Design, Development and Analysis of Rapid tooling mold and mold inserts for minimum Shrinkage and Warpage

Submitted in

fulfillment of the requirements for the degree of

Doctor of Philosophy

by

Sagar Kumar

(2013RME9049)

Under the supervision of

Dr. Amit Kumar Singh

DEPARTMENT OF MECHANICAL ENGINEERING

MALAVIYA NATIONAL INSTITUTE OF TECHNOLOGY, JAIPUR

JAIPUR-302017 RAJASTHAN, INDIA

MARCH 2019

© Malaviya National Institute of Technology Jaipur-2019

All rights reserved.

Declaration

I, Sagar Kumar (2013RME9049) declare that this thesis titled **"Design, Development and Analysis of Rapid tooling mold and mold inserts for minimum Shrinkage and Warpage"** and the work presented in it , are my own. I confirm that:

- This work was done wholly or mainly while in candidature for a research degree at this University.
- Where ant part of this thesis has previously been submitted for a degree or any other qualification at this university or any other institution, this has been clearly stated.
- Where I have consulted the published work of others this is always clearly attributed.
- Where I have quoted from the work of others, the source is always given. With the expectation of such quotations, this thesis is entirely my own work.
- I have acknowledged all main sources of help.
- Where the thesis is based on work done by myself, jointly with others, I have made clearly exactly what was done by others and what I have contributed myself.

Date: **Sagar Kumar**

(2013RME9049)

Certificate

This is to certify that the thesis entitled "**Design, Development and Analysis of Rapid tooling mold and mold inserts for minimum Shrinkage and Warpage"** being submitted by **Mr. Sagar Kumar** to the **Malaviya National Institute of Technology, Jaipur** for the award of the degree of **Doctor of Philosophy** is a bonafide record of original research work carried out by him under my supervision in conformity with rules and regulations of the institute.

The results contained in this thesis have not been submitted, in part or in full, to any other University or Institute for the award of any Degree or Diploma.

Dr. Amit Kumar Singh
Assistant Professor
Mechanical Engineering Department
Malaviya National Institute of Technology, Jaipur
Jaipur-302017, India

Place: Jaipur
Date:

Acknowledgement

I would like to express my deep and sincere gratitude to my thesis supervisor, Dr. Amit Kumar Singh, for his invaluable guidance and support. He is an excellent teacher and his knowledge and logical way of thinking has been of great value for me. This research is impossible without his inspiring guidance, experience, and subject knowledge.

I also take this opportunity to express my heartfelt thanks to the members of Departmental Research Evaluation Committee (DREC), Dr. Amar Patnaik and Dr. Harlal Singh Mali, who spared their valuable time and experiences to evaluate my research plan and the synopsis. I would also like to thank Prof. G. S. Dangayach, Head of the Mechanical Engineering Department, and his office team for helping in all administrative works regarding the thesis.

I also like to convey my heartfelt gratitude to seniors Dr. Chitresh Nayak, Dr. Kailash Chaudhary and Manoj Gupta for sharing their valuable knowledge. I also like to thanks my friends Vimal Kumar Pathak, Prashant Athanker, Ramanpreet Singh, NRNV Gowripathi Rao, Chandramani Goswami and Gaurav Kumar Badhotiya for their support and help which was extremely needed to complete my work successfully. Finally, but not the least I am very thankful to my parents, my brothers and my wife Ritu Shree who have surrendered their priority and time for me.

Sagar Kumar

Department of Mechanical Engineering

Malaviya National Institute of Technology, Jaipur

ABSTRACT

Traditional tool making in the case of plastic injection molding is time consuming, expensive and creates a lot of waste. Recent developments in rapid tooling technology by implementing the use of advanced manufacturing process like additive manufacturing (AM) is of large significance to the industry. In the same context, this thesis aims to provide an initial feasibility study to examine whether the polymer rapid tools are realistic and can be used as practical injection mold without any major downsides. In addition, prime objective of the research is to determine whether different benchmark features can be molded repeatedly on the proposed polymer rapid tool.

Understanding the tool survivability is a critical issue that need to be verified for the tooling to be successful. The tool survivability is analysed using simulation and experimental study in this thesis. The research work begins with investigating initial feasibility on determining whether room temperature vulcanizing (RTV) and polymer rapid tool (PRT) can be used as functional injection mold tooling. Initially, simple geometric shapes were formed and studied, which represent commonly molded features. This was followed by the molding of more complex and commercially available plastic components. The result shows that the parts fabricated using soft tooling RTV shows lot of shrinkage and also it will be not useful for high temperature injection molding. The complex features are difficult to be built as there is chance of breaking the part. Moreover, the Polyjet polymer mold shows better results as compared to soft tooling in terms of shrinkage. Experimental results showed that the mold was cracked initially possibly due to increase in pressure. But after optimizing the parameters the parts fabricated shows good quality results.

Furthermore, the digital ABS material is analysed for checking its feasibility in injection molding applications. The mechanical properties of the samples were considered and further bending, tensile and impact tests were performed by measuring their hardness. In addition the physical characterization was also performed. The outcome of the results are positive and showing that different parts can be manufactured using a commercial injection molding machine with digital ABS inserts in absence of any

catastrophic failure for the typical shape, molding compound and injection times used in this study. After 50 trials, the cavity undergo a slight and permanent distortion, but the quality of the surface was virtually unaffected and the surface remains same as its original quality. Thus, Digital ABS expresses good surface and dimensional stability at the time of injection process. Initially, there is a small increase in tension as well as modulus that is expected as point out by the outcome of other studies. Further, the impact strength increased by 30% or more, which was a conspicuous improvement.

Next study was performed to investigate whether the standard benchmark features have any effect on the dimensional behaviour of the parts fabricated using injection molding. Therefore, twelve standard benchmark CAD model were selected with different geometric attributes. Subsequently, simulation analysis was performed on all CAD model using Moldflow® (MFA) simulation software. Additionally, regression analysis is applied to identify the effect of injection molding parameters on the volumetric shrinkage of part made using rapid tooling mold insert of digital ABS material. It is found that maximum volumetric shrinkage (18.75 %) is observed for square pyramid frustum, conical frustum, and solid torus. On the contrary, hollow rectangular prism shows minimum shrinkage effect having 12.61 % of volumetric shrinkage. Further, this study is extended for complex feature component, and the results are experimentally validated with contactless laser-scanning systems.

The last stage of the thesis presents an integrated methodology for developing mathematical models and predicting the values of shrinkage and warpage by correlating them with process parameters of plastic injection molding process for making the case study part i.e. electronic relay of PBT and PET polymer material. The parameters considered for the prediction of shrinkage and warpage are Melt temperature, Packing temperature and Packing time. To find the optimum value of process parameters, the analytical model using regression analysis was developed. To further improve the optimum values a recently developed modified particle swarm optimization algorithm was used.

CONTENTS

Certificate i

Acknowledgements..... ii

Abstract iii

Contents v

List of Figures viii

List of Tables..... xi

CHAPTER-1 BACKGROUND & MOTIVATION

1. Introduction 1-3

1.2 Background 4

1.2.1 Rapid tooling and its history 4-5

1.2.1.1 Direct Tooling 5-6

1.2.1.2 Indirect Tooling 7

1.3 Additive manufacturing 8-9

1.4 Reverse Engineering for part inspection 10-11

1.5 Thesis Statement 12

1.6 Thesis Organization 12-14

1.7 Chapter Summary 14

CHAPTER-2 LITERATURE REVIEW

2.1 Rapid tooling techniques used for production of parts in injection molding 16-18

2.2 Use of cooling channels and additive manufacturing techniques for improving part quality 19-22

2.3 Material Jetting process 22

2.4 Directed Energy Deposition 23-24

2.5 Powder Bed Fusion 24

2.6 Binder Jetting 24-25

2.7 Vat photopolymerization 25-26

2.8 Sheet Lamination 26

2.9 Material Extrusion 26-28

2.10 Injection molding process parameter selection and optimization 28-30

2.11 Advances in 3D scanning systems for quality inspection 31-34

2.12 Discussion on mechanical and physical properties of mold in injection molding 35-37

2.13 The Knowledge Gap in Earlier Investigations 37-38

2.14 Research objectives 38-39

2.15 Chapter summary 39

CHAPTER-3 MATERIALS AND METHODS

3.1 Investigations of Room Temperature Vulcanizing (RTV) soft tooling as functional injection Molding 40

3.2 Experimental set up 40

3.2.1 Selection of Test pattern (Model) 41

3.2.2 Entry Level Additive Manufacturing (ELAM) for generation of RP pattern- 41-42

3.2.3 Selection of RTV Silicon compound 42-43

3.3 Methodology to prepare RTV silicon rubber mold 43

3.3.1 RTV Mould preparation 44

3.4. Pattern by Wax injection 44

3.5 Process parameters for the production of wax patterns 45-46

3.6 Experiment and Observation 46

3.7 The responses 47

3.8 Results & discussion 48-51

3.9 Investigation of FDM modeled Polymer Rapid Tooling (PRT) for Plastic Injection Molding 51-54

3.10 Methodology to develop PRT mold 54

3.11 Material selection and properties 55

3.12 Working principle of Polyjet Direct 3D printing 56-57

3.13 Hand Injection Moulding machine to develop the part 58-60

3.14 Reverse engineering to check the accuracy of RP 61-65

3.15 Chapter Summary 65

CHAPTER- 4 MECHANICAL AND PHYSICAL CHARACTERIZATION OF DIGITAL ABS

4.1 Sample geometry and used materials 66-67

4.2 Mould inserts materials 67

4.3 Design and manufacturing of mould 68-69

4.4 Process parameter and material selection for injection molding experiments 69-72

4.5 Dimensional and Surface analysis 73

4.6 Mechanical and DSC analyses 73-76

4.7. Results and discussion 76-81

4.7.1 Mechanical properties and Crystallinity 81-83

4.8 Chapter Summary 83

CHAPTER-5 VOLUMETRIC SHRINKAGE ESTIMATION OF BENCHMARK PARTS

5.1 Design and development of benchmark feature component 84-85

5.2 Material selection and properties 85-87

5.3 General considerations for design of standard benchmark parts 87-88

5.3.1 Geometric Attributes consideration 91

5.3.2 Volume Ratio (VR) 91

5.3.3 Thickness Ratio (TR) 91

5.3.4 Draft Angle Ratio (DR) 91

5.3.5 Part Weight Ratio (WR) 91

5.3.6 Quality Prediction Ratio (QR) 92

5.3.7 Cycle Time Ratio (CTR) 92

5.4 Mold design for standard benchmark pats using Autodesk inventor 3D modeling software 93

5.4.1 Design procedure to generate a core and cavity 93

5.4.1.1 Procedure to create the patching surface 93-96

5.5 Moldflow Simulation Results and Analysis for the Benchmark Parts 96-101

5.6 Result and discussion 102-103

5.7 Chapter Summary 103-104

CHAPTER-6 VOLUMETRIC SHRINKAGE AND WARPAGE ESTIMATION OF COMPLEX PARTS

6.1 Development of Core and Cavity for complex feature component 105-106

6.2 Design of injecting plastic part 106

6.2.1 Best gate location 107

6.3 Employed parameters 107-108

6.4 Simulation study for PBT and PET materials 108-110

6.5 Taguchi method 111

6.6 Analysis for injection molding 111

6.7 The obtained values from the analysis 112

6.8 Regression analysis method 112

6.9 Warpage and shrinkage analysis for results evaluation 113-117

6.10 Experimental verification 118

6.10.1 The evaluation of rapid tooling by developing the test mold 118

6.10.2 Manufacturing of the rapid tooling mold by polyjet technology 118

6.10.3 Process parameter and Material selection for Injection molding Experiments 119-121

6.11 Comparison of the outcome of simulation results with experimental data using 3D scanners 121-122

6.12 Scanning methodologies 122

6.12.1 Environmental Conditions 122-123

6.13 Chapter Summary 124-125

CHAPTER 7 OPTIMIZATION OF RAPID TOOLING MOLDED COMPLEX FEATURED COMPONENT

7.1 Introduction 126-129

7.2. Experimental Details 129-131

7.3 Results 131-137

7.4 Modified particle swarm optimization algorithm 137

7.4.1 Standard particle swarm optimization algorithm 137-141

7.5 Optimization problem formulation 141

7.5.1 Identification of design variables 141

7.5.2 Objective function and constraints 141-142

7.6 Discussion 142-144

7.7 Chapter Summary 145

CHAPTER 8 CONCLUSION AND FUTURE WORK 146-149

8.1 Scope for Future work 150

REFERENCES 151-192

LIST OF PUBLICATIONS 193

BIODATA 194

List of Figures

Figure 1.1 Line diagram of Injection molding process 2

Figure 1.2 Classification of rapid tooling 5

Figure 1.3 Relations in material quantity of parts and selected RT technique 6

Figure 1.4 Example of silicon rubber soft tooling 7

Figure 1.5 Layer by Layer depositions to build a product 8

Figure 1.6: Flowchart for basic phases of reverse engineering 11

Figure 1.7 Schematic of 3D scanner mechanism 11

Figure 2.1 Schematic of DMLS technique 16

Figure 2.2 Metal mold used in injection molding 17

Figure 2.3 Conventional and Conformal cooling channel 20

Figure 2.4 Mold cavities with and without cooling channel 21

Figure 2.5 Schematic of Directed energy deposition (DED) process 23

Figure 2.6 Schematic of Vat photopolymerization process 25

Figure 2.7 Schematic diagram of FDM based AM process 27

Figure 2.8 Fishbone diagram for injection molding process parameters 30

Figure 2.9 Laser triangulation principle 32

Figure 3.1 Stepped bar pattern developed by additive manufacturing 41

Figure 3.2 Schematic of R3D2 entry-level AM Printer 42

Figure 3.3 Si rubbers for RTV soft tooling 43

Figure 3.4 (a) RTV silicon rubber mold 44

Figure 3.4 (b) Mold and Patterns 44

Figure 3.5 vacuum wax injection machines 45

Figure 3.6 Ishikawa cause effect chart for wax pattern 45

Figure 3.7 Effect of process parameters on linear shrinkage and S/N ratio 50

Figure 3.8 Applications of additive manufacturing 53

Figure 3.9 Revenues from the production of parts 54

Figure3.10 Designed geometry with dimension of striker mold 54

Figure 3.11 Monomers used in thermoplastic ABS 55

Figure 3.12 Polyjet 3D printers for printing mold 56

Figure 3.13 3D printed core and cavity 57

Figure3.14 Hand Injection Molding (HIM) Machine for trail 58

Figure3.15 Damaged mold at the injection point 59

Figure 3.16 Metals (MS) plate for minimizing temperature and pressure intensity at the injection point 59

Figure 3.17 Progressive stages of the component made in the trial runs 58

Figure 3.18(a) Part sticks to the mold cavity 60

Figure 3.18 (b) Quality part (striker) productions 61

Figure 3.19 3D scanner for inspection of part component 62

Figure 3.20 Inspection of specimen with 3D scanner 62

Figure 3.21 Inspection results of component 63

Figure 3.22 Digital Vernier Caliper for measurement 64

Figure 4.1 (a) Tensile sample 65

Figure 4.1 (b) Bending test specimen 67

Figure 4.2 (a) 3D model of mold inserts (b) Numerical simulation using Moldflow 68

Figure 4.3 Metal inserts with cooling channels 68

Figure 4.4 Digital ABS mold inserts 69

Figure 4.5 Digital ABS Insert with tensile cavity 70

Figure 4.6 Temperature of Digital ABS Insert after supercritical CO2 is sprayed 71

Figure 4.7 Plastic Tool Strain at Break Varying Melt Temp, Injection Speed and Supercritical CO2 72

Figure 4.8 EMICDL2000 Universal Tensile Testing Machine 74

Figure 4.9 TA Q20 Differential Scanning Calorimeter 74

Figure 4.10 CNC Bridgeport Mill used to Post Process the Digital ABS Mold and Tensile 75

Figure 4.11 Milling the Edges of a Molded Tensile Bar 75

Figure 4.12 Three-dimensional surface profile of cavity as (a) printed, after (b) 20 shots and (c) 40 shots 78

Figure 4.13 CMM Measurement 79

Figure 4.14 2D waviness profile (at 1.80 mm) 80

Figure 4.15 Surface details of the tensile sample after 6 shots 80

Figure 5.1 3D Model of benchmark parts using Autodesk inventor solid modeling software 85

Figure 5.2 Process flow diagrams for simulation and analysis 86

Figure 5.3 Procedure to create patching surface 94

Figure 5.4 Create runoff areas 94

Figure 5.5 Core and Cavity for all Benchmark features 96

Figure 5.6 Moldflow® (MFA) simulation results for Rectangular Prism Hollow with Cylinder 97
Figure 5.7 Simulation results of all benchmark features using Autodesk simulation moldflow software 100
Figure 5.8 Regression graph for volumetric shrinkage percentage 103
Figure 6.1 Development of Core and Cavity for test part 106
Figure 6.2 Result of best gate location analysis 107
Figure 6.3 Simulation results of complex feature component for 0.8, 0.9 and for 1 mm wall thickness for PBT/PET materials 109
Figure 6.4 The exact gate location and finite element mesh 112
Figure 6.5 Normal probability plot for warpage of 1 mm wall thickness 114
Figure 6.6 Typical response surface plots 115
Figure 6.7 Normal probability plot for volumetric shrinkage of 1 mm wall thickness of PBT and PET standardized residuals at 95% of confidence interval 116
Figure 6.8 Typical Response Surface plots for shrinkage 117
Figure 6.9 Arburg 370S 700 – 290 injection molding machine 119
Figure 6.10 3D polyjet mold mounted on for experiment 120
Figure 6.11 Cracked mold after performing 150 shots 120
Figure 6.12 ABS mold insert with metal die 121
Figure 6.13 Steinbichler Comet L3D during scanning 122
Figure 6.14 Deviation between 3D scan and CAD model 123
Figure 6.15 Volumetric shrinkage of cylinder and hollow rectangular prism 124
Figure 7.1 Electronic relay mesh file with cooling channel 130

Figure 7.2 Variation of the S/N ratio of (a) Shrinkage (b) Warpage 133

Figure 7.3 Percentage deviation in prediction of shrinkage 135

Figure 7.4 Percentage deviations in prediction of warpage 137

Figure 7.5 Flowchart of modified particle swarm optimization (MPSO) algorithm 141

Figure 7.6 Convergence plot of (a) Shrinkage (b) Warpage of PBT 143

Figure 7.7 Shrinkage analysis using optimized parameter 144

Figure 7.8 Warpage analysis using optimized parameter 144

List of Tables

Table 2.1 Summary of important literature for Mechanical and physical properties of mold. 37

Table 3.1 Constituent of RTV Si rubber for soft tooling 43

Table 3.2 L16 experiment Factors and Levels 46

Table 3.3 L16 Responses of Experimental work 47

Table 3.4 Response Table for S/N Ratio 50

Table3.5 Parameters of Polyjet 3D printer 54

Table 3.6 Dimension of measured part using 3D scanner 60

Table 3.7 Dimensional results using Vernier Caliper 61

Table 4.1 Properties of SAE 1045 and Digital ABS materials 67

Table 4.2 Injection-moulding parameters for inserts 70

Table 4.3 Molding parameters to conduct the experiments 72

Table 4.4 Digital ABS cavity surface quality 76

Table 4.5 Digital ABS cavity CMM measurements 79

Table 4.6 Average Dimensions of PET samples after injection in the Digital ABS cavity 81

Table 4.7 PET specimens Crystallinity test results after injection in mold inserts 82

Table 4.8 PET specimens tensile test results after injection in mold inserts 82

Table 4.9 PET specimens bending test results after injection in mold inserts 82

Table 4.10 PET specimens impact test results after injection in mold inserts 83

Table 4.11 PET specimens Hardness test results after injection in mold inserts 83

Table 5.1 Input parameter of thermoplastic material polyethylene terephthalate (PET) 85

Table 5.2 Input parameter of mold material (Digital ABS) 87

Table 5.3 Simulation process setting parameter for Digital ABS mold 87

Table 5.4 General consideration for bounding box volume of benchmark features 89

Table 5.5 Geometric attribute data compiled for regression analysis 92

Table 5.6 (B1), (B2) Moldflow® (MFA) simulation results compiled for regression analysis 101

Table 5.7 Input parameter of simulation of PET injection molding – simulation design 102

Table 6.1 Optimal process parameters and levels 108

Table 6.2 Simulation results for Shrinkage and Warpage of PBT and PET materials for 0.8, 0.9 and 1 mm wall thickness 110-111

Table 6.3 L9 (3^2) Orthogonal Array Variance for Experiment 113

Table: 6.4 Regression model for warpage and the R^2 values for PBT/PET material 114

Table 6.5 (a), (b) Regression model for Shrinkage and the R^2 values for PBT and PET material 116

Table 6.6 Plastic Injection Molding Machine 119

Table 6.7 Operating parameter Steinbichler Comet L3D 121

Table 7.1 Physical properties of PBT/ PET material 130

Table 7.2 Process Parameters and their levels 131

Table 7.3 The layout of L9 orthogonal array 131

Table 7.4 Shrinkage and warpage values of PBT and PET material 132

Table 7.5 ANOVA result for PBT shrinkage model 134

Table 7.6 ANOVA result for PET shrinkage model 135

Table 7.7 ANOVA Analysis for warpage PBT model 136

Table 7.8 ANOVA Analysis for warpage PET model 136

Table 7.9 Optimum parameters prediction using PSO and MPSO 142

Table 7.10 Confirmation simulation trials 144

Table 7.11 Comparison of shrinkage and warpage improvement with literature 145

CHAPTER-1

BACKGROUND & MOTIVATION

1. Introduction

The manufacturing scenario of the today's twenty-first century is continuously evolving into one of the volatile consumer markets with fast moving product technologies. These continuous changes are forcing the industries to be competitive along different front including design, manufacturing, quality, inspection etc. Historically, the manufacturing sector has not been at best but it has assured of providing better results in the coming days. In the last few years, the rapid growth in the manufacturing technologies and their applications has given rise to the production of complex profile parts with improved accuracy. In addition, the market globalization has forced the manufacturing scenario to be extremely competitive and volatile. To survive in such a volatile scenario, it is expected for the manufacturing industries to not only producing high quality products but also look into the aesthetics, cost as well as customer desires. In order to achieve these goals, manufacturing firms are required to adopt flexibility in their production system and reducing the time to market for their products.

Nowadays, to accomplish the objectives, reducing cycle time and for faster product development, injection molding with rapid tooling is adopted in industries. Injection molding is one of the most extensively applied and established processes in current manufacturing scenario. The process commences from the heating of a thermoplastic material which is further enforced into a mould impression under pressure. The material inside of the mold cavity cools, solidifies, and is then removed as a developed product. The moulds are also referred to as a tool which helps the resin to get the required shape and are typically machined from metals such as aluminum, hardened steel, and various copper-based alloys (Lebrun et.al., 1996) for improved and longer tool life.

Injection molding has been the most common technique for producing plastic product due to high efficiency and manufacturability. The Plastic injection molding primarily consists of three processes: filling and packing, cooling and lastly ejection. Among these three processes cooling step is the most important stage as it not only affects the quality of the product, also the productivity gets hampered. The cooling process account for nearly two-third of the total time taken by the injection molding product cycle. To improve the efficiency of the cooling stage, an effective cooling system is required. An efficient cooling channel can be incorporated to reduce the internal stresses and differential shrinkage by providing appropriate cooling the entire part. The cooling system during their design also needs to keep in mind the manufacturability of the system for controlling construction cost.

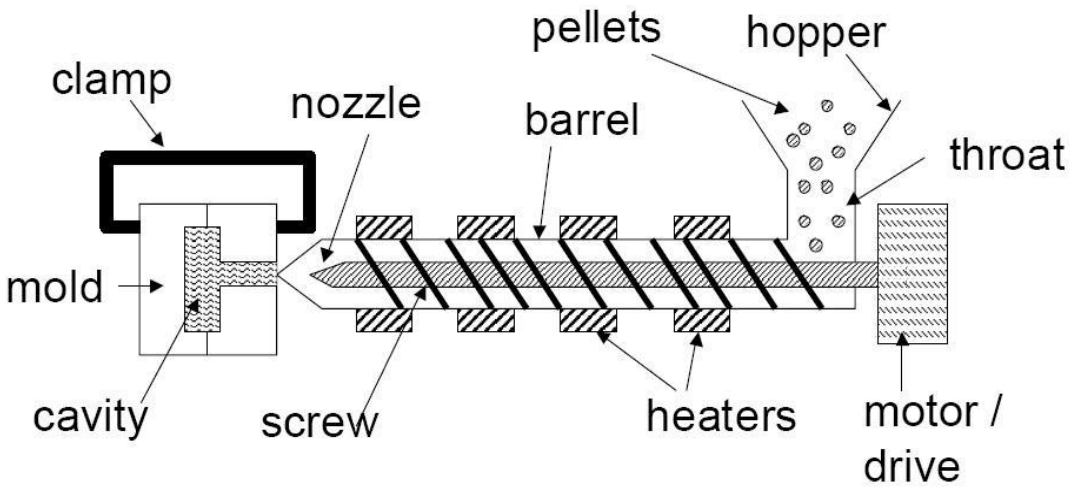

Figure 1.1 Line diagram of Injection molding process

The other method to improve the final part quality is by means of rapid tooling. The traditional tool making is time consuming, expensive and produces a great deal of waste. The conventional tools may take lot of time to produce and can be very costly. For fabricating such tools, highly skilled and expertise personnel are required. In addition, mostly the parts are fabricated at distant places from the places where they are planned to be used, thus requiring expensive and lengthy transportation. The summation of all these problems, in the initial stages of producing a new component, the design of the developed mold leads to some changes. The changes are due to the modifications in the product's

dimensions or because of mold refining to better meet desired part specifications. Whatever may be the reason for these changes, each modification needs extensive and expensive alterations. In few cases, the changes incorporated in the mold are so severe that it is advisable to reproduce it from scratch.

The injection molds are expected to produce components that are near to their original specifications. The mechanical properties, thermal conductivity and accuracy of the mold have a substantial impact on part quality, geometric complexity, molding cycle and competitiveness (Lee & Subramanian, 2007). However, for producing prototyped components or mold verification, the major and primary cost is driven by the cost of the mold. To improve the effectiveness, productivity and compress the mold cycle of the injection molding process, one of the possible alternatives to conventional tooling in those instances is Rapid Tooling (RT). RT generally, is the term proposed for either indirectly or directly exploiting a 3D printed prototype as a tooling part (Sachs et.al, 1992). Moreover, a rapid tool is a mold which can fabricate similar products as a traditional tool, at significant good quality; however, it must be fabricated within a small amount of time and expense. These tools are not used to completely replace the traditional tooling methods nor will they be used for producing components in high volume. In contrast, the RTs are ideally used for prototyping the products and for short batch run applications which necessitate maximum flexibility. There are numerous approaches available for creating rapid tools.

The most recent approach involves the application of Additive Manufacturing (AM) process. Usually, the AM route was applied for developing the injection mold indirectly. Though, the most ideal use for AM-produced rapid tools is their direct use as a functional injection mold. The success of some of the AM techniques resides on the adequate availability of materials. With ever increasing progress in the developments of new AM materials and techniques, it may now practical to fabricate plastic molds and apply them in the form of functional tools. Moreover, the thermal behaviors of plastic molds are also different from the conventional metal molds. The present research work aims for an early feasibility study to determine whether the rapid tools based on different polymer are possible as injection mold tools by analyzing and determining if they can produce specified dimensions over different cycles.

1.2 Background

This section provides a brief overview of the subject matter and terminology normally used within this research. The subject matter includes rapid tooling history, additive manufacturing for pattern making, injection molding and the use of rapid tools within the injection molding.

1.2.1 Rapid tooling and its history

Till late 1990s, the rapid tooling always has the requirement of conventional and customized tools such as jigs and fixtures. In addition, the hardware and moulds are also used for pervasive injection molding and die manufacturing within the rapid tooling scenario. The moulds are earlier developed using expensive and time taking subtractive manufacturing processes, depending on the complexity of the part. Moreover, there is limited flexibility for further improvement and any error in the manufacturing of such object may lead to the increase in cost of product cycle. In contrast, with the advent of 3D printing technology, the moulds are printed in short period of time by additive manufacturing (AM) process. In comparison to conventional tooling practice, the mould preparation using 3D printing involves less cost and less time (Bassoli et.al, 2007; Ferreira, 2004 and Hofmann, 2014)

The different rapid tooling processes available are classified and shown in Figure 1.2. Earlier, the researchers have classified the RT process based on the quantity of parts produced, cost and time taken by conventional tooling (Chua et.al, 2015; Mueller & Kochan, 1999; Levy et.al, 2003). In context of tooling, mainly plastic injection

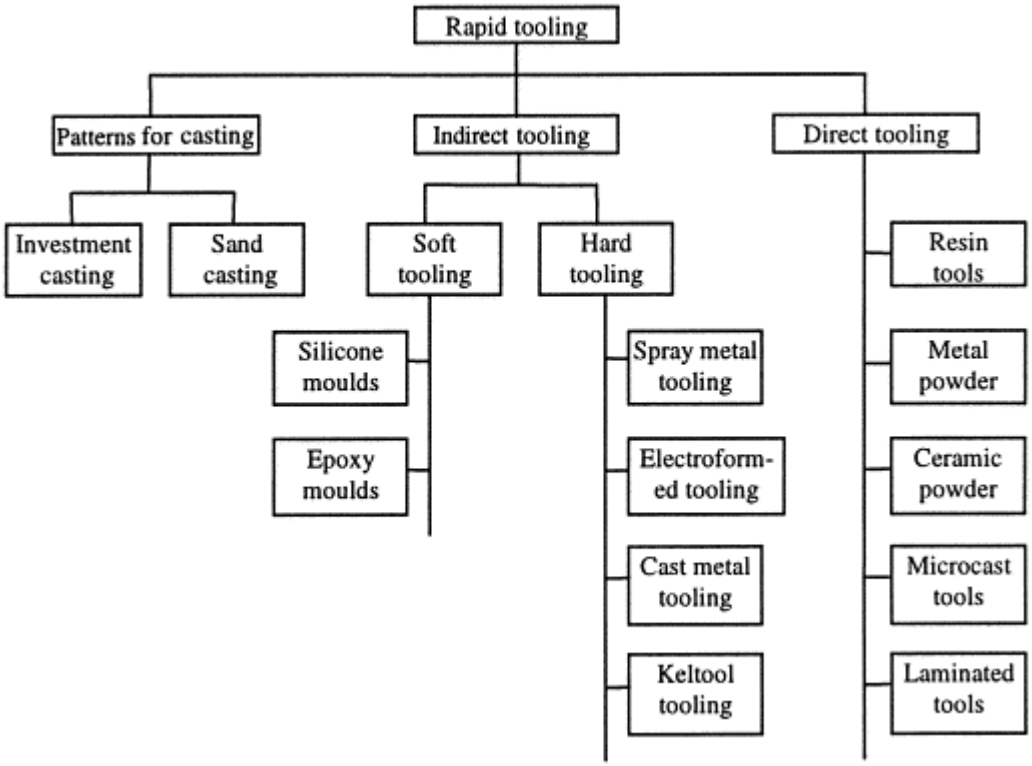

Figure 1.2 Classification of rapid tooling (Rosochowski & Matuszak, 2000)

molding tools are considered, as these are commonly used forming tools. The rapid tooling options may also be classified based on the material quantity and the amount of quantity required as shown in Figure 1.3. It is quite clearly evident that for strong technical parts with more number of quantity, more refined tooling option has to be considered. The choice of selecting the adequate rapid tooling technique solely depends on the requirement of quantity, its quality and time to produce components. Moreover, skill and expertise are important tools that are required for effective selection of rapid tooling processes.

1.2.1.1 Direct Tooling

Direct tooling referred to as process in which an AM part can be directly used as mold or pattern. The part manufactured using additive manufacturing doesn't require any post processing ideally and can be directly used in production floor for fabrication of product

at a rapid pace. Since the inception of this concept, it has not been widely accepted in industries as a main scale

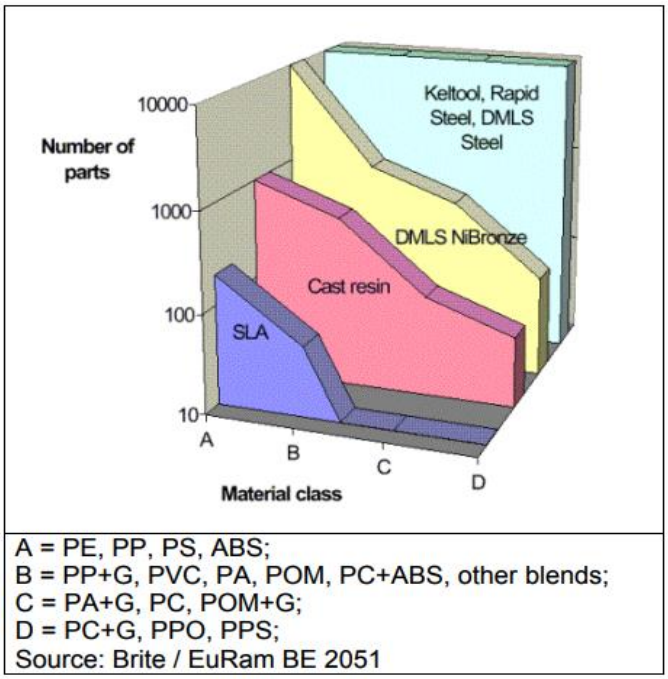

Figure 1.3 Relations in material quantity of parts and selected RT technique (Hilton, 2000)

manufacturing technology. The direct tools generally made of durable material and used to produce larger number of components. Spray metal tooling is used as tooling for low pressure processes. In recent years, with the development of spraying methods and technologies, it is preferred as tooling for injection moulding prototypes of low production. Cast metal tooling is widely used in injection moulding and die casting.

Ceramic tooling is applied for producing more accurate components which are precise in their size and dimension with minimum shrinkage. Further, metal powder tooling is extensively used for direct tool production. Usually, the automotive components are fabricated from this type of tooling that requires maximum tensile strength. The use of laminated metal sheets is widely accepted but only drawback is to keep in mind to resolve the bonding technique to ensure structural integrity.

1.2.1.2 Indirect Tooling

The indirect tooling refers to the process in which a model is build using an RP method, in any suitable material that is not required to be metallic. Using the master pattern, a mould is developed out of a certain specific material such as soft metal, silicone rubber and epoxy resin. It is broadly divided into two primary groups' i.e. soft tooling and hard tooling depending on the type of component and the number of quantities required for production. Soft tooling refers to the low cost and soft material process which is used interchangeably. Mostly, the parts produced in RT are using soft tooling techniques. One example of soft tooling is use of silicon rubber for producing mould cavity about a master rapid prototyping pattern as shown in Figure 1.4. The various other examples of soft tooling include epoxy molds and castable ceramics.

Figure 1.4 Example of silicon rubber soft tooling

Though the use of soft tooling is widely accepted in industries but the shift is now beginning to change to use hard tooling. These tools are widely used for short prototype runs especially 100-200 parts batch production (Jamal et.al, 2004). The principal

advantage of direct tooling comes as the production of injection molding bridge or “firm” tools.

1.3 Additive manufacturing

Additive manufacturing (AM) is also well-known by the names of layered manufacturing (LM), freeform fabrication (FFF), rapid prototyping (RP), and automated fabrication. RP is an advanced technology useful in developing physical models at a rapid pace and fabricating functional prototypes in small batches directly from a virtual computer aided design (CAD) model. It involves addition of material sequentially layer by layer until a complete 3D object is fabricated. The AM processes developed part by addition of material, in contrast to to removing material as performed in conventional manufacturing processes. Therefore, it helps in minimizing the wastage of material as compared to the traditional manufacturing. Usually, the AM techniques work by splitting the computer model into similar cross-section layers. The buildup of these layers from bottom to top created a physical object (see Figure 1.5).

Figure 1.5 Layer by Layer depositions to build a product (Prest et.al, 2013)

The various AM technologies are commonly similar to each other by adding and joining materials in layer-wise method to form the objects. This is directly contrary to the

classical techniques such as milling and forging. Prior to that, objects are made of mechanical removal of material, and later mechanical forces, the material is constantly deformed in the desired form. The beginning for each RP process is the cause of the abstract geometry of the object being created. From this, a record must be created that describes the geometry. The created record must be manipulated to produce the instructions needed to control the process in the final phase of the actual manufacture of the component. The input at the beginning of the RP process may be a point cloud obtained by sampling techniques (Reverse Engineering) or 3D CAD models produced by many solid modelers or mathematical data acquired by analytical equations. The entire process of creating an object by any RP method can be classified into two stages (Shirazi et.al, 2015 and Stevenson, 1993).

STEP 1: At this stage STL (stereolithography) file is created with tessellating 3D model, that is cut and retained, and the generated data is stored in standard formats that can be interpreted by RP machines. This information will be used in step 2. At this stage, the most important parameters are the choice of the orientation of the parts and the layer thickness, since the construction time, the surface quality, the number of supporting structures; the costs etc. are affected by them.

STEP 2: In this step, a physical model is generated. This step is different for the processes of RP and depends on the basic principle of deposition used in the RP machine. The software operating the RP system generates laser scan paths (in processes such as selective laser sintering, stereolithography etc.) or material deposition paths (in processes) such as fused deposition modeling from the slice information obtained in step 1. At this stage, various process-related information such as tolerance (surface finish), material, machine (such as laser spot diameter, cutting speed, temperature, etc.) is provided (Badrinarayan & Barlow, 1994; Dalgarno & Stewart, 2001). There are several known RP technologies available on the market, including only a few stereolithography (SL), selective laser sintering (SLS), laminated object production (LOM), fused deposition modeling (FDM), 3D printing (3DP), multi-jet modeling (MJM) and Solid Ground Curing (SGC) (Bassoli et.al, 2007; Bernard et.al, 2002, Cheah et.al, 2005).

1.4 Reverse Engineering for part inspection - Although a traditional engineering process initiates with a design concept, in contrast reverse engineering begins with capturing the data of actual shape of an object. The major advantage of the reverse engineering process is data capturing of the free-form surface. It is imperative to capture the shape point data of physical object. The accuracy of the reconstructed model largely depends on the quality, type of the data captured and type of measuring instrument. In industries, till date part inspection was performed mostly by gauges, templates and Coordinate measuring machines (CMM). However, in recent times the conventional gauges and CMMs are replaced by 3D scanners because of their improved accuracy and fast data acquisition (Galantucci et.al, 2003; Gao et.al, 2006; Onuh et.al, 2006) In addition, the CMMs are also not suitable for measuring soft materials; also the sampling speed is very low. The steps for the reverse engineering process consist of measuring part geometry through a contact or non-contact instrument, developing a computer-aided geometric model from the measurement data and possible technical refinements of part design, developing the manufacturing plan, selecting the materials, and finally becoming the real one Production model developed. The basic flow of reverse engineering process is shown in figure 1.5.

Reverse engineering with 3D scan data is a rapid and efficient way to generate CAD models when an object has a complex structure or when a 3D model does not exist for an object. The 3D scanning device takes the physical geometry of the component and converts it into 3D digital model. The mechanism of laser scanner used in this work is shown in Figure 1.7. The 3D laser scanning process begins with laser line projection on the surface of the object. The laser beam is reflected and CCD sensor is placed to capture surface data in the form of 3-dimensional point data.

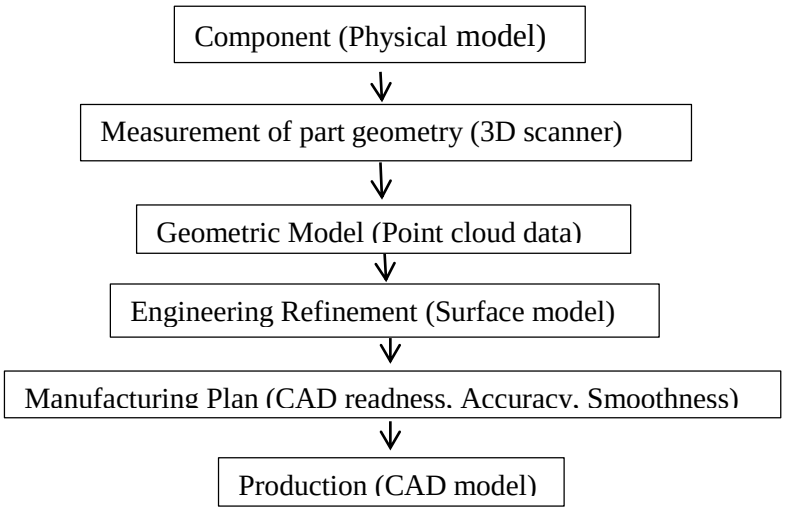

Figure 1.6: Flowchart for basic phases of reverse engineering

The point data of object surface is acquired using triangulation method. Scopes of an object are scanned simultaneously so that hundreds or thousands of closely positioned points can be captured simultaneously. Without making the contact with the object the process of laser scanning is performed.

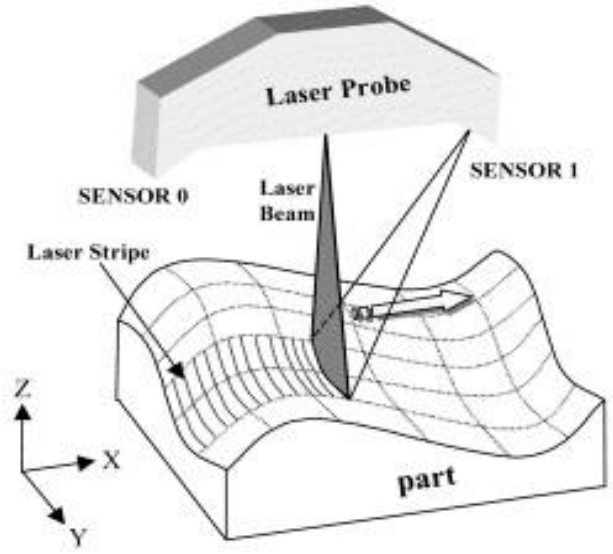

Figure 1.7 Schematic of 3D scanner mechanism

For rapid product development (RPD) newly established equipment and techniques are used that support the designers and manufacturers in surviving the demands for the reduction of product development time. For example, injection molding companies need

to dramatically reduce tool and development times for die. By introducing the reverse engineering methodology, a three-dimensional product or model can be quickly tested in digital form, re-modeled and exported for rapid prototyping or rapid tooling or for rapid manufacturing.

1.5 Thesis Statement

This thesis presents the practical applicability of digital ABS mold and inspection of developed specific feature component followed by a regression model. The main objective of the research is to improve the quality of the part through optimizing process parameter of a plastic injection molding machine followed by a 3D inspection process, beginning with manufacturing to the final model developed. During the injection molding process, the analysis of rapid tooling mold on the dimensional and surface stability and the final casting process is studied in detail. The CAD model is used for analysis with Moldflow software. The mechanical and physical properties of the samples were analyzed by tensile, bending and impact test as well as by measuring their hardness. Further, a framework for systematic methodology is developed to determine optimal injection molding conditions for minimum shrinkage and warpage in a thin wall relay part for Polybutylene Teraphthalate (PBT) and Polyethylene terephthalate (PET) materials using newly developed Modified Particle Swarm Optimization (MPSO) algorithm.

1.6 Thesis Organization

The rest of this thesis is organized as follows:

Chapter 1: Background and Motivation

The background, motivation and importance of research to develop most ideal use for AM-produced rapid tools is their direct use as a functional injection mold for effective and accurate industrial applications are presented in this chapter. It also emphasizes the contours of the dissertation organization.

Chapter 2: Literature review

This chapter presents a literature review on various challenges and issues related to PRT mold, followed by Injection molding machine operated at optimal process parameter for data collecting and verifying the results by 3D scanning system. The discussion is followed by volumetric shrinkage and warpage error evaluation and optimization method for effective inspection of developed part and mold.

Chapter 3: Materials and methods

This chapter includes the selection and employability of materials for the use of functional injection mold tooling. The main purpose of this study was to determine whether the Room Temperature Vulcanizing (RTV) and Polymer Rapid Tooling (PRT) mold could develop a distinctive feature for specific geometry within the acceptable tolerance limit and can perform this repetitively. Initially, it was created and studied by simple geometric shapes, which represent the most commonly developed features. Further this was followed by the molding of more complex feature component.

Chapter 4: Mechanical and physical characterization of Digital ABS

The present study deals with the analysis of digital ABS on dimensional and surface stability as well as the final casting properties. The mechanical properties of the samples were analyzed by measuring bending, tensile and impact tests and their hardness. Differential scanning calorimeter (DSC) was used to measure PET crystallization.

Chapter 5: Volumetric Shrinkage Estimation of Benchmark parts

The work of this chapter proposes an effective shrinkage estimation of twelve reference benchmark features commonly used in an injection molded plastic component. To determine the influence of shape and geometry parameters on volume shrinkage and warpage, a systematic methodology based on Moldflow® (MFA) software is used. Furthermore, a statistical regression technique was used to identify the percentage contribution of geometrical attributes to volumetric shrinkage and warpage. The regression equation followed by geometric parameters was developed to estimate the percentage of volumetric shrinkage of injected part.

Chapter 6: Volumetric Shrinkage and Warpage Estimation of Complex Parts

This chapter deals with the study of volume shrinkage and warpage results for complex parts that consist all the benchmark features. For this purpose an electronics component relay is considered as a sample produced from digital ABS mold integrated with straight cooling channels. A systematic methodology is proposed for analyzing volumetric shrinkage and warpage in an injection molded part having a thin shell structure during the injection molding process. The outcomes were experimentally validated with reverse engineering technique.

Chapter 7: Optimization of rapid tooling molded Complex featured component

This chapter discusses a systematic methodology for analyzing volume shrinkage and warpage in an injection molded component with a thin shell structure during the injection molding process. First, the impact of parameters of the injection molding process on shrinkage and warpage for various wall thicknesses was investigated using the Taguchi method. The shrinkage and warpage values were found by Moldflow insight software. The result of confirmation experiments and analysis of variance (ANOVA) ensures that the quadratic models of the shrinkage and warpage are well fitted with the values simulated at optimal values. The shrinkage and warpage are examined and predicted by the mathematical model obtained for the individual influences of all parameters.

Chapter 8: Conclusion and Future Scope

The results of this study are summarized in this chapter. It also deals with the contribution and the future directions of this research.

1.7 Chapter Summary

This chapter begins with a background followed by a brief introduction of rapid tooling, its applications and advantages. Further reverse engineering principles with its importance in industrial applications is discussed. The significance of rapid tooling for inspection in industries is presented. The motivation behind developing an iterative and detailed inspection plan is presented here. At last, brief information about various chapters is discussed.

CHAPTER – 2

LITERATURE REVIEW

This chapter presents an extensive literature survey which provides background information on the research topics of the present investigation. Since, the present work emphasis is on the rapid tooling and the parts produced using additive manufacturing mold, this chapter summarizes overview of different rapid tooling techniques used in production, additive manufacturing (AM) techniques, injection molding process parameter selection, optimization and advances in 3D scanning systems for quality inspection. Furthermore, the discussion on mechanical and physical properties of additive manufacturing mold is also been performed. The topics briefly reviewed all the relevant literature and still needs further research to minimize the above covered challenges and issues for industrial applications.

The literature was classified on the following basis:

2.1 Rapid tooling techniques used for production of parts in injection molding

2.2 Use of cooling channels and additive manufacturing techniques for improving part quality

2.3 Injection molding process parameter selection and optimization

2.4 Advances in 3D scanning systems for quality inspection

2.5 Discussion on mechanical and physical properties of additive manufacturing mold

At the end of this chapter, an overview of the literature survey and a knowledge gap in the previous investigations are presented.

2.1 Rapid tooling techniques used for production of parts in injection molding-

Since early 1990's, several attempts have been made for producing parts in injection molding using rapid tooling. The prime objective of applying rapid tooling concept is to reduce the product lifecycle and producing faster product in injection molding (Levy et al., 2003). With the use of rapid tooling, the tool delivery time can be reduced upto 50%. Past studies suggests that metallic rapid tools are widely applied rapid tools in injection molding for production of components. There is number of research available that shows the successful implementation of metallic material for rapid injection mold development (Rosochowski & Matuszak, 2000). Initially, the rapid tooling involves the use of Direct Metal Laser Sintering (DMLS) additive manufacturing technology. The strength of the sintered mold was increased by bonding together the powder particles using oven heating (Dalgarno & Stewart, 2001). The DMLS techniques were used to produce metallic molds using different alloys material involving steel, aluminium, zinc and titanium etc (Barlow, Beaman, & Balasubramanian, 1996). These RT techniques are used for producing the conventional hard molding tools which are further useful in producing parts in full time production. Based on past publications data, it was found that the DMLS rapid metallic tools are capable of producing 250 to 1000 parts. In addition, the metallic mold fabrication takes three to four weeks in mold fabrication (Pham, 2000). Similar work reported on DMLS process used the mold which is built on a steel plate for facilitating mold assembly.

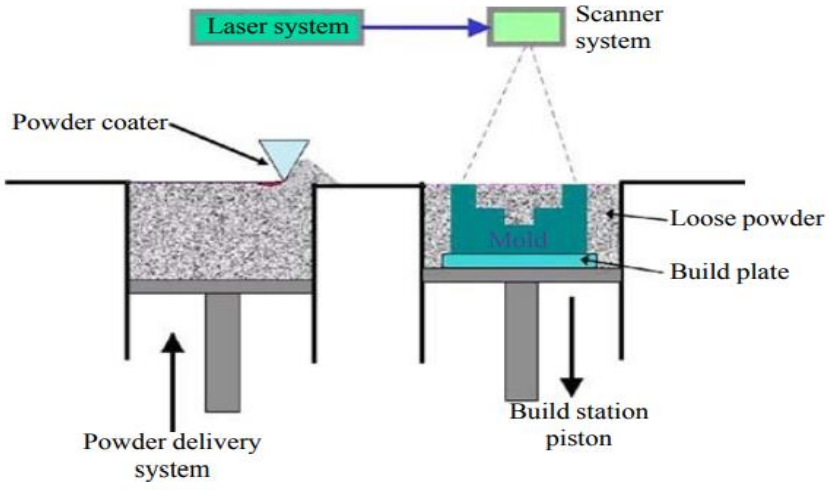

Figure 2.1 Schematic of DMLS technique (Barlow, Beaman, & Balasubramanian, 1996)

By implementing the similar techniques metallic powders are also sintered to form loose sponge. After successful sintering process, the sponge matrix is allowed to permeate with a known alloy by means of a vacuum method. The aforesaid methods develop the molds or tools that have the capabilities of firm tooling or more advanced. Nevertheless, this process involves the need of post processing operation for removing the porosity from the initial prototyped model in metal that also takes a percentage of lead time and expense (Badrinarayan and Barlow, 1994).

Another method available in literature for creating paper-based prototypes, based on the laminated object manufacturing (LOM) principle, which has been used for making metallic laminated tools and parts (Dickens, 1997). This process requires the bolting of metal sheets together in place of glueing or brazing. Therefore, there is an absence of complete adhesion between the layers making it unsuitable for injection molding processes involving liquid metal as material. Moreover, the LOM process has an intrinsic incapability of adaptive layer thickness and in addition suffers from excessive wastage of material (Bryden et al., 2004).

Figure 2.2 Metal mold used in injection molding (Dickens, 1997)

Furthermore, distinctive droplet producing processes have been developed that includes welding, thermal spraying and micro-casting for creating metallic tools to enhance the deposition eminence and to achieve the defined profile shape and size (Spencer et al., 1998). The other commonly investigated technique involves spraying of metallic particles that are highly energized (Krunakaran, 2004). This process is quite alike in its procedure

to ink jet printers. The method produces highly inflexible and thermally active tools of firm tooling abilities. Depending on the size of the developed metallic tool and their intricacy, hard tooling status can be attained. The major shortcomings of all the aforesaid methods are that accessibility of metals is limited as compared to the part produced by plastics materials. In addition, the components build up using metallic materials are expensive in contrast to plastic components.

Moreover, the machines use to develop metallic tools and parts can cost twofold times the amount of a substitute machine. An additional drawback is that metallic-based AM technologies have very limited build volumes, due to the restrictions in size of build volume and tool. Several other attempts have been made for producing the polymer rapid prototype as an injection mold tool. In the mid 90's, (Jacobs, 1996) a modified Stereolithography technique is implemented using epoxy solid style of rapid tooling. The epoxy's mold has the ability to run for more number of cycles as compared to traditional resin mold tool. The polymer molds are beneficial in the way that only a fraction of cost is incurred in their development in comparison to metal molds (Dickens, 1997). The initial phase of polymer mold involves the use of SLA resin which is very soft to resist the amount of heat at high temperature and pressure in the injection molding process (Dickens, 1997). Therefore, the dimensional tolerances of the parts developed are of great concern as the shape and dimensional sizes will change as the pressure and heat increases or decreases (Dawson, 1998).

Furthermore, one important study carried out by (Palmer & Colton, 2000) found that some shearing action will take place in mold and results in failing mainly depending on the directionality of the resin as mold cavity is filled in. The aforementioned problem in the SLA mold results in infeasibility in its use for industrial applications. During the last decade due to technological growth in developing new materials and polymers, it has now become quite easy to develop material of highest strength and low heat deflection properties. Due to the rapid advancement in materials development along with expansion of entry level (low cost) polymer-based-AM machines, the use of polymer rapid tool for developing injection molds would be more beneficial choice for batch and highly flexible production. Moreover, very few past studies have been performed to conform the use

polymer based rapid tooling. The present thesis will be the extension of the work on the suitability of polyjet printed rapid tooling mold.

2.2 Use of cooling channels and additive manufacturing techniques for improving part quality

With the improvement in manufacturing technology and intricate profile, the need for using the polymer injection molding is increasing day by day. Appropriate thermal management of injection molding tooling is important for accomplishing concurrent enhancements in production rate and part quality (Sachs et al., 2000). The cooling channels generally manage to flow out heat outside of the plastic mold. Generally, the conventional cooling channels are machined using a straight line approach. The conventional methods provide unpredictable results as the cooling throughout the mold are not reliable and accurate. Due to non-uniformity in cooling along different parts leads to extended cycle times, also uneven cooling can happen, warpage and scrap also produced. A significant reduction in the manufacture time of a plastic part collected to an improved product quality is expected with the use of conformal cooling channels (Dimitrov and Moammer, 2010). The cycle time and cooling time can be effectively reduced in an injection moulding by optimum utilization of cooling channels (Dalgarno and Stewart, 2001).

Although, a number of past research are available that deals with the design and modeling of conformal cooling channels in injection molding tooling, the concept of conform tooling design is not so deep-rooted. Conformal cooling channel shows a possible alternative with increasing acceptance (Hall and Krystofik, 2015). The schematic of traditional cooling channel and conformal cooling channel is shown in Figure 2.3. The major benefit of using conformal cooling channel is that it minimizes the cooling time and provides uniform cooling. In comparison to traditional straight cooling channels conformal one has proved to be more effective than the conventional cooling channels in terms of a rate of production and accuracy of molded parts. In addition, greater surface area for the cooling in conformal cooling channel as compared to the conventional straight-drilled cooling systems, resulting in unvarying circulation of heat. Some of the geometrical features needed in conformal cooling channel are very difficult to

manufacture using conventional machining or manufacturing techniques. For the aforementioned reasons rapid tooling (RT) techniques are best suited for the fabrication of conformal cooling channels.

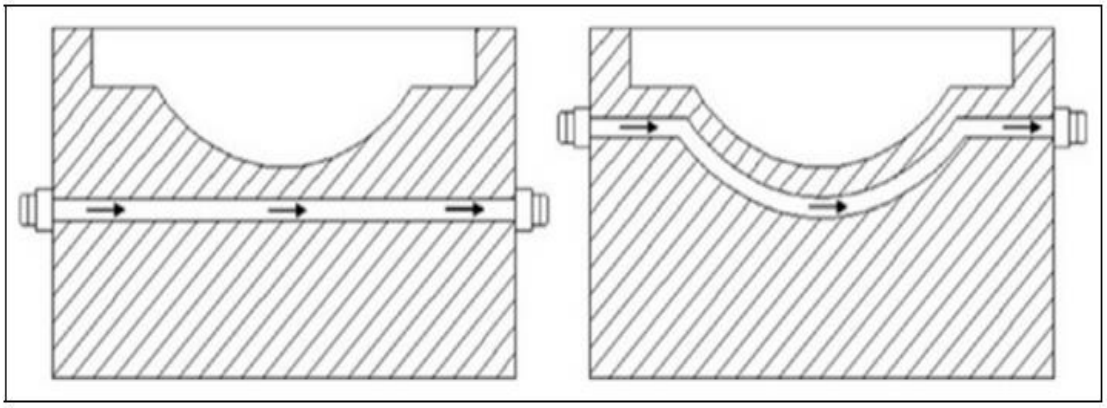

Figure 2.3 Conventional and Conformal cooling channel (Dimitrov and Moammer, 2010)

Past studies performed by different researchers depicts the advantages of the cooling channels in plastic injection molding. Au and Yu, (2007) in their study suggested a scaffolding design for conformal cooling channel fabrication. The study also performed the comparison of the mold cavity by incorporating and removing the scaffolding assembly using virtual simulation procedure (Figure 2.4). The Moldflow plastic insight interface was used and porous scaffolding structure was investigated. The results of the study concluded that the scaffold cooling structure provided improved cooling inside the mold cavity. One similar study (Hearunkyaji et al., 2014) was performed that applied the concept of fins for improving the efficiency of cooling channels. Furthermore similar studies were presented by Saifullah ABM and Masood, (2007), they performed simulation for comparison in between square cooling channel and straight cooling channels. Their results confirmed that the conformal cooling channel reduced the cycle time as well as cooling time significantly in contrast to traditional straight cooling channels. Another similar study conducted by Park and Dang, (2010) used Moldflow software for simulating the behavior of cooling channels with baffles for radiator grills using ABS polymer. After the significant analysis and comparison with straight cooling

channels, the baffled cooling channel provided much better temperature variation which is comes out to be significantly uniform.

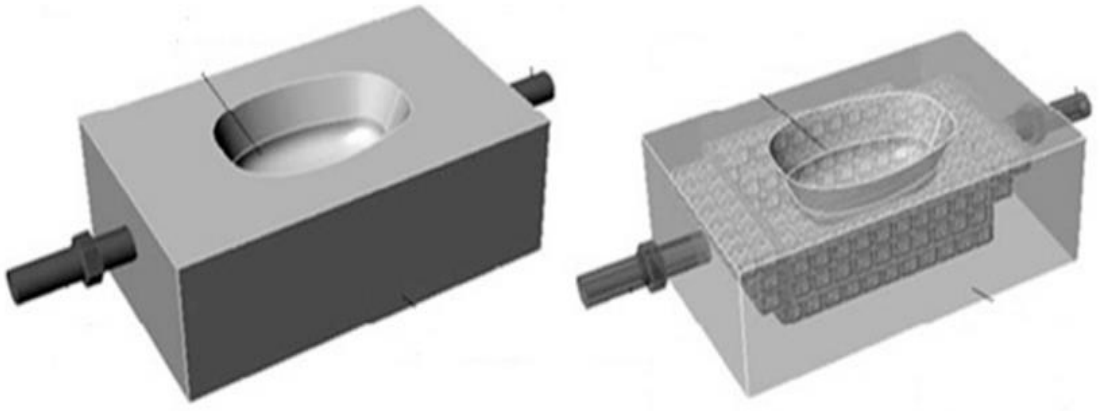

Figure 2.4 Mold cavities with and without cooling channel (Au and Yu, 2011)

In other comparable study, Altaf et al., (2011) investigated the effect of circular cooling channels in comparison to profiled cross-sectional cooling channel using ANSYS interface. The results showed that profiled cooling channel have improved heat flow of approximately 15 % in comparison to the simple one. One specific design was proposed by Au and Yu, (2011) with porous design that mainly based on the duality principle. The projected design delivers a more even cooling performance than the traditional conformal cooling channel design. One of the advanced studies on the design of conformal cooling channel was performed by Wang et al., (2011). They proposed an algorithm based on Voronoi diagram to modify the structure of conformal cooling channel. The conclusions indicated that the presented algorithm efficiently minimizes the cooling time and in addition maintains the temperature uniformity as well as linear and volumetric shrinkage.

Au and Yu (2014) further studied the effect of changing the distance between the mold cavities and cooling channel. This method helps in balancing the heat flow through the cooling channel starting from inlet to the outlet. One specific study performed by Khan et al., (2014) designed dissimilar types of cooling channels and studied their effects in Mold flow Advisor interface. The cooling channel used for the analysis includes conventional, series, parallel and cooling channel with additive cooling lines for cooling a food container. The results depicted that the most efficient cooling channel is the one using additive cooling and also it takes less cooling time. Similarly, Wang et al., (2015)

proposed a novel method for designing the structure of cooling channel in spiral form and then comparison is made with other cooling channels available in literature. It was found that the cooling time for spiral conformal cooling channel is less as compared to Voronoi diagram cooling channels. One of the recent study provided by Brooks and Bridgen (2016) provided the novel concept for conformal cooling channels in layers for providing high heat transfer rates and very low variation in temperature.

There are number of studies available that give the idea that for effective fabrication of complex conformal cooling channels rapid prototyping is a better alternative in comparison to traditional manufacturing techniques. The rapid prototyping techniques have been used for the development of metallic tool inserts as well as conformal cooling channels. Among them for the fabrication of complex-shaped conformal cooling channel, different RP processes are used. RP technology has been in use since the early 1980s. In 1991, various additive manufacturing processes were classified as powder-based, liquid-based and solid-based systems (Kruth, 1991). based on the different types of materials for part fabrication. Further, various AM processes and systems using a functional classification scheme has also been presented (William, 2014). The basic additive manufacturing processes are discussed in brief in the following sections;

2.3 Material Jetting process

Material jetting is similar to the inkjet printing in which droplets of wax or photopolymer material are selectively deposited through an orifice to build a 3D artefact (Calvert, 2001; Gans et al., 2004; Stucker, 2012). In material jetting process, material droplets are created using two different modes: (1) Continuous inkjet (CIJ) and (2) Drop on demand (DoD). Generally, CIJ systems are used at places where high printing speed is required. In contrast, DoD is used where higher accuracy along with small droplets are required (Vaezi et al., 2013). A lot of researches have been done in the field of direct ink jetting, which suggests that different parameters and factors are responsible for improving the quality of ink jetting process.

The material jetting process can successfully print with multi-materials as well as functionally graded materials (FGM). Several researchers have applied inkjet printers for printing structures using different FGM materials. In the late 90s, one dimensional FGM based structure was printed using a thin zirconia-alumina (Mott and Evans, 1999; Wang and Shaw 2006). Some of the studies reported modify the design and fabrication of commercial inkjet printers for printing multi-materials (Ibrahim et al., 2006; Xie et al., 2010). Researchers have used this process successfully for different applications such as wearable products (Yap and Yeong, 2014), functional lightweight honeycombs (Yap and Yeong, 2015) and scaffolds (Naing et al., 2005). Besides, the advantages discussed above, the material jetting process growth is clogged by the limited choice of materials such as wax and photopolymer are only commercially available materials. The other drawback is the part accuracy which is not as good as material extrusion process.

2.4 Directed Energy Deposition

Directed energy deposition (DED) process uses a focused thermal energy (laser beam) for creating a molten pool and subsequently fusing the material as it is being deposited (Kakinuma et al., 2016). The multi-axis table is rastered to develop the cross-section of each layer. The laser head is incremented upwards until all the desired cross-sectional slices of the part are created and 3D model is developed (see Figure 2.5). The process

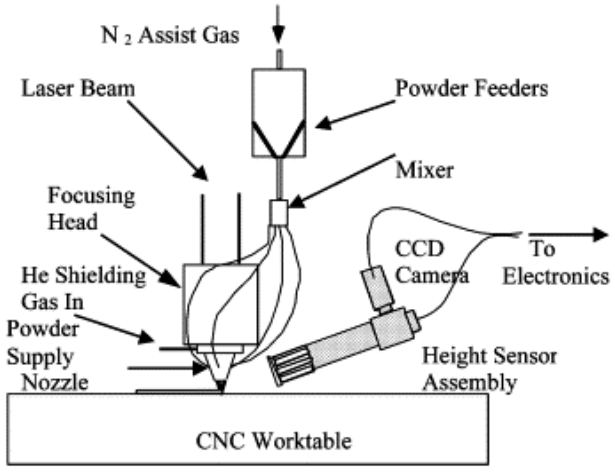

Figure 2.5 Schematic of Directed energy deposition (DED) process (Shin et al., 2003)

parameters responsible for improving the quality of DED process includes powder flow rate, laser diameter, scanning rate, laser power (Laeng et al., 2000). Recent research shows that a powder material characteristic is also a key factor in improving the quality of printed part (Kakinuma et al., 2016). The prime advantage of this process is its controlling ability in the microstructure of build parts. Another advantage of this process is in improving the tribological properties of printed parts by allowing coating to the surfaces (Wilson et al., 2013).

2.5 Powder Bed Fusion

Powder bed fusion process is one of the first commercialized AM processes. This process used a thermal source to melt and fuse the powder particles of metal, ceramics and polymers into the desired patterns (Stucker, 2012). Some of the most popular powder bed fusion systems known are Selective Laser Sintering (SLS), Selective Laser Melting (SLM) and Electron Beam Melting (EBM). The SLS and SLM system employs laser source while EBM uses a scanned electron beam (Kruth et al., 2005; Buchbinder et al., 2011; Murr et al., 2012). Several studies have been reported for determining the process parameters (over 50) characterizing the bed fusion processes. The process parameter can be categorized into mainly four groups namely, laser related, scan related, temperature related and powder related parameters.

2.6 Binder Jetting

In the early 1990s, binder jetting methods based on ink jet technology was introduced in Massachusetts Institute of Technology (MIT) and commercialized by Z Corp. and Ex one. The process deals with printing a binder in to powder bed to build a structure. The binder droplet helps in sticking the powder material together providing desire shape to the part. Once this step is complete, it is followed by lowering the powder bed and new layer is deposited and again the above process is repeated (Sachs et al., 1992). A wide choice of materials are processed through binder jetting process such as metals (Williams et al., 2010), foundry sand (Snelling et al., 2013), ceramics (Yoo et al., 1993), and polymers (Lam et al., 2002; Leong et al., 2003; Lee et al., 2005; Tay et al., 2007).

Distinguished researchers have worked on binder jetting process involving different applications. One of the main applications include scaffold development (Sherwood et al., 2002), The prime significance of this process is fast build time of parts as very less amount of material is dispensed through orifice. Additionally, the combination of metal powder and additive in binder enables material composition not easily achieved by other AM processes (Gibson et al., 2010). However, the parts printed employing the bender jetting process have inferior accuracy and poor surface finish as compared to parts of material jetting process.

2.7 Vat photopolymerization

In the early 80s, C. Hull introduced first AM system commercially based on SLA process. SLA is the main photopolymer method in which ultraviolet laser is used to polymerize the UV curable resign selectively, layer by layer (Cooper, 2001; Noorani, 2006) as shown in Figure 2.6. Most of the research found for this process involves the processing of ceramics (Chartier et al., 2008; Bian et al., 2012; Chopra et al., 2012). The process of vat photopolymerization is widely used in different applications like dental fillings, ear hearing aids and scaffolds (Bartolo, 2011; Sirrine et al., 2015).

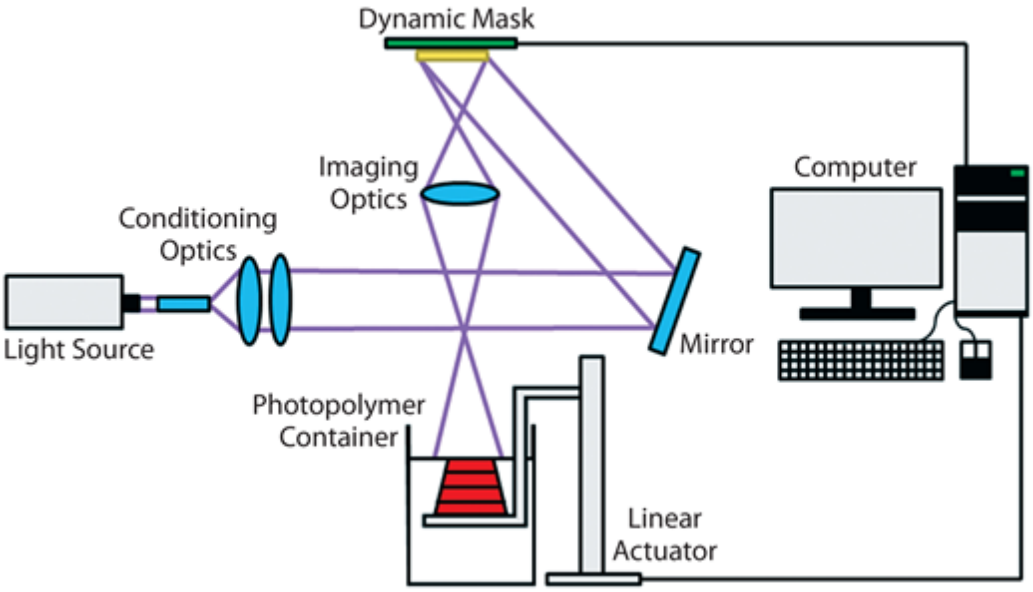

Figure 2.6 Schematic of Vat photopolymerization process (Chartrain et al., 2016)

The prime advantage of this process is its high resolution and ability to fabricate complex objects. However, main limitation of this process is its inherency to use only photopolymers. Further, some of the more problems reported by different studies includes errors caused by overcuring, scanned line shape, trapped volumes and shadowing obstruction of earlier build layers (Kim et al., 2011; Wong and Hernandez, 2012; Choi et al., 2011).

2.8 Sheet Lamination

The manufacture of sheet lamination additives is the process of bonding sheets of material to form an object. There are two systems that have been commercialized are Laminated Object Manufacturing (LOM) and Ultrasonic Consolidation (UC) (Mueller and Kochan, 1999; Ram et al; 2007). Usually, the sheet lamination AM processes was used to fabricate metal parts stacking, cutting, and gluing outlined metallic laminates. In the late 1990, few studies reported the first laminated tooling sheets for sheet metal fabrication (Himmer et al., 1999). Several researchers have tried to enhance the laminated bonding (Wimpenny et al., 2003; Janaki Ram et al., 2006) with reduced stair step effects (Walcyzk and Yoo, 2009).

2.9 Material Extrusion

AM machines based on material extrusion deposit material through nozzle by pressure created using tractor-feed system in continuous layer form to fabricate objects. Fused deposition modeling (FDM) is among the most commonly used AM process (Wohlers, 2011). The FDM based printer was developed by Stratasys in 1988 that produced sliced layers by extruding molten thermoplastic material (Bernard and Fischer, 2002; Noorani, 2006; Kai et al., 2010). FDM process used amorphous thermoplastics for part manufacturing having acrylonitrile butadiene styrene (ABS) being the most common. The other materials available in market for FDM process are poly lactic acid (PLA), polyimide, and polyphenylsulfone.

The gradual expiring of a few valuable patents in 2009 offers a level playing field for the technology innovators to incubate, alter or harness the FDM process (Gridlogics,

2014). FDM based AM process schematic is shown in Figure 2.7. In FDM process, material is melted and flow through liquefier head and passed through the nozzle. Further, the material is deposited layer by layer as shown in below Figure 2.7. The FDM process is clean, safe, and highly automatic and also produces minimum waste. Other FDM advantages include easiness of support removal, short cycle time, and easy integration with CAD software. These features make it appropriate for variety of applications (Chua et al., 2010; Ingole et al., 2009; Elliot et al., 2013). Lately, a new trend in FDM has emerged, which can be referred to as entry level additive manufacturing (ELAM) that is comparatively inexpensive, desktop sized and usually have an open chamber (Lotz et al., 2012).

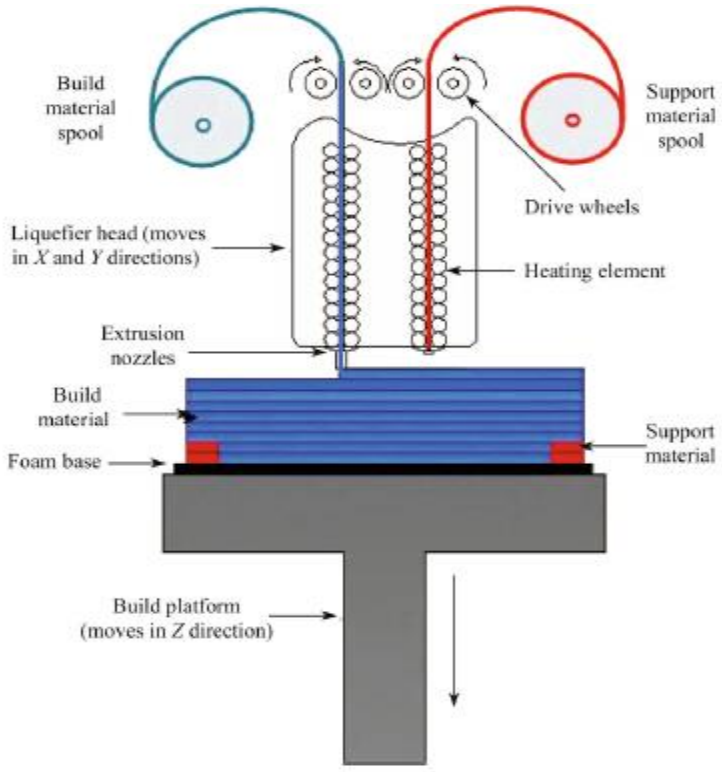

Figure 2.7 Schematic diagram of FDM based AM process

Among the above AM technologies, mainly the powder based AM process are only used. One study performed by Donnchadha BO and Tansey (2003) used SLS method for producing tool inserts, which helped in reducing the lead time and incurred cost. Directed

metal deposition is used in one specific study for reducing the production cycle time as well as without affecting the part quality (Davis et al., 2003). One important study by MIT reveals that 3D printing based on FDM principle was used to create mold with conformal cooling channel which was further used in injection molding machine (Xu et al., 2001). In the recent study of Eiamsa-Ard and Wannissorn (2015), the authors applied metal deposition method for creating mold along with the conformal cooling channel. This thesis deals with the use of Polyjet printed mold along with conformal cooling channel in place of metal mold in injection molding application. The Polyjet printer was based on FDM principle which was very rarely used till date for mold production.

2.10 Injection molding process parameter selection and optimization-The plastic injections molding (PIM) processes are widely used for producing intricate shaped plastic parts with distinctive geometric features and have shorter production cycles. The PIM process is a repeated one which consists of filling and packing, cooling and ejection (Noble et al., 2014). Injection molding helps in producing products for computer, communication, and consumer electronic (3C) such as portable computers and cell phones. The 3C products are generally thin, light, short and small (Chiang et al., 2007, Chen et al., 2009). However, with the increasing demand of more complex products having less wall thickness, the PIM process is prone to face more challenging tasks (Ozcelik and Erzurumlu, 2005). Consequently, the quality of the parts produced using PIM process is affected by the appropriate selection of the various process parameters and the mold design (Liao et al., 2004, Chiang, 2007). In contrast, the inappropriate process parameter values led to produce part defects, resulting in long lead times and high cost (Hasan et al., 2007).

Warpage and Shrinkage are one of the most imperative drawbacks used to measure the quality of injection molded part. Previous studies indicate that shrinkage and warpage are mostly related to injection molding process parameters. The influence of packaging parameters and gate geometry on the final part has been studied by Leo and Cuvelliez (1996) and it was found that thinner gates obtain more uniform shrinkage in processes with the same packing pressure. Galantucci and Spina (2003) applied double skin model for investigating the warpage defect and further concluded that melt temperature was among the most influencing factor for minimizing warpage. Huang and

Tai (2001) in their study applied computer simulation and experiment for analyzing the factor affecting warpage in a thin shell injection molded components. Tang et al. (2007) applied Taguchi method for minimizing the warpage in the design of improved plastic injection mold. Similarly, Taguchi and ANOVA are used in a study for obtaining optimal shrinkage injection molding conditions (Park and Ahn, 2004). The results suggested that optimized parameter reduces shrinkage by 1.244 % and 0.937 % for Polypropylene (PP) and Polystyrene (PS), respectively.

Similarly, Park and Dang (2012) in their study suggests that runner and cooling channel geometry can improve the final quality of products. One specific study was found for minimizing the warpage in thin shell plastic parts by employing the response surface methodology (RSM) and genetic algorithm (GA). Hakimian and Sulong (2012) in their study applied Taguchi method to analyze the shrinkage and warpage in micro gears of polymer composites. Choi and Im (1999) found that residual stress is an important factor that affects the shrinkage and warpage defect in injection molded components. Liao et al., (2004) in their study provided optimum conditions for minimizing shrinkage and warpage problems. The cyclone scanner and polyworks software was used for determining the shrinkage and warpage problem. The packing pressure was found to be the most influencing factors. Kikuchi and Koyoma (1996) have applied finite element method for studying the relation among warpage, part thickness and anisotropy.

In a recent study, Othman et al., (2017) also optimizes the shrinkage and warpage in their study for composite material. In addition, effects of different process parameters are discussed in recent studies of Mohan et al., (2017). One recent study used simulation based methods for prediction of shrinkage and warpage in the injection molding process (Zwicke et al., 2017). Dan and Bistany (2000) applied RSM for examining the sink marks in injection molding lab experiments. The study includes determining the effect of different injection molding parameters like melt temperature, mould temperature, injection rate cooling time, pack time, pack pressure on final part quality. Beryllium copper as mold material was found to be effective and efficient in minimizing the sink marks.

Some literatures are also available which mainly focuses on relating the polymer microstructure to molding ability (Crawford, 1998; Tadmor and Gogos, 2007). However, it is not in scope of the present work. Moreover, several studies found have used response surface methodology (RSM) individually or integrating with genetic algorithm (GA) for determining the interaction and relationship among factors and process parameters (Kurtaran and Erzurumlu, 2006; Pathak and Singh, 2017). Similar studies have been found that uses neural model (Lin, 2002), modified complex method (Li and Li, 2008), grey-fuzzy logic for thin shell feature (Chiang and Chang, 2006) for optimization of warpage in different thermoplastic parts. The fishbone diagram for determining the effect of different injection molding parameters on final part quality is shown in Figure 2.9.

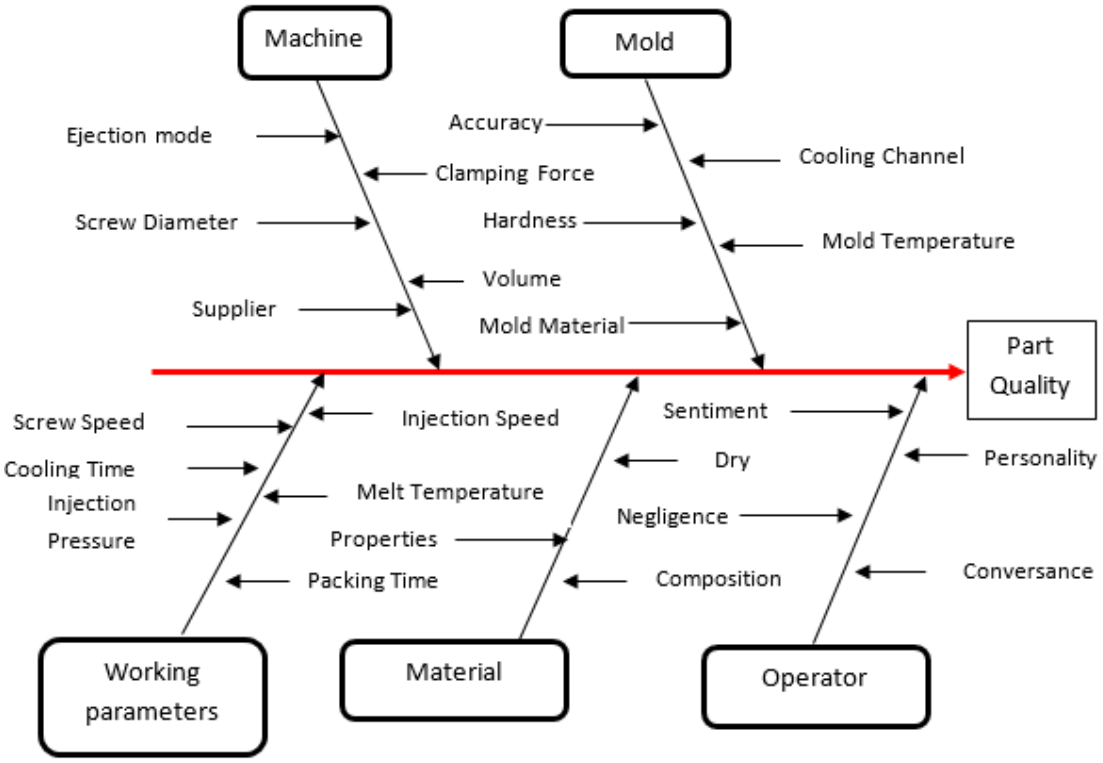

Figure 2.8 Fishbone diagram for injection molding process parameters (Lin, 2002)

2.12 Advances in 3D scanning systems for quality inspection

From the past few years, the use of non-contact scanning devices is gaining an increasing interest in reverse engineering (RE) applications for data acquisition of real-world free form shapes, in addition to inspection purposes. These devices provide masses of accurate three-dimensional point cloud data within very less time making it an important alternative for measurement and metrology in industrial applications. The contactless scanning devices provides raw and unorganized point cloud data in the case of intricate free-form shapes like warped surfaces. The contactless scanning systems works on specific principles that includes time-of-flight, triangulation, structured light and photogrammetry (Varady et al., 1997; Schwenke et. al., 2002). Wang et al., (1999) developed a contactless scanning system having 4 axis for data acquisition. Furthermore, several researchers have developed scanning devices based on laser diode and (Charged Couple Device) CCD sensor for data acquisition of the objects surface using laser stripes (Yau et al., 2000; Chang and Chang, 2002). Chang and Chang developed an integrated approach for data capturing by using touch probe as well as laser scanner which are mounted on a CMM.

The non-contact devices are classified as active and passive system by Isgro et al., (2005). Active systems works on using light patterns on any scene to spot its position for measurement. Passive systems, on the other hand, use naturally occurring images produced by reflected light from a natural or artificial source, and they do not use any other type of energy to help the sensors. At the present time, these contactless scanning systems have get hold of good level of confidence for RE applications and laser scanners mainly are engaged for part inspection in industrial applications (Lin et al., 2010; Jorge et al., 2011; Xu et al., 2011; Pathak et al., 2016).

Past literature provides the information about use of coordinate measuring machines (CMMs) for data acquisition, accurate shape, and also quality inspection to conform to the GD&T specifications (Gao et al., 2006; Martinez et al., 2010). Most often, the probe CMMs are used to acquire point data from basic features such as holes, slits, steps, etc., since these features require only a few samples to determine their identification. However, the data collection process with CMM is substantially slow,

since the probe must make contact at each point where a scan is to be performed. In addition, some studies have shown that the planning of CMM data acquisition is a difficult and complex task, as complicated free-form surfaces require higher sample points (Elkott et al., 2002).

With increasing free-form in the industry, whether for aesthetic or functional purposes, data collection becomes an important task for accurate inspection. Since, the parts having free-form shape are costlier and plays an imperative role in final assembly, the complete part data measurement is imperious for effective functionalities (Curles, 1997; Lindau et al., 2013). Moreover, the CMM has ineffectiveness in free-form shape measurement. In addition, the contactless scanners have ability of obtaining millions of point cloud in short duration of time, along with the improved precision in recent times. For all these reasons, the non-contact 3D scanners be used for quality control of industrial components. A general schematic of such a non-contact 3D scanning device is shown in Figure 2.8.

Since, the usages of laser scanners are becoming progressively common in other industrial fields also, it is essential to understand wisely different factors that can be chosen to get the best results. Besides the several improvements in accuracy control of 3D scanners, there are some other factors that influences the overall quality and accuracy of scanned point data (Lee and Chang, 2006; Ali et al., 2006; Mian et al., 2015)

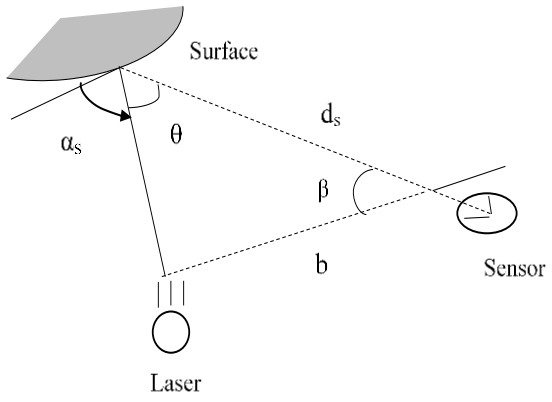

Figure 2.9 Laser triangulation principle (Curles, 1997), (α_s is incident scanning angle) (2001)

predicted digitization error considering the effect of scan depth and projected angle on measurement accuracy. The prediction model developed calculates the systematic error having maximum deviation of 25 μm. Shuo and Dar has developed a laser scanning system and suggested in their study that error compensation of the inclination angle data can be used to improve the precision of the system. Mian et al., (2015) performed experimental study and investigated the influence of different scanning factors on the final accuracy of the reverse engineered model. The scanning parameters they considered include laser power, shutter time, measuring field and threshold for reflection. It was found that the laser power and shutter time are inversely related to the final accuracy of model. Threshold for reflection has major influence on the surface accuracy.

Past studies have suggested countless different parameters that are either related to scanning parameters or acquisition instrument whereas current study proposes specific parameters for the same process. Some of the factors that are associated with acquisition device includes scanner resolution (Liang et al., 2016), field of view (Mian et al., 2015) and accuracy (Yin et al., 2014). Ghazali et al., (2011) reveal that scanner resolution significantly affects the accuracy of points captured by comparison of data points captured using 3D scanner with GPS observation. Subsequently, the factors addressed related to scanning factors includes laser power, shutter time and threshold for reflection (Ali et al., 2008). Their study found that the most important factor which affect the quality of point data acquired is laser power. Gestel et al., (2009) proposed a test method for laser scanners based on a planar test artifact. The study also addresses the systematic error evaluation which is based on in-plane, out-of-plane angle and scan depth effect. One similar study was reported, which investigated the influence of range and surface reflectance as the scanning parameters on the data acquisition (Tornincasa and Vezzetti, 2005). In addition, some studies have indicated that the ambient light conditions and the properties of the scanned object are few other factors that are responsible for measurement accuracy. In the research of Lemes and Uzunovic (2009), the influence of ambient lighting on the quality of scanned data has been reported. An empirical relationship was established between the color of the surface of the object, the ambient illumination, and the quality of the laser scan. Similarly, Blanco et al. (2008) in their study evaluates the effect of ambient light on the scanning process. It has been found that

different type of light produce different results which is not uniform. Further, Voisin et al. (2007) in their study shows the influence of illumination (ambient light) on structured light based scanner performance. It was observed that the ambient light more or less affects the range accuracy depending on the original color.

The laser scanning and the touch probe CMM comparative test shows that the ultimate accuracy of the part to be scanned depends on the scanning strategy. The study suggested that single-head alignment is preferable to multi-head alignment during scanning (Martinez et al., 2010). Few specific studies are based on the study of the effects of laser intensity that depends on the roughness of the surface. This study suggests that the intensity of the laser is directly related to the machining process and further an extensive range of intensities for maximum data acquisition were suggested (Cuesta et al., 2009). Further, Kaasalainen et al., (2010) pointed that target object moisture has an effect on the laser scanning performance and its output. In a continuing effort (Kaasalainen et al., 2011), effect of two important parameters such as incidence angle and range on the intensity measurement and radiometric calibration for different Terrestrial laser scanner (TLS) scanners were studied for establishing a correction scheme. In addition, few studies have identified methods for collecting data from transparent and glossy surfaces. They suggested that the provision of coating sprays on the surface would be the solution to such objects. Further, it was clarified from the result that only a variation of the actual surface area of 5-15 μm was obtained is added in actual surface (Mahmuda et al., 2011). Pesci and Teza, (2008) in their study evaluated the influence of surface irregularities (roughness) on the point data provided by laser scanning.

Most of the previous studies consider various factors of the contactless scanning system to obtain a precisely scanned surface. However, attempts to study the influence of scanned surface topology and local geometry have rarely been investigated in the literature (Xi et al., 2001; Shiou and Ali, 2005; Uzunovic and Lemes, 2010; Mian et al., 2015). The effects of relationship among object, image, and the error of the measuring device have been studied (Xi and Shu, 1999). The study shows an absolute error with respect to the nonlinear relationship between the precalibrating factors. This preceding error was also discussed in (Lee et al., 2002), and it was established that distance between laser head and object lead to out-of-plane error.

2.13 Discussion on mechanical and physical properties of mold in injection molding

Additive manufacturing since its inception has come a long way from automobile to biomedical applications. Nowadays, one of the significant applications of additive manufacturing technology is the use in rapid tooling. From the past research, it is now clear those RT tools, as injection molds can be used to produce conventional and practical samples for small or sometimes large-batch production (Pham et al., 1998; Hilton and Jacobs, 2000; Chua et al., 2010). The selection of mold material and their processing have an influence on how it executes during its use throughout its life cycle in injection molding process (Martinez et al., 2011). The different thermal properties of mould materials have significant effect on the mechanical properties of the polymer parts produced in the injection molding.

In 2007, Sadabadi and Ghasemi examined various injection molding process parameters that can affect the mechanical properties in polystyrene composite mold. In another similar study, Yang (2006) studied the influence of different injection molding conditions on the mechanical and tribological behavior of poly corbonate material. In early 2000, Guerrica et al., (2001) performed experiments for determining the effect of melt temperature, injection rate and screw rotation on the mechanical properties of the plastic injection molding parts. In one similar study, Kenig et al., (2001) applied regression analysis and neural network for investigating the effect on the mechanical properties of injection mold parts. In 2000, Bociaga performed a specific study and found that the mold temperature has significant impact on the mechanical and thermal properties of the high density poly ethylene (HDPE) mold. In addition, the effect of injection velocity has also been discussed and reported.

Nagaoka et al., (2005) studied the mechanical behavior of polypropylene material as mold in injection molding. Furthermore, Shi (2008) study investigated the effect on mechanical properties of polypropylene material by optimizing injection molding process parameters using neural network. Tang et al., (2007) found the effect of process parameters on the mechanical properties of two aluminium composites. The experimental trials were performed using Taguchi method and linear relation was found using regression analysis. Ozcelik et al., (2010) observed the influence of melt temperature,

packing pressure on the mechanical properties of ABS polymer material in their study. The mechanical properties include flexural modulus, impact strength and tensile strength. In a similar study performed by Chien et al., (2004) on the examination of mechanical properties and molding behavior of polypropylene parts, it was found that with increase in foaming content from 0.8 to 1.6 % the mechanical properties reduced significantly. Park and Young (2009) studied the effect of mold temperature on different mechanical properties of polyether polymer.

Lee et al. (2007) investigated the compressive strength in layered parts as a function of build direction and determined that the compressive strength is greater for the axial FDM specimens than for the transverse. Panda et al., (2006) in their study performed investigation by measuring the influence of process parameters on different part characteristics that includes surface roughness, dimensional and mechanical strengths. Further, several researchers have studied the effect of processing conditions on the morphological structure that in turn can affect the physical and dimensional characteristics of the mold (Michael and Menges, 1989). Polosky et al. (1998) inspected the impact and tensile strength for polycarbonate and nylon 6, 6 molded in a SL tool and a steel tool. The authors found a 10 % variance in tensile strength between SL and steel tools and the stress levels were usually lesser in the parts from the SL tool due to the sluggish cooling rate permissible relaxation of the parts.

Mohd et al., (2016) in their study determine the tensile strength and dimensional variation of ABS polymer when mixed according to the loading ratio. Their study concluded that high injection pressure and melting temperature will produces less shrinkage. In a similar study, Mehat and Kamaruddin (2010) applied Taguchi and ANOVA analysis to confirm that injection timing is the most significant factor that affects the flexural modulus of the injection molded parts. Seldon (2004) also investigates the effect of molding parameters on mechanical properties on injection mold for different material using experimental design. In a recent study by Farotti and Natalini (2017), process parameters effect in injection molding is considered by determining the change in the mechanical properties of polypropylene polymer. Their study concluded that holding pressure and mold temperature have significant effect on the mechanical properties of mold.

Table 2.1 Summary of important literature for Mechanical and physical properties of mold

Investigator	Year	Properties	Material
Bociaga	2000	Mechanical and thermal behavior	High density poly ethylene (HDPE)
Nagaoka et al	2005	Mechanical behavior	Polypropylene
Yang	2006	Mechanical and tribological behavior	Polycarbonate
Shi	2008	Mechanical behavior	Polypropylene
Tang et al.	2007	Mechanical behavior	aluminium composites
Ozcelik et al.	2010	flexural modulus, impact strength and tensile strength	ABS polymer
Chien et al.	2004	mechanical properties and molding behavior	Polypropylene
Park and Young	2009	mechanical properties	Polyether polymer
Mohd. Et al.	2016	tensile strength and dimensional variation	ABS
Farotti and Natalini	2017	Mechanical behavior	Polypropylene

2.14 The Knowledge Gap in Earlier Investigations

This exhaustive literature review, presented above, shows the following knowledge gap that assisted to define the objectives of this research:

1. Though a lot of research work has been done on metallic mold. Due to many drawbacks in metallic mold like heavy weight, high cost, rusting and poor surface finish, difficult machining of metallic mold, application of possibility of employability of rapid tooling mold need to be investigates.
2. Several studies have been reported to improve parts quality in terms of volume shrinkage and warpage and to optimize important parameters of injection molding. In addition, some of the reported literature used nature inspired algorithms such as PSO and its modifications to predict optimal parameters.

3. Earlier the dimensional accuracy of developed component from mold is investigated with vernier caliper or CMM. That makes the inspection process slow and inaccurate, that require adequate skill and expertise. Also, very view literature is available presenting the inspection planning for advance manufacturing process i.e. benchmark part and complex feature parts especially developed by Rapid tooling mold.
4. As far as quality of the part is concerned, most of the work reported is using difficult mathematical approximations, which requires lot of skill and expertise, but only very few of them considered software based conversion. None of them have provided the critical parameters, there factors value and the path for accurate product development.
5. None of literature has proposed for inspection of quality of any benchmark part and complex feature parts developed by rapid tooling mold and evaluation of mold strength, to perform more experiment through rapid tooling mold insert.
6. No work has been proposed yet for the Optimization of warpage and shrinkage of rapid tooling molded thin wall component using modified particle swarm optimization for various injection molding materials.

2.15 Research objectives

The objectives of this research work are outlined as follows:

1. Investigate the possibilities of employing rapid tooling mold inserts in place of metallic mold for injection molding.
2. Development of mathematical model for standard benchmark features to reduce the defects (volumetric shrinkage and warpage) of parts developed by RP mold using Moldflow simulation software.
3. Confirmation and validation of dimensional accuracy of test specimen developed by RP mold using 3D scanner (COMET plus and INSPECT plus software)
4. Optimization of warpage and shrinkage of rapid tooling molded thin wall component using modified particle swarm optimization.
5. Analyses the effects of all the process parameters on the performances of shrinkage and warpage obtained by mathematical models. Find the optimum

value of process parameters, by the analytical model using regression analysis and improve the optimum values by a recently developed modified particle swarm optimization algorithm.

6. Comparison of outcomes (Volumetric shrinkage and warpage) with conventional molds using 3D Scanner and previous literature.

2.16 Chapter summary

The chapter reviews the literature available on different rapid tooling techniques used in production, additive manufacturing (AM) techniques, injection molding process parameter selection, optimization and advances in 3D scanning systems for quality inspection. Furthermore, the discussion on mechanical and physical properties of additive manufacturing mold is also been performed. Based on literature discussed, the research gap in the past research is determined and based on that objectives of the present work are determined.

CHAPTER- 3

MATERIALS AND METHODS

The research work presented in this chapter is focused on investigating initial feasibility on determining whether room temperature vulcanizing (RTV) and polymer rapid tool (PRT) can be used as functional injection mold tooling. The main objective of the research was to determine whether the RTV and PRT could mold a set of distinctive features for a specific dimension within the usual tolerance limits and do this repeatedly. Initially, simple geometric shapes were formed and studied, which represent commonly molded features. This was followed by the molding of more complex and commercially available plastic components.

3.1 Investigations of Room Temperature Vulcanizing (RTV) soft tooling as functional injection Molding

Rapid Prototyping is being recognized worldwide by industries for its potential in saving on process time and cost effectively. Rapid Tooling helps rapid prototyping grow beyond its conventional "Feel & Fit" status to "Feel –Fit – Function" status and increasingly becoming popular in product development sector. But it's potential for short or normal production run is still not realized. One alternative is to use silicon molds for replicating (multiplying) sufficient number of models. As this appends an additional stage in the tooling process it is evident to estimate and predict the dimensional deviation from RP model and its wax replica. This work investigates the dimensional accuracy of the wax replicas generated out of component molded on rapid prototyping machine. Further, to study the influence of process a 3 factor 4 level (L16) orthogonal array experiment is designed as per Taguchi method and result is reported.

3.2 Experimental set up

The fused deposition modeling based native R3D2 ELAM machine was used for modeling the pattern (Shrinkage Stepped bar). The build material used was ABS wires of

1.7mm diameter size. RTV molds were planned and made with Mold Max 60 Part A & Part B supplied by ***smooth-on*** products distributors Mumbai. A wax injector 2.5 Kg was used for injecting the wax into the silicon rubber molds. The respective wax replicas dimensions were recorded for calculating dimensional deviations and ANOVA.

3.2.1 Selection of Test pattern (Model)

In view to win the acceptance of precision casting industries, it was decided to use the most popular test pattern used by the industry, hence stepped shrink test bar was selected. The important dimensions to be observed in X, Y and Z directions and a cylindrical hole were included for dimensional deviation study, as in the figure 3.1. It is a good choice for its shape, size, manufacturability etc.

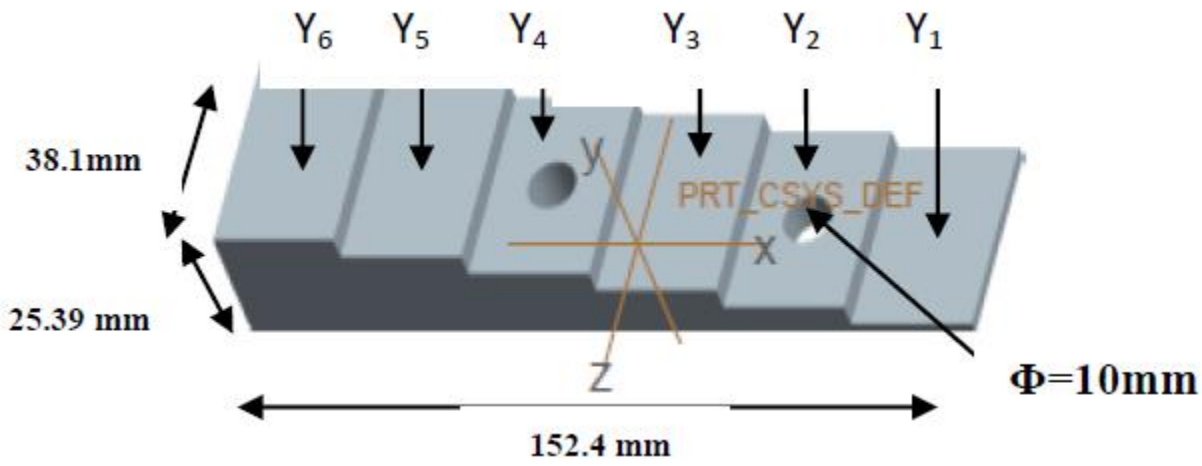

Figure 3.1 Stepped bar pattern developed for additive manufacturing

3.2.2 Entry Level Additive Manufacturing (ELAM) for generation of RP pattern-

The use of affordable AM machines is now locating its place in education where students can feel, fit and sense the fabricated objects. One of such low-cost ELAM machines was used as shown in Figure 3.2. One of the advantages of ELAM systems is that they can use open source slicing software such as Slic3r, Cura, kisslicer. Another advantage is that these machines come with a single nozzle and the support material can be extruded through the same nozzle in a sparse manner. This cuts the cost of machine as wide choice of feedstock filaments are possible. It comprises a horizontally translating (x-y) heated bed platform with a functional build area of 200 mm x 220 mm and vertical translating

(z-direction) extruder attached with a nozzle. The maximum build height of the machine is 200 mm. The extrusion process is governed by a stepper motor with a feed of 1.7 mm diameter ABS filament into a heated 0.15 mm diameter nozzle. The R3D2 ELAM machine used to construct parts with a layer thickness of 0.075 mm. The process of printing the parts on R3D2 ELAM system begins with the CAD model saved in STL format. The surface defining the design must not contain any discontinuity (non-manifold edge). The part could be re-oriented and repaired for optimum print quality using Netfabb and MeshMixer. Slic3r software was used to slice the part with suitable layer thickness and for adjusting other print parameters before G-code generated. Initially, the extruder head and printer bed were heated to a predefined temp and then extruder head begins to extrude molten plastic to build prototype taking shape from bottom to top layer by layer. Acetone-ABS mixture is used on printer bed for effective part adherence. Acetone solution offers a satisfactory adhesion of the part on printer bed during the printing process.

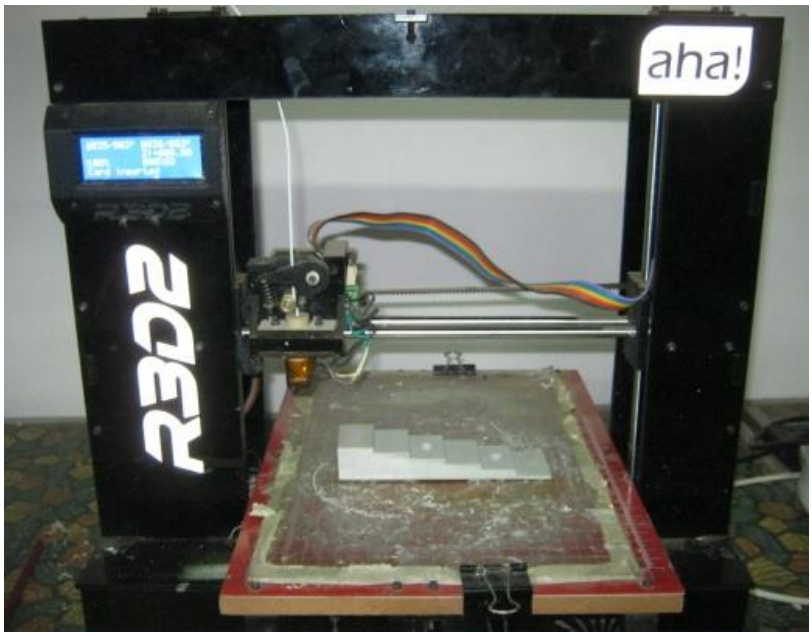

Figure 3.2 Schematic of R3D2 entry-level AM Printer

3.2.3 Selection of RTV Silicon compound

Mold Max 60 RTV compounds were selected for its relatively high shore hardness (60),low linear shrinkage .0015 in/in, high mixed viscosity (20,000cps),thermal conduc-

tivity (0.347W/mK), pot life (40min),Cure time(24hrs) etc. The constituents for RTV were shown below in Table 3.1.

Table 3.1 Constituent of RTV mold and Si rubber for soft tooling

Mold star series	Mold star 15 slow
Platinum Si rubber	Platinum Si rubber
Polyorganosiloxanes	Polyorganosiloxanes (Mixed)
Amorphous silic	Petroleum Distilate
Platinum Silixane	Mineral filler
Mineral filler	-
Si rubber compound	Polyosiloxanes
Triglyceride sand rubber	Carlinoria Proposition
Butganotin	-

Figure 3.3 Si rubbers for RTV soft tooling

3.3 Methodology to prepare RTV silicon rubber mold –

Mix required amount of liquid rubber compound into mixing container (1A:1B) by volume thoroughly. Pour over prepared model (RP pattern) and let it cure to a solid up to 24 hrs. After solidification the bottom part will be prepared known as Drag. Similarly make top part of mold known as Cope.

3.3.1 RTV Mould preparation-The mould box consist of cope and drag as in the Figure 3.4 (b). Required weight of the compound A and B are mixed in a jar and bottom mould was made. After 24 hrs of curing time top mould was also made. Mould alignment and guide pins are very important and were taken care. The pattern was removed and mould was ready for filling. It is recommended to use a suitable release agent to perform a compatibility test between the rubber compound and the plastic RP pattern. Just observe whether the rubber becomes gummy when smearing on a small uncritical area of the pattern. Use protective wear (nasal mask, sleeves, gloves, goggles). Care! If the mixture is spilled, the work area to be damaged.

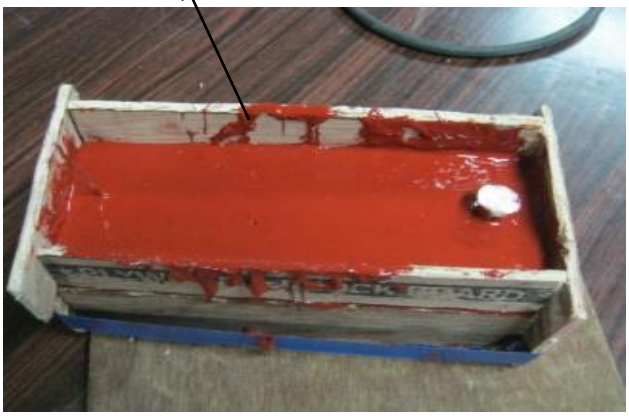

Figure 3.4 (a) RTV silicon rubber mold

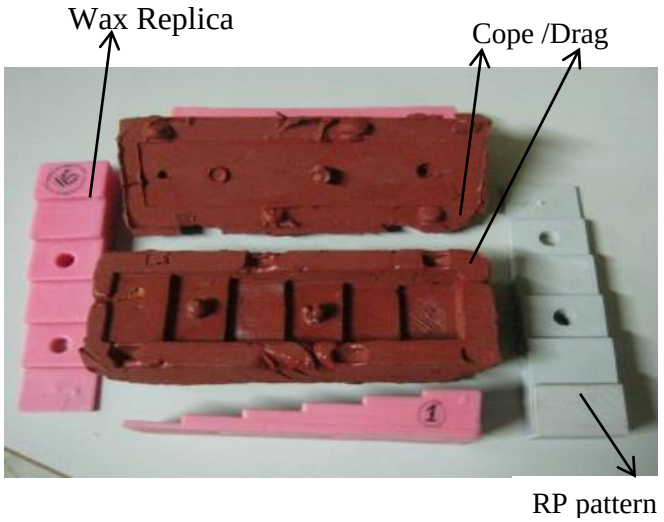

Figure 3.4 (b) Mold and Patterns

3.4 Pattern by Wax injection - It was decided to use a wax injector of 2.5 Kg, with temperature (range 30-150^{o}C PID controller) and pressure (range 0- 2Kg/cm^{2}) control provisions. Refer Figure 3.5 adequate number of runs were performed before getting the injector stabilized. Further trial runs were also tried to understand the process parameters suitable for the proposed test bar. Then the factors and levels were decided to perform design of experiments. Sixteen combinations were tried and wax replicas were identified as 1 to 16.

Figure 3.5 vacuum wax injection machines

3.5 Process parameters for the production of wax patterns

To identify the process parameters that affect the quality of the investment cast parts, an Ishikawa Cause and Effect diagram was created as shown in Figure 3.6. The dimensional stability of the wax pattern produced by the IC process may be affected by the following process parameters, as presented in the Ishikawa Cause Effect Chart.

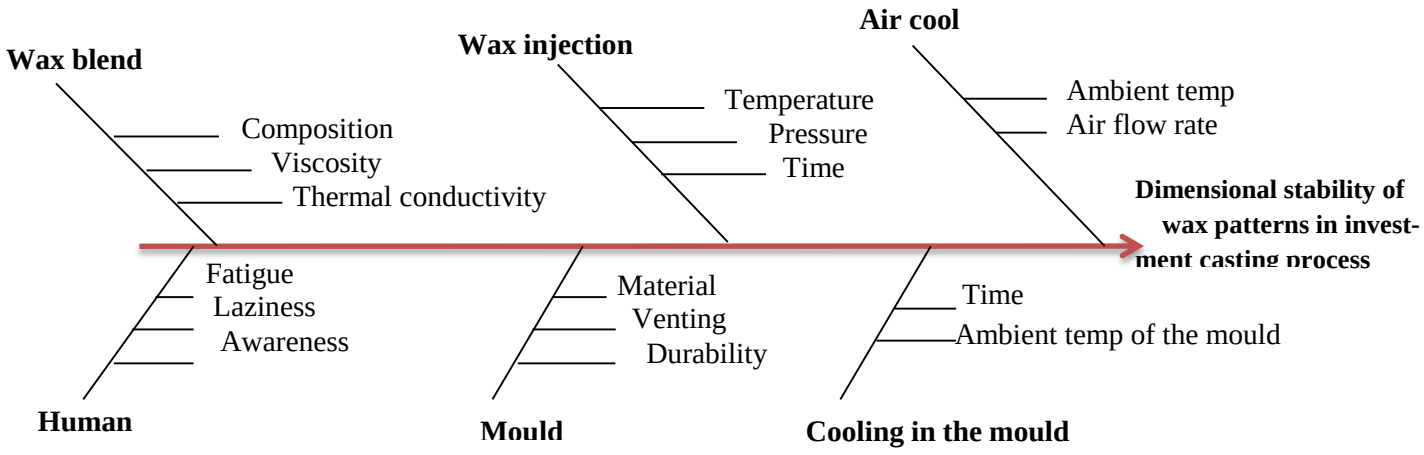

Figure 3.6 Ishikawa cause effect chart for wax pattern

Variables for Wax mixture – composition includes different waxes and additives, viscosity, thermal conductivity.

Variables for Wax injection – injection temperature, injection pressure, injection time.

Mould Variables for inside cooling – cooling time, ambient temperature of the mould.

Air cool based variables – ambient temperature, ratio of air flow.

Variables for mould – mould material, durability, sufficient venting.

Individuals based variables – fatigue, idleness, awareness

The process parameters, injection temperature, injection pressure and injection time were considered to demonstrate their influence on the dimensional stability of the wax pattern made by the IC process. Additional parameters such as wax composition, ambient temperature, and vacuum pressure, the pattern cooling inside the mold and after ejection from the mold were stable throughout the analysis. The range of selected process parameters were determined by performing the experiments with one variable at a time approach. Table 3.2 shows the process parameters, their design symbols and ranges. Based on preliminary experiments performed in the laboratory, the injection temperature range of 75 to 90°C was selected. The results showed that the fluidity of wax was not proper at temperatures below 75°C, the wax mixture used in the experiment resulted in incomplete filling of the mold cavity, and wax injection at temperatures above 90°C resulted in more wax mold shrinkage. The injection pressure was chosen in the range of 0.8 to 1.1 kg/cm ^{2}. The wax shrinkage was observed to be minimal within this range. The range of injection time between 4 -10 seconds was chosen for the reason that the cavity was not completely filled when the injection time was less than 4 seconds, and that when the injection time exceeded 10 seconds, liquid overflow was caused to wax out from the mold. In this study the response parameter was linear shrinkage (LS), expressed in percentage, which is calculated by finding the difference between the pattern size and dimensions of the mold.

3.6 Experiment & observation

A four level three factor DoE was planned for Table 3.2 and Taguchi L16 orthogonal array experimentation procedures were performed to generate the respective responses.

Dimensions of the RP replicas (Wax patterns) were measured and compared with respective CAD dimensions and RP contraction was calculated as shown in the Table 3.3.

Table 3.2 L16 experiment Factors and Levels

		Levels			
S. No.	**Factors**	**1**	**2**	**3**	**4**
A	Temperature (^{0}C). T	75	80	85	90
B	Pressure (Kg/cm^2). P	0.8	0.9	1.0	1.1
C	Time (min).t	4	6	8	10

3.7 The responses - The linear dimensional deviation in X, Y, Z and Hole diameter were calculated taking the respective RP dimensions as references. And percentage deviations were calculated as given in the Table 3.3. In most of the cases it was shrinkage hardly expansion was noticed. The S/N ratios were calculated, trend graphs were plotted for Temperature, Pressure & time. The responses were used for calculating the ANOVA using MINITAB16.

$$\frac{S}{N} = -10log\left[\frac{1}{n}\sum_{i=1}^{n} y_i^2\right] \text{ ——— } \quad (3.1)$$

Table 3.3 L16 Responses of Experimental work

Dimensions (Refer fig 3.1)			**Responses for L$_{16}$ Taguchi experiment combinations (Dimensional variations)**															
	CAD	**RP**	**1**	**2**	**3**	**4**	**5**	**6**	**7**	**8**	**9**	**10**	**11**	**12**	**13**	**14**	**15**	**16**
Y$_2$	7.11	7.26	7.8	6.92	7.2	6.7	6.92	6.98	7.1	7.11	6.9	6.92	7.1	7.9	6.90	7.2	7.17	6.72
Y$_3$	11.68	11.64	11.00	10.9	11	10.8	10.94	11	10.9	11.08	10.78	11	11.04	11.28	11.02	11.1	11.1	11.02
Y$_4$	16.25	15.80	14.92	14.88	14.8	14.82	14.82	15	14.8	14.92	14.9	14.98	14.92	15.1	15.22	15.32	14.74	14.96
Y$_5$	20.82	20.58	19.38	19.32	19.28	19.48	19.42	19.52	19.34	19.56	19.4	19.48	19.4	19.72	19.84	19.62	19.4	19.74
Y$_6$	25.39	24.52	23.96	24.0	24	24	23.7	23.9	24.12	24.1	23.9	24.14	24.02	24.22	24.20	24.42	24.06	24.22
X$_7$	152.40	152.2	147.96	147.6	147.3	147.92	147.22	147.48	147.66	148.76	147.4	147.58	147.5	147.5	148.06	147.6	148.4	148
Z	38.10	38.2	36.7	36.74	36.48	36.7	36.62	36.78	36.72	36.66	36.60	36.56	36.72	36.60	36.58	36.78	36.98	36.96

H	10.00	9.26	9.21	9.34	9.42	9.63	9.26	9.29	9.19	9.32	9.23	9.25	9.35	9.32	9.27	9.31	9.31	9.12
			Percentage Shrinkage calculated from above responses															
Y(Y_2 to Y_5)			5.09	5.74	4.73	6.61	5.63	4.88	3.64	4.09	5.93	5.17	4.66	3.12	4.38	3.28	4.57	5.5
X (X_7)			2.78	3.02	3.21	2.81	3.27	3.10	2.98	2.26	3.15	3.03	3.08	3.08	2.72	3.02	2.49	2.75
Z			3.92	3.82	4.50	3.92	4.13	3.71	3.87	4.03	4.18	4.29	3.87	4.18	4.24	3.92	3.19	3.24
H (hole)			0.53	-0.86	-1.72	-1.72	0	-0.32	0.75	-0.64	0.32	0.10	-0.97	-0.43	-0.10	-0.53	-0.53	-1.72

3.8 Results & discussion

For the sake of simplicity the dimensional deviation of RP replica with reference to RP pattern is termed as shrinkage. Then percentage shrinkage are estimated in X, Y, Z directions. The selected test bar for the study in this paper is the one being regularly used in the precision casting sector. This might enhance the adaptability and acceptance from the end users and hence linking the findings with the industry might become easy. Since FDM models(patterns) have contraction in X,Y ,Z directions it was advised to quantify the contraction compensation of wax (RP replicas) also in X,Y ,Z directions. This might help when we decide for providing total (cumulative) compensation on CAD drawing stage. It may be avoid estimate individual.

It can be read out from the experiment that the shrinkage in

Y Direction is 3.5 to 6 %

Z Direction is 3.5 to 4.5%

X Direction is 2.5 to 3.5 %

Shrinkage on one typical internal dimension (Hole diameter) is an example for restricted dimensions, and it is clear that when the wax is restricted by the mould it hardly shrinks. The shrink value observed is +0.50 to – 1.7%. One can well assume the average value as approximately – 1.0%. ie it has an apparent expansion on the restricted dimensions; this is a complex phenomenon, it may even explore the thermal expansion of the RTV, accuracy of RP on cylindrical dimensions etc. to explain it. Above values reported represents 'RP to Replica contraction' and the 'alloy contraction 'always is available with the shop floor for different alloys cast. But the RP contraction is quite a controversial in spite of

several technical publications. However academia agrees with RP model's behavior that it shrink in X, Y& Z directions differently and it tends to expand in its z direction. The typical values we got to represent RP contraction is 0.34 to -3.0%,-0.2% and 0.13% respectively on Y, Z and X direction. Once we put together all the three contraction components we can quantify the compensation require on the CAD. It's worth to recall now that wax contraction is hardly 1% in metallic mould, it shows wax behaves differently in metal moulds and in RTV moulds .This may be due to the difference in the respective thermal conductivity (Thermal diffusivity) and modulus.

In the precision castings sector the above findings are unacceptable and remain irrelevant as it is quoted without reference and limits. It's very important to notice that in X direction which is taken along the direction of wax flow /wax injection the wax replica has a tendency to shrink less compared to Z direction which is taken to be perpendicular to the wax flow. This conform to the technical literature published by RTV suppliers that its shrinks less in the flow direction [www.xiameter.com]. The applicability of above shrinkage values is 0 – 150mm, 0- 40mm and 0-25 mm for X, Z and Y axes respectively. The Taguchi experiment S/N ratio and trend charts gives us the impact of Wax temperature(T) ,Hold time (t) and Wax injection pressure (p) on the output we measured in the form of shrinkage. It's may be inappropriate to term the response as shrinkage ; it is shear 'dimensional deviation' since it is not attributed to just a phase change ,in fact there appears an interplay of thermo physical properties of RTV compound and process factors involved in mould making, like thermal diffusivity, thermal conductivity, mould wall thickness, Modulus (strength) ,wax flow direction, size & geometry besides the process factors we considered. It can state from the trend graph that 80 – 90 ^{0}C wax temperature, Pressure at 1 bar and hold time 8 minutes give best result in Y direction where in Z direction pressure is not very impactful –Temperature and Hold time is more impactful and it is more evident as values are increased. The Injection temperature is more impactful in all the cases.

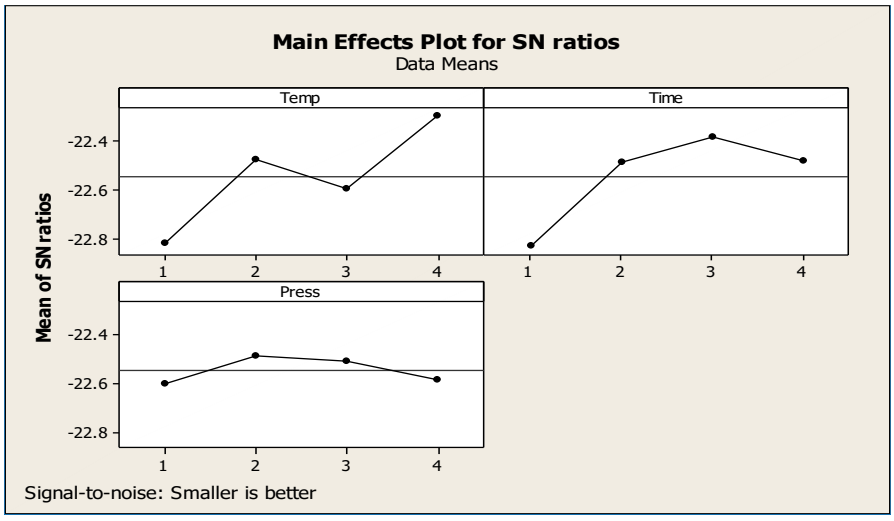

Figure 3.7 Effect of process parameters on linear shrinkage and S/N ratio

It is observed that impact of pressure is very different in Z & X directions, in Z direction it is found more impactful, may be, the hydrodynamic pressure is more on across the flow, i.e perpendicular to X (injection) direction.

The response table of the S/N ratio gives the optimum value against each factor of the process. This is based on highest value criteria. As such 90^0C (D1) for Temperature, 0.9 Kg/cm^2 (B3) for Pressure and 8 minutes (C2) for Time constitute the best combination of set of values ensues the optimum and minimum shrinkage on the wax replica, with factor Temperature and Pressure respectively as the most influential and the least influential in the experiment. And it is observed 2.0 to 2.5 %, 3.0 to 3.5% and around 5% shrinkage on X, Y and Z dimensions after optimization of shrinkage on wax replicas.

This work reports shrinkage behavior of wax in the RTV silicon rubber compounds under the influence of wax injection temperature, Mold hold time and Wax injection pressure and help open up the black box of 'cumulative shrinkage compensation' required on the CAD drawing when integration of RP with precision castings is attempted. This is the need of the present day precision casters but unfortunately it is a complex issue and a live challenge to the academic community and researchers. Though the wax pattern generated by RTV demonstrates its capability to be an alternative to metallic moulds its full potential can be realized only when RTV & RP go hand in hand. Though sporadic commercialization of RTV & RP integration is being reported a comprehen-

sive optimization and standardization is essential before we could win the trust of precision cast house.

Table 3.4 Response Table for S/N Ratio

	Factors	A	B	C	D	Delta	Rank
1	Temp	-22.82	-22.48	-22.53	**-22.30**	0.52	1
2	Time	-22.83	-22.49	**-22.38**	-22.48	0.45	2
3	Pressure	-22.60	**-22.49**	-22.51	-22.58	0.12	3

The data in optimizing the shrinkage on the wax replica using process parameters Temperature, Time and Pressure with Taguchi L16 orthogonal array experiment are shown in table 3.3. This study optimizes the factors for minimum shrinkage. S/N ratio is calculated as the equation (3.1) with lower the better criteria. Where Yi is the value of the quality features for the i^{th} attempts, n is the number of iterations.

3.9 Investigation of FDM modeled Polymer Rapid Tooling (PRT) for Plastic Injection Molding - As stated in previous section, in order for the RTV mold to be feasible for use, it must be able to mold the product that meets to the specified geometry and do this repeatedly and within the tolerance range limits. This means that the mold must be stable and robust. For the purposes of this study, the stability of the mold refers to a form that corresponds to specified dimensions for several cycles, which results in acceptable components. Robustness refers the resistance of mold to degradation and, consequently, limiting the change in size from part to part. To investigate the robustness and stability of PRT shapes, parts were selected and molded using both PRTs and conventional metallic tools. Each molded part contained several important functions. After molding, the preselected characteristics were measured in comparison with the calculated dimensions and evaluated with high accuracy. Then, the measurement data were tracked from shot to shot to determine behavior and robustness produced parts.

The measurement data from the molded parts will then be analyzed to determine:

-If the part reaches the required size (within the specified tolerance)

- If the component meets the size of most components generate

-the rate at which the parts changed in dimension depending on the number of shot cycles that the shape experienced. Although length and Width are not necessarily geometric features, it is a simple way to compare a molded component regardless of overall complexity. To a lesser extent, diameters were also examined to depict non-linear features such as cylinders, pads, fillets and curves.

With the advances in materials along with the new access and low cost plastic based AM equipment, direct use Polymer Rapid Tools (PRTs) would be a far more advantageous option in creating injection molds for low and highly flexible production. However, the use of polymer based direct rapid tooling by industries is curtailed due to the issues with the dimensional stability of the polymer based rapid tooling molds. Apart from dimensional tolerances, there are also issues with the life of these polymer based mold as they wear fast and are also not able to sustain high injection pressures in an Injection molding machine. Another, major problem with the polymer based rapid tooling is the poor thermal conductivity of polymeric materials due to which there is an increase in the cooling time and ultimately leading to decrease in productivity. Therefore, before proposing polymer based rapid tooling as a solution to industries to reduce the product development time and bring down the costs, a thorough study of the issues related to the same is imperative. This primary objective of this work is to investigate the dimensional accuracy of striker (RP) component produced by ABS mold inserts. For dimensional accuracy a reverse engineering technique 3D scanning is used which is compared with CAD file and inspected with COMET plus software. Further, the outputs are validated with vernier caliper. The mold insert is manufactured by Fused Deposition Modeling (FDM) technology which is used on injection molding machine.

With short production cycles, excellent surfaces of the products, tight tolerance complete automation capability and facile molding of complex part geometry, Injection molding (IM) is crowned as the most popular molding process for manufacturing thermoplastic parts. However IM requires complex and costly tooling and it is almost uneco-

nomical to plan a short production run. Hence IM personals are confronted when a one–off production or trial run for product development are warranted. The proliferation of rapid Prototyping (RP) tends to rope in IM tool design and development simplified. RP in late eighties began with rapid generation of prototypes for feel and fit purposes. Today, Rapid prototyping (RP) has emerged as a third industrial revolution reengineering the entire manufacturing transforming the way in which products and systems are designed and manufactured as a fascinating area of study called rapid manufacturing (RM) covering >50% of the additive manufacturing (AM) output (see Figure 3.8). This is affected through emergence of a new field of science called Rapid Tooling (RT). RT is being expanded as Soft Tooling, Hard Tooling, Direct Tooling, and Indirect Tooling and is the link between RP and RM.

Today, RP technology is slowly being recognized as a class of commercially viable production techniques characterized by significantly low tooling cost and lead time. The revenues from end-product manufacturing accounts for 34.7% of the total additive manufacturing (AM) market, which, according to Wohler's report, reaches $ 1 billion (see Figure 3.9). AM has a host of technologies (FDM/SLA/SLS/3D printing/poly jet) employing different types of feed materials like solids(filaments), liquids(resins), powders but majority employ polymer based feed stock hence the thermal resistance and fatigue strength are always a concern when it was employed to endure extreme conditions of stress and temperature entailed in tooling. However as per the sporadic information available in the literature; the development of

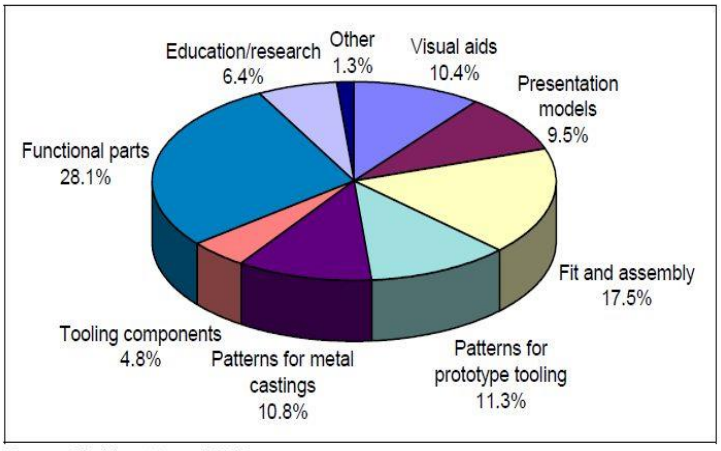

Source: Wohlers Report 2013

Figure 3.8 Applications of additive manufacturing

SLA based IM tooling was seen attempted however no commercialization has yet been reported. Metal based AMs are the best but are unaffordable. FDM with its conventional ABS and poor part density it is being ruled out for IM tooling project. One promising option is FDM based Polyjet technology which employs digital ABS, rubber like elastopolymers etc. This work investigates the development of IM tooling through Polyjet technology.

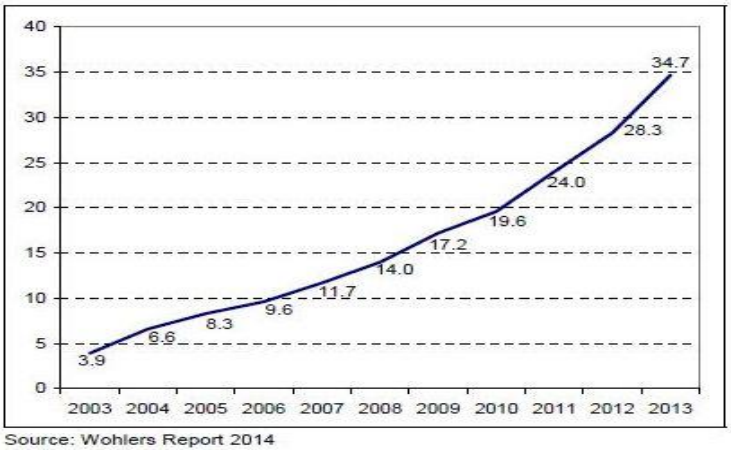

Figure 3.9 Revenues from the production of parts

3.10 Methodology to develop PRT mold - Polyjet technology is a variant of FDM technology licensed to Stratasys. These machines manifest extreme level of surface finish (Ra 3) and part definition with improved density, physical properties etc. Before manufacturing of mold inserts of part component on 3D Polyjet it is created on Autodesk inventor 3D modeling software according to their dimension as shown in Figure 3.10.

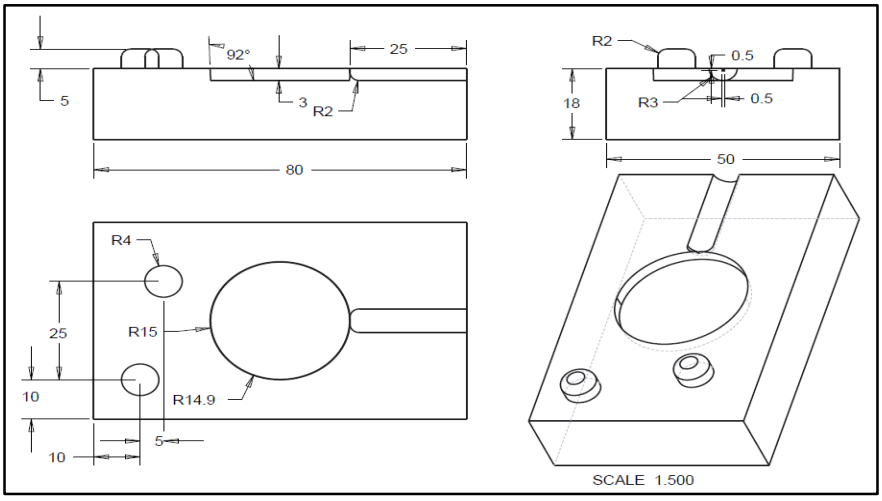

Figure3.10 Designed geometry with dimension of striker mold

3.11 Material selection and properties-

The digital acrylonitrile butadiene styrene (ABS), available from Stratasys Inc was used as a matrix polymer. This ABS is an FDM grade polymer used by Stratasys for the production of recommended prototypes on the FDM machine. The specific gravity of ABS was 1.05 g / ml. Acrylonitrile-butadiene-styrene is an amorphous thermoplastic consisting of three monomers, usually containing 15-35% of acrylonitrile, 5-30% of butadiene and 40-60% of styrene (see figure 3.11). The Properties of ABS means, Acrylonitrile: chemical resistance, heat resistance and high strength, Butadiene: toughness, impact strength and low-temperature property preservation, Styrene: rigidity, surface appearance (gloss) and process ability. Its properties may vary according to the volume fractions of the monomers used in the mixture. While acrylonitrile is responsible for the bonding of contiguous chains and the resulting strength of the ABS terpolymer, styrene imparts a shiny and impermeable appearance to it. The rubbery butadiene provides the ductility and impact resistance of the ABS (Designing Site Retrieved May 2010). The FDM-ABS is an environment-stable thermoplastic without significant distortion, shrinkage or moisture absorption. It is 40% stronger than standard ABS over impact and flexural strength. Its more robust layer makes the perfect material to create long-term parts for form, fit and functional applications. Due of these advantages, Digital ABS was preferred as a matrix in the development of the new metal-polymer composite.

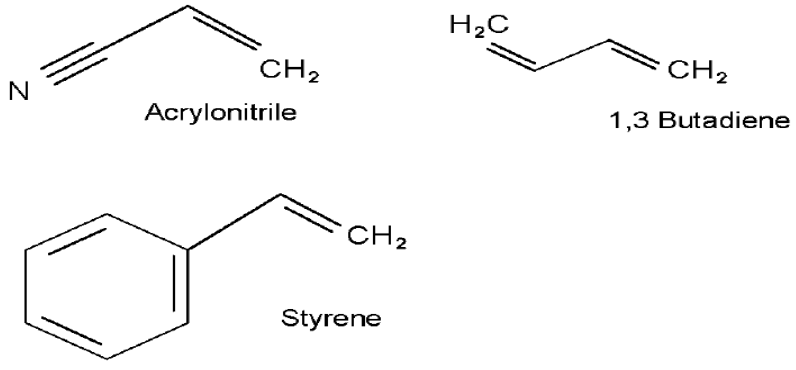

Figure 3.11 Monomers used in thermoplastic ABS

3.12 Working principle of Polyjet Direct 3D printing - Poly-Jet Modeling is an additive manufacturing technique with a selectively ink jetting of UV-curable photopolymer resin as shown in Figure 3.12. First, the photopolymer is jetted onto the buildup platform by the printing head. Simultaneously the photopolymer drops are leveled by a roller and solidified by a UV- light. Subsequently the platform is lowered. Like this, a part is generated layer by layer. The replication and enhancement of the photopolymer material layers is a solid three-dimensional model than it is not perfect. In order to prevent collapse of structures during production, gel-like support in the material is designed specifically for intricate geometry with the model materials. After the model is completed, the substrate can be easily removed by hand and sprayed with water to leave only the cured photopolymer material.

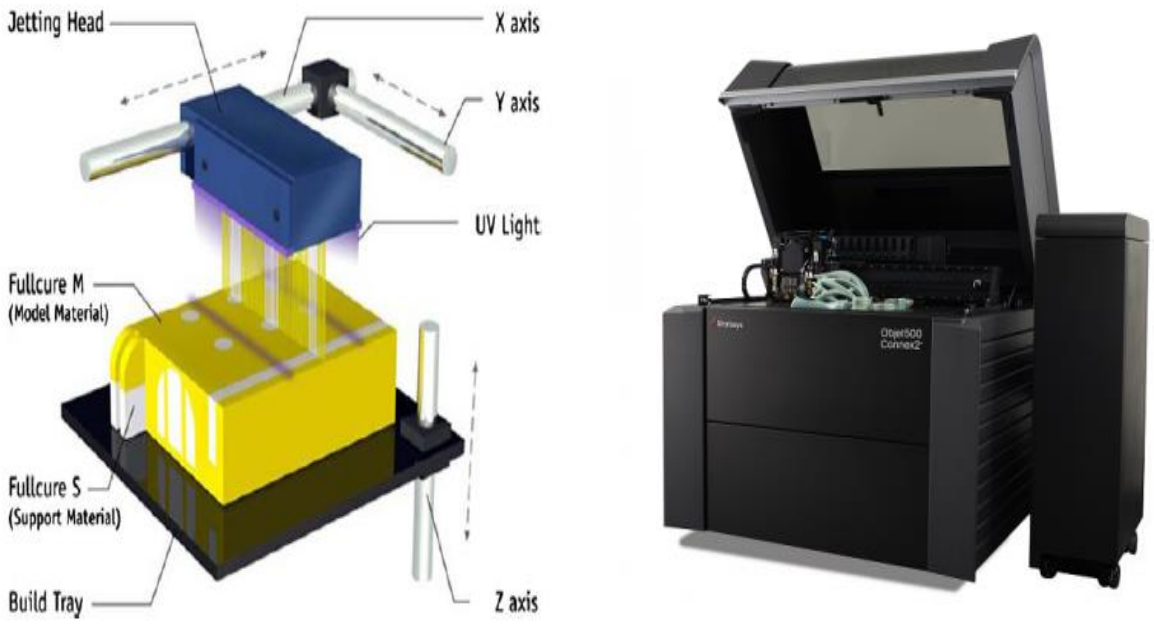

Figure 3.12 Polyjet 3D printers for printing mold, Barnatt C. (2013)

Table3.5 Parameters of Polyjet 3D printer Component/mold

Type	Stratasys Objet350 Connex
Material	Digital ABS
Bed temperature	35^0C
Chamber temperature	35^0C
Layer Thickness	0.032 mm

Digital ABS is suitable for simulation of parts requiring high impact resistance and shock absorption of 65-80 J / m and a deviation of heat temperature at 58-68 ° C (136-154 ° F). It is a high temperature material synthesis of unprecedented dimensional stability of heat resistance. The material can simulate the thermal performance of engineering plastics and is ideal for testing applications such as hot polymer flow in mold insert cavity.

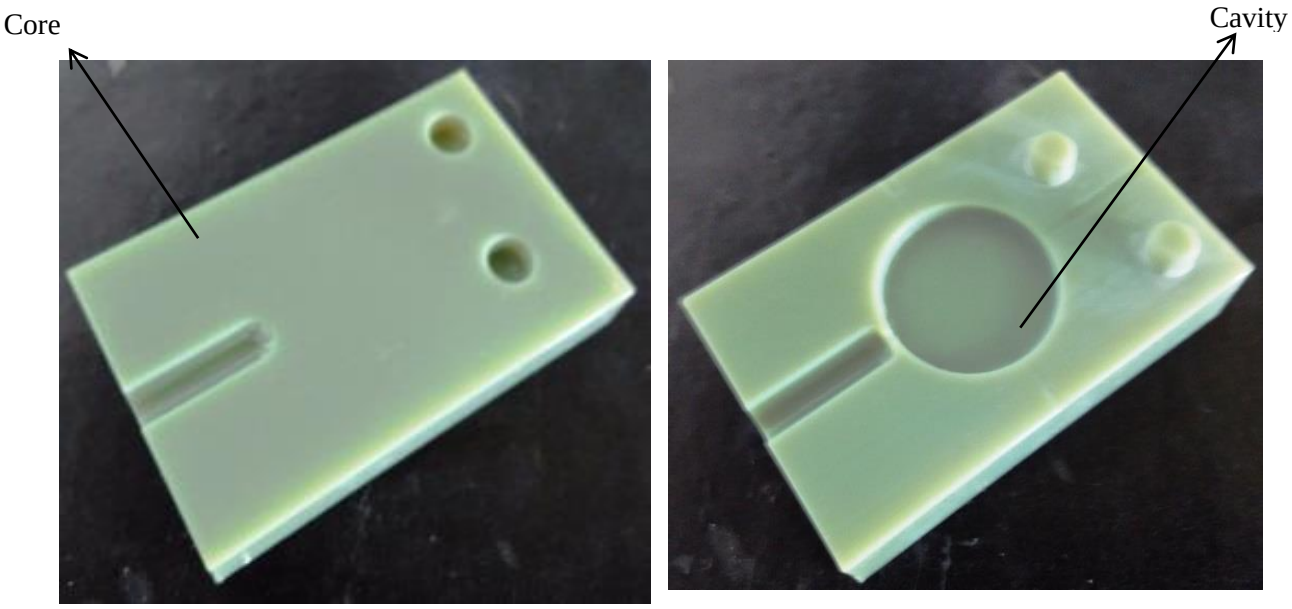

Figure 3.13 3D printed core and cavity

3.13 Hand Injection Moulding machine to develop the part

Thermoplastic or thermoset material is heated to be plasticized in a cylinder at a controlled temperature and then forced under pressure through a nozzle into a gate, runner, sprues and cavities of the mold. The solidification of resin undergoes rapidly. After solidification of molten material mould is opened and the part gets eject. Injection moulding is propagates in the production of glass-reinforced parts.

The mold forms, shapes and cools the plastic material into the required product shape. The temperature setting for the PP injection is based on the MP of the PP (164°C) it was advisable to set a temperature 180°C to start with the experiment. The PP beads were heated in the barrel to test the melting and oozing out of the liquid plastic threads the nozzle by manually pressuring through the plunger. The molding was uniformed hence the temperature was gradually increased in steps from 190, 200 and 210° C.

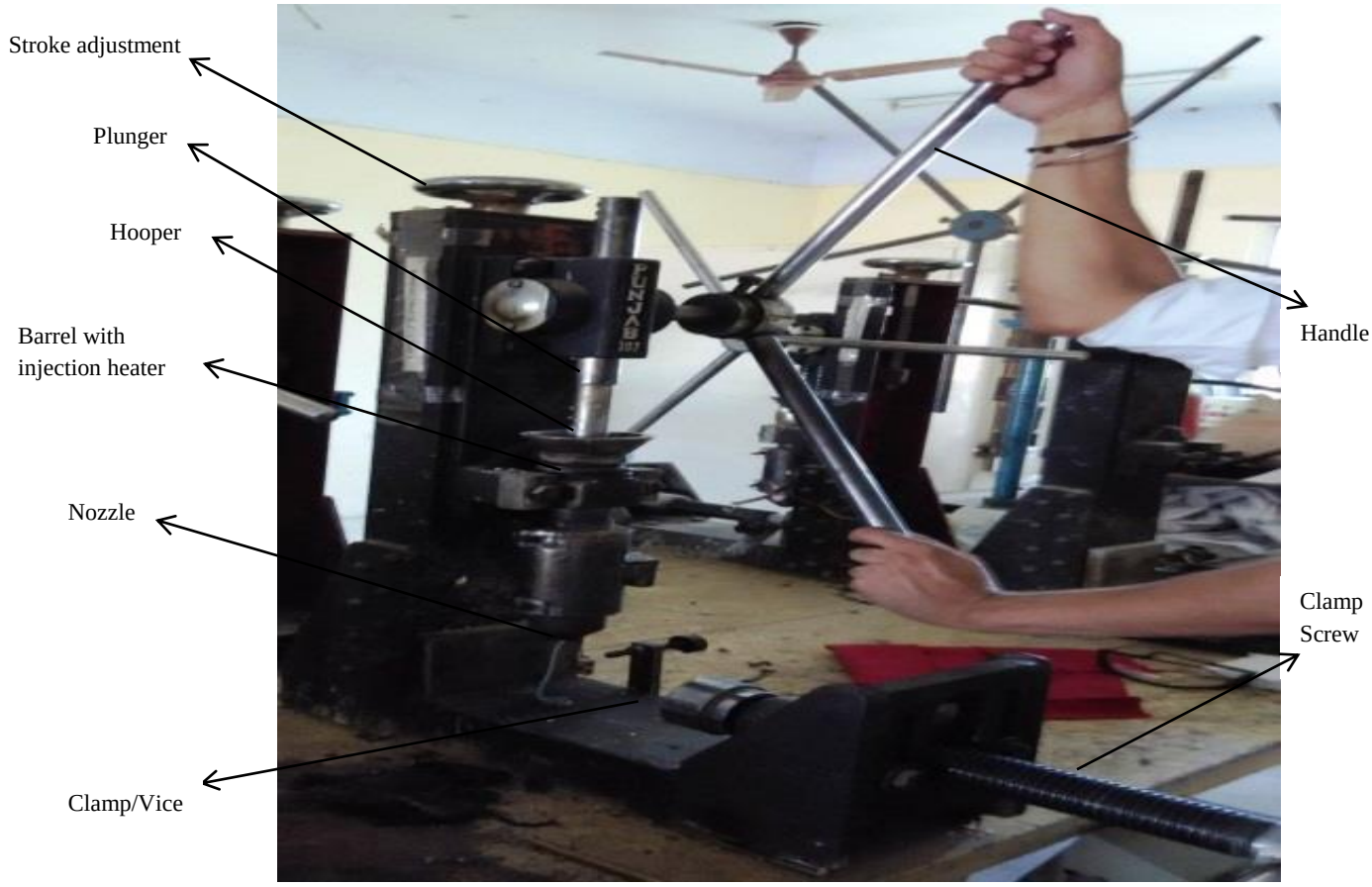

Figure 3.14 Hand Injection Molding (HIM) Machine for trial

It was observed that the mold was getting damaged at the injection point due to applied pressure (at the plunger runner contact area). Always it needs to avoid the direct machine nozzle contact to printed tool. Here a metals (MS) plate is used to resolve the problem by minimizing temperature and pressure intensity at the injection point and converted point load to uniformly distributed load.

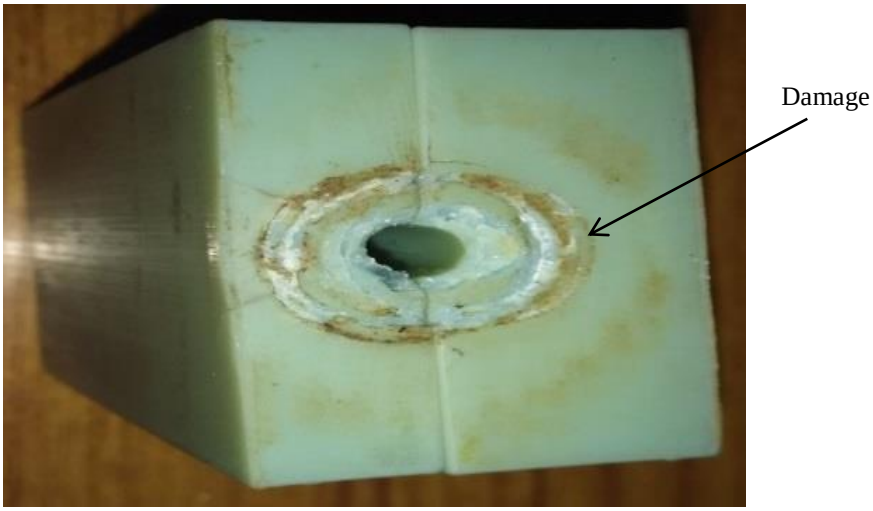

Figure 3.15 Damaged mold at the injection point

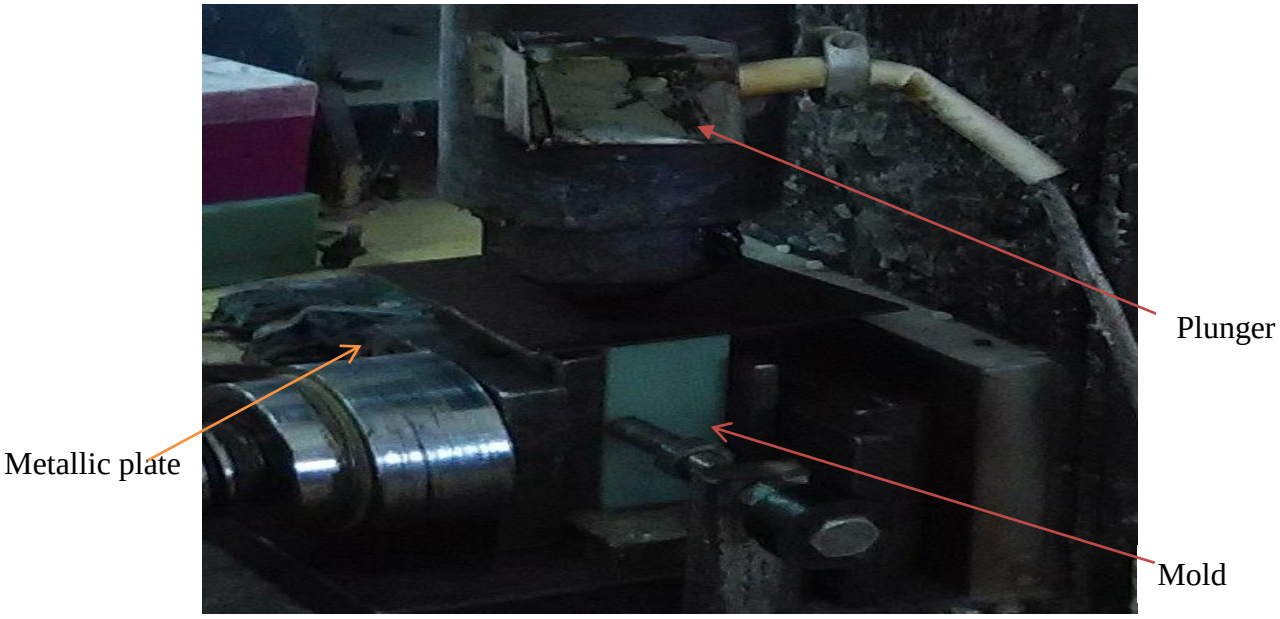

Figure 3.16 Metals (MS) plate for minimizing temperature and pressure intensity at the injection point

Figure 3.17 Progressive stages of the component made in the trial runs

During the run time whenever the mold got over heated the component got sticky and gummy and did not form well. It needs to be probed. Designing of proper Cooling channels may be a solution. The next figure shows the damage and non- formation of the part due to high temperature 200˚C and above. The part non-formation during the run was not possible to run the mold continuously. It was found the temperature 190ºC was good to get excellent mouldings. The product coming from the nozzle temperature controlling from 170 to 190 ˚C is acceptable.

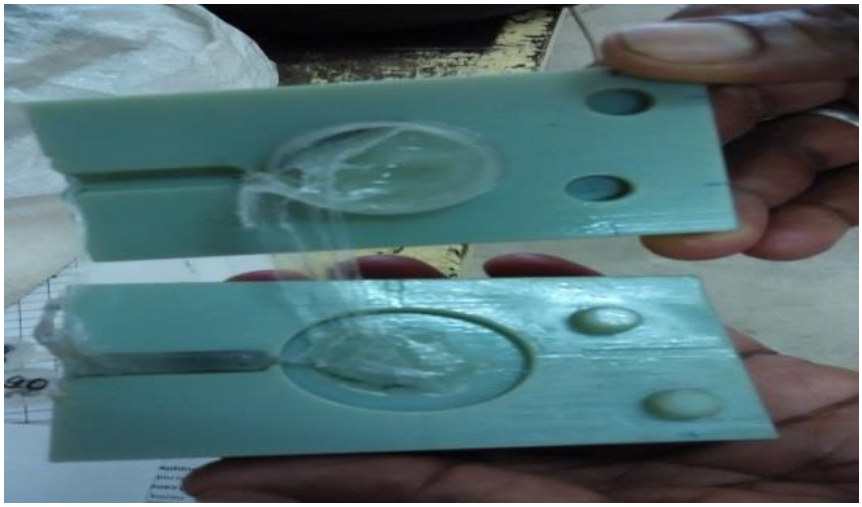

Figure 3.18 (a) Part sticks to the mold cavity

Figure 3.18 (b) Quality parts (striker) productions

It was found at temperature above 200^{o} C the part formed were rejected. This was applicable even at low temperature injection after a brief run of 5 shots. This was due to mold getting over heated due to dull dissipation of heat from the mould cavity.

3.14. Reverse engineering to check the accuracy of RP- A three-dimensional scanner is used to capture the physical object's features through lasers, lights, or X-rays and generates dense dot or polygonal meshes. Before scanning a striker mold part is placed on the table. The physical object can be digitized using 3D scanning technologies such as Coordinate Measuring Machine (CMM) or non-contact 3D scanning technologies such as laser scanners, structured light digitizers, and so on. The point cloud of a manufactured part will be aligned to a CAD model and compared to check for differences after inspection. The part production procedure was established in the HIM machine and the readings on dimensional accuracy of the part are shown in Figure 3.19

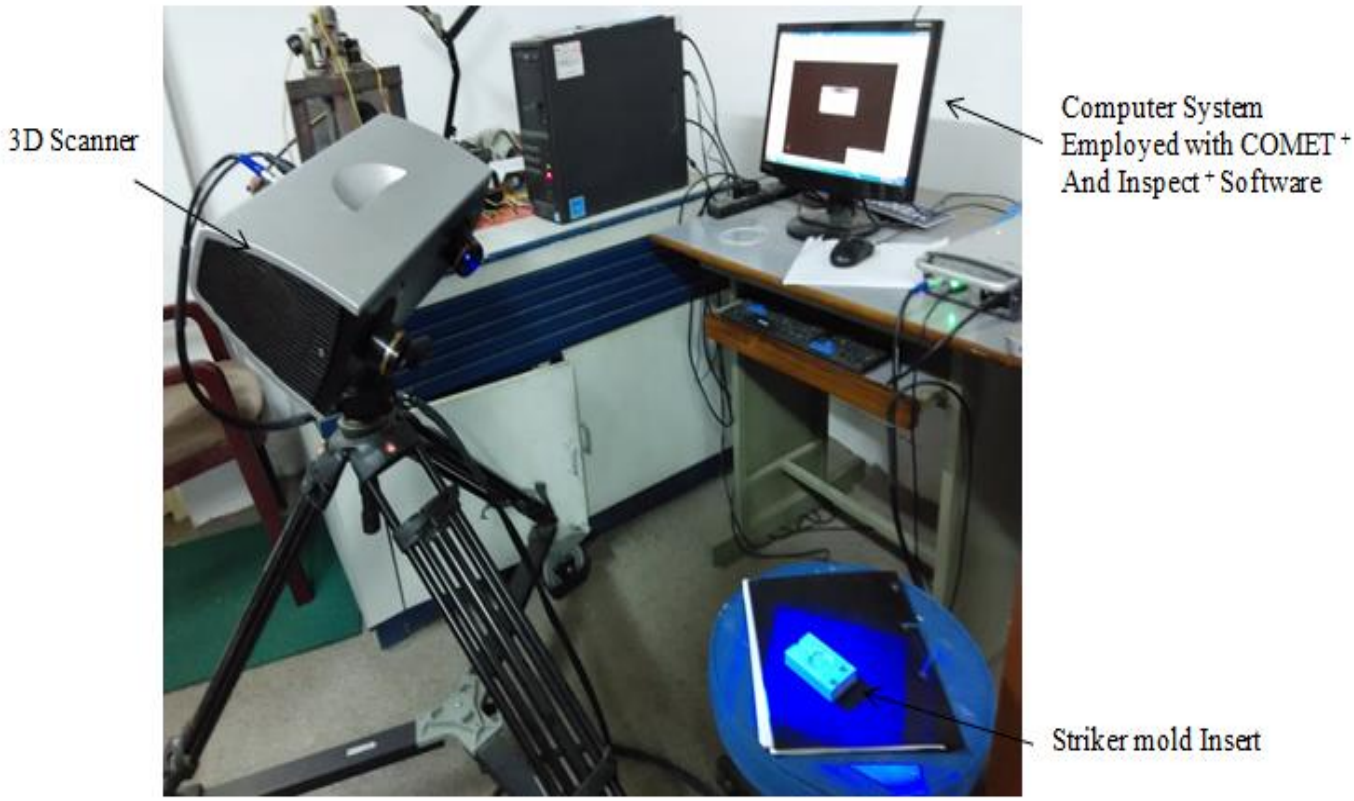

.

Figure 3.19 3D scanner for inspection of part component

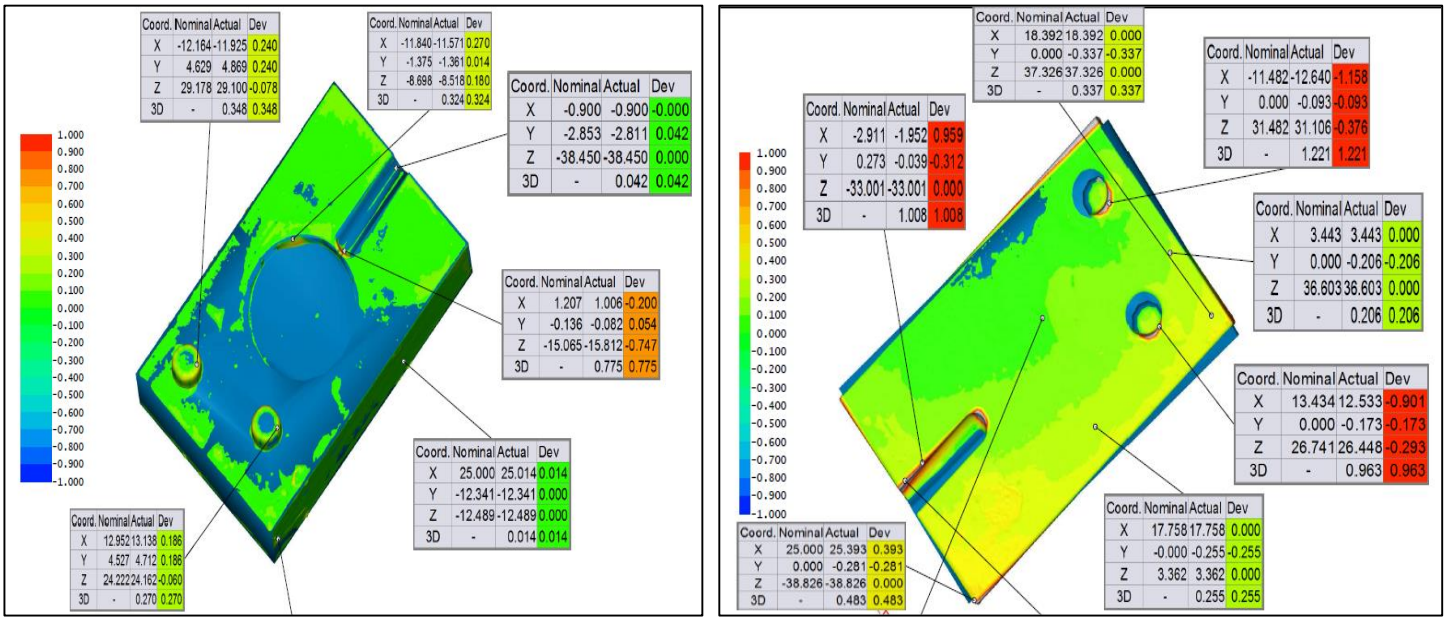

Figure 3.20 Inspection of specimen with 3D scanner

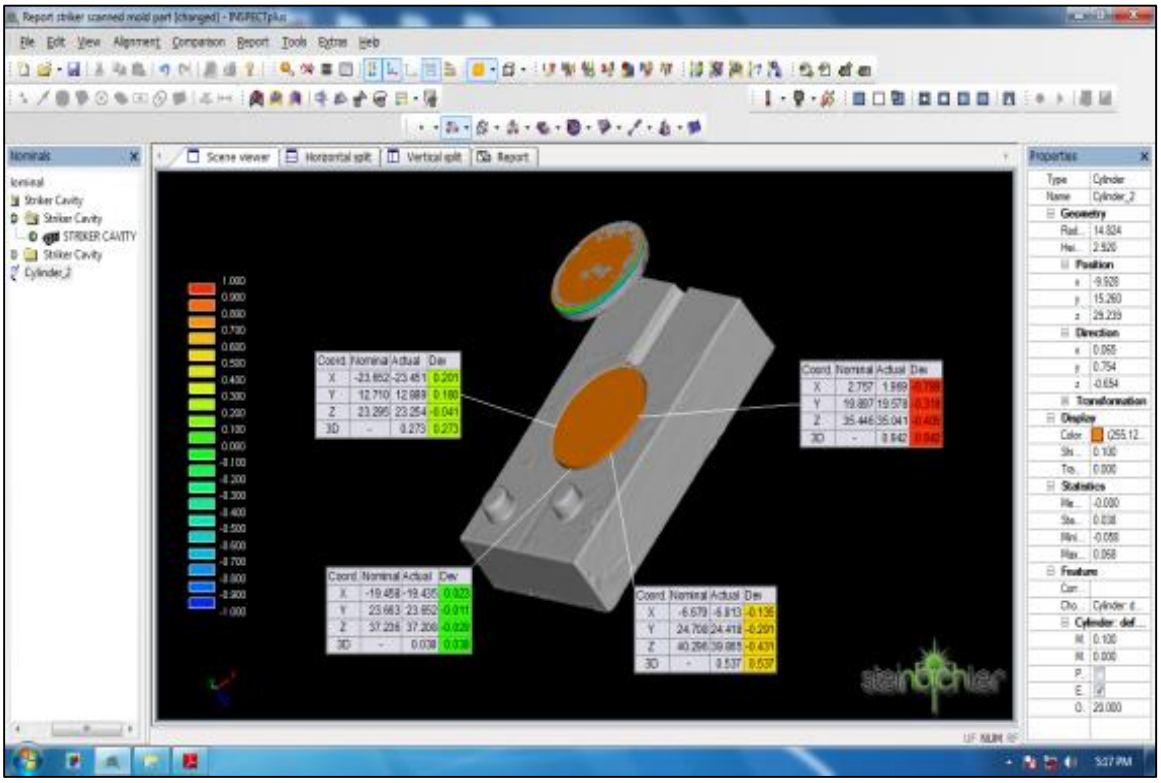

Figure 3.21 Inspection results of component

Table 3.6 Dimension of measured part using 3D scanner

Dimensions (mm)	Nominal	Mold	Part
Diameter	30	29.628	29.54
Thickness	3	2.920	2.98

The Digital Caliper is a precision tool that makes it extremely accurate to measure inside and outside distances (see Figure 3.22). The instrument shown below is a digital caliper as the distances/measurements, are read out from a LCD display. The display is operated with the on/off button. The external jaws should then be brought together until they touch each other and the zero buttons need to be pressed. The digital caliper can then be used to measure distances. Always go through this practice while turning on the display for the first time.

Figure 3.22 Digital Vernier Caliper for measurement

The material to be measured is located between the outer jaws and carefully brought together. Tighten the locking screw so that the jaw does not move apart. The digital display is then able to read. The measured distance can be note down by in metric and imperial values by operating the inch/mm button. Table 3.7 shows the dimensional results using vernier caliper for comparison with reverse engineering results. As clearly seen the results are in accordance with reverse engineering results.

Table 3.7 Dimensional results using Vernier Caliper

SI. No.	Thickness (mm)	Diameter (mm)
1.	2.9	29.31
2.	2.98	29.54
3.	2.95	29.36
4.	2.95	29.41
5.	2.93	29.29
6.	2.89	28.9
7.	2.89	29.32
8.	2.96	29.15
9.	3.02	29.26
10.	2.96	29.20
Average	2.943	29.274

The injection molding is an intensive mass production process hardly amenable to product developmental short run trials. In the fast changing product style and customer taste

the plastic industries are felt the paradox of prototyping and mass production increasingly. Hence it's a global need to introduce new Time Compression Technologies (CTC) to manufacturer prototyping molds economically. Polyjet based additive manufacturing (AM) is potential and promising CTC technology to prototype injection molds for typical short runs. Polyjet CTC is going to be a viable answer to the long standing prototyping issues in the polymer injection molding industries. As compared with measure dimension through vernier caliper the scanned part of striker cavity is almost similar.

3.15 Chapter Summary

The key motive for this study was to investigate feasibility by determining whether PRT/RTV shapes can meet the desired physical dimensions within tolerance limits across a range of geometries and complexities. In particular, it was investigated whether the dimensional stability observed on a simple feature object can be consistently maintained in components with a higher degree of geometric complexity. At the same time, the dimensional stability of PRT/RTV molds was evaluated by cycling the molds until failure and tracking changes and deviations over time.

In addition, the degradation of the PRT form was investigated use of conventionally produced metal molds as a basis for comparison. In addition, information was collected during the course of the experiments to support future research and feasibility.

CHAPTER- 4

MECHANICAL AND PHYSICAL CHARACTERIZATION OF DIGITAL ABS

This chapter introduces the digital ABS polymer for mould material, manufactured by means of Polyjet technology and was examined as an alternative for rapid tooling. Based on the manufacturer description, digital ABS is a resin particularly developed to protect against high temperatures and pressure. The key purpose of the present study is to examine a new material for the mold fabrication during the injection process. In this study, the analysis is carried out on digital ABS for the dimensional and surface stability and also studies the final casting properties. For the aforementioned analysis, mechanical properties of the samples were considered and further bending, tensile and impact tests were performed by measuring their hardness. For measuring the PET crystallation differential scanner calculators (DSC) are used.

4.1 Sample geometry and used materials- The geometry of the part considered in the present study is shown in Figure 4.1. It is in accordance with the ASTM D638 standard for polymeric part and testing for the ASTM D790 standard tensile test. The bending as well as the impact strength analysis was performed on the similar samples, since based on ASTM standard the sample dimension should be between a thickness range of 3.0-12.7 mm and width must be of 12.7 mm. The same tensile specimen was used for hardness test also.

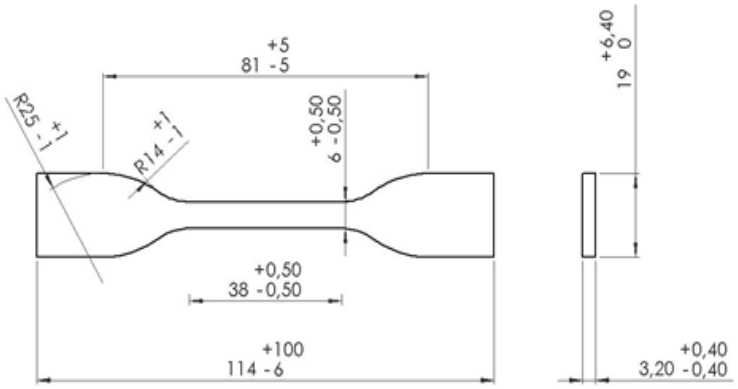

Figure 4.1 (a) Tensile test sample

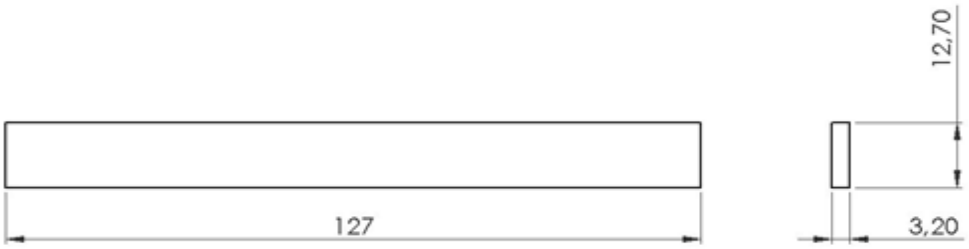

Figure 4.1 (b) Bending test specimen

The moulding material CP 204 PET was considered as it is extensively used in industry and is not difficult to mould. To make a heterophasic (stereoblock) copolymer (Braskem, 2012) it is copolymerized with ethylene-propylene rubber (EPR).

4.2 Mould inserts materials

The digital ABS polymer is a mixture of two materials having RGD515 and RGD535 that encompasses acrylic and metacracheal monuments, urine oligomes, isoborine, epoxy and other acrylic (Stratasys, 2011a; Stratasys, 2011b). Based on manufacturer specification, when removed from the 3D printer, it has a shock resistance of 55-70 J / m and a heat transfer temperature (HDT) of 48-58 °C. The digital ABS mold can be manufactured through a polyjet machine that can mix the polymers RGD535 and RGD515 in a predefined ratio. The SAE 1045 steel insert was considered for comparing the effect of mold insert on the final properties of mold, extensively used in injection molding. The main properties of these two materials are shown in Table 4.1.

Table 4.1 Properties of SAE 1045 and Digital ABS materials

Properties	SAE 1045	Digital ABS
Thermal conductivity [W/m.K]	52.7	0.17-0.19
Density [g/cm³]	7.65	-
Specific heat [J/kg.K]	790	-
Coefficient of thermal expansion [K^{-1}]	12.3	-
Modulus of elasticity [GPa]	190	2.5-3.0
Tensile strength [MPa]	410	55-60

4.3 Design and manufacturing of mould

The two different samples used in the present research are joined in a pair of mold inserts as shown in figure 4.2 (a). The arithmetical simulation was performed on Moldflow interface to check runner balancing and filling in the injection process [see figure 4.2(b)].

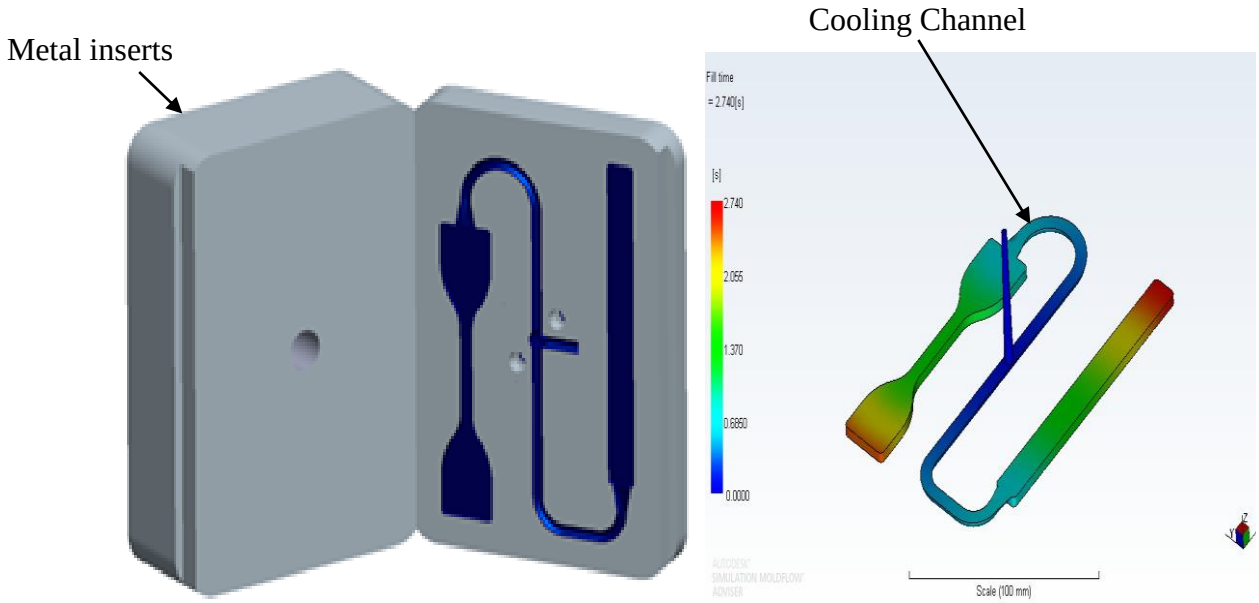

Figure 4.2 (a) 3D model of mold inserts; (b) Numerical simulation using Moldflow

The runner channel is semicircular (radius 3 mm) and the profile of the gate is fan shape. Since the shape of the cavity is extremely simple and easy removal is possible by hand, the need of an ejector system not required for the mold. Furthermore, a cooling system arrangement was also installed for the used metal inserts (Figure 4.3).

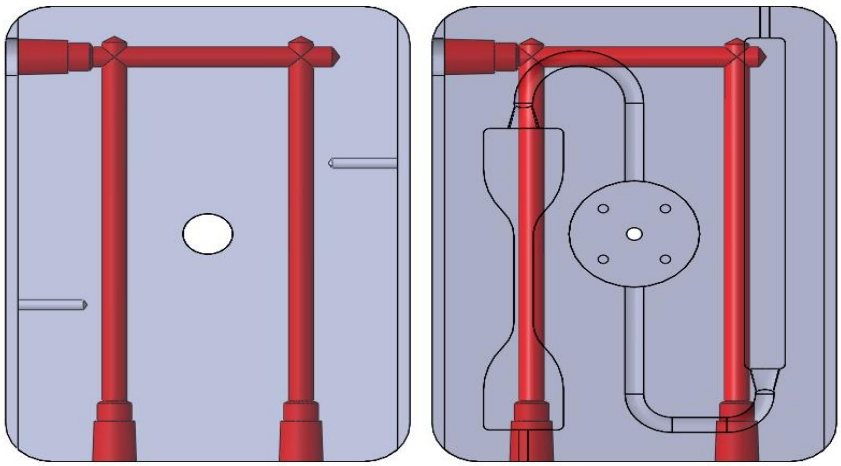

Figure 4.3 Metal inserts with cooling channels

A CNC machine is used to machine the SAE 1045 insert, and the digital ABS insert (see Figure 4.4) was printed on the Stratasys Connex 500 by means of a shiny selection with the cavity shape on top. As Zonder and Sella (2013) suggested, the direction of printing selected in such a way that the polymer flow direction is aligned with the printed line. The digital ABS insert has not been surface finished, in order to analyze the surface of the insert during the plastic injection process. It was necessary to adjust the insert just by slightly adjusting the sandpaper so that the metal mold plate can be attached to the insert and the metal sprue bush can be assembled. In order to execute the injection, all metal inserts are assembled into metal injection molded specially planned for the aforementioned purpose.

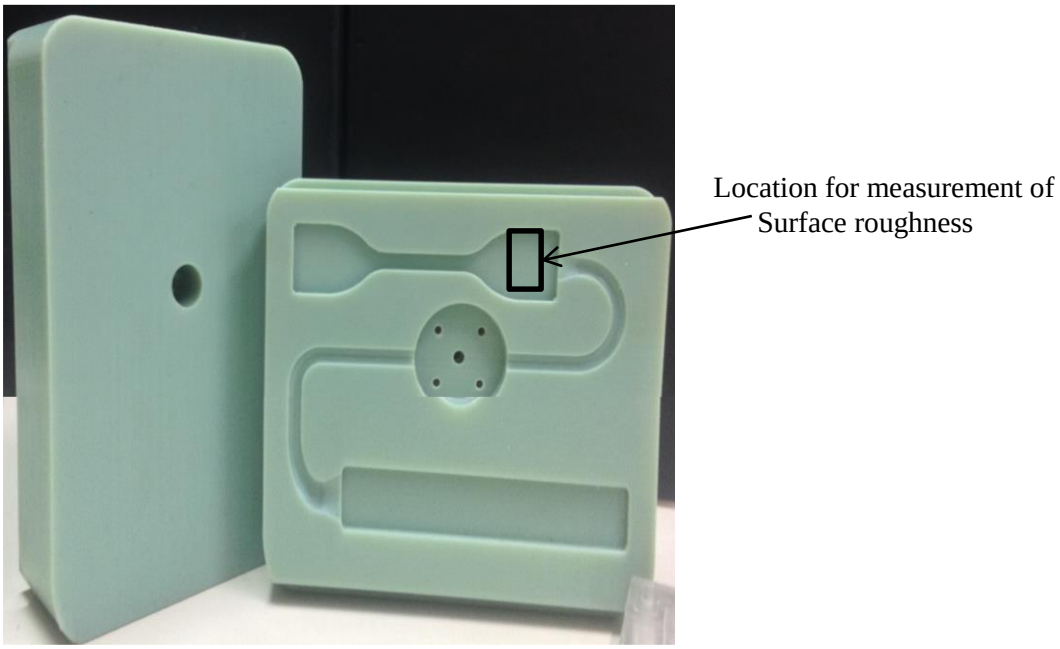

Figure 4.4 Digital ABS mold inserts

4.4 Process parameter and material selection for injection molding experiments

An Advanced injection molding machine Arburg 370S 700-290 is used and based on previous experience and past studies, the process parameters are defined in the cavity shape and mold used here (Volpato et al., 2011). Table 4.2 exhibit the parameters that are mainly involved in injection of metal inserts. These values are used as a preliminary point for defining the process parameters of the digital ABS material. As shown in Table 4.2, there

are 5 shots are needed to do this. This is usually a commonly employed method with use of polymer inserts in the injection molding (Salmoria et al.2008; Bareta et al., 2007).

Figure 4.5 Digital ABS Insert with tensile cavity

Table 4.2 Injection molding parameters for inserts

Parameters	SAE 1045	Digital ABS
Injection time (s)	12	20
Injection temperature (°C)	210	195
Injection pressure (MPa)	35	18
Injection speed (mm/s)	15	10
Holding pressure (MPa)	24	21
Clamping pressure (MPa)	100	32
Holding time (s)	12	32
Mould temperature (°C)	35	30
Cooling time (s)	8	40

The different parameters used were determined by considering the lowest strength of the chosen material. Usually, it is general exercise to apply polymer resin inserts for injection molding (Salmoria et al., 2008; Bareta et al., 2007). The temperature senses for digital ABS inserts were measured with a contactless digital infrared temperature gun thermometer having resolution of 1°C at varying locations on the insertion surface. Supercritical CO_2 was used as a cooling fluid. An experiment was performed to test the effect of spraying a cooling fluid on the digital ABS tool to rapidly cool it between shots. The next shot was taken immediately after spraying the cooling fluid onto the digital ABS mold. After the supercritical CO_2 sprayed on the tool, it was measured that the mold temperate is dropped to 9 ° C as shown in the figure 4.6.

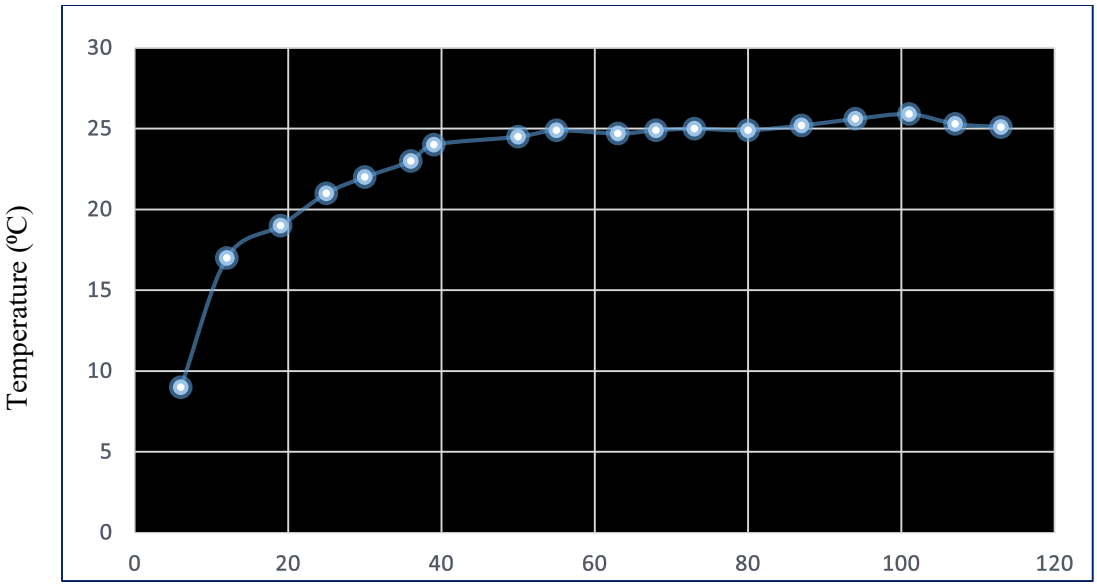

Figure 4.6 Temperature of Digital ABS Insert after supercritical CO2 is sprayed

The injection temperature was set at 25° C for the insert materials. Therefore, the next cycle of injection begins only when this temperature was reached. After setup, giving of total 50 shorts, 45 samples were made with digital ABS. The metal inserts temperature was controlled by incorporating a cooling system and maintained at 25°C prior to the start of the new cycle.

Table 4.3 Molding parameters to conduct the experiments

Properties	Steel Tool-Recommended	Digital ABS Tool-Modified Conditions
Mold Open Time (s)	9	240
Melt Temperature (°C)	210	182
Injection Time (s)	1	4
Packing Pressure (psi)	170	175
Packing Time (s)	20	30
Cooling Time (s)	30	30
Molding Material	PET	PET

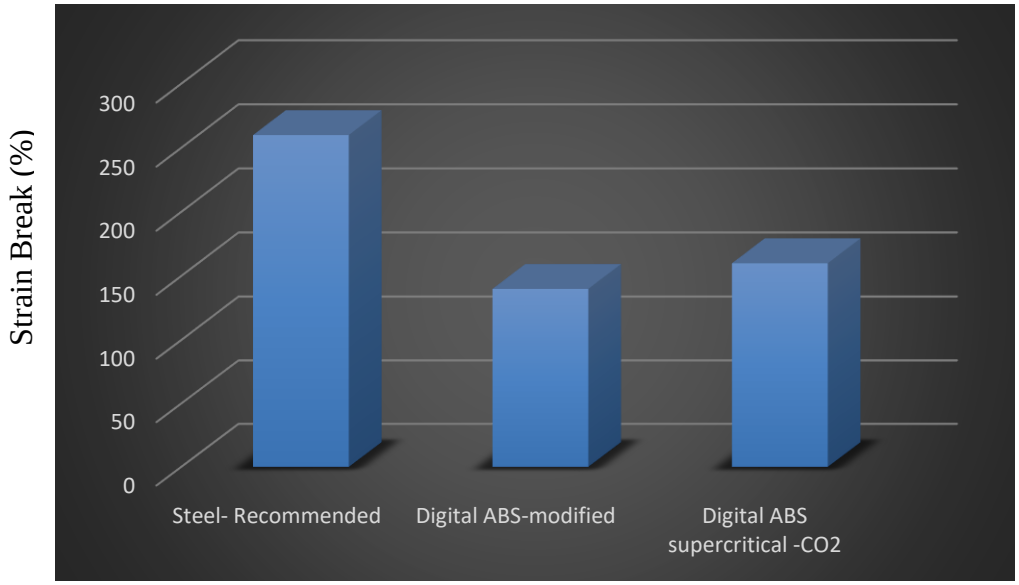

Figure 4.7 Plastic tool strain at break varying melt temp, injection speed and supercritical CO2

The fracture strain from molding using polypropylene in a plastic mold with an initial mold temperature of supercritical CO2 of around 9°C is shown in Figure 4.7.

4.5 Dimensional and Surface analysis- The main dimensions for performing the dimensional investigation of the cavity and samples made using digital ABS inserts is illustrated in Figure 4.1 (length, width and thickness). The sample was measured and reading are recorded with a vernier caliper having a least count of 0.01 mm. A Coordinate Measuring Machine (CMM) (Zeiss, UM550) was employed to recognize deformation within the cavity insert. Furthermore, a 3D profilometer is employed to analyze the surface of the digital ABS inserts. Figure 4.4 shows that the measurements were performed inside the tensile cavity, near the gate. All the measurements of the cavity were executed prior to the material injection and after 20 and 40 cycles of injection. Afterwards, precise measurements were made using CMM, three times in each phase after the removal of the cavity insert from the mold plate. This process is envisioned to deliver evidence on the everlasting cavity distortion and thus on the insert material stability.

4.6 Mechanical and DSC analyses- The samples were tested using an Universal testing machine at ASTM D 638 for tensile testing and ASTM D 790 (10 specimens each) for bending test at a speed of 5 mm/s (Figure 4.8). The impact study was performed with CEAST Resil impactor according to ASTM D 256 using hammer and Izod type. A notch (dimension A: 10.32 mm, angle: 45 ° and radius: 0.25 mm) with ten samples are prepared. The shore hardness (ASTM D2240) was measured and recorded by using a durometer in the broadest segment of the sample specimen. In this test, a sample fabricated with different variety of material insert was used. In addition, the results are reported in the form of standard deviation and mean deviation.

Figure 4.8 Universal Tensile Testing Machine (EMICDL2000)

A TAQ20 Differential Scanning Calorimeter (DSC) in figure 4.9 was used to measure the percentage crystallinity of the mouldings. The sample mass was weighing 8 mg, the heating rate was 10° C / min and the nitrogen flow rate was 50 ml /min. To avoid the skin region, samples were taken from the central region of the tensile specimens (Harris et al., 2004).

Figure 4.9 TA Q20 Differential Scanning Calorimeter

A computer numerical control (CNC) Bridgeport mill was used in two experiments to determine whether post-processing of 3D printing dies helped to increase the ductility of molded tensile bars. In the other experiment the same CNC mill shown in figure 4.10 the edges of the molded tensile bars were machined as shown in Figure 4.11.

Figure 4.10 CNC Bridgeport Mill used to post process the Digital ABS mold and tensile

Figure 4.11 Milling the Edges of a Molded Tensile Bar

In DSC analysis, a single scan was performed for individual specimen to record the past thermal data of the polymer. In order to avoid heat due to mechanical cutting, the sample was cut with a hand cutter and extracted from the molded product. Before going to testing, samples were stored in desiccant crystals.

4.7. Results and discussion

During the inspection of digital ABS insert a catastrophic failure was not observed. Figure 4.12 demonstrates the three dimensional surface outline of the printed digital ABS, after 20 shots and after 40 shots. Table 4.4 shows the surface quality data of the cavity considered. The "line" produced in the course of printing process are apparent in figure 4.12. As shown in figure 4.12, the peak-to-peak mean distance is 0.68 mm, and the waviness profile is shown at the mid of the measurement surface in figure 4.12 (a). The generated contours were duplicated on the molding surface and easily seen in Figure 4.14. In addition, no surface finishing was performed. Consequently, better surface quality in molding can be achieved by post processing of the insert cavity prior to injection for removing these ‘lines’. Figures 4.12 (b) and 4.12 (c) and Table 4.4 illustrates that there is no significant change in the quality of surface profile after 20 and 40 injection cycles.

Table 4.4 Digital ABS cavity surface quality

Tensile cavity	**Insert Stage**		
	As printed	20 shots	40 shots
Max. peak height (μm)	10.43	12.46	11.89
Roughness (Sq) = root mean square of height (μm)	5.192	5.472	5.033
Max. valley depth (μm)	15.45	14.02	13.69

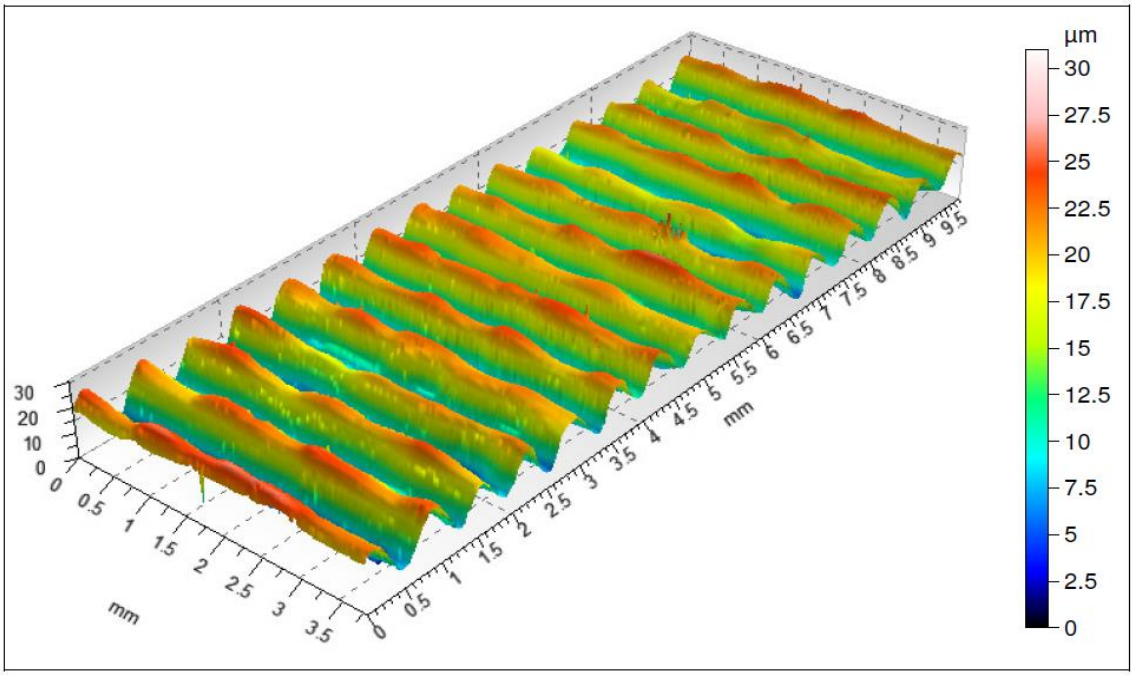
µm
30
27.5
25
22.5
20
17.5
15
12.5
10
7.5
5
2.5
0
mm
mm

(a)

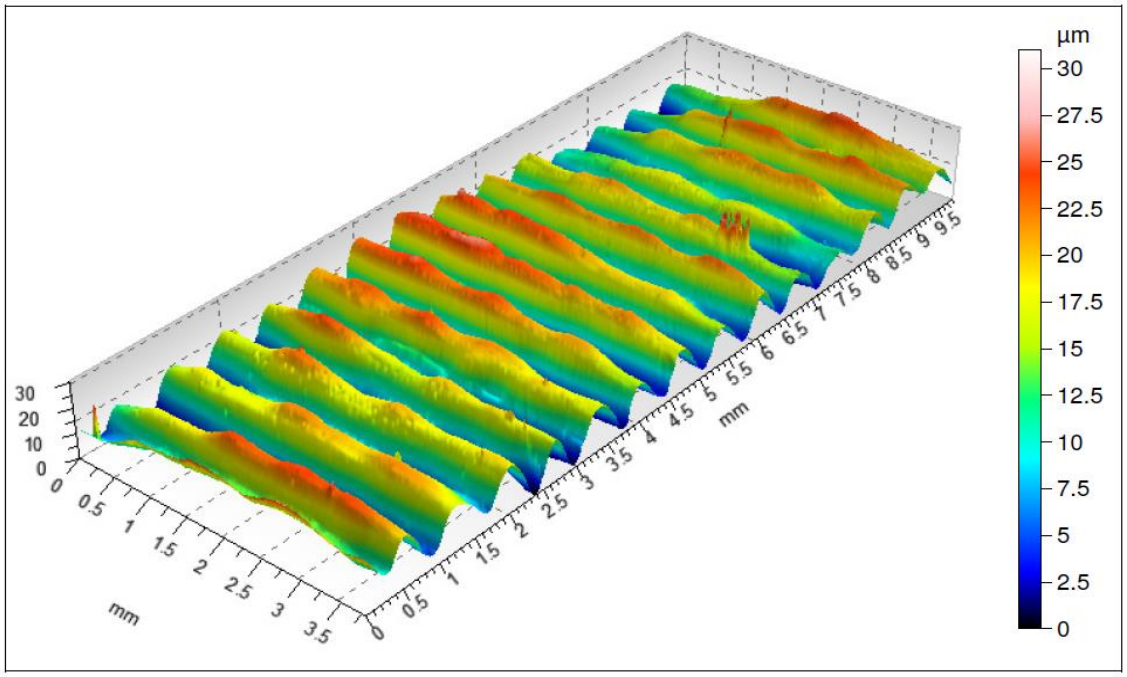
µm
30
27.5
25
22.5
20
17.5
15
12.5
10
7.5
5
2.5
0
mm
mm

(b)

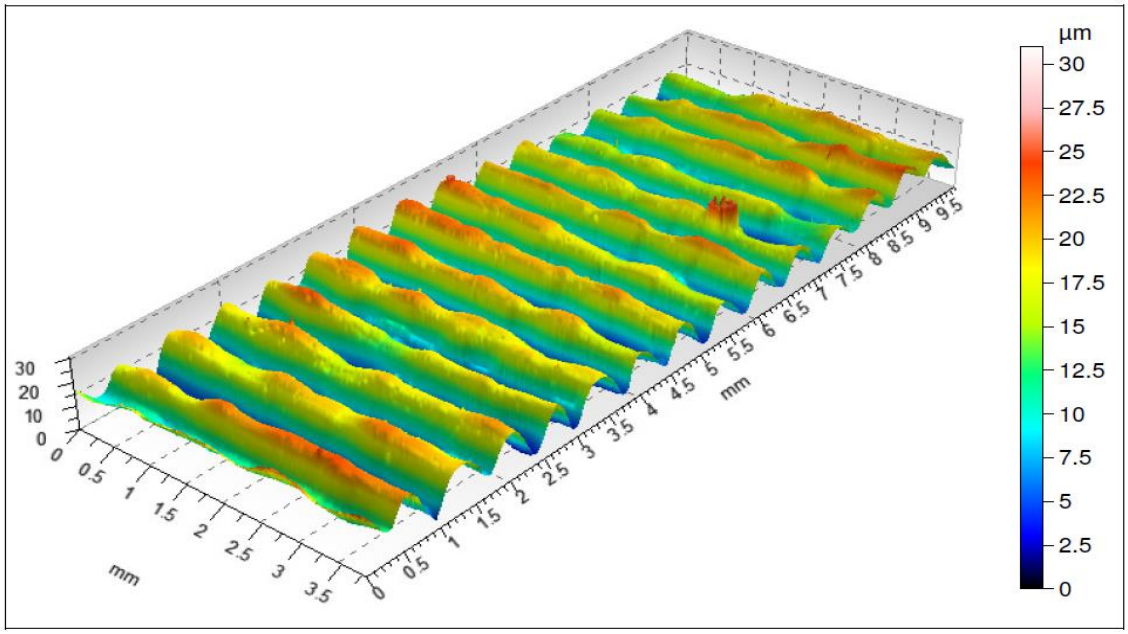

(c)

Figure 4.12 Three-dimensional surface profile of cavity as (a) printed, (b) after 20 shots and (c) after 40 shots

The peak attenuated slightly and the common surface profile (i.e. 'line') was upheld. In addition, the distance did not change either between peak and valley. The peak was anticipated to stabilize, but this did not happen. These results point out that the digital ABS is exceptionally stable against the number of trials and the number of injection parameters used. Table 4.5 clearly shows the dimension measurement results of the digital ABS cavity which is obtained by means of CMM after 20 shots and 50 shots and also Figure 4.15 confirms the same results. The dimensional specifications of the cavity including the length and breadth are slightly increased after 20 shots and decreased after 40 shots. The necessary clamping force to hold the mold closed is the main cause of the minor everlasting distortion (length and width reduction) at the end of the injection. To evade sparks, the mold structure inserts were mounted so that their surfaces touched against the metal plates. In contrast to dimensional characteristics that were reduced, there is slight increase in the cavity depth. The differences witnessed in all the three measurements are less and within the 3D printer precision.

Figure 4.13 CMM Measurement

Table 4.5 Digital ABS cavity CMM measurements

Parameters (mm)	**stage**		
	As printed	**20 shots**	**40 shots**
Tensile Cavity			
Length	118.325 (0.013)*	118.351 (0.067)	118.310 (0.024)
Width (middle)	6.072 (0.003)	6.145 (0.026)	6.035 (0.018)
Depth	3.605(0.032)	3.587(0.094)	3.679(0.074)
Bending Cavity			
Length	131.005 (0.022)	131.012 (0.041)	130.961 (0.033)
Width (middle)	13.027(0.009)	13.041 (0.025)	12.989 (0.056)
Depth	3.375 (0.031)	3.354 (0.045)	3.438 (0.059)

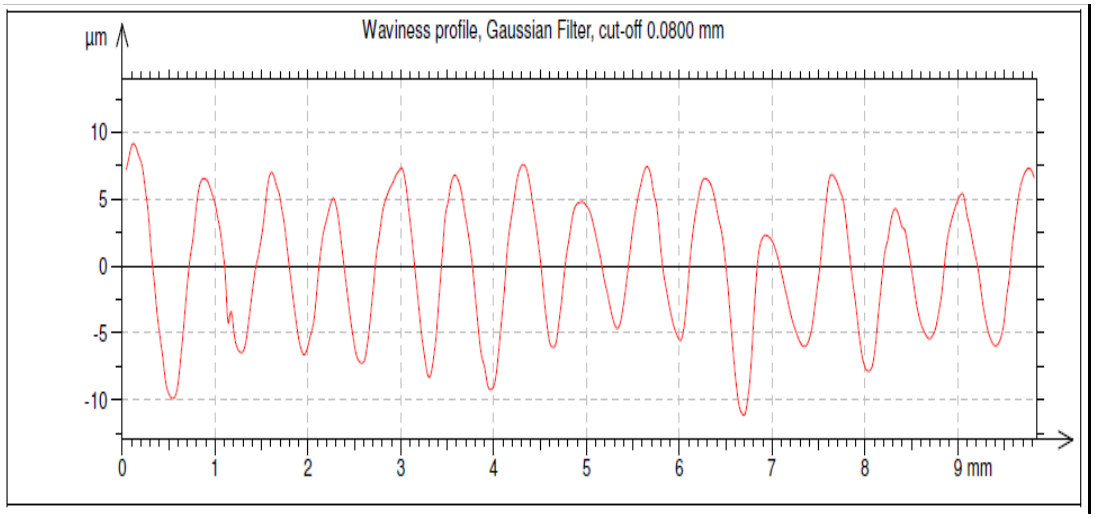

Figure 4.14 2D waviness profile (at 1.80 mm)

Figure 4.15 Surface details of the tensile sample after 6 shots

Table 4.6 shows the variations in the dimensions of the molded parts. The table shows the mean size of 5 samples at the commencement, 5 injected into the middle (18-23) and the last 5 during the injection process. The sample length increases marginally as the number of shots increases (0.16% from the first sample to the last sample). A minor decrease in the dimension was detected in the mold cavity (Table 4.4) and is not identified in the sample. The primary reason is because of the usage of dissimilar resolutions of the measuring instruments and the different techniques.

Table 4.6 Average Dimensions of PET samples after injection in the Digital ABS cavity

Features (mm)	Specimens		
	Shots 1 - 5	**Shots 18 -23**	**Shots 35-40**
Tensile specimen			
Length	118.05 (0.12)	119.06 (0.13)	119.12 (0.03)
Thickness	3.57 (0.01)	3.67 (0.04)	3.78 (0.02)
Width	6.37 (0.02)	6.42 (0.01)	6.46 (0.03)
Bending specimen			
Length	129.60 (0.21)	130.46 (0.12)	130.56 (0.23)
Thickness	3.33 (0.02)	3.40 (0.04)	3.37 (0.01)
Width	13.23 (0.03)	13.31 (0.02)	13.26 (0.02)

4.7.1 Mechanical properties and Crystallinity - Table 4.7 shows the crystallinity of PET molded products of the two inserts used. For molded articles made with insert of digitalized ABS, the crystallation is lesser in comparison to the manufactured steel insert. The present outcomes were not anticipated, because the poor heat transfer rate in case of digital ABS reveals that the PET material solidify slowly in order to give polymer chains more time to self-organize (Segal and Campbell, 2001; Martinho et al., 2009). In addition, the heat transfer rate is increased with integration of cooling system inside the metal inserts. Bareta et al. (2007) found nearly the same values for PET injected into P20 steel feed (39.28%) and epoxy resin feed (39.18%) using similar calculation method of crystallinity. Salmoria et al. (2008) reported using another method 87.4% for a crystallinity of PET injected into an epoxy resin insert and 70.5% for PET injected into a steel mold. In both cases a PET homo-polymer is used. Crystallinity is not reported in both the cases, but Cunha et al. (1992) found several changes in the form of PET homo-polymer and PET copolymer.

Table 4.7 PET specimens Crystallinity test results after injection in mold inserts

Insert material	SAE 1045	ABS
Heat of fusion ΔH (J/g)	81.24	71.65
Crystallinity χ (%)	39.27	34.59

Tables 4.8 and 4.9 illustrated the results of tensile and bending tests respectively. In the tensile test case, the material injected into the insert of digital ABS have a elasticity modulus of about 3% improved than its equivalent value for the molded object made with the SAE 1045 insert. Though, the tensile strength is quite similar for the inserts.

Table 4.8 PET specimens tensile test results after injection in mold inserts

Insert material	SAE 1045	Digital ABS
UTS (MPa)	22.14 (0.47)	23.35 (0.46)
Modulus of elasticity (MPa)	896.68 (46.91)	916.54 (49.96)

In the bending test, a comparison of the molded parts produced by Digital ABS and SAE 1045 result the maximum tensile strength of about 24% and in the elastic modulus of about 19% is increased. Other similar studies have reported the increase in modulus of elasticity

Table 4.9 PET specimens bending test results after injection in mold inserts

Insert material	SAE 1045	Digital ABS
Tensile strength (MPa)	23.35 (0.92)	27.75 (1.33)
Modulus of elasticity (MPa)	638.19 (22.51)	764.69 (39.34)
Yield strength (MPa)	17.87 (0.71)	20.69 (1.45)

The increase of tensile strength and elastic modulus of digital ABS and SAE 1045 is shown in table 4.9. The impact test results are shown in Table 4.10. The impact strength of the injected PET material into the digital ABS insert was about 32% more than the corresponding numerical value of the molded part manufactured using the SAE 1045 insert.

Table 4.10 PET specimens impact test results after injection in mold inserts

Insert material	SAE 1045	Digital ABS
Impact strength (J/m)	40.78 (4.93)	54.47 (3.59)
Absorbed energy (J)	0.13 (0.02)	0.17 (0.01)
Absorbed energy %	12.96	15.67

Cunha et al. (1992) attracted the attention for the fact that the influence on impact strength is not only by crystalline but also by spherical and sized thickness. Therefore, for a better understanding of these effects, more detailed morphological analysis is required. Table 4.11 shows the hardness test results of PET specimens injected into the insert. No significant changes were detected.

Table 4.11 PET specimens Hardness test results after injection in mold inserts

Insert material	SAE 1045	Digital ABS
Hardness (Shore D)	64 (0.7)	65 (0.5)

4.8 Chapter Summary

This chapter examined the use of digital ABS material on RT applications, taking into consideration the surface stability along with the dimensional stability in the injection process and their effect on the ultimate molding properties. The outcome of the results reveal that a simple geometry, molding material and the total number of injections shots can be performed in a commercial injection molding machine with insert of digital ABS without any shattering calamity. After the fifty trails, there is a minor sufferings in the cavity, which is permanent distortion, however the surface quality is not affected and the surface maintained its original feature. Thus, digital ABS has shown a decent dimensional and texture stability for the duration of the plastic injection molding process. The digital ABS mold insert properties differed slightly from those of molded parts with metal inserts. First of all, a slight improvement in elasticity module and tensile strength is noted based on different studies performed. Second, there was a 30% or more significant improvement in impact strength is observed. The same hardness among was found in the molded articles produced using two different inserts.

CHAPTER-5

Volumetric Shrinkage Estimation of Benchmark parts

This chapter determines the volumetric shrinkage of common benchmark features for thermoplastic polyethylene terephthalate (PET) injection molded components made using digital Acrylonitrile butadiene styrene (ABS) mold. These benchmark features are found almost in each and every mold component. The effect of each benchmark feature on the dimensional characteristics of the parts produced is examined in this section. Therefore, twelve standard benchmark CAD model were selected with different geometric attributes. Subsequently, simulation analysis was performed on all CAD model using Moldflow® (MFA) simulation software. Additionally, regression analysis is applied to recognize the effect of injection molding parameters on the volumetric shrinkage of part made using rapid tooling mold insert of digital ABS material. It is found that maximum volumetric shrinkage (18.75 %) is observed for square pyramid frustum, conical frustum, and solid torus. On the contrary, hollow rectangular prism shows minimum shrinkage effect having 12.61 % of volumetric shrinkage. This study predicted that shrinkage is the main concern for these three geometric features (i.e. square pyramid frustum, conical frustum, and solid torus) and must be looked for its minimization. This work is extended in the next chapter for complex feature component. In that the component consist the standard benchmark features in a single part and the results are experimentally validated, by 3D scanner integrated with COMET plus and Inspect plus software. Since shrinkage estimation for digital ABS mold using Rapid Tooling technique has not been attempted before, therefore, this study provides guidance for the optimum parameter selection and assigning suitable shrinkage compensation values for digital ABS mold made using direct rapid tooling.

5.1 Design and development of benchmark feature component

In this study, PET material is selected for simulation of the plastic injection molding process using digital ABS rapid tool mold insert. Properties of the selected polymer

material are listed in table 5.1. The selected twelve benchmark parts (figure5.1) consists of standard geometric features which are generally used in any industrial component.

1.Cylinder	2. Rectangular Prism	3.Hollow Cylinder	4.HollowRectangular Prism
5.Square Pyramid	6.Square Pyramid Frustum	7.Hollow Square Pyramid Frustum	8.Conical Frustum
9.Hollow Conical Frustum	10.Rectangular Prism Hollow with Cylinder	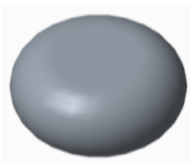 11.Solid Torus	12.Hollow Torus

Figure 5.1 3D Model of benchmark parts using Autodesk inventor solid modeling software

5.2 Material selection and properties- Digital ABS is selected for mold material. The properties of the digital ABS are detailed in chapter 3. The material PET is selected to inject inside the mold for development of test specimen. The input parameters and range of PET material is reported in table 5.1.

Table 5.1 Input parameter of thermoplastic material polyethylene terephthalate (PET)

Parameter	**Range Value**	
Elastic Modulus (MPa)	1574.77	1530.86
Coefficient of thermal expansion (1/ ^{0}C)	0.00010	0.00015
Poisson ratio	0.35	0.44

Parameter	Value
Melt density Liquid (g/cm^3)	0.73
Melt density Solid (g/cm^3)	0.89
Shear modulus (Mpa)	523.90
Specific heat ($J/kg-^0C$)	2740
Thermal conductivity ($W/m-^0C$)	0.16

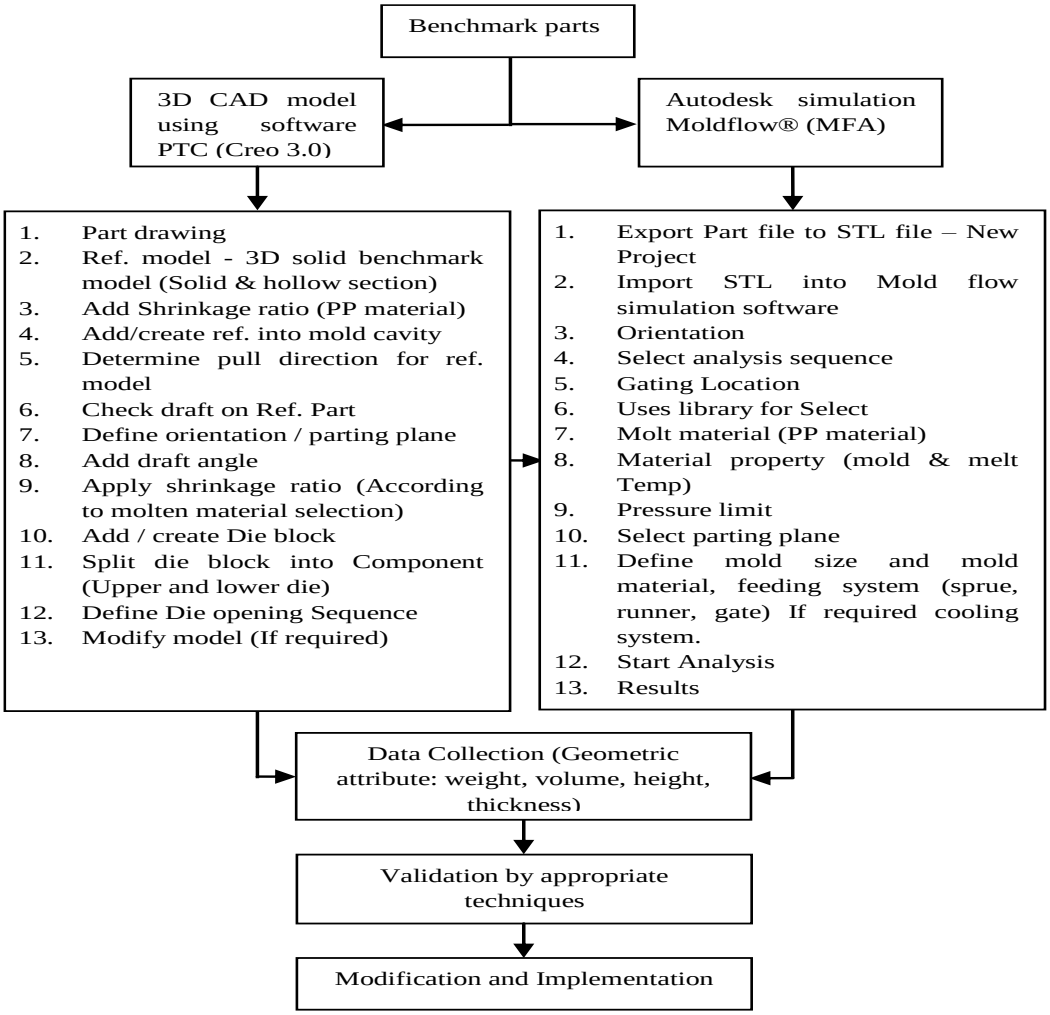

Figure 5.2 Process flow diagrams for simulation and analysis

Figure 5.2 shows the process flow diagram describing a sequence of steps for modeling and simulation of twelve benchmark parts using Autodesk inventor 3D modeling and Moldflow® (MFA) software respectively. Tooling design requires (i) orientation of the

parting plane (ii) scaling the model to accommodate for shrinkage allowance according to molten material selection (iii) generating draft angle (iv) splitting the part geometry at parting line to create die and cavity shapes.

The value of shrinkage ratio is different for different material and depends upon type of molten plastic material. One of the significant steps for modeling the benchmark part is to apply shrinkage ratio actually for particular material. Standard benchmark CAD model in .stl file format is used as an input for simulation study.

Table 5.2 and 5.3 shows the mold material (Digital ABS) properties and default simulation setting parameter is considered for PET material respectively. The Moldflow® (MFA) analysis is performed after assigning a molten material with similar analysis for all benchmark parts throughout the injection molding process. The material used to perform this experiment is commercially available for injection molding of products, refer table 5.1.

Table 5.2 Input parameter of mold material (Digital ABS)

Thermal Properties		**Mold mechanical properties**	
Parameter	**Value**	**Parameter**	**Value**
Mold density (g/cm^3)	1.2	Elastic modulus (MPa)	3000
Mold specific heat (J/kg-°C)	1900	Poisson ratio	0.23
Mold thermal conductivity (W/m-°C)	0.27	Mold coefficient of thermal expansion (1/°C)	0.0000074

Table 5.3 Simulation process setting parameter for Digital ABS mold

Melt temperature (^0C)	240
Mold temperature (^0C)	40
Packing pressure (MPa)	80
Packing time (s)	10
Maximum machine injection pressure (MPa)	180

5.3 General considerations for design of standard benchmark parts – Before development of core and cavity of all the standard benchmark features, the bounding box volume need to be calculated according to the input parameters. The input parameters for

bounding box volume for individual parts are bounding box dimension, height, draft degree, thickness; shrinkage value of injected material is reported in table 5.4

Table 5.4 General consideration for bounding box volume of benchmark features

	Parts Images	Bounding Box Dimension (L×W×H) mm	H (mm)	Draft degree	Thickness (mm)	Shrinkage for Polyethylene material	Part volume before Shrinkage (mm)	Part volume after shrinkage (mm)	BB vol for BM parts
1. Cylinder		35×35×20	20	1.5	20	0.001	19242.3	20424.5	24500
2.Rectangular Prism		31×31×20	20	1.5	20	0.001	19220	20479	19220
3.Hollow Cylinder		65×65×20	20	1.5	10	0.001	18849.6	21454.9	84500
4.Hollow Rectangular Prism		55×55×20	20	1.5	10	0.001	2000	22764.4	60500
5.Square Pyramid		54×54×20	20	0	20	0.001	19440	20029.1	58320

6.Square Pyramid Frustum		35×35×20	20	0	20	0.001	18166.7	18717.1	24500
7.Hollow Square Pyramid Frustum		40×40×20	20	0	10	0.001	20361.7	20978.7	32000
8.Conical Frustum		40x40x20	20	0	20	0.001	19373.2	19960.2	32000
9. Hollow Conical Frustum		50×50×20	20	0	10	0.001	21991.1	22657.5	50000
10.Rectangular Prism Hollow with Cylinder		45x45x20	20	1.5	10	0.001	21257.7	23468.1	40500
11.Torse	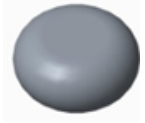	40*40*20	20	0	20	0.001	20341.6	20958	32000
12. Hollow Torse 10thk		50*50*20	20	0	10	0.001	19739.2	20337.3	50000

5.3.1 Geometric Attributes consideration

Geometric attributes are used to estimate the dimensional accuracy of the part features developed by a particular machine. The geometric features (shape and size) like volume of part, height, thickness and draft angle considered in this study. The weight of benchmark part model and the total weight (included sprue) of a same part model measured from the CAD software (considering the density value of PET molten material = 0.000738 g/mm^3), the volume is obtained of all twelve benchmarks parts with using mass property function in Autodesk Inventor 3D modeling software.

5.3.2 Volume Ratio (VR): It is the ratio of the benchmark parts volume as obtained using the 1+S formulas for shrinkage factor calculation, Here 'S' denote shrinkage ratio to the bounding box volume. The bounding box volume assumes the maximum length, width, and height of the part geometry. The volume of all the reference parts considered is the same and is nearly about to 20000 mm^3, where S = Shrinkage ratio (0.01 to 0.025).

$$V_R = V/V_B \tag{5.1}$$

5.3.3 Thickness Ratio (TR): This is the ratio of the minimum thickness of benchmark part to the maximum height of the same part.

$$T_R = T_{Min}/H_{Max} \tag{5.2}$$

5.3.4 Draft Angle Ratio (D_R): It is the ratio of draft angle in parts to the standard draft angle consideration which is maximum up to 3^0 depending on the height of parts. In this study, the height constraint of all twelve benchmarks parts is same (20 mm).

$$D_R = \frac{D_A}{S_{DA}} \tag{5.3}$$

5.3.5 Part Weight Ratio (W_R): It is the ratio of part weight to the total weight of the part.

$$W_R = \frac{W}{W_T} \tag{5.4}$$

5.3.6 Quality Prediction Ratio (Q_R): This is the ratio of quality prediction percentage to the desired quality (say 100 %) of all benchmarks parts.

$$Q_R = \frac{QP\%}{QP_{100\%}} \tag{5.5}$$

5.3.7 Cycle Time Ratio (CT_R): This is the ratio of cooling time to the total cycle time.

$$CT_R = \frac{C_T}{TC_T} \tag{5.6}$$

Table 5.5 Geometric attribute data compiled for regression analysis

Part Sr. No.	V	V_B	V_R	T_{Min}	H_{Max}	T_R
1	19242.3	24500	0.7854	20	20	1
2	19220	19220	1	20	20	1
3	18849.6	84500	0.223072	10	20	0.5
4	2000	60500	0.330579	10	20	0.5
5	19440	58320	0.333333	20	20	1
6	18166.7	24500	0.741498	20	20	1
7	20361.7	32000	0.636303	10	20	0.5
8	19373.2	32000	0.605413	20	20	1
9	21991.1	50000	0.439822	10	20	0.5
10	21257.7	40500	0.524881	10	20	0.5
11	20341.6	32000	0.635675	20	20	1
12	19739.2	50000	0.394784	10	20	0.5

Part Sr. No.	**D_A**	**S_{DA}**	**D_R**	**W**	**W_T**	**W_R**
1	1.5	3	0.5	14.19	15.606	0.90939
2	1.5	3	0.5	14.18	15.694	0.903244
3	1.5	3	0.5	13.9	18.593	0.747717
4	1.5	3	0.5	14.75	19.855	0.742926
5	0	3	0	14.35	15.464	0.92775

6	0	3	0	13.41	14.337	0.935133
7	0	3	0	18.2	16.308	1.116262
8	0	3	0	14.3	15.256	0.937165
9	0	3	0	16.23	17.39	0.933264
10	1.5	3	0.5	15.69	18.139	0.864889
11	0	3	0	15.46	15.946	0.969355
12	0	3	0	14.57	15.543	0.937241

The above steps were involved in design criteria framework for Rapid Tooling injection molding process; it includes tooling design (die and cavity), simulation and the statistical technique. Finally, these results are validated by using regression method.

5.4 Mold design for standard benchmark parts using Autodesk inventor 3D modeling Software – In this section, the mold was prepared according to their part geometry. The stepwise methods are given below.

5.4.1 Deign procedure to generate a core and cavity -The defined work piece feature allows you to create a rectangular or cylindrical work piece that is a prerequisite for creating the core and cavity. For a rectangular work piece, set the length, width, height, and distance to control the shape of the work piece. For a cylindrical work piece, set the diameter and height of the work piece. The defined work feature offers product dimensions as design references. A preview function immediately displays the changes in the dimensions. Creating a satisfactory parting surface (interface) is a critical step in designing a successful injection molding tool. The right interface guarantees that the construction of core and cavity is suitable. It also ensures that the plastic part can be removed from the mold. In Inventor Mold Design, the interface is divided into two parts, the patch surface and the runoff surface also called drain surface.

5.4.1.1 Procedure to create the patching surface

Many plastic parts have holes or slots that need to be patched. It can be create a patch interface for an internal opening using the following patch tools:

Figure 5.3 Procedure to create patching surface

In this process patch a plastic part with several holes. Then, use manual selection or auto-detection to create patch surfaces. After that, patch the loop with open end. For the existing surfaces, Use this option if you cannot create a patch surface with other patch tools. Although creating a patch surface is the most common command, the others are helpful if you have different requirements. After designing the work piece, define the runoff area. The runner off surface divides the work piece and removes the plastic part from the mold. To generate a runoff area the following tools: The Create runoff feature uses manual selection or automatic detection to generate a runoff surface. If automatic loop recognition is not appropriate for your needs, edit the loop and select it manually. If the automatic runoff surface that is created automatically is not appropriate, it can use the remaining methods to create a runoff surface. If it cannot create a runoff surface using these methods, then use “existing surface" function is the other option. It can create faces in the part and design environment and import them as a runoff surface. The Create Runoff Surface function manually selects or automatically determines the runoff cycle on the plastic part and creates a runoff surface on the loop. If you want to select edges in an area without edges, use the Split Face tool to divide the part. Then select the resulting edges to create a runoff loop.

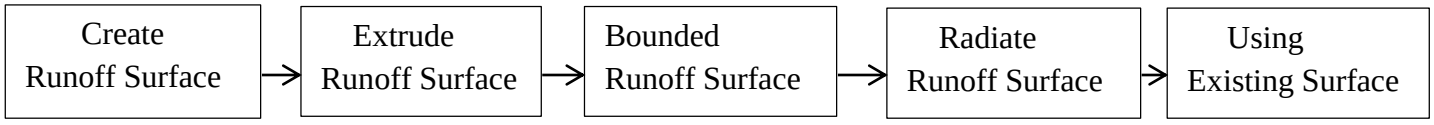

Figure 5.4 Create runoff areas

A single runoff loop is selected on the part. Sometimes the recognized runoff loop is correct, but the surface based on the runoff loop is not generated accurate. In this case, change the direction of the surface to obtain a satisfactory runoff area. If the design of the part is complex, it takes more time to detect the runoff loop.

1. Cylinder

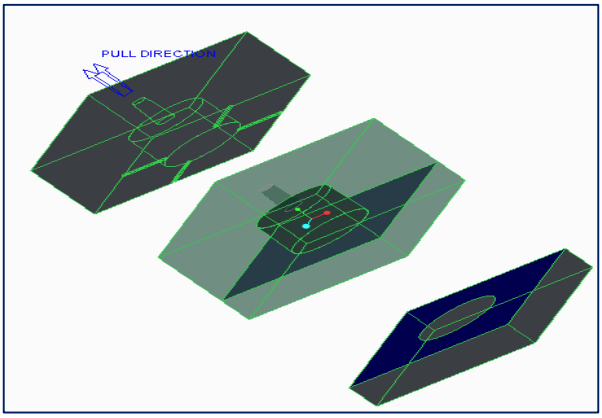

2. Rectangular prism

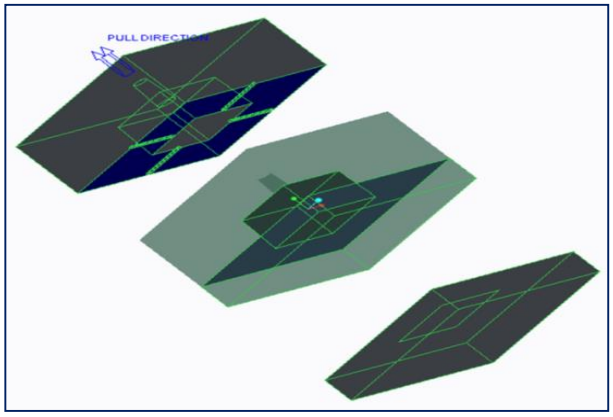

3. Hollow Cylinder

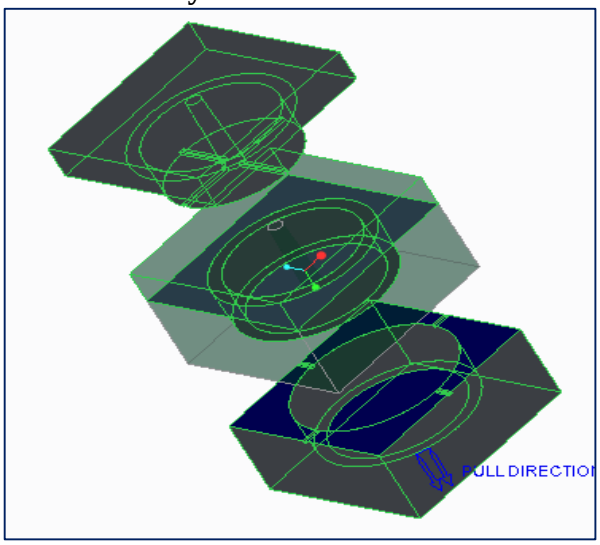

4. Hollow rectangular prism

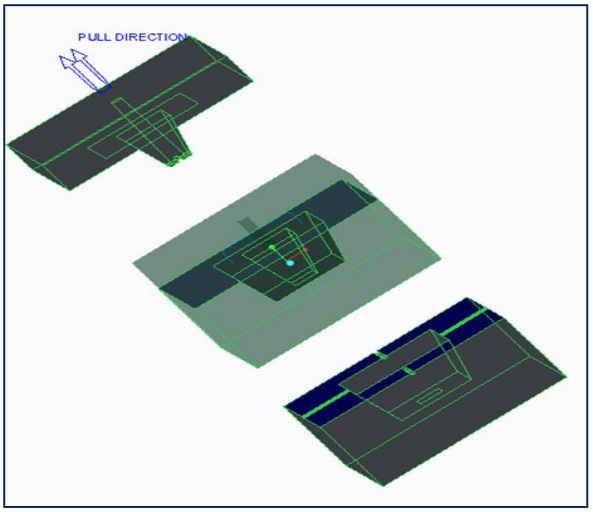

5. Square pyramid

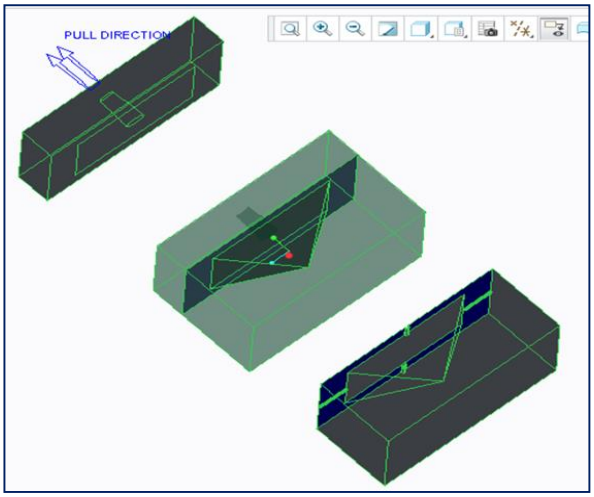

6. Square pyramid frustum

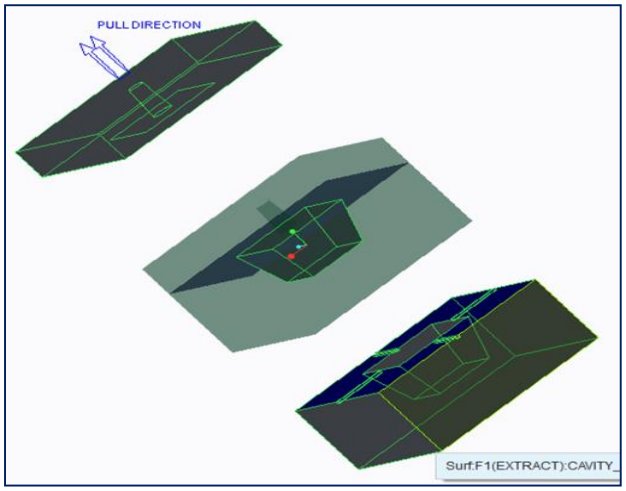

7. Hollow Square pyramid frustum

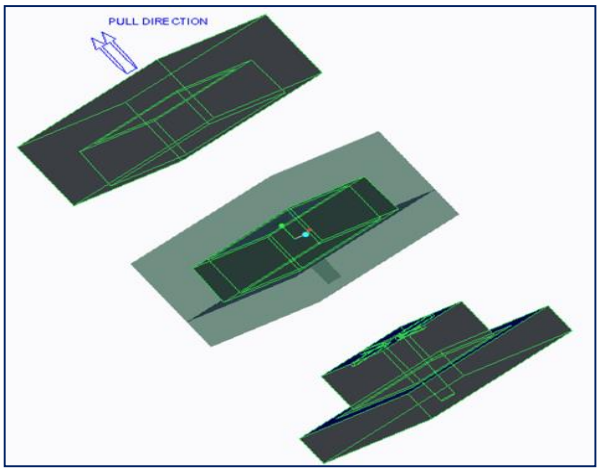

8. Conical Frustum

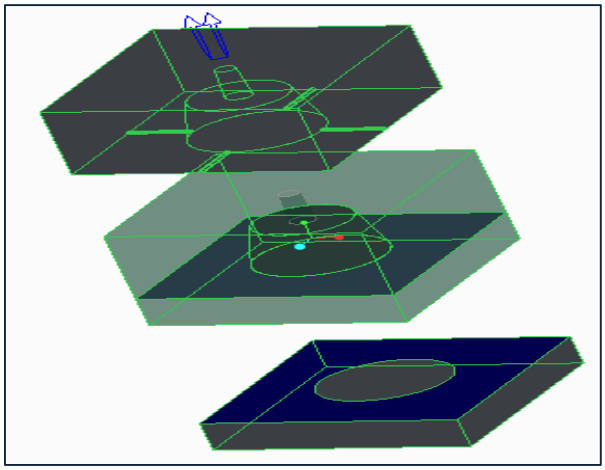

9. Hollow Conical Frustum

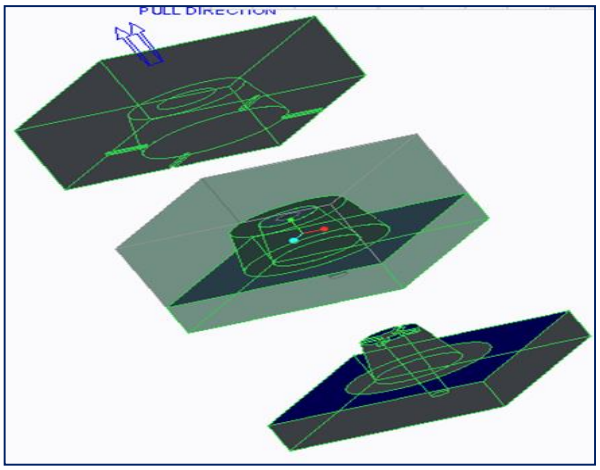

10. Rectangular prism Hollow with cylinder

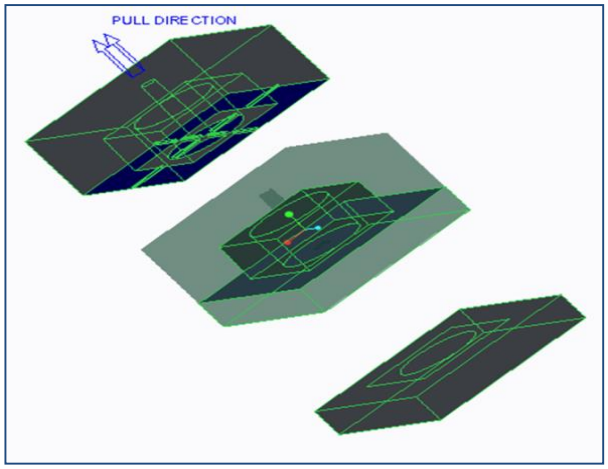

Figure 5.5 Core and Cavity for all Benchmark features

5.5 Moldflow Simulation Results and Analysis for the Benchmark Parts

Simulation is performed on Moldflow® (MFA) FEM software. Simulation study was done to evaluate and advise the injecting location, observed defects (air trap, weld lines, shrinkage, warpage), cycle time (fill time, packing time, cooling time, mold-open time) in order to be able to improve the accuracy in the injection molded parts made using Digital ABS Rapid Tooling Mold Inserts. In this process, Solid Geometry imports mesh from Parasolid®-based CAD systems, Autodesk Inventor software, and STEP universal files. Then, scan imported geometry and automatically fix errors that may occur during translating a model from the CAD software. After that review, correct, repair, and

make it simple; solid models carried from 3D-CAD systems to prepare them for simulation. Then, perform 3D simulations for all features using a fixed, tetrahedral finite element mesh technique. The result of the simulation study for a single benchmark part is shown in figure 5.6 as an example; similarly it is preceded for the rest of the benchmark parts reported in figure 5.7.

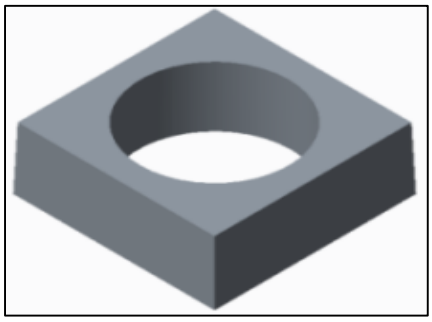

Part model

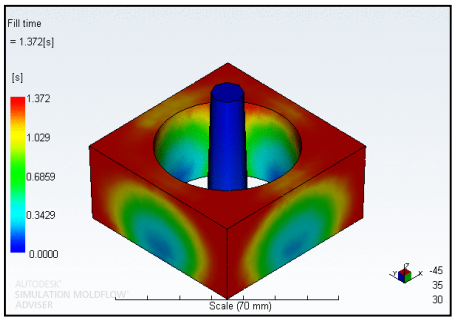

Filling time

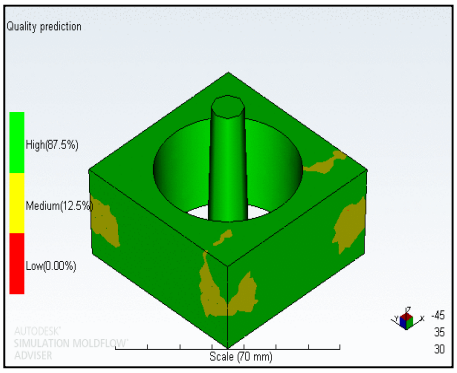

Quality prediction percentage

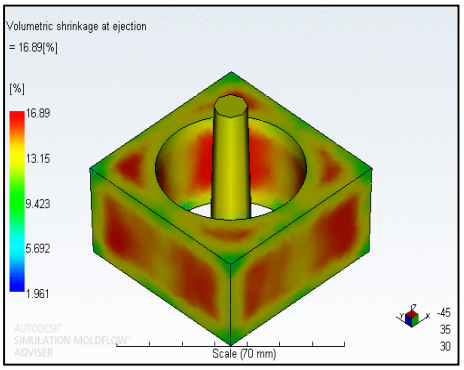

Volumetric shrinkage percentage

Figure 5.6 Moldflow® (MFA) simulation results for Rectangular Prism Hollow with Cylinder

1. Cylinder

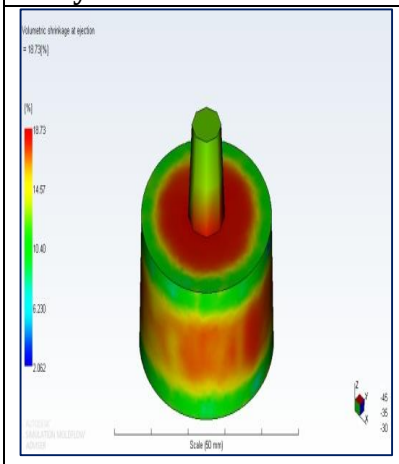

Volumetric shrinkage -18.73%

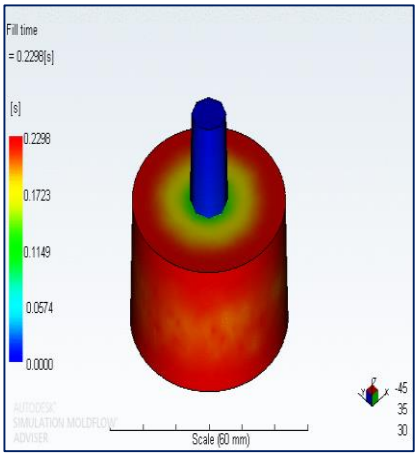

Filling Time - 0.2298

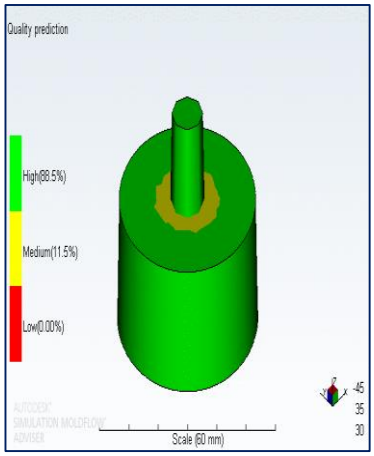

Quality prediction % 88.5

2. Rectangular prism

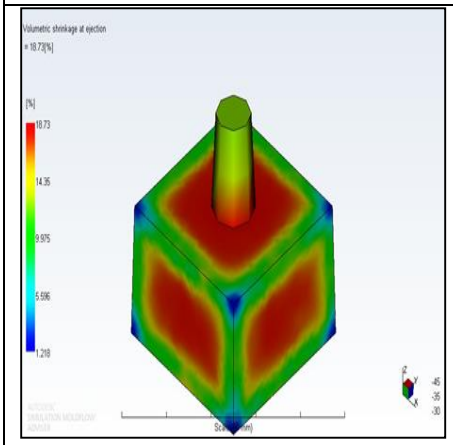

Volumetric shrinkage -18.73 %

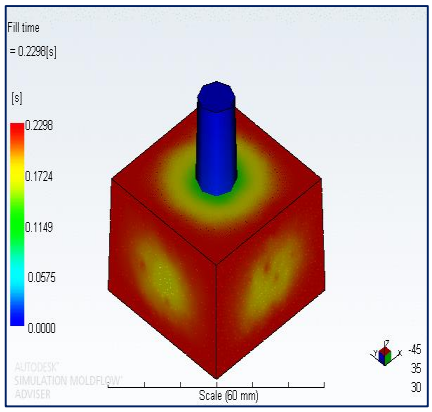

Filling Time - 0.2298

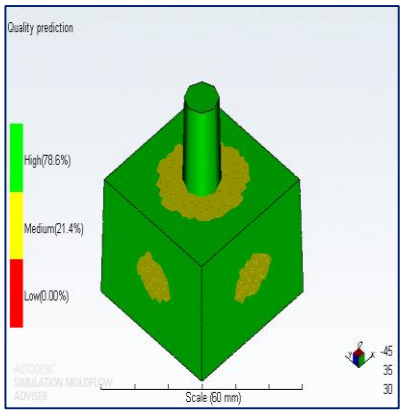

Quality prediction % **78.6**

3. Hollow cylinder

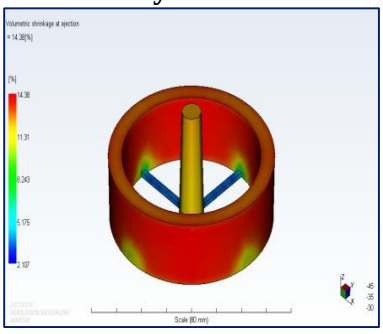

Volumetric shrinkage- 14.38 %

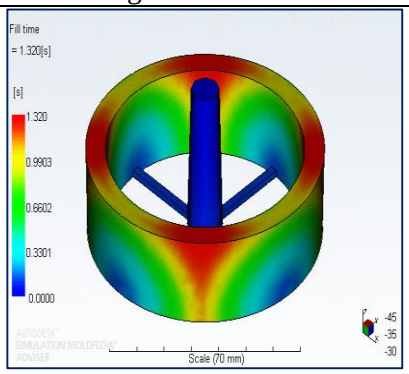

Filling Time -1.320

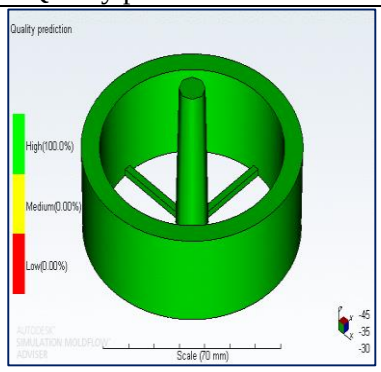

Quality prediction % 100%

4. Hollow rectangular prism 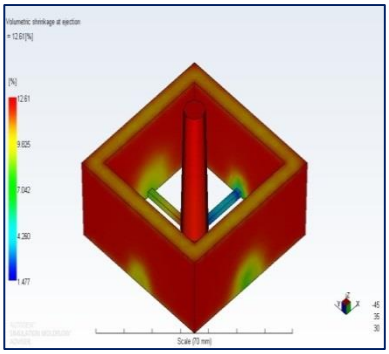 Volumetric shrinkage -12.61 %	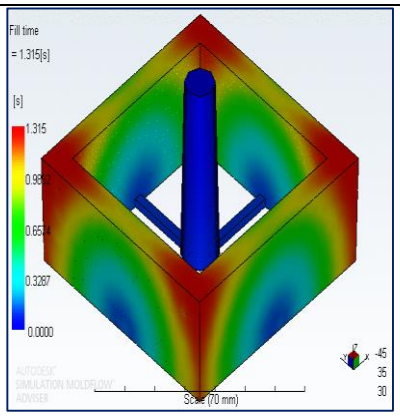 Filling Time -1.357	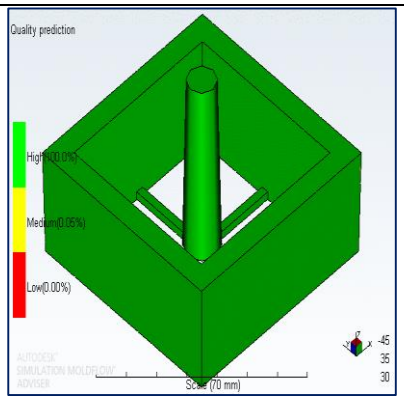 Quality prediction % 100%
5.Square pyramid 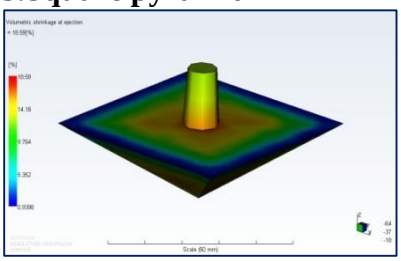 Volumetric shrinkage -18.59 %	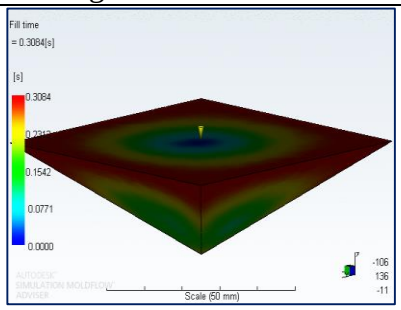 Filling Time - 0.3084	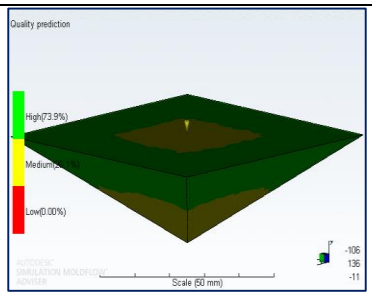 Quality prediction % 73.9
6. Square pyramid frustum 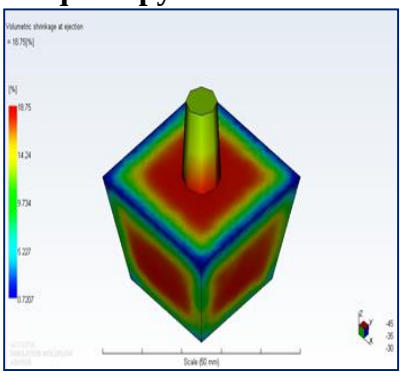 Volumetric shrinkage -18.75 %	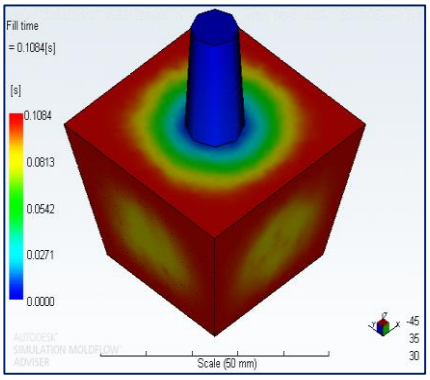 Filling Time - 0.1084	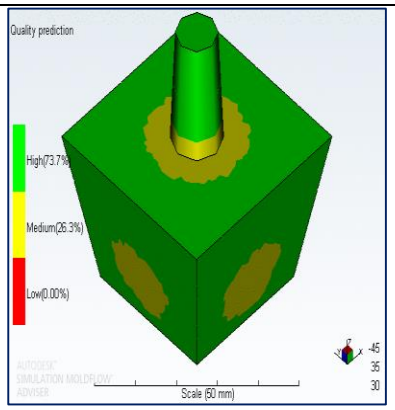 Quality prediction % **73.7**
7. Hollow Square pyramid frustum 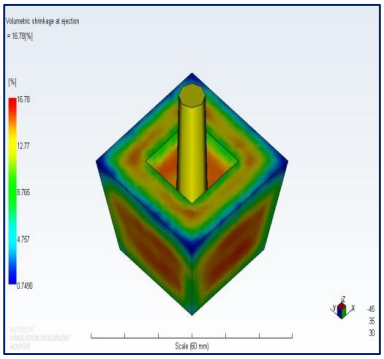 Volumetric shrinkage - 16.78 %	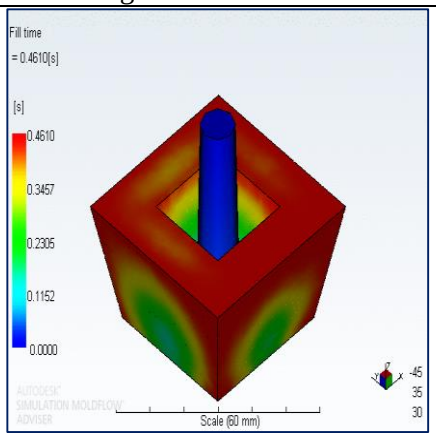 Filling Time – 0.4610	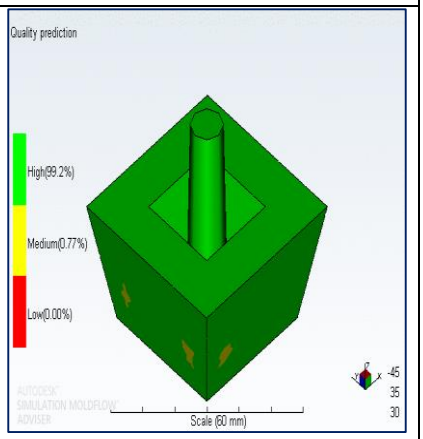 Quality prediction %99.2

8. Conical Frustum 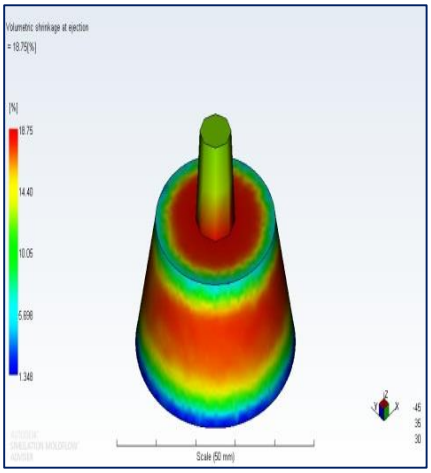 Volumetric shrinkage – 18.75 %	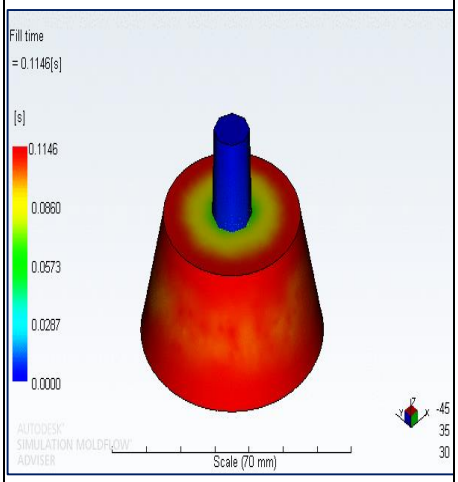 Filling Time – 0.1146	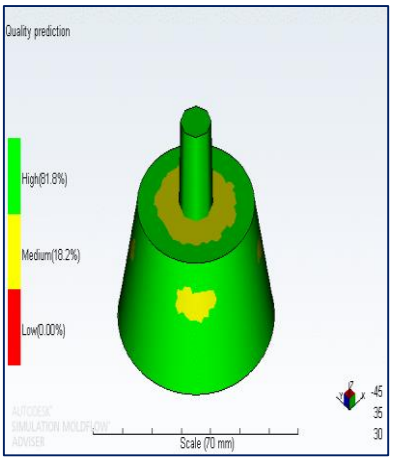 Quality prediction %81.4
9. Hollow Conical Frustum 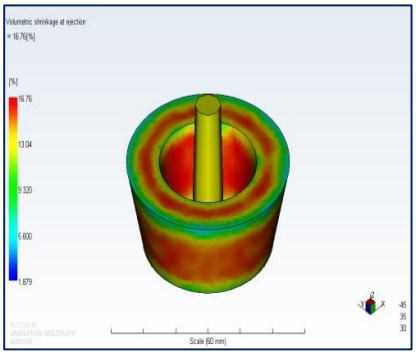 Volumetric shrinkage – 16.76 %	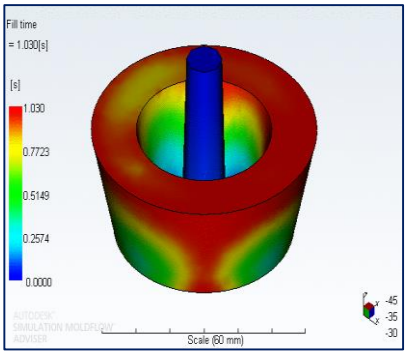 Filling Time – 1.030	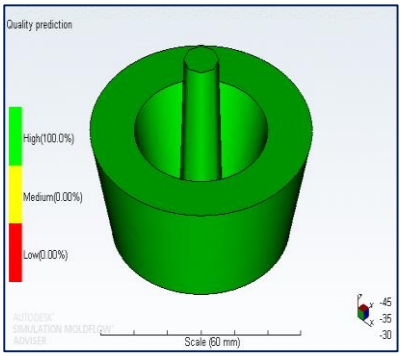 Quality prediction % 100
10. Rectangular prism hollow with cylinder 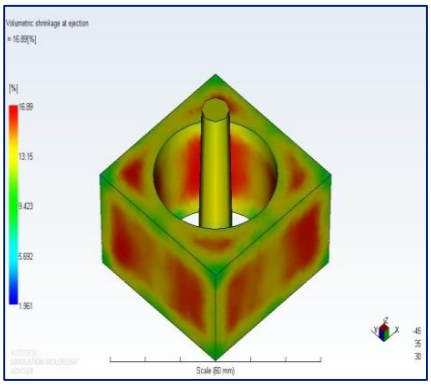 Volumetric shrinkage – 16.89%	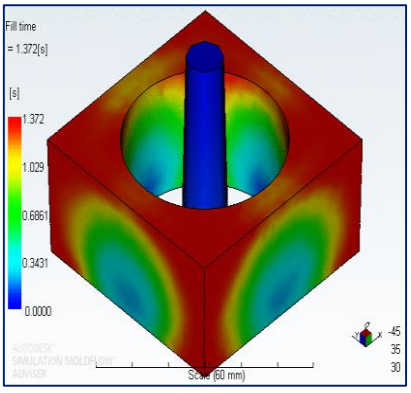 Filling Time – 1.372	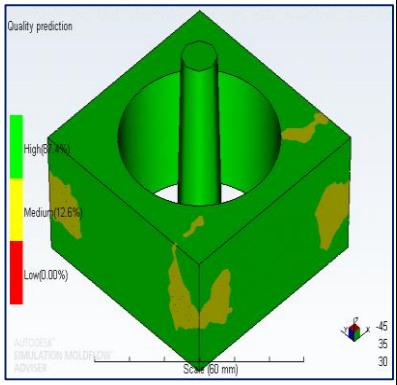 Quality prediction % 87.4

Figure 5.7 Simulation results of all benchmark features using Autodesk simulation moldflow software

The geometric features were related to the die and cavity, and the injection molding process consists of melting of the polymer and then it is injected into the mold cavity. After the determination of the number of input parameters and the range of their changeability, the design of experiments performed by statistical software.

Table 5.6 (B1) Moldflow® (MFA) simulation results in data compiled for regression analysis

Part Sr. No.	**QP**	**$QP_{100\%}$**	**QP_R**
1	88.5	100	0.885
2	79.8	100	0.798
3	100	100	1
4	100	100	1
5	72.4	100	0.724
6	73.7	100	0.737
7	99.4	100	0.994
8	81.4	100	0.814
9	100	100	1
10	87.5	100	0.875
11	97.4	100	0.974
12	100	100	1

Table 5.6 (B2) Moldflow® (MFA) simulation results compiled for regression analysis

Part Sr. No.	C_T	TC_T	CT_R	VS %
1	495.85	511.07	0.970219	18.73
2	483.33	498.54	0.969491	18.73
3	32.75	49.05	0.667686	14.38
4	32.75	49.04	0.667822	12.61
5	329.62	344.84	0.955864	18.59
6	459.3	474.41	0.96815	18.75
7	296.2	311.66	0.950395	16.78

8	485.66	500.88	0.969613	18.75
9	141.48	157.51	0.898229	16.76
10	165.8	182.17	0.910139	16.89
11	512.39	527.61	0.971153	18.75
12	131.14	147.38	0.889809	16.8

5.5 Result and discussion

The mathematical model is developed in term of the polynomial equation that is established to show the influence of geometric attribute and processing parameters on the volumetric shrinkage percentage equation 5.7. The software Minitab® was used to analyze and obtain different coefficients of the polynomial equation for the purpose.

Table 5.7 Input parameter of simulation of PET injection molding – simulation design

Benchmark Parts	V_R	T_R	DA_R	QP_R	W_R	CT_R	VS%	FITS	RESI	SRES	COEF
1	0.7854	1	0.5	0.885	0.90939	0.970219	18.73	18.78087	-0.05087	-0.1368	2.969242
2	1	1	0.5	0.798	0.903244	0.969491	18.73	18.55407	0.175932	0.48532	-0.78007
3	0.223072	0.5	0.5	1	0.747717	0.667686	14.38	13.53569	0.844313	2.181226	2.188646
4	0.330579	0.5	0.5	1	0.742926	0.667822	12.61	13.47175	-0.86175	-2.2225	-0.09633
5	0.333333	1	0	0.724	0.92775	0.955864	18.59	18.73608	-0.14608	-0.61613	0.795644
6	0.741498	1	0	0.737	0.935133	0.96815	18.75	18.61514	0.134863	0.388234	-3.66397
7	0.636303	0.5	0	0.994	1.116262	0.950395	16.78	16.83422	-0.05422	-0.83577	17.43075
8	0.605413	1	0	0.814	0.937165	0.969613	18.75	18.80062	-0.05062	-0.10286	
9	0.439822	0.5	0	1	0.933264	0.898229	16.76	16.75346	0.006535	0.015468	
10	0.524881	0.5	0.5	0.875	0.864889	0.910139	16.89	16.99762	-0.10762	-0.37201	
11	0.635675	1	0	0.974	0.969355	0.971153	18.75	18.81321	-0.06321	-0.18385	
12	0.394784	0.5	0	1	0.937241	0.889809	16.8	16.62726	0.17274	0.380694	

$$\textbf{VS\%} = 2.97 - 0.78\ V_R + 2.19\ T_R - 0.10\ DA_R - 3.66\ W_R + 0.80\ QP_R + 17.43\ CT_R \quad (5.7)$$

$$S = 0.562051,\ R\text{-sq} = 96.37\%,\ R\text{-sq (adj)} = 92.01\%$$

The regression equation for estimating volumetric shrinkage percentage for all twelve benchmark parts designs using geometric attributes and the Moldflow® (MFA) simulation results obtained in Table 5.6 and Regression graph show in Figure 5.8.

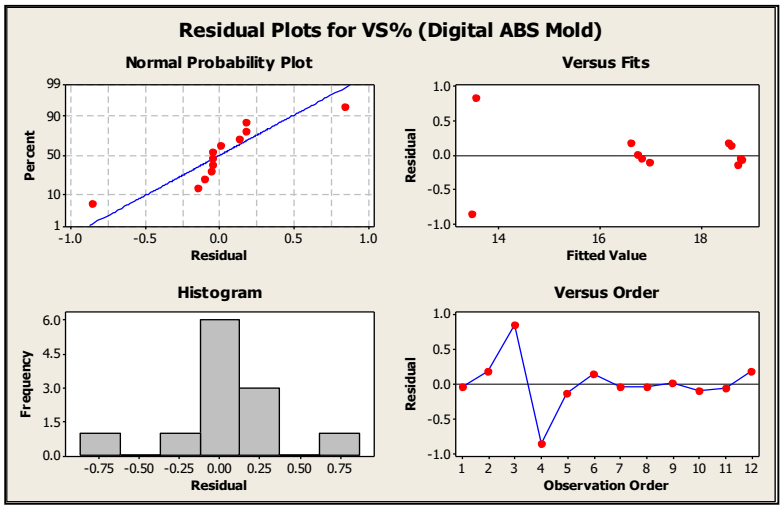

Figure 5.8 Regression graph for volumetric shrinkage percentage

5.6 Chapter Summary

Linear regression models are most powerful statistical techniques for solving optimization problems and can affluence complicated relationships among several variables. They help in explaining the correlation between dependent variable (volumetric shrinkage), with determined values of one or more independent variables (VR, TR, DAR, WR, QPR, CTR). To model the process, a mathematical function with a linear polynomial curve is used. Therefore, correlation coefficients, R_ Square value, of the equations for volumetric shrinkage of 96.37%, calculated which explores the volumetric shrinkage of a linear relationship between the simulation data and the expected values from the regression model. Based on this R^2 test, quadratic polynomial models are best fitted for the output. The normal probability distribution of shrinkage defect residuals of the ABS mold shows that the residuals are mostly fall on a straight line, with the errors being normally distributed and obviously showing that the resulting quadratic modal is precisely more accurate. It can easily notice from the Table 5.7, highest volumetric shrinkage percentage (18.75 %) results are obtained for square pyramid frustum, conical frustum, and solid torus, and the lowest volumetric shrinkage percentage of 12.61 % is achieved for the hollow rectangular prism, which is investigated through Moldflow® (MFA) simulation software.

Hence, from the above literature it can be determined that, the process of rapid tooling plays a significant role in injection molding and simultaneously this process is an important issue also. The exact numerical simulation of this process is a challenging task. In this work, the polyjet technology was adopted to manufacture the component by injection mold inserts. The work is carried out for complex feature component in the next chapter, where these benchmark features are integrated in a solitary part and it is experimentally checked.

CHAPTER- 6

Volumetric Shrinkage and Warpage Estimation of Complex Parts

This chapter deals with the study of volume shrinkage and warpage results of complex parts that is extended work of previous chapter for benchmark parts. For this purpose an electronics component relay is considered as a sample produced from digital ABS mold integrated with straight cooling channels. The resulting volumetric shrinkage and warpage is investigated for various benchmark features integrated in a solitary component. The PBT/PET molten material is used to inject into the mold to produce the required constituent. A systematic methodology is proposed for analyzing volumetric shrinkage and warpage in an injection molded part having a thin shell structure during the injection molding process. Initially, the effects of the injection process parameters on shrinkage and warpage for various wall thicknesses were examined using Taguchi method. The shrinkage and warpage values were found by Moldflow insight software. The shrinkage and warpage was analyzed and predicted by the acquired mathematical models for the individual effects of all parameters. The results of performing confirmatory experiments and analysis of variance (ANOVA) ensure that the quadratic models of shrinkage and warpage are well fitted with the simulated values at the optimum value.

6.1 Development of Core and Cavity for complex feature component

Digital ABS is used in the present study to make mold inserts with cooling channel to improve the part quality and mold efficiency. The straight cooling system is inserted in mold. The results that belong to cooling system were taken as (cooling channel diameter: 8 mm, the distance between cooling channel and the part: 8mm, No of straight cooling channels: 4, the distance between the channels centers: 8 mm).

For this study, the diameter of cooling channel and gate location are considered as design factors along with melt temperature, packing pressure and packing time as process parameters are used to model and optimize the results of shrinkage and warpage for a

relay cover. The resulting volumetric shrinkage and warpage is investigated for the benchmark features that are mounted in the component.

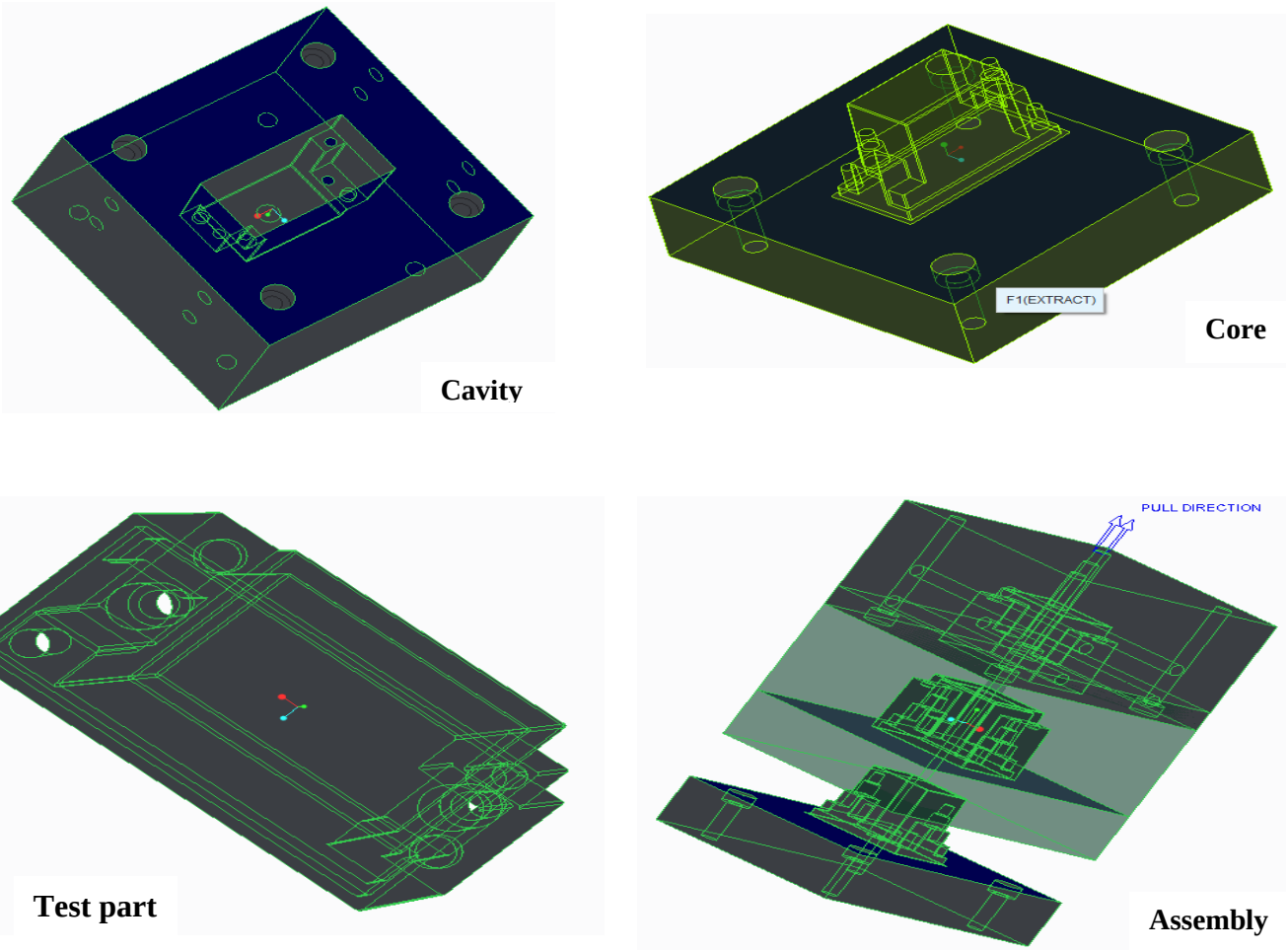

Figure 6.1 Development of Core and Cavity for test part

6.2 Design of injecting plastic part

An electronic part component (relay) as shown in figure 6.1 was considered as a sample for analysis contains complex geometry. It was designed with Autodesk Inventor 3D modeling software. The dimensions of the part component are 72 mm× 34 mm × 48.5 mm. Three different wall thickness 0.8 mm, 0.9mm and 1 mm was considered for the analyses.

6.2.1 Best gate location

An analysis of the best gateway location was done in the MPI software to determine where to place the location of the gateway in simulations. Figure 6.2 shows the outcome of this analysis. Based on the result of the analysis using MPI software, it is required to put the gate to the red colour area as in figure 6.2.

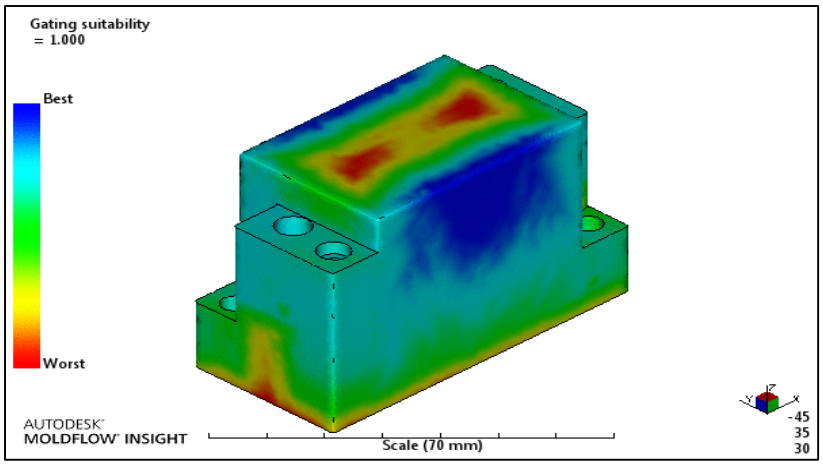

Figure 6.2 Result of best gate location analysis

6.3 Employed parameters

Some of the important processing parameters such as filling time, mold temperature, gate dimensions and locations, melt temperature, packing pressure, and packing time are always used in injection molding. The mold temperature, melt temperature, packing time, packing pressure respectively are the most influential factors to determine warpage defects. In this study, the injection parameters are considered as Melt temperature, packing time and packing pressure for digital ABS material.

The operating parameters which were used for the shrinkage and warpage analysis for this work are melt temperature, packing pressure, packing time. The parametric values for the analysis are shown in Table 6.1.

Table 6.1 Optimal process parameters and levels

Levels	A: Melt temperature (°C)	B:Packing pressure (MPa)	C: Packing time (s)
1.	254	25	10
2.	266	30	15
3.	278	35	20

In Table **6.1**, the values for the melt temperature, the packing pressure and packing time were taken from MPI 4.0 database. Here, the mold temperature is not considered because of its poor thermal conductivity, the heat transfer rate is very slow between the mold and the part. The mold takes more time to cool Hence; the defective parts are produced which need to be improved. To provide uniform and rapid cooling, a straight cooling channel is inserted inside the mold and simultaneously employs a supercritical CO2 cooling spray on plastic mold to decrease the plastic mold temperature to 9°C before each shot. Later, the experiments were performed by molding with PBT/PET in the Digital ABS tool at a slower injection speed and a lower melt temperature.

6.4 Simulation study for PBT and PET materials - Simulation of (1mm, 0.9mm and 0.8 mm) wall thickness for Polybutylene Teraphthalate (PBT) as well as Polyethylene terephthalate (PET) plastic material at optimum process parameters: By L9 Orthogonal array using Moldflow Insight software.

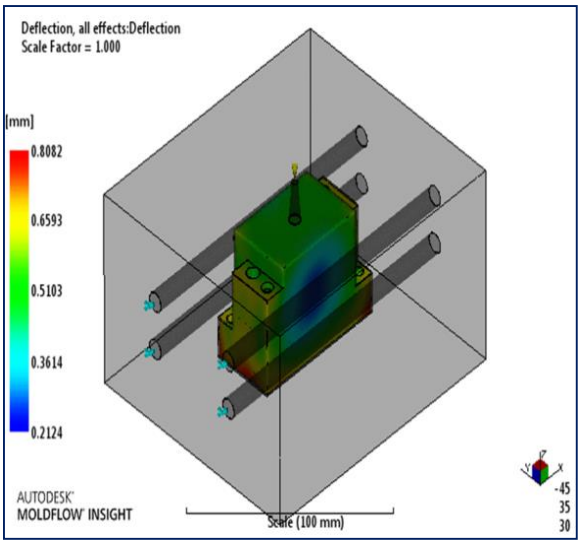

Deflection, all effects: Deflection

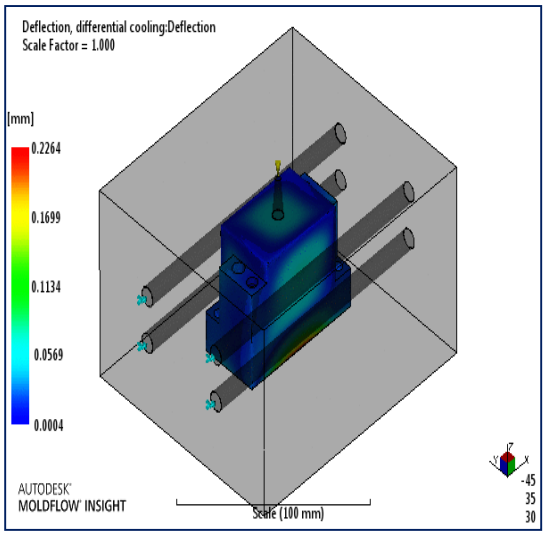

Differential cooling: Deflection

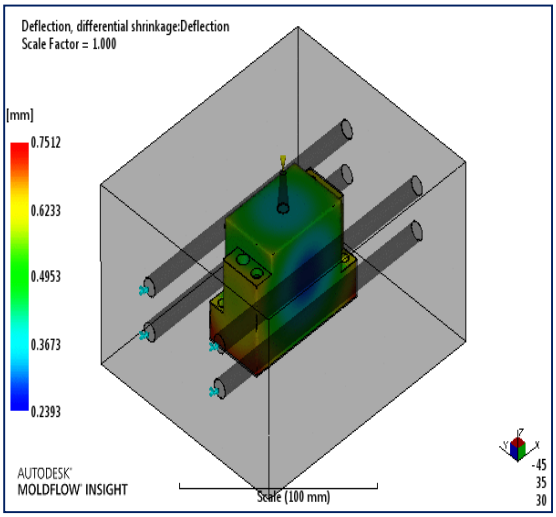

Differential shrinkage: Deflection

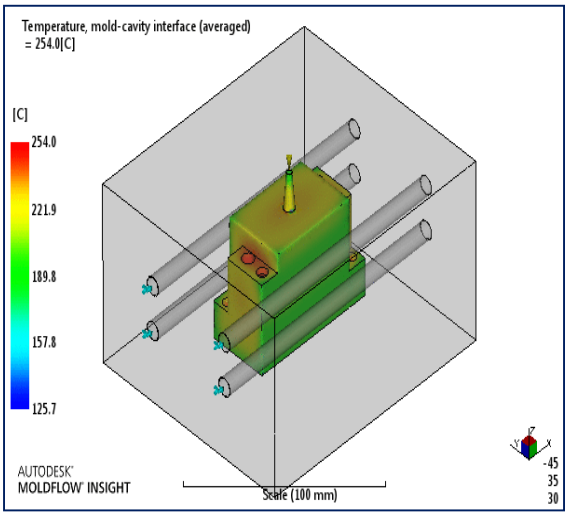

Temperature, mold-cavity interface (averaged)

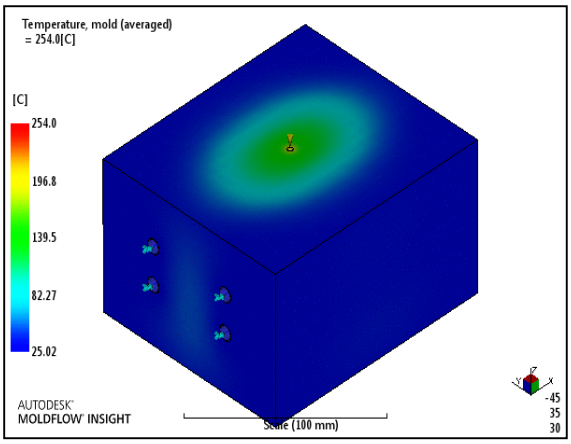

Temperature, mold (averaged)

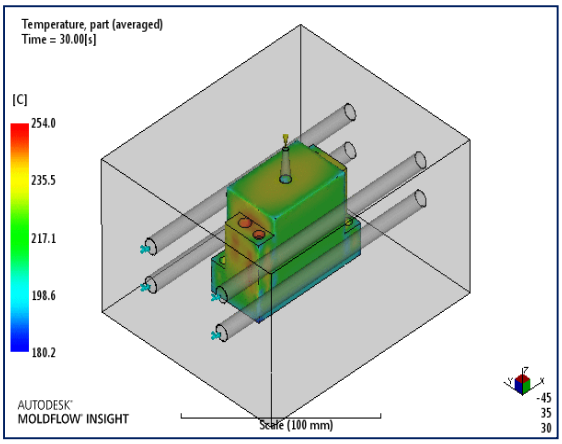

Temperature, part (averaged)

Figure 6.3 Simulation results of complex feature component for **0.8, 0.9** and for **1 mm** wall thickness for **PBT/PET** materials.

$$\text{Shrinkage} = \frac{Volume\ of\ liquid\ material}{Volume\ of\ Solidified\ material} < 1$$

Table 6.2 Simulation results for Shrinkage and Warpage of PBT and PET materials for 0.8, 0.9 and 1 mm wall thickness

For 0.8 mm part thickness					***Polybutylene Terephthalate* (PBT)**			***Polyethylene terephthalate* (PET)**		
	Melt Temp(°C) (A)	Packing Pressure MPa (B)	Packing Time (s) (C)	Deflection: all effect: deflection	Deflection: differential Shrinkage :Deflection	Volumetric shrinkage %	Deflection: all effect: deflection	Deflection: differential Shrinkage :Deflection	Volumetric shrinkage %
1	254	25	10	0.9432	0.8555	14.14	0.682	0.6427	13.38
2	254	30	15	0.9164	0.8318	14.29	0.6508	0.629	13.35
3	254	35	20	0.8813	0.8045	14.33	0.6198	0.6136	13.3
4	266	25	15	0.9341	0.8413	15.11	0.6525	0.6076	13.89
5	266	30	20	0.8931	0.8062	15.35	0.6222	0.5972	13.83
6	266	35	10	0.857	0.7737	15.41	0.5942	0.5865	13.78
7	278	25	20	0.9076	0.8076	16.59	0.6108	0.5745	14.36
8	278	30	10	0.8596	0.7665	16.16	0.5874	0.568	14.31
9	278	35	15	0.801	0.7246	16.58	0.5701	0.5601	14.26

For 0.9 mm part thickness				***Polybutylene Teraphthalate* (PBT)**			***Polyethylene terephthalate* (PET)**		
	Melt Temp (°C) (A)	Packing Pressure MPa (B)	Packing Time (s) (C)	Deflection: all effect: deflection	Deflection: differential Shrinkage: deflection	Volumetric shrinkage %	Deflection: all effect: deflection	Deflection: differential Shrinkage: Deflection	Volumetric shrinkage %
1	254	25	10	0.9367	0.8388	15.17	0.66	0.6506	13.5
2	254	30	15	0.9029	0.822	15.31	0.6237	0.6321	13.47
3	254	35	20	0.8634	0.8029	15.34	0.6078	0.6138	13.35
4	266	25	15	0.9125	0.8085	16.09	0.6293	0.6132	13.96
5	266	30	20	0.8502	0.7761	16.08	0.5973	0.6005	13.92
6	266	35	10	0.7962	0.7624	16.13	0.579	0.5868	13.86
7	278	25	20	0.8117	0.7519	16.9	0.592	0.5784	14.38
8	278	30	10	0.7715	0.7374	16.88	0.571	0.5672	14.35
9	278	35	15	0.7441	0.7263	16.84	0.5546	0.558	14.3

For 1 mm part thickness					***Polybutylene Teraphthalate (PBT)***			***Polyethylene terephthalate (PET)***		
		Melt Temp (°C) (A)	Packing Pressure (MPa) (B)	Packing Time (s) (C)	Deflection: all effect: deflection	Deflection: differential Warpage: Deflection	Volumetric shrinkage %	Deflection: all effect: deflection	Deflection: differential Warpage: Deflection	Volumetric shrinkage %
	1	254	25	10	0.8082	0.7512	16.12	0.6497	0.5951	13.73
	2	254	30	15	0.8021	0.7463	16.12	0.6362	0.5704	13.76
	3	254	35	20	0.8045	0.7424	16.12	0.6797	0.5838	13.71
	4	266	25	15	0.7623	0.698	16.84	0.6289	0.5694	14.24
	5	266	30	20	0.7603	0.696	16.85	0.6241	0.5671	14.21
	6	266	35	10	0.7699	0.6982	16.81	0.6339	0.5703	14.23
	7	278	25	20	0.7491	0.6815	17.42	0.6105	0.5436	14.71
	8	278	30	10	0.7555	0.6816	17.42	0.6139	0.544	14.72
	9	278	35	15	0.7511	0.6812	17.4	0.6118	0.5437	14.73

6.5 Taguchi method

In this study, L9 (3^2) orthogonal array is shown in Table 6.2 which is employed with design of experiment method. Analyses were performed after locating the values from Table 6.4 to Table 6.5.

6.6 Analysis for injection molding

The analyses of the component has been done by MPI software. The type of the mesh was “3D tetrahedral”. The model consists for analysis is 23374 elements. PBT/PET materials were used for three different thickness values. MPI software is used to determine the best gate location to inject the molten material. The analysis has been done for cool +fill+ warp using MPI software. The total warpage and shrinkage values were found in X, Y and Z co-ordinates.

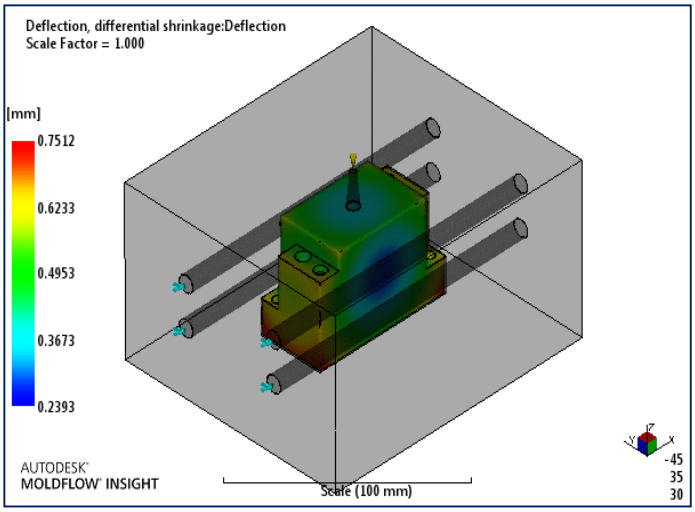

Figure 6.4 the exact gate location and finite element mesh

6.7 Analysis of three various wall thickness for PBT/PET materials

Analysis has been performed for three various wall thickness values 0.8, 0.9 and 1.0 mm using PBT/PET materials. Table 6.3 shows the results of these analyses. The shrinkage and warpage characteristics for these three values can be compared from these results. To evaluate the results of the analysis for PBT/PET materials, statistical methods have been used for these thickness values. The analyses were performed by Regression and ANOVA methods using MINITAB software for these values.

6.8 Regression analysis method

Regression analysis is the most versatile tool employing in research area. The basic concept of this technique is determining the effect of various factors on the outcomes during performing the experiments. The replication of the experiments may be one or more and the factors may be direct or indirect. The observation and the effected parameters must be shown with mathematical model while doing Regression analysis. The regression model also called generated model. The mathematical model includes variables while investigating the regression analysis. The variables must be able to count and can be measure also.

Table 6.3 L9 (3^2) Orthogonal Array Variance for Experiment

SI.	A	B	C	Warpage						Shrinkage					
Materials				PBT	PET	PBT	PET	PBT	PET	PBT	PET	PBT	PET	PBT	PET
Wall Thickness				0.8mm		0.9 mm		1.0mm		0.8mm		0.9mm		1.0 mm	
1.	1	1	1	0.9432	0.682	0.9367	0.66	0.8082	0.6497	15.17	13.38	14.14	13.73	16.12	13.5
2.	1	2	2	0.9164	0.6508	0.9029	0.6237	0.8021	0.6362	15.31	13.35	14.29	13.76	16.15	13.47
3.	1	3	3	0.8813	0.6198	0.8634	0.6078	0.8045	0.6797	15.34	13.30	14.33	13.71	16.18	13.35
4.	2	1	2	0.9341	0.6525	0.9125	0.6293	0.7623	0.6289	16.09	13.89	15.11	14.24	16.84	13.96
5.	2	2	3	0.8931	0.6222	0.8502	0.5973	0.7603	0.6241	16.08	13.83	15.35	14.21	16.85	13.92
6.	2	3	1	0.857	0.5942	0.7962	0.579	0.7699	0.6339	16.13	13.78	15.41	14.23	16.81	13.86
7.	3	1	3	0.9076	0.6108	0.8117	0.592	0.7491	0.6105	16.9	14.36	16.59	14.71	17.42	14.38
8.	3	2	1	0.8596	0.5874	0.7715	0.571	0.7555	0.6139	16.88	14.31	16.16	14.72	17.45	14.35
9.	3	2	2	0.801	0.5701	0.7441	0.5546	0.7511	0.6118	16.84	14.26	16.58	14.73	17.4	14.30

6.9 Warpage and shrinkage analysis for results evaluation

For the consideration of warpage as a mathematical model, more than one variable can be accepted that directly or indirectly effected in shrinkage and warpages. Now, for PBT material of 0.8 mm wall thickness the minimum and maximum warpage values are 0.801mm and 0.9432 mm respectively. Similarly for PET material for same wall thickness, the minimum and maximum warpage values are 0.5701mm and 0.682mm. For 0.9 mm wall thickness the minimum warpage for PBT material is 0.7441 mm and maximum warpage is 0.9367. For PET, it is 0.5546 mm is minimum and 0.66 mm is maximum. For 1.0 mm wall thickness, they are 0.7491mm minimum and 0.8082 mm is the maximum for PBT whereas, for PET it is 0.6105 mm and 0.6797 mm respectively.

Similarly, the minimum and maximum shrinkage of PBT material for 0.8 mm wall thickness is 15.17mm and 16.1 mm respectively. For PET material, it is 13.30 mm is the minimum and 14.30 mm is the maximum value. For 0.9 mm wall thickness, the minimum shrinkage for PBT material is 14.14 mm and 16.59 mm is the maximum shrinkage. Next, for the same thickness of PET material, it is 13.71 mm is the minimum and 14.76 mm is the maximum shrinkage. For 1 mm wall thickness, the minimum shrinkage for PBT material is 16.12 mm and maximum shrinkage is 17.45 mm. For PET material it is 13.35 mm is minimum and 14.38 mm is the maximum value of the shrinkage. The most influential factor for warpage and shrinkage of ABS material is packing pressure.

Table 6.4 Regression model for warpage and the R^2 values for PBT/PET material

Thickness (mm)	Regression model for PBT material	R^2 %
0.8	Warpage = 0.925 - 0.0322 Melt temp - 0.0336 Packing Pressure + 0.00377 Packing Time	90.9
0.9	Warpage = 1.05 – 0.0626 Melt temp– 0.0429 Packing pressure + 0.00348 Packing Time	96.9
1.0	Warpage = 0.831 - 0.0265 Melt Temp + 0.00098 Packing Pressure - 0.00328 Packing Time	97.6

Thickness (mm)	Regression model for PET material	R^2%
0.8	Warpage = 0.740 - 0.0307 Melt Temp - 0.0269 Packing Pressure - 0.00180 Packing Time	78.8
0.9	Warpage = 0.711 - 0.0290 Melt Temp - 0.0233 Packing Pressure - 0.00215 Packing Time	98.3
1.0	Warpage = 0.658 - 0.0216 Melt Temp+ 0.00605 Packing Pressure + 0.00280 Packing Time	98.7

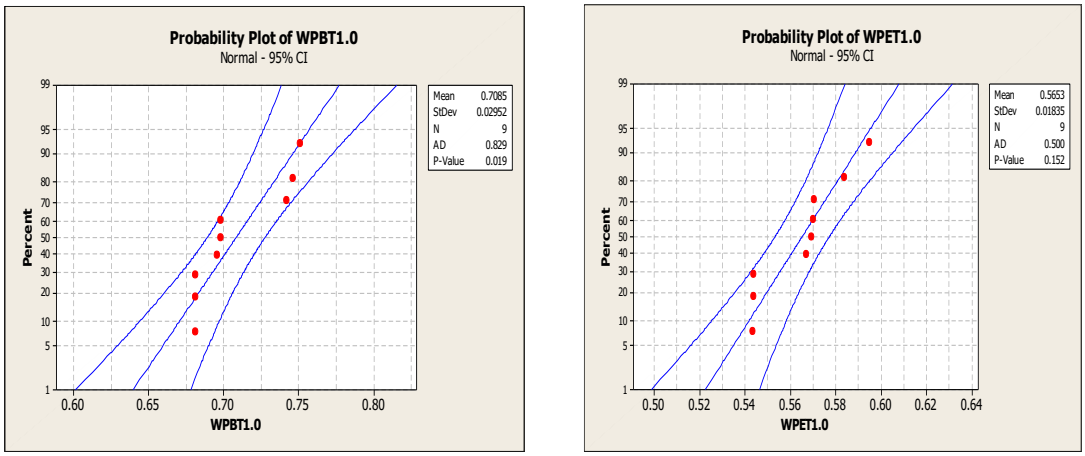

Figure 6.5 Normal probability plot for warpage of 1 mm wall thickness

The results of the Anderson-Darling (AD) standardity test are shown in Figure 6.5 for the respective distortion of PBT and PET for residues of 1 mm wall thickness. Since the p-value of the normality diagrams is over 0.05, it means that the rest follows the normal distribution, and the given models are suitable for practical technical applications. From the response surface plot (see Figure 6.6) it is observed that the warpage first decreases and then increases with increasing layer thickness for PBT and PET materials.

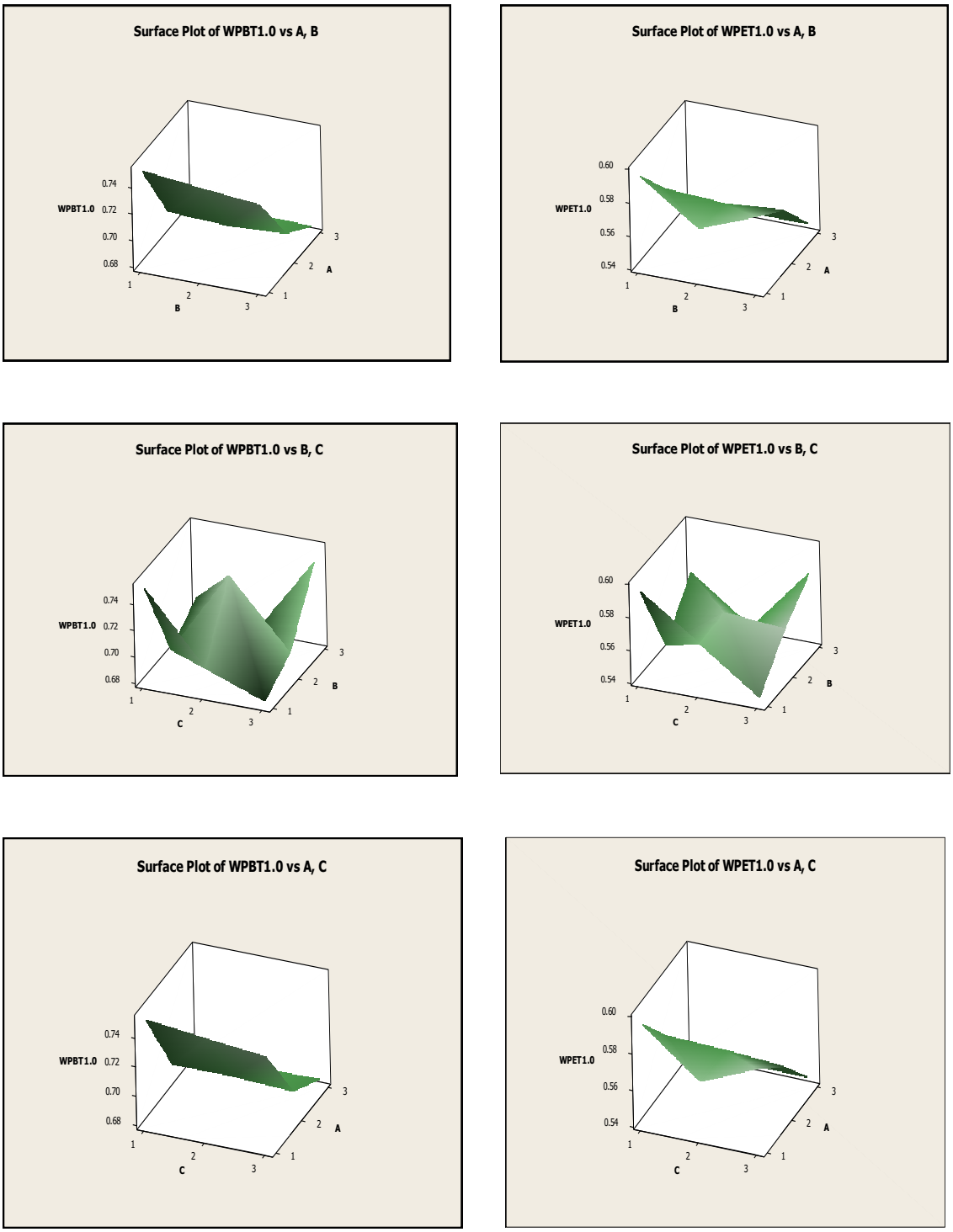

Figure 6.6 Typical response surface plots

Table 6.5 (a) and (b) Regression model for Shrinkage and the R^2 values for PBT and PET material

Thickness (mm)	Regression model for PBT material	R^2 %
0.8	VS = 14.4 + 0.800 Melt temp + 0.0250 Packing Pressure + 0.0233 Packing Time	98.6
0.9	VS = 15.5 + 0.647 Melt temp - 0.0083 packing Press + 0.0067 Packing time	99.6
1.0	VS = 12.8 + 1.09 Melt temp + 0.0800 Packing Pressure + 0.0933 Packing Time	99.6

Thickness (mm)	Regression model for PET material	R^2%
0.8	VS = 13.0 + 0.483 Melt temp - 0.0483 Packing Pressure + 0.00333 Packing Time	99.7
0.9	VS = 13.3 + 0.493 Melt temp - 0.00167 Packing Pressure - 0.00833 Packing Time	99.9
1.0	VS = 13.1 + 0.452 Melt temp - 0.0550 Packing Pressure - 0.0100 Packing Time	100

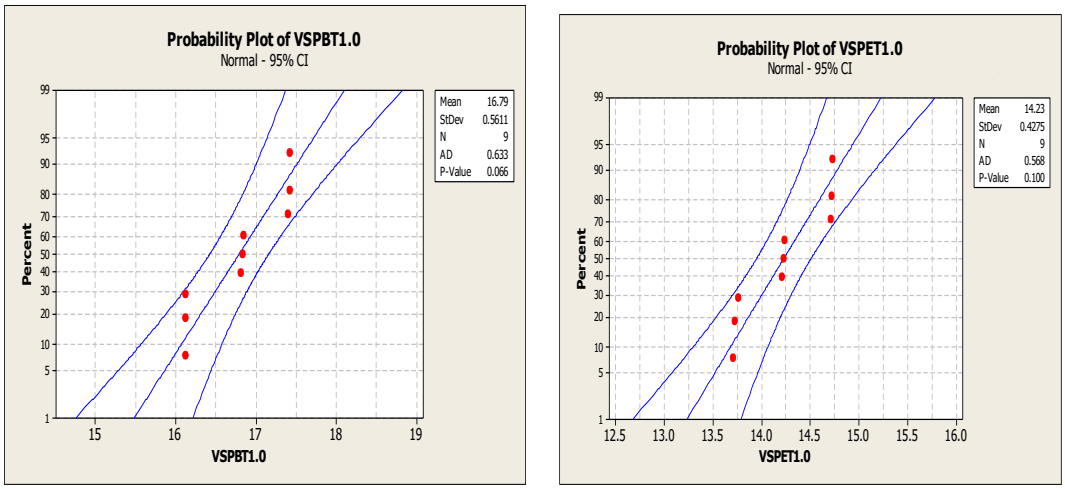

Figure 6.7 Normal probability plot for volumetric shrinkage of 1 mm wall thickness of PBT and PET standardized residuals at 95% of confidence interval

Similarly, the results of the Anderson-Darling (AD) normality test are shown in Figure 6.7 for the respective shrinkage of PBT and PET for a 1 mm thick residue. Since the p value of the normality plot has been found to exceed 0.05, this means that the residues follow a normal distribution and the given model is suitable for practical engineering applications.

To determine the results obtained from the analysis is acceptable or not for PBT/PET materials for three thickness values regression analysis method is used. The model above is used to predict shrinkage and warpage values within the range of factors studied from the regression model and the R^2 value of warpage and contraction depends on the wall thickness analysis. Here, the R^2 values is more than 90%, it is acceptable. During warpage and shrinkage analyses, three injection parameters were used. These parameters are melt temperature, packing pressure and packing pressure. After finding the shrinkage and warpage values, the effect of each injection parameter was examined for each material.

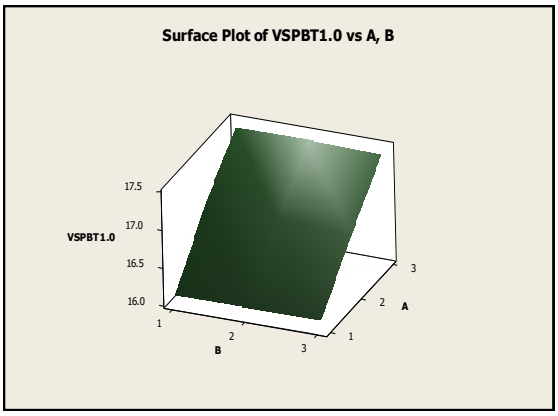

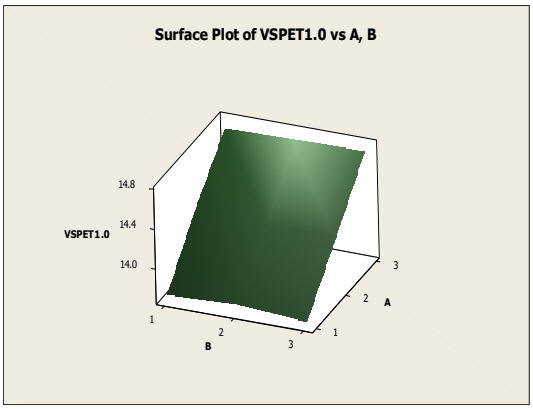

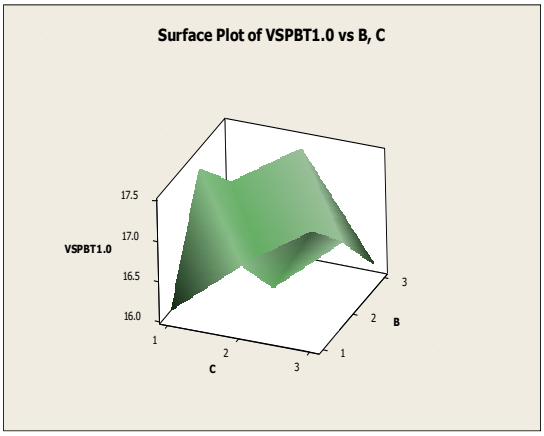

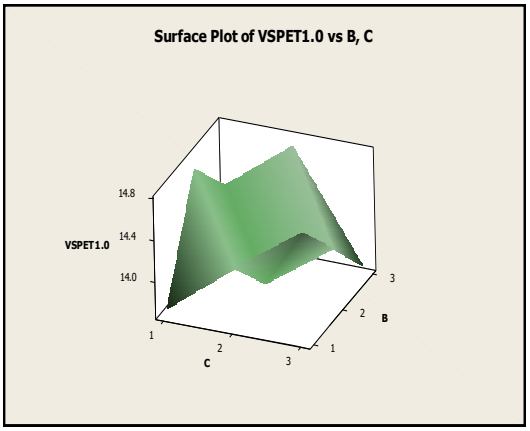

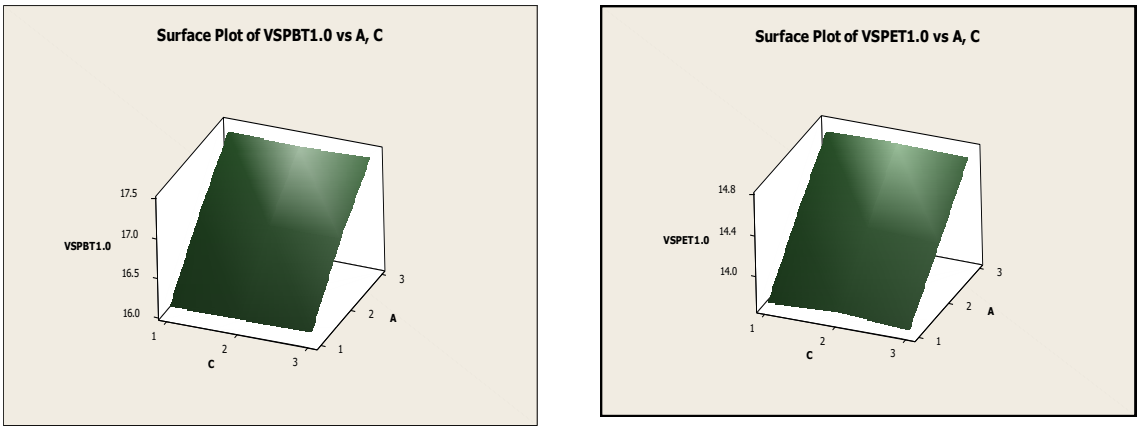

Figure 6.8 Typical Response Surface plots for shrinkage

The typical response surface of typical interactions is depicted in Figure 6.8. It is easy to recognize that the shrinkage value increases as wall thickness increases.

6.10 Experimental verification- In this section, inspection of the part developed by ABS mold and mold inserts is performed experimentally on injection molding machine.

6.10.1 The evaluation of rapid tooling by developing the test mold- A special geometry part was designed to depict the effect of rapid tool mold properties. The effect of mold design, mold materials, various technological parameters, and geometrical attributes can be easily estimated by developed parts.

6.10.2 Manufacturing of the rapid tooling mold by polyjet technology

A mixture commonly used for AM IM tools is a material called Digital ABS. It is made by mixing two different polymers in the machine (Gibson, 2015; Stratasys, 2017a). To produce the rapid tooling mold inserts, An rapid prototyping machine (Object Alaris 30) is used. Thin 28 μm layers having resolution of 600×600×900 dpi is used in Alaris 30 printers. The mold inserts were printed using support material (Fullcure705) and building material (Fullcure720) which was removed by NaOH (5%) solution refer Chapter 3 for working principle of Polyjet Direct 3D printing Figure 3.12.

6.10.3 Process parameter and Material selection for Injection molding Experiments

For the test, an advance injection molding machine Arburg 370S 700 – 290 having screw diameter of 30 mm was used. The operating parameters like Injection volume (44 $cm^{3)}$, the injection rate (50 cm^3/s), the switch –over point (12 $cm^{3)}$, clamping force (50 t), and the pressure limit (400 bar) and melt temperature (20^0 C) was used. Coolant temperature was 20° C in the case of polyjet mold.

Table 6.6 Plastic Injection Molding Machine

Operating parameters	
Temperature- 210°C	Clamp force – 15 KN
Injection pressure-300 bar	Shot size – 60 cc
Holding pressure-1000 bar	Cooling time – 300 sec
Holding time – 8 sec	

Figure 6.9 Arburg 370S 700 – 290 injection molding machine

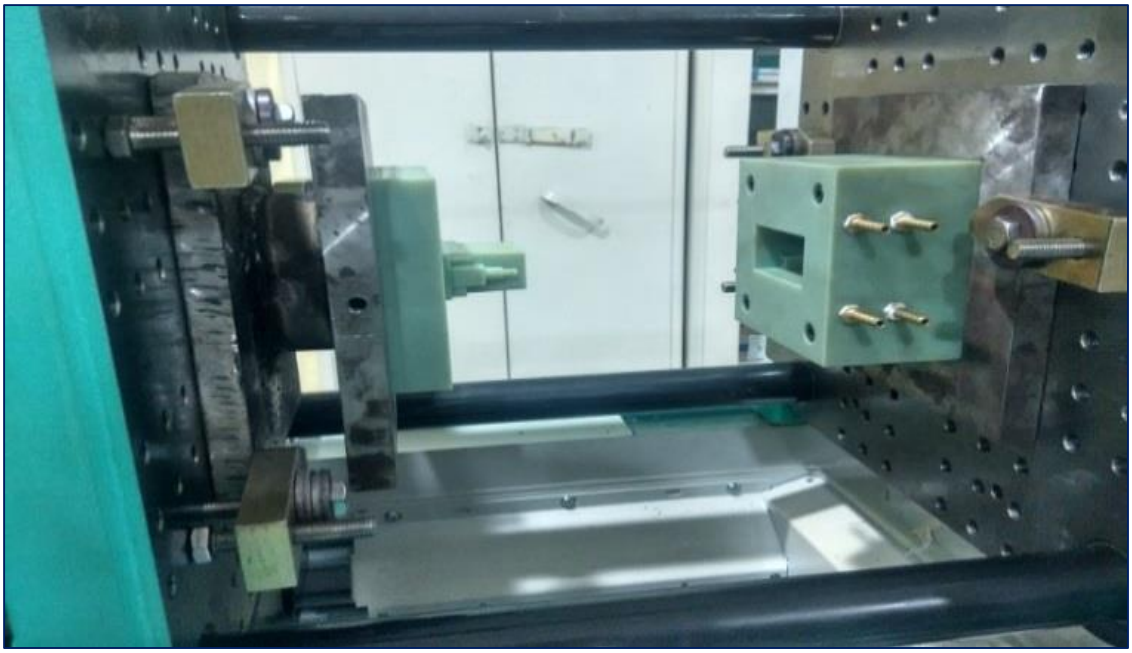

Figure 6.10 3D polyjet mold mounted on for experiment

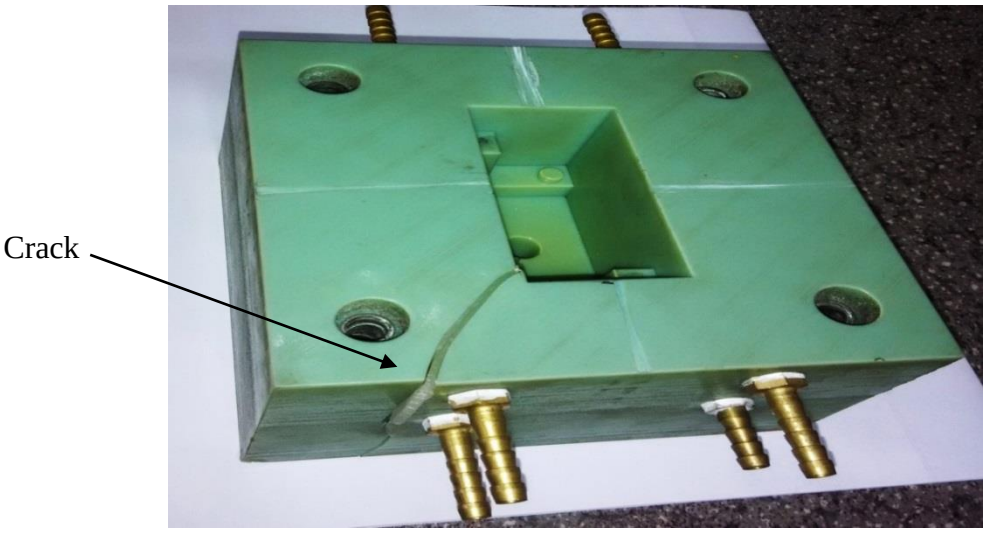

Figure 6.11 Cracked mold after performing 150 shots

During the experiment the PRT mold breaks after 140-150 shots see figure 6.11. In all instances was that the part adhered to the surface of the mold cavity and prevented part extraction. Regardless of the application of the release agent, the part would be fused to the mold so that the part could not be extracted without destroying the mold cavity. At the time of extraction process, the mold usually chip and destroys the gate or surrounding

parting line, making the insert unusable. So, to overcome this problem, the mold is inserted inside a metallic core and cavity, and performed the experiments on plastic injection molding machine to improve the strength of the mold and getting more number of trials to develop the parts refer figure 6.12.

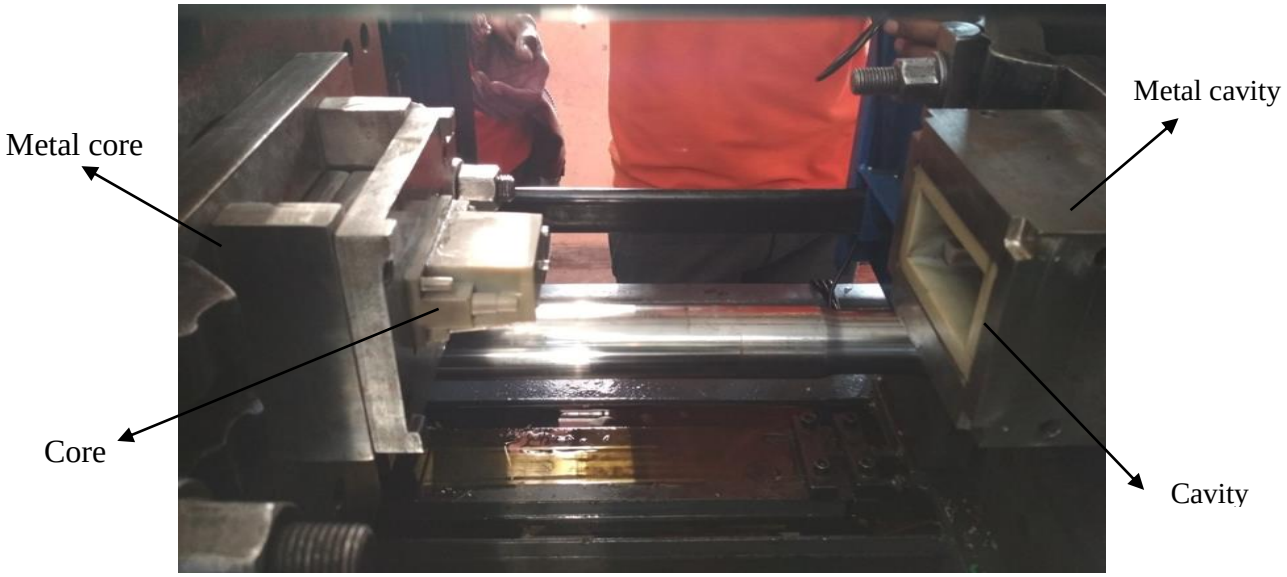

Figure 6.12 ABS mold insert with metal die

6.11 Comparison of the outcome of simulation results with experimental data using 3D scanners

The Steinbichler Comet L3D enables non-contact optical scanning. The version used for the comparison is with resolutions of 2 MPX and 1600 × 1200 pixels. With this portable scanner, a scanning head is mounted on a tripod during scanning. The Rotary table can be used for positioning (rotating) measurement data. The Basic change of scanned data, comparison with model and export in STEP, IGES, and STL format (Figure 6.13) have to be done by using software (COMET PLUS , INSPECT PLUS).

Table 6.7 Operating parameter Steinbichler Comet L3D

Resolution of camera [dpi]	1600×1200
Field Measurement [mm]	400
Volume Measurement [mm^3]	400×300×250
Point to point distance [μm]	250

Figure 6.13 Steinbichler Comet L3D during scanning

6.12 Scanning methodologies- For study the geometric features of the developed complex part is inspected in this section using 3D scanner operated with softwares.

6.12.1 Environmental Conditions – During scanning it was required to maintain the basic parameters of the environment such as temperature, humidity, lightning etc. without changing it. In order to stabilize thermal properties it was essential to leave the scanned sample in the room where the scan was done. If the object has a glossy surface, it is essential to repair it with a powdery choke sprayed on it. As a result, a position marker is placed on the object and / or its surroundings.

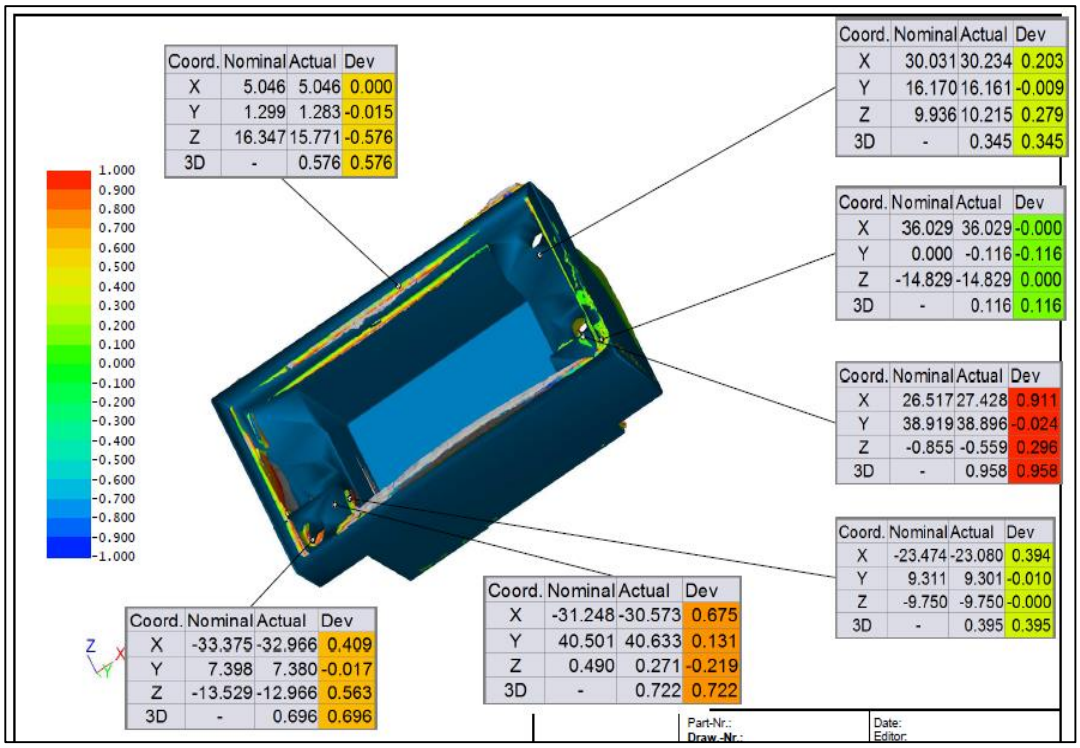

Figure 6.14 Deviation between 3D scan and CAD model

The Independent assessment of the deviations between the CAD model of the sample and the obtained mesh was performed. The BEST-FIT function is used for comparison of a 3D scan against the model, where the rapid, rough alignment is followed by a precision adjustment. The evaluation distance is set as 1 mm. In graphic processing, the color gamut was set to ± 0.2 mm; Values over and above this limit are indicated. Volumetric shrinkage estimation of benchmark features using Inspect plus software.

From figure 6.15 it can be easily recognized that 18.79 % is the maximum volumetric shrinkage found in cylinder feature and 11.57 % is the least volumetric shrinkage in hollow rectangular prism among all the features.

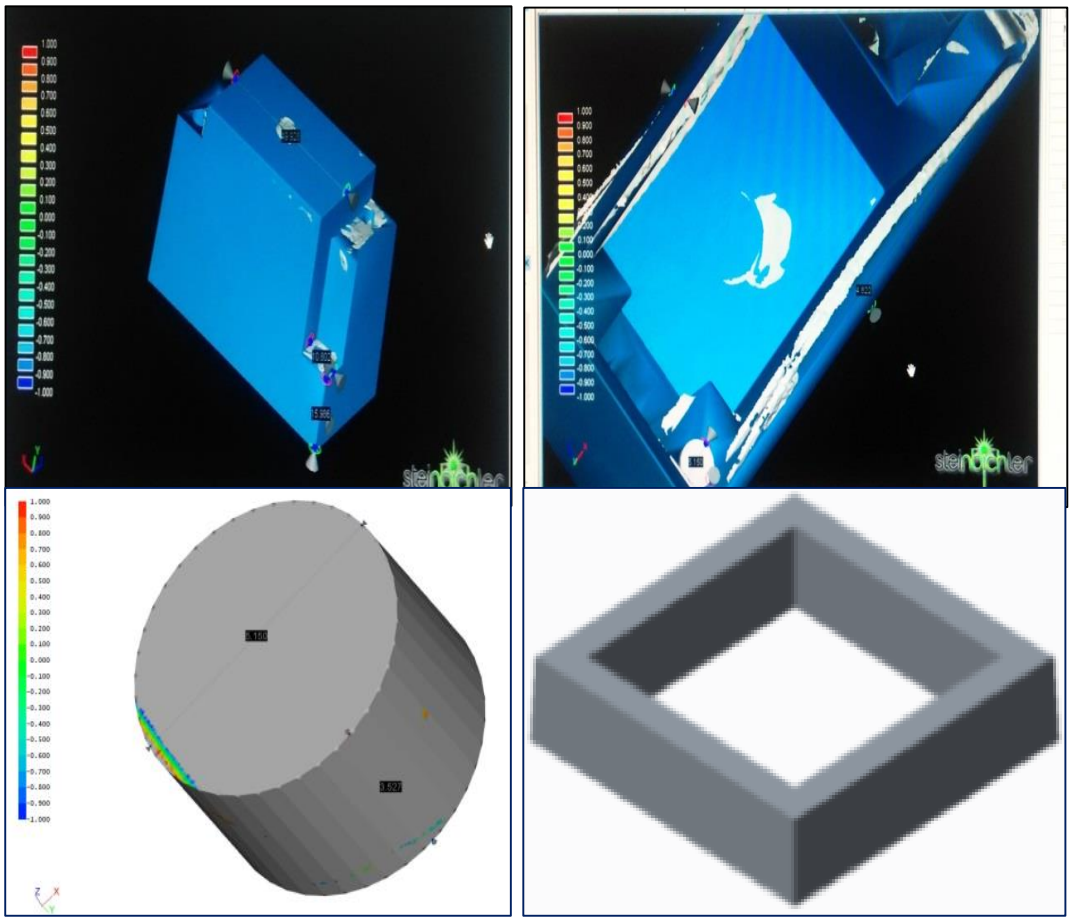

Highest Volumetric shrinkage = 18.79% Lowest volumetric shrinkage = 11.57%

Figure 6.15 Volumetric shrinkage of cylinder and hollow rectangular prism

6.13 Chapter Summary

The aim of this research work is to identify the exact location, where the possibility of shrinkage occurs in injection molded part, provide modification for better part quality. In this present change driven environment, determining the volumetric shrinkage percentage during design stage can help in comparing alternative design solution before the start of plastic part production. In this methodology, geometrical parameter involves such as volume, height, weight, draft angle, thickness, quality prediction percentage, total cycle time. With the help of integrating software package, CAD model is used for analysis with Moldflow® (MFA) simulation. Regression

analysis using twelve benchmark parts criteria were determining the coefficient of the geometric parameter equation in previous chapter. The regression equation can be employed in early phases of part lifecycle, significantly in design for manufacturability; the designer can easily estimate the volumetric shrinkage percentage of an injected part (from its CAD model), allowing comparison of alternate designs in term of the influence on die and cavity material. The outcomes were experimentally validated with 3D scanner integrated with inspection softwares.

CHAPTER 7

Optimization of Rapid Tooling Molded Complex Featured Component

The work of this chapter presents a systematic methodology to determine optimal injection molding conditions for minimum warpage and shrinkage in a thin wall relay part using modified particle swarm optimization algorithm (MPSO). Polybutylene terephthalate (PBT) and polyethylene terephthalate (PET) were injected in a thin wall relay component for different processing parameters: melt temperature, packing pressure and packing time. Further, simulation analysis using Taguchi's design of L_9 array is used to consider the interaction effects of the above parameters. A predictive mathematical model for shrinkage and warpage is developed for the above process parameters using regression analysis. An ANOVA analysis is performed to determine statistical implication within the injection molding parameters. The developed predictive model is further optimized using a newly developed MPSO algorithm and the process parameters values are predicted for minimizing shrinkage and warpage. The predicted values of warpage and shrinkage using MPSO algorithm are improved by approximately 30% as compared to the initial simulation values and comparable to previous literature results.

7.1 Introduction

The plastic injection molding (PIM) process is extensively applied for producing intricate shaped plastic parts with distinctive geometric features and has shorter production cycles. The PIM process is a repeated one which consists of the process beginning with filling and packing, after that cooling and at last ejection. Injection molding helps in producing products for computer, consumer electronic and communication (3C) i.e. computers that are portable and mobile phones. Generally, the 3C products are thin, light, short and small. However, with the increasing demand of more complex products having less wall thickness, the PIM process is prone to face more challenging tasks. Consequently, the quality of the parts produced using PIM process is affected by the appropriate selection of

the various process parameters and the mold design. In contrast, the inappropriate process parameter values led to produce part defects, resulting in long lead times and high cost.

Warpage and shrinkage are among the most important deficiencies used to measure the quality of injection molded components. Previous studies suggest that shrinkage and warpage are highly related to injection molding process parameters. The effect of gate geometry and packing parameters on the end part investigated, and it was found that a thinner gate gets a more uniform shrinkage in the process with the unchanged packing pressure. Galantucci et al. (2009) applied double skin model for investigating the warpage defect and further concluded that melt temperature was among the most influencing factor for minimizing warpage. Huang and Tai (2001) in their study applied computer simulation and experiment for analyzing the factor affecting warpage in a thin shell injection molded components. Tang et al. (2007) applied Taguchi method for minimizing the warpage in the design of improved plastic injection mold. Similarly, Taguchi and ANOVA are used in a study for obtaining optimal shrinkage injection molding conditions. The results suggested that optimized parameters reduce shrinkage by 1.244 % and 0.937 % for Polypropylene (PP) and polystyrene (PS), respectively.

Similarly, Park and Dang (2010) in their study suggests that runner and cooling channel geometry can improve the final quality of products. One specific study was found for minimizing the warpage in thin shell plastic parts by employing the genetic algorithm and response surface methodology. Hakimian and Sulong (2012) in their study applied Taguchi method to analyze the warpage and shrinkage in micro gears of polymer composites. Choi (1999) found that residual stress is a significant factor that influence the warpage and shrinkage defect in injection molded components. Liao et al. (2004) in their study provided optimum conditions for minimizing shrinkage and warpage problems. The cyclone scanner and polyworks software was used for determining the shrinkage and warpage problem. The packing pressure found to be the most influencing factors. Kikuchi and Koyoma (1996) have applied finite element method for studying the relation among warpage, part thickness and anisotropy. Othman et al. (2017) also optimizes the shrinkage and warpage in their study for composite material. In addition, effect of different process parameters is discussed in recent studies of Mohan et al. (2017) One recent study used simulation based methods for estimation of shrinkage and warpage in the injection molding

process. Some literature are also available which focusses on relating the polymer microstructure to molding ability, however, it is not in scope of the present work. Moreover, several studies found have used response surface methodology (RSM) individually or integrating with genetic algorithm (GA) for determining the interaction and relationship among factors and process parameters. Similar studies have been found that uses neural model, modified complex method, grey-fuzzy logic for thin shell feature for optimization of warpage in different thermoplastic parts.

Generally, the warpage problem in thin-wall injection molded plastic parts has been reported in many literatures. As thickness of the part decreases, the shrinkage defect becomes even more complex and causes significant warpage of the plastic component. However, few of them have shown the effective processing variables and their optimization for the dimensional shrinkage and warpage minimization under high-speed injection molding process. The past literatures have used only GA for the determination of optimal injection molding conditions. The current study takes into consideration a newly developed modified particle swarm optimization (MPSO) algorithm for optimal injection molding process parameter determination.

In this study, a systematic methodology is presented using regression analysis and a newly developed MPSO algorithm for determining the optimum process parameters. The Particle Swarm Optimization (PSO) algorithm has proven to be a successful tool for resolving optimization applications because of the simplicity of the concept with less parametric adjustments compared to other nature inspired optimization algorithms. However, the usual PSO faces some disadvantages. For example, a fragile local search that can lead to an inclusion of local minima that affect the convergence performance, leading to uncertainties in the obtained results. To improve PSO's exploitation capabilities, the MPSO is offered by Pathak et al. (2018) which is modified version of classical PSO. Based on the new improved particle position, which is different from global and local best positions. An effective greedy selection procedure is employed to get a better position to decide on a new position and a candidate based on fitness values.

Furthermore, a real life case study of an electronics component relay is considered for injection molding process. The PBT/PET molten material is injected into the mold to

produce the required constituent. An effective methodology is proposed for analyzing volumetric shrinkage and warpage in an injection molded part having a thin shell feature at the time of injection molding process. Initially, the effects of the injection process parameters on shrinkage and warpage for various wall thicknesses were examined using Taguchi method. The shrinkage and warpage values were found by Moldflow insight software. The results of confirmation experiments and analysis of variance (ANOVA) assure that quadratic shrinkage and buckling models are well equipped with simulated values at the optimum value. The quadratic shrinkage and warpage models are well fitted with simulated values at the optimum value. The analysis of dimensional behavior including shrinkage and warpage have been performed and the developed mathematical models helps in prediction of the specific effects of different parameters.

7.2. Experimental Details

An electronic relay part, with an overall dimension of 72 mm × 34 mm × 48.5 mm was designed in Autodesk inventor 3D modeling software and was used as a model, using a 3D mesh type. The analytical model consists of 29, 812 elements. The analysis were performed using three thickness values of 0.8, 0.9 and 1.0 mm. Figure 7.1 shows the mesh file of relay component with the cooling channels. The default values were determined using an injection molding machine (maximum machine injection rate, 6000 m^3/s) and acrylonitrile butadiene styrene (ABS) mold material (mold density, 1.5 g/cm^3; mold specific heat, 1300 J/kg °C). The injection molded electronic relay was either made of PBT or PET material, due to wide application of these materials in academic and industries. The PBT and PET polyesters are important commercial material having many attractive properties. They have high strength and toughness, good abrasion and heat resistance, good chemical resistance, low creep at elevated temperatures, and excellent dimensional stability, particularly when glass-fiber reinforced. Both are semi-aromatic. These are amorphous thermoplastic materials when solidified by rapid cooling or semi-crystalline thermoplastic materials that are easily formatted and thermoformed. The physical properties of these materials are summarized in Table 7.1, acquired from Moldflow Insight library.

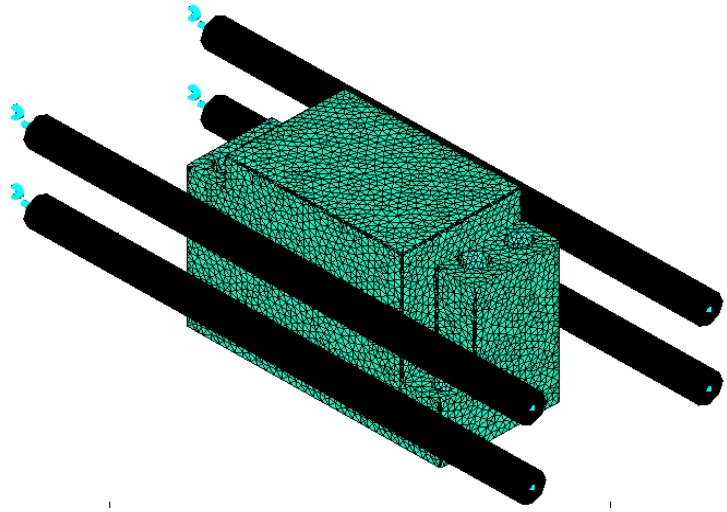

Figure 7.1 Electronic relay mesh file with cooling channel

Table 7.1 Physical properties of PBT/ PET material

Property	PBT	PET
Melt density (g/cm^3)	1.31	0.72 - 0.76
Solid density (g/cm^3)	-	0.86 - 0.96
Mold temperature (°C)	40 - 60	80 – 120
Melt temperature (°C)	220 - 280	265 - 280
Poisson ratio	0.3902	035 – 0.45
Material structure	Semi-crystalline	Amorphous

The parameters considered for shrinkage and warpage analyses are melt temperature (A), packing pressure (B) and packing time (C). The values of these parameters are provided in Table 7.2. The injection time was fixed at 3 seconds for all experiments. An L_9 (3^3) orthogonal array was selected for the experimental design for each of the three factors. The three levels for the three factors were identified during the 9 experiments (see Table 7.3). The signal-to-noise ratios (S/N) for every trials were determined using the signal-to-noise ratios (S/N) for every trials were determined using

$$\frac{S}{N} = -10log\left[\frac{1}{n}\sum_{i=1}^{n} y_i^2\right] \qquad \text{-------} \qquad [7.1]$$

where n is the number of shrinkage and warpage data sets (equal to 9) and y_i is the shrinkage and warpage value for the i^{th} data sets. The ANOVA analysis is performed using the Minitab software.

Table 7.2 Process Parameters and their levels

Factors	Description	Coded Symbol	Unit	PBT Levels			PET Levels		
				1	2	3	1	2	3
A	Melt Temperature, t_m	X_1	°C	254	266	278	252	264	276
B	Packing Pressure, p_p	X_2	MPa	25	30	35	22	28	34
C	Packing Time, p_t	X_3	s	10	15	20	12	18	24

Table 7.3 The layout of L9 orthogonal array

Exp. No.	A	B	C
1	1	1	3
2	1	2	2
3	1	3	1
4	2	1	2
5	2	2	1
6	2	3	3
7	3	1	1
8	3	2	3
9	3	3	2

7.3 Results

The Taguchi method was applied to predict the effect of injection molding process parameters on the shrinkage and warpage. The measured values of shrinkage and warpage and the signal-to-noise ratios are measured and reported in Table 7.4. The signal-to-noise ratio is an important quality indicator that researchers used to determine the influence of varying a particular parameter on the performance. For the current study, smaller the better

characteristic was selected when calculating the S/N ratio, which is based on equation 7.1, as shown in Table 7.4. It was found that the best process parameter value can be determined by selecting the level with the best values at each factor. Figure 7.2 illustrates the variation of the S/N ratio of warpage and shrinkage for different PBT and PET material. Based on shrinkage results in Table 7.4 and Figure 7.2 (a), it was found that PET material had higher S/N ratio (-6.02) value than the PBT material, because it exhibits least shrinkage as compared to PBT. Similarly, the warpage result shows that PET also has least warpage in comparison to PBT warpage values. It was clearly seen from the results that PET material is better for producing relay component in comparison to PBT material due to its least shrinkage and warpage.

Table 7.4 Shrinkage and warpage values of PBT and PET material

Exp. No.	**PBT**		**PET**		**PBT**		**PET**	
	Shrinkage %	S/N ratio	**Shrinkage %**	S/N ratio	**Warpage (mm)**	S/N ratio	**Warpage (mm)**	S/N ratio
1	2.1982	-7.1293	2.0409	-6.2237	0.2432	12.2841	0.1682	15.3867
2	2.1392	-2.3451	1.972	-6.0301	0.2164	13.2956	0.1608	15.8743
3	2.0932	-6.8343	1.9145	-5.5843	0.2813	11.0166	0.1619	15.815
4	2.1523	-7.0749	1.8832	-5.4029	0.1341	17.4521	0.2521	11.9685
5	2.0123	-6.1452	1.9923	-6.0940	0.1931	14.2844	0.2912	10.7161
6	1.945	-5.7231	1.9639	-5.927	0.1857	14.6237	0.1972	14.1018
7	1.9197	-5.5938	2.021	-6.1512	0.2076	13.6554	0.2102	13.5473
8	1.9921	-6.0927	1.9715	-6.0211	0.1596	15.9397	0.1821	14.6143
9	1.9772	-6.0312	1.9218	-5.7439	0.1801	14.8897	0.1717	15.305

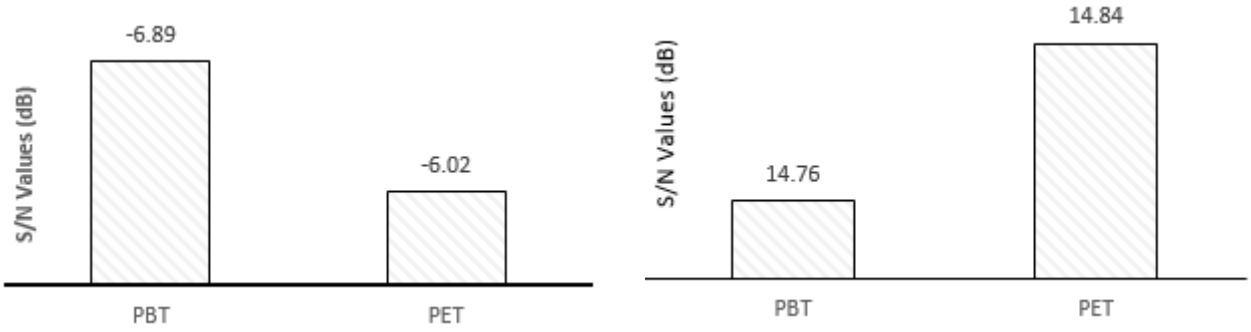

(a) (b)

Figure 7.2 Variation of the S/N ratio of (a) Shrinkage (b) Warpage

For further analyzing the obtained results and determining the significance of each parameter, regression analysis and ANOVA test was performed. These analyses were performed on Minitab V14 software. Due to change in response statistics drastically with the control parameters, it is very challenging to develop an analytical model. The regression analysis may be the solution to this problem which is useful in searching the effect of factors to an event while examining that event. There may be factors which are either direct or indirect. The regression analysis is worthwhile when the focus is on determining the relationship between dependent and one or more independent variables. While using multiple regression analysis, the equation of the form given below is used to explain the relationship between the independent variables X_1, X_2 and X_3 and the response variable Y.

$$\boldsymbol{Y} = \beta + \beta_1 X_1 + \beta_2 X_2 + \beta_3 X_3 + \beta_{11} X_1^2 + \beta_{22} X_2^2 + \beta_{33} X_3^2 + \beta_{12} X_1 X_2 + \beta_{13} X_1 X_3 + \beta_{23} X_2 X_3$$

Based on the above generalized regression model, the following analytical model was obtained for shrinkage of PBT and PET in the form of coded unit:

Shrinkage (S1) = $0.326440 + 0.201507X_1 - 0.034872X_2 + 0.065912X_3 - 0.003173X_1^2 - 0.029771X_2^2 - 0.004712X_3^2 + 0.033242X_1X_2 + 0.023560X_1X_3 + 0.048322X_2X_3$

Shrinkage (S2) = $0.462270 + 0.305915X_1 - 0.048202X_2 + 0.079210X_3 - 0.002320X_1^2 - 0.041725X_2^2 - 0.003712X_3^2 + 0.045902X_1X_2 + 0.043450X_1X_3 + 0.054721X_2X_3$

In addition, the model significance is further validated using ANOVA analysis. The ANOVA results for PBT and PET material are shown in Table 7.5 and Table 7.6 respectively. The model was built for 95% confidence level. The correlation coefficient (r^2) of the developed analytical models for PBT and PET was found to be 0.973 and 0.962 (nearer to the ideal value of 1). The adequate value of regression coefficient indicates that the model is significant and further analysis and predictions can be performed. All the linear, square and interaction terms have significant effect on the response output. It was clearly seen from Table 7.5 and 7.6 that the F-value is significantly higher for both the ANOVA table, indicating that the model is significant. There is only a chance of 0.05% that such a high model F value might have occurred due to noise.

Table 7.5 ANOVA result for PBT shrinkage model

Source	**DF**	**Sum of squares (SS)**	**Mean square (MS)**	**F-Value**	**P-value**	
Regression	9	1.52827	0.16980	253.43	0.000	Significant
Linear	3	1.37281	0.45760	682.98	0.000	
Square	3	0.01430	0.00477	7.12	0.001	
Interaction	3	0.13092	0.04031	60.16	0.000	
Residual error	41	0.02744	0.00067			
Lack of fit	5	0.02205	0.00441	6.58	0.000	
Pure error	36	0.00438	0.00012			
Total	50	1.5572				

Table 7.6 ANOVA result for PET shrinkage model

Source	**DF**	**Sum of squares (SS)**	**Mean square(MS)**	**F-Value**	**P-value**	
Regression	9	2.72891	0.30321	133.57	0.000	Significant
Linear	3	2.43011	0.81003	356.84	0.000	

Square	3	0.08260	0.02753	12.13	0.000
Interaction	3	0.25109	0.08370	36.87	0.000
Residual error	41	0.09344	0.00227		
Lack of fit	5	0.08704	0.01741	7.67	0.000
Pure error	36	0.00812	0.00012		
Total	50	2.92391	0.00025		

Furthermore, the performance of the developed model of warpage for both materials was tested using ten randomly selected experiments other than the used in Table 7.4. The random values chosen from ten experiments are compared with the values obtained through developed analytical model. The results of percentage deviation in prediction of shrinkage for the PBT and PET material are shown in Figure 7.3. It was clearly seen from Figure 7.3, the percentage deviation in shrinkage prediction for PBT and PET are 3.56 and 5.55 respectively. However, the percentage deviation for shrinkage for PBT is less as compared to PET material. Similarly, the following analytical model for warpage was developed using non-linear regression model for both the material i.e. PBT and PET.

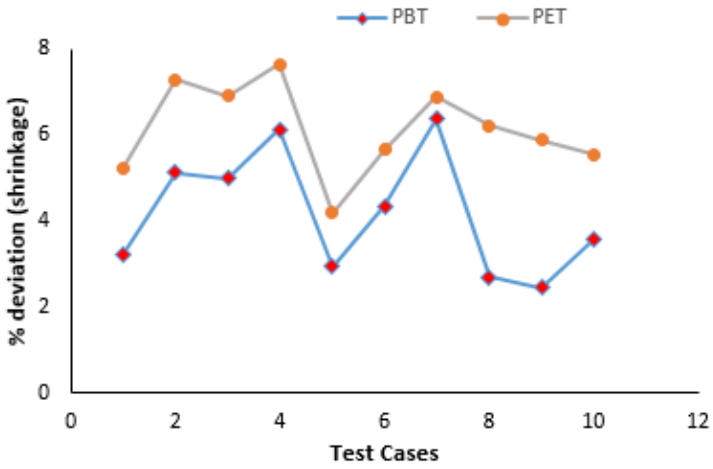

Figure 7.3 Percentage deviation in prediction of shrinkage

Warpage (W_1) = $1.23966 + 0.772017X_1 + 0.005873X_2 - 0.347592X_3 - 0.027631X_1^2 - 0.000987X_2^2 - 0.012283X_3^2 + 0.000533X_1X_2 + 0.010937X_1X_3 + 0.000272X_2X_3$

Warpage (W_2) = $1.78218 + 0.817812X_1 + 0.007291X_2 + 0.192205X_3 - 0.051140X_1^2 - 0.001723X_2^2 - 0.027831X_3^2 + 0.000612X_1X_2 - 0.033147X_1X_3 + 0.000721X_2X_3$

The developed regression model significance is further tested using ANOVA analysis. The ANOVA results for PBT and PET material are reported in Table 7.7 and Table 7.8 respectively. The model was built for 95% confidence level. The correlation coefficient (r^2) of the developed analytical models for PBT and PET was found to be 0.941 and 0.924 (nearer to the ideal value of 1). The adequate value of regression coefficient indicates that the model is significant and further analysis and predictions can be performed. Moreover, all the linear, square and interaction terms have significant effect on the response output. It was clearly seen from Table 7.7 and 7.8 that the F-value is significantly higher for both the ANOVA table, indicating that the model is significant. There is only a chance of 0.05% that such a high model F value might have occurred due to noise.

Table 7.7 ANOVA Analysis for warpage PBT model

Source	**DF**	**Sum of squares (SS)**	**Mean square (MS)**	**F-Value**	**P-value**	
Regression	9	202.317	22.48	40.43	0.000	Significant
Linear	3	112.34	37.45	67.36	0.000	
Square	3	43.22	14.41	25.92	0.000	
Interaction	3	29.23	9.74	17.52	0.000	
Lack of fit	5	16.26	3.252	5.56	0.000	
Pure error	36	6.52	0.181			
Total	50	225.097				

Table 7.8 ANOVA Analysis for warpage PET model

Source	**DF**	**Sum of squares (SS)**	**Mean square (MS)**	**F-Value**	**P-value**	
Regression	9	195.794	21.755	49.55	0.000	Significant
Linear	3	106.91	35.64	81.48	0.001	
Square	3	35.18	11.73	26.72	0.000	
Interaction	3	25.76	8.59	19.55	0.000	
Lack of fit	5	12.54	2.508	5.72	0.000	
Pure error	36	5.48	0.152			
Total	50	213.814				

Furthermore, the performance of the developed model of warpage for both materials was tested using ten randomly selected experiments other than the used in Table 7.4. The random values chosen from ten experiments and compared with the values obtained developed analytical model. The results of percentage deviation in prediction of warpage for the PBT and PET material are shown in Figure 7.4. It was clearly seen from Figure 7.4, the percentage deviation in warpage prediction for PBT and PET are 3.22 and 4.23 respectively. However, the percentage deviation for warpage for PBT is less as compared to PET material.

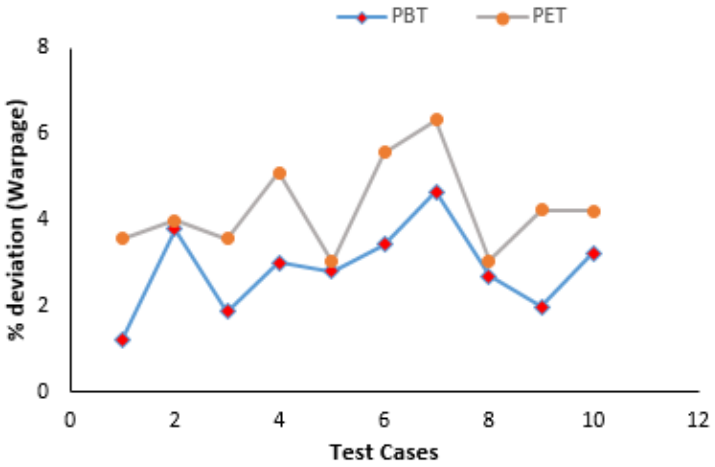

Figure 7.4 Percentage deviations in prediction of warpage

7.4 Modified particle swarm optimization algorithm

In this section, the modified version of the classic particle swarm optimization algorithm to evaluate the developed analytic model in Eq. (7.3). Since the exploitability directly affects the quality of the results. The modified variant will help overcome the classic PSO disadvantage of low convergence due to lack of exploitation capabilities. The modified version will help to overcome the classic deficiency of PSO in low convergence due to the lack of ability to operate.

7.4.1 Standard particle swarm optimization algorithm

The basic particle swarm optimization is a population-based method proposed by Kennedy and Eberhart in 1995. PSO is modeled on simulating the social behavior of birds in a herd. PSO is initialized by randomly distributing each particle in the D-dimensional

search space. The performance of each particle is measured using a fitness function that depends on the optimization problem. Each particle *i* represented as:

x_i, the current position of the particle i

v_i, current velocity of the particle i

p_i, personal best position of the particle i

The personal best position is the best position the particle has reached so far. The adaptive function is highest at that position in the i[th] particle. Here, the velocity behaves like a vector, and it helps to guide the particle from one position to another. Personal best position of i th particle depending on time step t as:

$$P_i(t) = \begin{cases} p_i(t) & if\ f\big(x_i(t)\big) \geq f\big(p_i(t)\big) \\ x_i(t) & if\ f(x_i(t)) < f(p_i(t)) \end{cases} \tag{7.3}$$

New position and velocity for i^{th} particle is updated at each iteration and expressed as:

$$v_i(t+1) = v_i(t) + c_1 * r_1\big(p_i(t) - x_i(t)\big) + c_2 * r_2(g_i(t) - x_i(t)) \tag{7.4}$$

$$x_i(t+1) = x_i(t) + v_i(t+1) \tag{7.5}$$

r_1 and r_2 are two independent uniformly distributed random numbers within given interval [0,1]. c_1 and c_2 are two accelerating coefficients whose value are generally 2 each for almost all applications, $p(t)$ is the best position parameter of an individual particle and $g(t)$ is global best position parameter of entire swarms. Shi and Eberhart (2000) introduced an inertia weight w into the velocity updating of the PSO that helps in controlling the scope of the search. Often, w decreases linearly from 0.9 to 0.4 over the whole iteration. High value of inertia weight helps in exploration whereas low value favors exploitation. The velocity update with inertia weight is shown in Eq. (7.6).

$$v_i(t+1) = w(t) * v_i(t) + c_1 * r_1\big(p_i(t) - x_i(t)\big) + c_2 * r_2(g_i(t) - x_i(t)) \tag{7.6}$$

A new version of PSO is proposed in this thesis. The exploration and exploitation capabilities are two important factors that are included in the design of an optimization algorithm. Exploitation means using existing information while exploration generates a new solution in the search space. In PSO, the new solution is replaced by the old, without actually comparing which is better. This shows that the ability to use PSO is unavailable and is merely an exploration trend, making it difficult to find the best possible solutions.

Due to the lack of exploitation strategy, the classical PSO still has disadvantages, such as poor local search capabilities, and may lead to entrapment in local minimum solutions. To overcome all of these issues, the modified variant of the PSO algorithm generates a new swarm position and fitness solution based on the new search equations (7.7) and (7.8):

$$v_{new} = p_{best} + rand(g_{best} - p_{best}) \tag{7.7}$$

$$x_{new} = p_{best} + v_{new} \tag{7.8}$$

Where $p_{best}$the best position of the particle, g_{best} is is the best global position of the particle. $rand$ is the random number between 0 and 1 that controls the speed at which the population evolves. The best sources of solutions to the current population are very useful to be used to improve the convergence performance. Also, Eq. (7.7), the new candidate solution can only drive around the best solution of the previous iteration. The proposed search and update equations described in Eq. (7.7) and (7.8) can increase the exploitation ability of the classic PSO. Any assortment strategy in the algorithm is commonly considered exploitation, since the fitness solution of the individual is used to determine whether a person should be exploited or not. Therefore, the MPSO particle swarms use a greedy selection process among two parallel fitness functions to update the best candidate solution, which also helps to improve the evaluation capability of the algorithm. The proposed transformation algorithm flowchart of the suspension is shown in Figure 7.5.

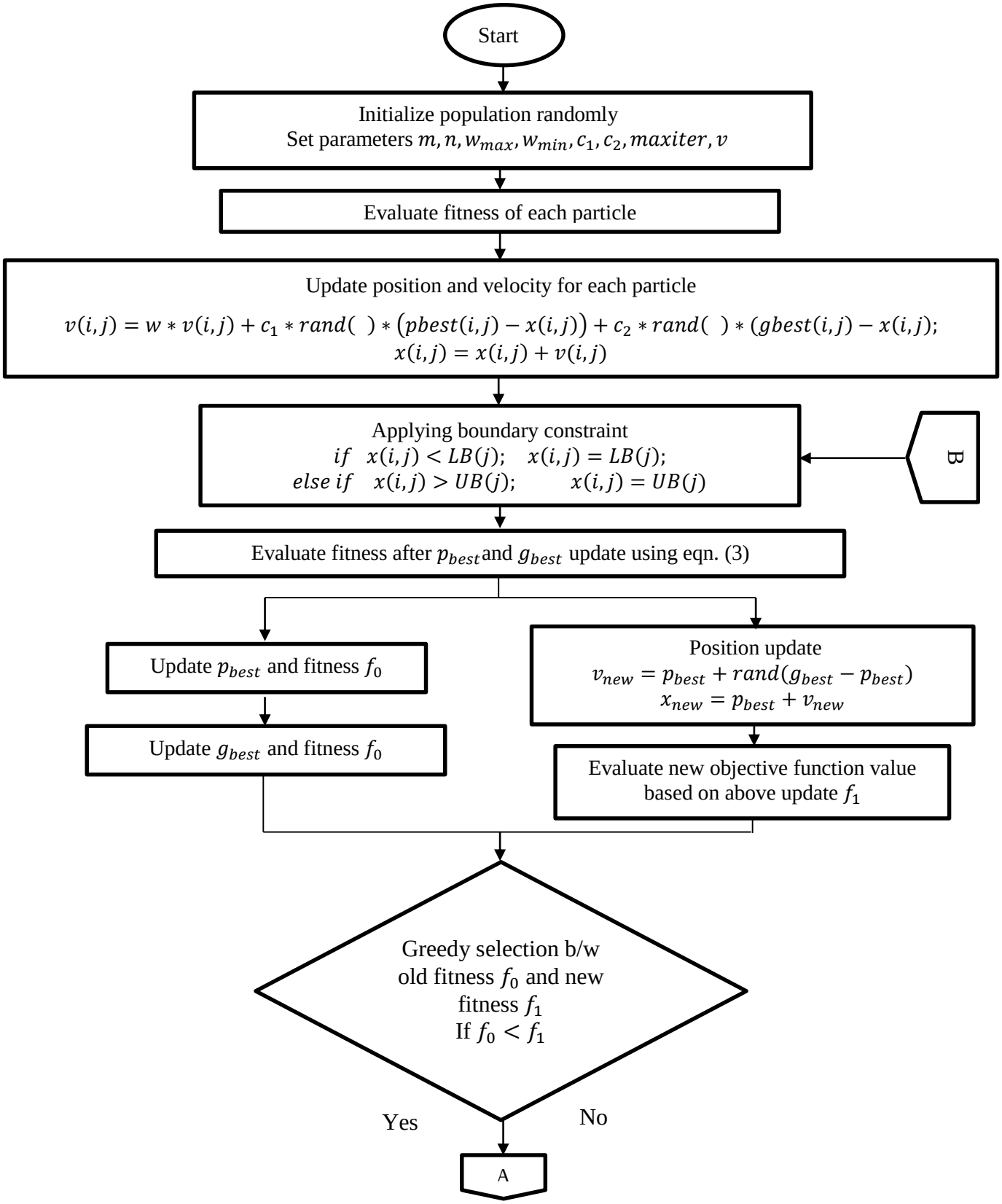
Start
Initialize population randomly
Set parameters $m, n, w_{max}, w_{min}, c_1, c_2, maxiter, v$
Evaluate fitness of each particle
Update position and velocity for each particle
$v(i,j) = w * v(i,j) + c_1 * rand(\ ) * \big(pbest(i,j) - x(i,j)\big) + c_2 * rand(\ ) * (gbest(i,j) - x(i,j);$
$x(i,j) = x(i,j) + v(i,j)$
Applying boundary constraint
$if \quad x(i,j) < LB(j); \quad x(i,j) = LB(j);$
$else\ if \quad x(i,j) > UB(j); \qquad x(i,j) = UB(j)$
B
Evaluate fitness after p_{best} and g_{best} update using eqn. (3)
Update p_{best} and fitness f_0
Update g_{best} and fitness f_0
Position update
$v_{new} = p_{best} + rand(g_{best} - p_{best})$
$x_{new} = p_{best} + v_{new}$
Evaluate new objective function value based on above update f_1
Greedy selection b/w old fitness f_0 and new fitness f_1
If $f_0 < f_1$
Yes
No
A

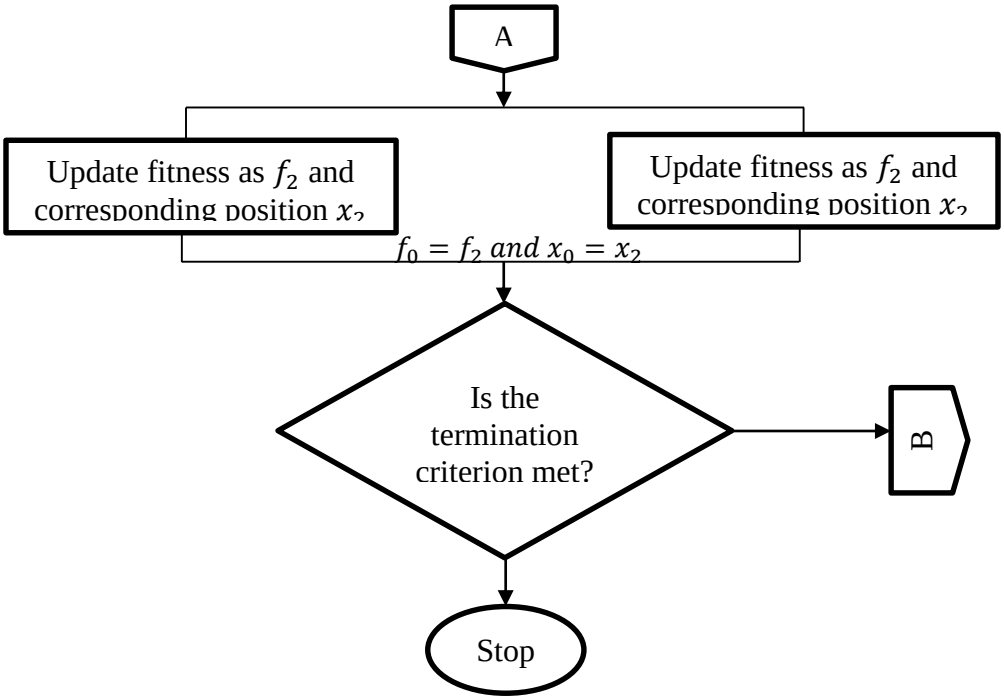

Figure 7.5 Flowchart of modified particle swarm optimization (MPSO) algorithm

7.5 Optimization problem formulation

In this study, a mathematical model of shrinkage and warpage is minimized to obtain optimal values for melting temperature, packing pressure and packing time. The values of optimal parameters are required to improve the injection molding process

7.5.1 Identification of design variables

The developed regression models for shrinkage and warpage consist of three important parameters such as melt temperatures, packaging pressure and packing time. These three parameters are design variables.

7.5.2 Objective function and constraints

To improve the final accuracy of injection molded components, the shrinkage and warpage in S_1, S_2 and W_1 and W_2 needs to be minimized. The optimization problem now is to be formulated as:

$$\text{Minimize } f(t_m, p_p, p_t) = S_1$$

$$f(t_m, p_p, p_t) = S_1;$$

$$f(t_m, p_p, p_t) = W_1;$$

$$f(t_m, p_p, p_t) = W_1;$$

In order to solve the optimization problem, a computer code that implemented the objective function and modified PSO as a solver in Matlab R2014a is developed.

The MPSO program used different settings of PSO parameters to predict the values of the injection molded parameters and to achieve minimized shrinkage and warpage values for the final components. To demonstrate the effectiveness of the proposed MPSO algorithm, its results are compared to those found from the standard PSO algorithm. The parameters for both algorithms are set as follows: c1, c2 = 2.05, number of population size = 10.

7.6 Discussion

The results predicted to minimize shrinkage and warpage with PSO and proposed MPSO for optimized values of melt temperature; packing pressure and packing time are shown in Table 7.11. From Table 7.11, it can be seen that the predicted values of the injection molded relay component by the MPSO algorithm provide a significant improvement over the PSO results as well as the simulation results by 36.47% for the PBT shrinkage and 19.31% for the PBT warpage, respectively demonstrate. Similar results are found for PET material having shrinkage reduction of 30.73% and warpage reduction of 28.79%. The convergence plot of the MPSO algorithm compared to the standard PSO for PBT material is depicted in Fig. 7.6. It can be observe from Figure 7.6 that the MPSO algorithm requires only 20 iterations to converge to the optimal solution compared to the classical PSO, which requires near about 60 iterations for the optimal solution. The low shrinkage and warping values confirm that the proposed MPSO algorithm provides better results. This improves the final accuracy and quality of the injection molded component and thus improves the result of the injection molding process.

Table 7.9 Optimum parameters prediction using PSO and MPSO

Parameters	**Melt temperature (T_m)**		**Packing pressure (P_p)**		**Packing time (P_t)**		**S1 (%)**	**S2 (%)**	**W1 (mm)**	**W2 (mm)**
	PBT	PET	PBT	PET	PBT	PET	PBT	PET	PBT	PET
Initial value	278	252	25	34	10	12	1.9197	1.9145		
	266	252	25	28	15	18			0.1341	0.1608
PSO	279.32	254.02	27.12	29.65	10.87	12.07	1.4203	1.5182		
	269.72	253.91	26.79	29.01	14.67	17.89			0.1221	0.1365
MPSO	281.09	254.15	28.54	35.17	10.34	12.53	1.2196	1.3298		
	268.26	253.12	27.91	28.34	15.91	18.22			0.1082	0.1145

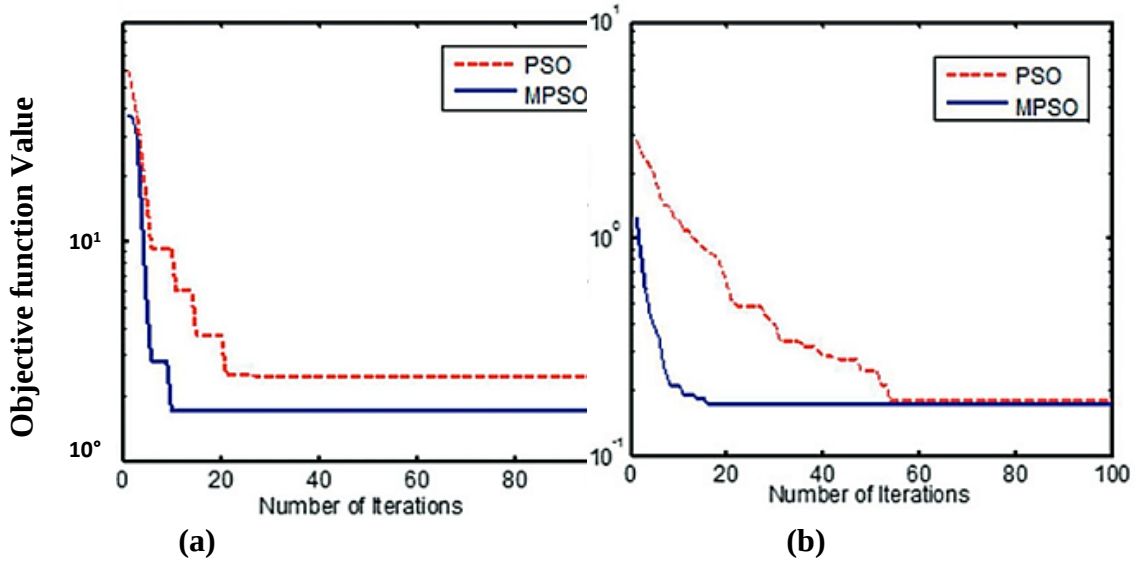

Figure 7.6 Convergence plot of (a) Shrinkage (b) Warpage of PBT material

To test the adequacy of the developed mathematical model and justify the use of newly developed MPSO algorithm, four simulation runs were performed for shrinkage (S1, S2) and warpage (W1, W2). The shrinkage and warpage results for PBT material is shown in Figure 7.7 and 7.8 respectively for the chosen parameter values. The collected confirmation trials data and their comparison with the envisaged values of shrinkage and warpage using MPSO algorithm is shown in Table 7.12. From Table 7.12, it is clearly seen that the predicted values of shrinkage and warpage are more accurate for the predicted model in comparison to the default simulation parameters. For further testing the adopted methodology, the results of shrinkage and warpage are compared with previous literature results for different polymer materials as tabulated in Table 7.13. It can be clearly seen from Table 7.13 that present study provide comparable results as compared to methods adopted in past research. The result confirms that the present methodology can be useful in plastic industries for producing accurate polymer products.

Table 7.10 Confirmation simulation trials

S. No.	Parameters			Shrinkage		Warpage (mm)	
	A	B	C	Simulation	Predicted	Simulation	Predicted
1	278	34	8	2.2289	2.2003	0.2922	0.2812
2	280	36	10	1.8722	1.7621	0.3681	0.3603
3	282	38	12	2.8021	2.745	0.2690	0.2231
4	281.09	35.17	10.34	2.321	2.019	0.2901	0.2521

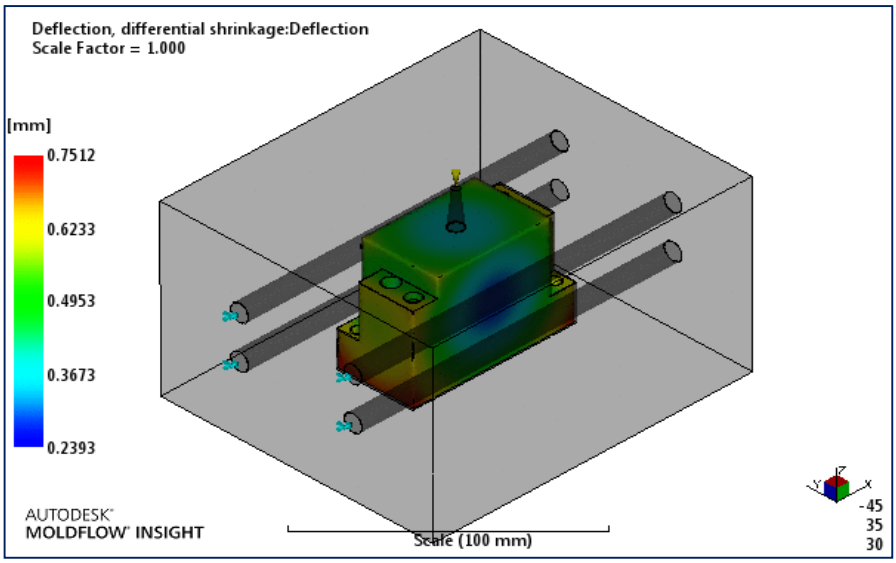

Figure 7.7 Shrinkage analysis using optimized parameter

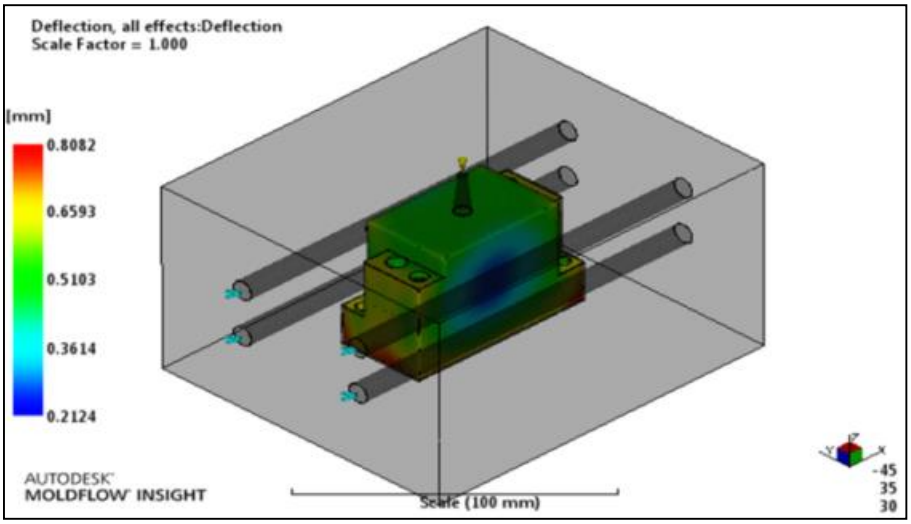

Figure 7.8 Warpage analysis using optimized parameter

Table 7.11 Comparison of shrinkage and warpage improvement with literature

Parameter	Hakimian et al.		Chiang & Chang	Present Study	
Shrinkage improvement (%)	34.5	12.68	1.04	36.47	30.73
Warpage improvement (%)	14.02	9.87	2.52	19.31	28.79

7.7 Chapter Summary

This paper presents an integrated methodology for developing mathematical models and predicting the values of shrinkage and warpage by correlating them with process parameters of plastic injection molding process for developing the electronic relay component of PBT and PET material. The parameters considered for the prediction of shrinkage and warpage are Melt temperature, Packing temperature and Packing time. To find the optimum value of process parameters, the analytical model using regression analysis was developed. To further improve the optimum values a recently developed modified particle swarm optimization algorithm was used. The conclusions of the research are as follows:

7.7.1 The results of the ANOVA analysis, which conduct confirmatory experiments, show that the analytical models of shrinkage and warpage are properly well with the simulation values. The effects of all process parameters on the performance of shrinkage and warpage are analyzed by the obtained mathematical models.

7.7.2 The predicted response of injection molding process also shows an improvement, using a newly developed MPSO algorithm. The MPSO algorithm overcomes the absence of classical PSO exploitation by introducing the search equation to improve performance based on the best outcome of the prior iteration. In addition, a greedy selection technique is added to improve the classical PSO's exploitation ability. The improvement in shrinkage and warpage is around 30% as compared to the initial values of shrinkage and warpage.

CHAPTER 8
Conclusion and Future Work

This dissertation presents a novel framework for improvement in part quality produced by rapid mold inserts and performs contactless inspection of samples having standard and complex feature using a reverse engineering approach. The proposed work mainly consist the development of important features of complex part integrated with standard benchmark features and from manufacturing to inspection of the industrial parts is discussed in the remaining chapters of the work. Based on the work carried out and the results obtained, this work is divided into five parts.

In the first part of thesis the investigation of employability of rapid tooling (RTV /PRT) as a functional injection molding is done. This work reports on the shrinkage behavior of wax in RTV silicone rubber under the influence of operating parameters of wax injector. Similarly, in the next part of this chapter feasibility of polymer rapid tools for plastic injection molding is also examined. Due to inadequate robustness and stability in RTV and PRT mold is used as an alternative tool for plastic injection molding process. The stability and robustness of PRT mold is tested on hand injection molding machine and using reverse engineering technique followed by 3D scanner it is found that PRT mold is suitable for making the simple part feature. The outcome of the test sample is compared with CAD file and inspected with COMET plus software. The results were validated with conventional tooling. After finding the suitability of PRT mold, the mechanical and physical characterization of Digital ABS used in PRT mold reporeted in chapter 3. The mechanical properties of the test specimen were analyzed by tensile, bending and impact test as well as by measuring their hardness. The results reported provided for the digital ABS in this research showed good dimensional and surface stability during the injection process. These produced parts will be functional and can be used in industrial applications for long time.

The chapter 4 of this thesis deals with estimating the part defects i.e. volumetric shrinkage and warpage for thermoplastic Polypropylene (PP) injection molded components

made using digital Acrylonitrile butadiene styrene (ABS) mold. For this purpose, twelve standard benchmark CAD model were selected with different geometric attributes. Subsequently, a systematic methodology is followed for simulation analysis, the Moldflow® (MFA) software is applied on all CAD model to identify the effect of shape and geometry parameters on the performance of volumetric shrinkage. Further, statistical regression technique used for determining the percentage contribution of geometric attributes on volumetric shrinkage. The basic purpose of the proposed methodology is to estimate volumetric shrinkage according to geometric attributes employed with RP-based rapid tooling design injection molding process. For modeling the process mathematical function including linear polynomial curve is used. Therefore, correlation coefficients, R^2 value, of the equations for volumetric shrinkage of 96.37%, calculated which explores the volumetric shrinkage of a linear relationship between the simulation data and the expected values from the regression model. Based on this R^2 test, quadratic polynomial models are best fitted for the output. The normal probability plot of residuals for the shrinkage defects of ABS mold notice that the residuals generally fall on straight line. The errors are normally distributed and obviously show that the quadratic modal obtained is precisely accurate. It can easily notice from the reported result in this chapter, highest volumetric shrinkage percentage (18.75 %) results are obtained for square pyramid frustum, conical frustum, and solid torus, and the lowest volumetric shrinkage percentage of 12.61 % is achieved for the hollow rectangular prism, which is investigated through Moldflow® (MFA) simulation software.

This study provides guidance to the personnel for the optimum parameter selection and assigning suitable shrinkage compensation values for digital ABS mold made using direct rapid tooling.

Similarly in the next section of this chapter, the investigation of warpage and shrinkage analysis of thin section part produce through Digital ABS Mold of the results for benchmark parts was extended for a complex part for a new PBT and PET materials. Analysis has been performed for three various thickness values 0.8, 0.9 and 1.0 mm using PBT/PET materials. To evaluate the results of the analysis for PBT/PET materials, statistical methods have been used for three different thickness values. Regression and ANOVA methods are used for these analyses. The analyses were performed by using

MINITAB software. To predict the values of shrinkage and warpage within the limits of the factors studied from the Regression model, the R^2 values for warpage and shrinkage are depends on wall thickness analysis. Here, the R^2 values is more than 90%, it is acceptable. The results of the Anderson-Darling (AD) standardity test are shown in this chapter for the respective distortion of PBT and PET for residues of 1 mm wall thickness. Since the p-value of the normality diagrams is over 0.05 for warpage and shrinkage, it means that the rest follows the normal distribution, and the models given by equations are suitable for practical technical applications. The developed complex part from the PRT mold is inspected with help of 3D scanner by choosing the best fit function against the model. The results can be easily recognized in this chapter is reported, 18.79 % is the maximum volumetric shrinkage found in cylinder feature and 11.57 % is the least volumetric shrinkage in hollow rectangular prism among all the features.

The last and the fifth chapter of this thesis a systematic methodology is presented using regression analysis and a newly developed MPSO algorithm for determining the optimum process parameters. In this method an efficient greedy selection procedure has been employed for obtaining better position between the newly generated and the current candidate solution based on the fitness value. Furthermore, a real life case study of an electronics component relay is considered for injection molding process. Initially, the effects of the injection process parameters on shrinkage and warpage for various wall thicknesses were examined using Taguchi method. The shrinkage and warpage values were found by Moldflow insight software. The results of confirmation experiments and analysis of variance (ANOVA) assure that the quadratic models of the shrinkage and warpage are well fitted with the simulated values at the optimum value. The shrinkage and warpage have been analyzed and predicted by the obtained mathematical models for the individual effects of all parameters. The adequate value of regression coefficient for shrinkage and warpage indicates that the model is significant and further analysis and predictions can be performed. Moreover, all the linear, square and interaction terms have significant effect on the response output. The influences of all the process parameters on the performances of shrinkage and warpage have been analyzed by the obtained mathematical models. The predicted response of injection molding process also shows an improvement, using a newly developed MPSO algorithm. The MPSO algorithm

overcomes the lack of classical PSO in exploitation behaviour through introduction of an improved search equation based on the best solution of the previous iteration. Additionally, a greedy selection procedure is added to improve the exploitation ability of the classical PSO. The improvement in shrinkage and warpage is around 30% as compared to the initial values of shrinkage and warpage.

On the basis of work carried out in this thesis, following conclusions have been reported in the five parts of this thesis as,

1. This work proposes a novel framework that replaces conventional molds and provides an AM direct PRT mold as a functional injection molding.

2. This work provided an alternating and optimum path for development of accurate part through PRT mold by minimizing various challenges, issues and by process parameter optimization of plastic injection molding machines. In addition, it investigates the critical parameters and there factors value for accurate feature reconstruction and improved accuracy of developed model.

3. This work proposes a novel inspection planning framework for eliminating conventional CMM/ Vernier caliper inspection planning requiring skill and expertise and provides a best way for inspection of soft materials like parts.

4. The work addresses the significance of 3D scanning process previously ignored in the literature. The effect of geometric attributes on the final accuracy of developed benchmark and complex feature part by PRT mold inserts using non-contact laser scanning is also studied.

5. This work also proposes a complex feature part having benchmark features for GD&T inspection and non-contact scanner characterization. The proposal of complex feature part and methodology for GD&T verification will provide a simple way of performance evaluation for contactless laser-scanning systems.

6. This work proposes an improved variant of classical particle swarm optimization named as modified particle swarm optimization (MPSO). The proposed algorithm overcomes the insufficiency of the classical PSO in terms of weak exploitation behaviour by introducing an improved solution search equation based on the best solution of the previous iteration. Additionally, a greedy selection procedure is added to further improve the exploitation ability of the classical PSO.

7. A simple objective function for geometric error of sample was formulated as an unconstrained optimization problem. Further, the minimum zone objective function was minimized using nature inspired algorithm like GA, PSO and MPSO.

8. The MPSO algorithm is further used in optimizing injection molding parameter and form error. Compared to conventional or existing heuristics optimization methods, the proposed MPSO algorithm not only has the advantage of a simple realization in computers and good flexibility, but it was shown to have improved evaluation accuracy.

Scope for Future work

This research work has given rise to some useful directions which forms the future scope of research. They are as follows:

1. Application of the proposed framework and adopted methodologies in inspection of components produced by other manufacturing processes.

2. Need to explore other injection molding parameters that affect the final output of the reverse engineered models.

3. This study proposes the novel framework for development of part from PRT mold and takes a step towards making the inspection process fully automatic. So, the next step will be to automatize the procedure described in the proposed framework by converting the steps into an algorithm for automatically extracting information from CAD to achieve an integrated GD&T-RE system.

4. Application of other advanced single and hybrid nature inspired optimization techniques for determining optimum injection molding parameters and GD&T error evaluation of developed part.

5. Application of advanced computational tools like Fuzzy sets and neural network will be highly interesting for optimum injection molding parameters and optimizing form error.

References:

Agazzi, A., Sobotka, V., Le Goff, R., Garcia, D., & Jarny, Y. (2010). A methodology for the design of effective cooling system in injection moulding. International journal of material forming, 3(1), 13-16.

Agazzi, A., Sobotka, V., LeGoff, R., & Jarny, Y. (2013). Optimal cooling design in injection moulding process–A new approach based on morphological surfaces. Applied Thermal Engineering, 52(1), 170-178.

Ahmad, A. H., Leman, Z., Azmir, M. A., Muhamad, K. F., Harun, W. S. W., Juliawati, A., & Alias, A. B. S. (2009, May). Optimization of warpage defect in injection moulding process using ABS material. In Modelling & Simulation, 2009. AMS'09. Third Asia International Conference on (pp. 470-474). IEEE.

Alias, A. B. S. (2009, May). Optimization of warpage defect in injection moulding process using ABS material. In Modelling & Simulation, 2009. AMS'09. Third Asia International Conference on (pp. 470-474). IEEE.

Ahmad, S. Darmoul, W. Ameen, M.H. Abidi, A. M. Al-Ahmar. Rapid Prototyping for Assembly Training and Validation. IFAC–PapersOnLine. 2015 Dec 31;48 (3):412-7.

Ahn, D. G., Park, S. H., & Kim, H. S. (2010). Manufacture of an injection mould with rapid and uniform cooling characteristics for the fan parts using a DMT process. International Journal of Precision Engineering and Manufacturing, 11(6), 915-924.

Ahmad, A. H., Leman, Z., Azmir, M. A., Muhamad, K. F., Harun, W. S. W., Juliawati, A., & Alias, A. B. S. (2009, May). Optimization of warpage defect in injection moulding process using ABS material. In Modelling & Simulation, 2009. AMS'09. Third Asia International Conference on (pp. 470-474). IEEE.

Altaf, K., Raghavan, V. R., & Rani, A. M. A. (2011). Comparative thermal analysis of circular and profiled cooling channels for injection mold tools. Journal of Applied Sciences, 11(11), 2068-2071.

Altaf, K., Rani, A. M. A., & Raghavan, V. R. (2011, September). Fabrication of circular and Profiled Conformal Cooling Channels in aluminum filled epoxy injection mould tools. In National Postgraduate Conference (NPC), 2011 (pp. 1-4). IEEE.

Altaf, K., Rani, A. M. A., Ahmad, F., Baharom, M., & Raghavan, V. R. (2016). Determining the effects of thermal conductivity on epoxy molds using profiled cooling channels with metal inserts. Journal of Mechanical Science and Technology, 30(11), 4901-4907

Altan, M. (2010). Reducing shrinkage in injection moldings via the Taguchi, ANOVA and neural network methods. Materials & Design, 31(1), 599-604.

Altan, T., Lilly, B., & Yen, Y. C. (2001). Manufacturing of dies and molds. CIRP Annals, 50(2), 404-422.

Amato, K. N., Gaytan, S. M., Murr, L. E., Martinez, E., Shindo, P. W., Hernandez, J., ... & Medina, F. (2012). Microstructures and mechanical behavior of Inconel 718 fabricated by selective laser melting. Acta Materialia, 60(5), 2229-2239.

Amran, M., Salmah, S., Zaki, M., Izamshah, R., Hadzley, M., Kasim, M. S., & Amri, M. (2014). The effect of pressure on warpage of dumbbell plastic part in injection moulding machine. In Advanced Materials Research (Vol. 903, pp. 61-66). Trans Tech Publications

An, J., Teoh, J. E. M., Suntornnond, R., & Chua, C. K. (2015). Design and 3D printing of scaffolds and tissues. Engineering, 1(2), 261-268.

Armillotta, A., Baraggi, R., & Fasoli, S. (2014). SLM tooling for die casting with conformal cooling channels. The International Journal of Advanced Manufacturing Technology, 71(1-4), 573-583.

Arobogast, T., Dawson, C. N., Keenan, P. T., Wheeler, M. F., & Yotov, I. (1998). Enhanced cell-centered finite differences for elliptic equations on general geometry. SIAM Journal on Scientific Computing, 19(2), 404-425.

Asproiu, S., & Străjescu, E. (2007). Influence of mold properties on the quality of molded parts. *UPB Sci. Bull. Ser. D Mech. Eng*, *69*(3), 39-46.

Au, K. M., & Yu, K. M. (2007). A scaffolding architecture for conformal cooling design in rapid plastic injection moulding. The International Journal of Advanced Manufacturing Technology, 34(5-6), 496-515.

Au, K. M., Yu, K. M., & Chiu, W. K. (2011). Visibility-based conformal cooling channel generation for rapid tooling. Computer-Aided Design, 43(4), 356-373.

Au, K. M., & Yu, K. M. (2011). Modeling of multi-connected porous passageway for mould cooling. Computer-Aided Design, 43(8), 989-1000.

Au, K. M., & Yu, K. M. (2014). Variable distance adjustment for conformal cooling channel design in rapid tool. Journal of Manufacturing Science and Engineering, 136(4), 044501.

Autodesk simulation moldflow Insight

Autodesk, 2015 Moldflow® simulation adviser help, www.autodesk.in.

B., Brezocnik, M., & Balic, J. (2006). Use of PolyJet technology in manufacture of new product. Journal of Achievements in Materials and Manufacturing Engineering, 18(1-2), 319-322.Communications in Heat and Mass Transfer, 37(9), 1359-1365.

Băcilă, C. G., & Baki-Hari, Z. G. (2006). The Rapid Tooling in the Product Development. In proceedings of the International Conference on Manufacturing Systems ICMaS (pp. 433-436).

Badrinarayan, B., & Barlow, J. W. (1994, September). Manufacture of injection molds using SLS. In Solid Freeform Fabrication Proceedings (pp. 371-8).

Barclift, M. W., & Williams, C. B. (2012, August). Examining variability in the mechanical properties of parts manufactured via polyjet direct 3D printing. In International Solid Freeform Fabrication Symposium (pp. 6-8). Austin, Texas: University of Texas at Austin

Barghash, M. A., & Alkaabneh, F. A. (2014). Shrinkage and warpage detailed analysis and optimization for the injection molding process using multistage experimental design. Quality engineering, 26(3), 319-334.

Barlow, J. W., Beaman, J. J., & Balasubramanian, B. (1996). A rapid mould-making system: material properties and design considerations. Rapid Prototyping Journal, 2(3), 4-15.

Barnatt, C. (2013). 3D printing: the next industrial revolution. Nottingham: Explaining The Future. com

Bartolo, P., Kruth, J. P., Silva, J., Levy, G., Malshe, A., Rajurkar, K., ... & Leu, M. (2012). Biomedical production of implants by additive electro-chemical and physical processes. CIRP Annals-Manufacturing Technology, 61(2), 635-655.

Bass, L., Meisel, N. A., & Williams, C. B. (2016). Exploring variability of orientation and aging effects in material properties of multi-material jetting parts. Rapid Prototyping Journal, 22(5), 826-834.

Bassoli, E., Gatto, A., Iuliano, L., & Grazia Violante, M. (2007). 3D printing technique applied to rapid casting. Rapid Prototyping Journal, 13(3), 148-155.

Beal, V. E., Ahrens, C. H., & Wendhausen, P. A. (2004). The use of stereolithography rapid tools in the manufacturing of metal powder injection molding parts. Journal of the Brazilian Society of Mechanical Sciences and Engineering, 26(1), 40-46.

Beringer, J., Arguin, J. F., Barnett, R. M., Copic, K., Dahl, O., Groom, D. E., ... & Yao, W. M. (2012). Review of particle physics. Physical Review D-Particles, Fields, Gravitation and Cosmology, 86(1).

Bernard, A., & Fischer, A. (2002). New trends in rapid product development. CIRP Annals-Manufacturing Technology, 51(2), 635-652.

Bian, W., Li, D., Lian, Q., Li, X., Zhang, W., Wang, K., & Jin, Z. (2012). Fabrication of a bio-inspired beta-Tricalcium phosphate/collagen scaffold based on ceramic stereolithography and gel casting for osteochondral tissue engineering. Rapid Prototyping Journal, 18(1), 68-80.

Bociaga, E. (2001). Effect of manufacturing conditions on the properties of injection molded polyethylene test specimens. Journal of Injection Molding Technology, 5(1), 15.

Bociąga, E., & Jaruga, T. (2007). Dynamic mechanical properties of parts from multicavity injection mould. Journal of Achievements in Materials and Manufacturing Engineering, 23(2), 83-86.

Brooks, H., & Brigden, K. (2016). Design of conformal cooling layers with self-supporting lattices for additively manufactured tooling. Additive Manufacturing, 11, 16-22.

Buchbinder, D., Schleifenbaum, H. B., Heidrich, S., Meiners, W., & Bültmann, J. (2011).

High power selective laser melting (HP SLM) of aluminum parts. Physics Procedia, 12, 271-278.

Calvert, P. (2001). Inkjet printing for materials and devices. Chemistry of materials, 13(10), 3299-3305.

Chang, H., Govindan, R., Jamin, S., Shenker, S. J., & Willinger, W. (2002, June). Towards capturing representative AS-level Internet topologies. In ACM SIGMETRICS Performance Evaluation Review (Vol. 30, No. 1, pp. 280-281). ACM.

Chang, T. C., & Faison, E. (2001). Shrinkage behavior and optimization of injection molded parts studied by the Taguchi method. Polymer Engineering & Science, 41(5), 703-710.

Chartier, C., Bastide, S., & Lévy-Clément, C. (2008). Metal-assisted chemical etching of silicon in HF–H2O2. Electrochimica Acta, 53(17), 5509-5516.

Cheah, C. M., Chua, C. K., Lee, C. W., Feng, C., & Totong, K. (2005). Rapid prototyping and tooling techniques: a review of applications for rapid investment casting. The International Journal of Advanced Manufacturing Technology, 25(3-4), 308-320.

Chen, C. C., Su, P. L., & Lin, Y. C. (2009). Analysis and modeling of effective parameters for dimension shrinkage variation of injection molded part with thin shell feature using response surface methodology. The International Journal of Advanced Manufacturing Technology, 45(11-12), 1087.

Chen, M. Y., Lee, D. J., & Tay, J. H. (2007). Distribution of extracellular polymeric substances in aerobic granules. Applied microbiology and biotechnology, 73(6), 1463-1469.

Chen, S. C. (2011). Understanding the effects of technology readiness, satisfaction and electronic word-of-mouth on loyalty in 3C products. Australian Journal of Business and Management Research, 1(3), 1.

Chen, W. C., Fu, G. L., Tai, P. H., & Deng, W. J. (2009). Process parameter optimization for MIMO plastic injection molding via soft computing. Expert Systems with Applications, 36(2), 1114-1122.

Chen, W. C., Tai, P. H., Wang, M. W., Deng, W. J., & Chen, C. T. (2008). A neural network-based approach for dynamic quality prediction in a plastic injection molding process. Expert systems with Applications, 35(3), 843-849.

Chen, W., & McCarthy, T. J. (1997). Layer-by-layer deposition: a tool for polymer surface modification. Macromolecules, 30(1), 78-86.

Chen, X., Lam, Y. C., & Li, D. Q. (2000). Analysis of thermal residual stress in plastic injection molding. Journal of Materials Processing Technology, 101(1-3), 275-280.

Cheng, X. Y., Li, S. J., Murr, L. E., Zhang, Z. B., Hao, Y. L., Yang, R., ... & Wicker, R. B. (2012). Compression deformation behavior of Ti–6Al–4V alloy with cellular structures fabricated by electron beam melting. journal of the mechanical behavior of biomedical materials, 16, 153-162.

Chiang, K. T. (2007). Modeling and optimization of designing parameters for a parallel-plain fin heat sink with confined impinging jet using the response surface methodology. Applied Thermal Engineering, 27(14-15), 2473-2482.

Chiang, K. T. (2007). The optimal process conditions of an injection-molded thermoplastic part with a thin shell feature using grey-fuzzy logic: A case study on machining the PC/ABS cell phone shell. Materials & design, 28(6), 1851-1860.

Chiang, K. T., & Chang, F. P. (2006). Application of grey-fuzzy logic on the optimal process design of an injection-molded part with a thin shell feature. International Communications in Heat and Mass Transfer, 33(1), 94-101.

Chiang, K. T., & Chang, F. P. (2007). Analysis of shrinkage and warpage in an injection-molded part with a thin shell feature using the response surface methodology. The International Journal of Advanced Manufacturing Technology, 35(5-6), 468-479.

Chiang, M., Low, S. H., Calderbank, A. R., & Doyle, J. C. (2007). Layering as optimization decomposition: A mathematical theory of network architectures. Proceedings of the IEEE, 95(1), 255-312.

Chien, W. T., Chen, C. S., & Chen, H. H. (2006). Resonant frequency analysis of fixed-free single-walled carbon nanotube-based mass sensor. Sensors and Actuators A: Physical, 126(1), 117-121.

Chin Fei, N., Mehat, N. M., Kamaruddin, S., & Mohamad Ariff, Z. (2013). Improving the performance of reprocessed ABS products from the manufacturing perspective via the Taguchi method. International Journal of Manufacturing Engineering, 2013.

Choi, D. S., & Im, Y. T. (1999). Prediction of shrinkage and warpage in consideration of residual stress in integrated simulation of injection molding. Composite Structures, 47(1-4), 655-665.

Choi, J. Y., Das, S., Theodore, N. D., Kim, I., Honsberg, C., Choi, H. W., & Alford, T. L. (2015). Advances in 2D/3D printing of functional nanomaterials and their applications. ECS Journal of Solid State Science and Technology, 4(4), P3001-P3009.

Chopra, K., Mummery, P. M., Derby, B., & Gough, J. E. (2012). Gel-cast glass-ceramic tissue scaffolds of controlled architecture produced via stereolithography of moulds. Biofabrication, 4(4), 045002.

Chua, C. K., Leong, K. F., & Lim, C. S. (2010). Rapid Prototyping: Principles and Applications (with Companion CD-ROM). World Scientific Publishing Company.

Chua, C. K., Leong, K. F., & Liu, Z. H. (2015). Rapid Tooling in Manufacturing. In Handbook of Manufacturing Engineering and Technology (pp. 2525-2549). Springer London.

Chua, C. K., Teh, S. H., & Gay, R. K. L. (1999). Rapid prototyping versus virtual prototyping in product design and manufacturing. The international journal of advanced manufacturing technology, 15(8), 597-603.

Clark, J. R., & Grant, M. B. B. (1992). The effect of surface finish on component performance. International Journal of Machine Tools and Manufacture, 32(1-2), 57-66.

Colao, F., Fantoni, R., Lazic, V., & Spizzichino, V. (2002). Laser-induced breakdown spectroscopy for semi-quantitative and quantitative analyses of artworks—application on multi-layered ceramics and copper based alloys. Spectrochimica Acta Part B: Atomic Spectroscopy, 57(7), 1219-1234.

Coleman, J. N., Lotya, M., O'Neill, A., Bergin, S. D., King, P. J., Khan, U., ... & Shvets, I. V. (2011). Two-dimensional nanosheets produced by liquid exfoliation of layered materials. Science, 331(6017), 568-571.

Cramez, M. C., Oliveira, M. J., & Crawford, R. J. (1998). Effect of pigmentation on the microstructure and properties of rotationally molded polyethylene. Journal of materials science, 33(20), 4869-4877.

Cuesta, E., Rico, J. C., Fernández, P., Blanco, D., & Valiño, G. (2009). Influence of roughness on surface scanning by means of a laser stripe system. The International Journal of Advanced Manufacturing Technology, 43(11-12), 1157.

Cui, X., Boland, T., D D'Lima, D., & K Lotz, M. (2012). Thermal inkjet printing in tissue engineering and regenerative medicine. Recent patents on drug delivery & formulation, 6(2), 149-155.

da Silva Bartolo, P. J., & Bártolo, P. (2010). Innovative Developments in Design and Manufacturing: Advanced Research in Virtual and Rapid Prototyping: Proceedings of the 4th International Conference on Advanced Research in Virtual and Rapid Prototyping, Leiria, Portugal, 6-10 October 2009. CRC.

Dalgarno, K. W., & Stewart, T. D. (2001). Manufacture of production injection mould tooling incorporating conformal cooling channels via indirect selective laser sintering. Proceedings of the Institution of Mechanical Engineers, Part B: Journal of Engineering Manufacture, 215(10), 1323-1332.

Dalgarno, K. W., Stewart, T. D., & Allport, J. M. (2001). Layer manufactured production tooling incorporating conformal heating channels for transfer moulding of elastomer compounds. Plastics, rubber and composites, 30(8), 384-388.

Dalgarno, K., & Stewart, T. (2001). Production tooling for polymer moulding using the RapidSteel process. Rapid Prototyping Journal, 7(3), 173-179.

Davim, J. P. (2001). A note on the determination of optimal cutting conditions for surface finish obtained in turning using design of experiments. Journal of materials processing technology, 116(2-3), 305-308.

De Gans, B. J., Duineveld, P. C., & Schubert, U. S. (2004). Inkjet printing of polymers: state of the art and future developments. Advanced materials, 16(3), 203-213.

Derrick, S. (2013). Use of Polymer Rapid Tools as Functional Injection Mold Tooling.

Dobrzański, L. A., Król, M., Bilewicz, M., & Viana, J. C. (2008). Microstructure and mechanical properties of Polypropylene/Polycarbonate blends. Journal of Achievements in Materials and Manufacturing Engineering, 27(1), 19-22.

Dickens, L.I. and Nanny, W.C., RADVA PLASTICS CORP, 1980. Composite panel structure and method of manufacture. U.S. Patent 4,241,555.

Dickens, P. M. (1997). Principles of design for laminated tooling. International Journal of Production Research, 35(5), 1349-1357.

Díez-Pascual, A. M., Ashrafi, B., Naffakh, M., González-Domínguez, J. M., Johnston, A., Simard, B., ... & Gómez-Fatou, M. A. (2011). Influence of carbon nanotubes on the thermal, electrical and mechanical properties of poly (ether ether ketone)/glass fiber laminates. Carbon, 49(8), 2817-2833.

Dimitrov, D. M., Moammer, A. A., & Harms, T. (2010). Cooling channel configuration in injection moulds.

Dimitrov, D., & Moammer, A. (2010). Investigation of the impact of conformal cooling on the performance of injection moulds for the packaging industry. Journal for New Generation Sciences, 8(1), 29-46.

Dimitrov, D., Moammer, A., & Harms, T. M. (2010). The impact of cooling channel layout on injection moulds.

Ding, Q. L., Ju, F., Mao, X. B., Ma, D., Yu, B. Y., & Song, S. B. (2016). Experimental investigation of the mechanical behavior in unloading conditions of sandstone after high-temperature treatment. Rock Mechanics and Rock Engineering, 49(7), 2641-2653.

Dobrzański, L. A., Król, M., Bilewicz, M., & Viana, J. C. (2008). Microstructure and mechanical properties of Polypropylene/Polycarbonate blends. Journal of Achievements in Materials and Manufacturing Engineering, 27(1), 19-22.

Donnchadha, B. O., & Tansey, A. (2003, October). Conformally cooled metal composite rapid tooling. In Proceedings of the 1st International Conference on Advanced Research in

Druschitz, A., Williams, C., Snelling, D., & Seals, M. (2014). Additive manufacturing supports the production of complex castings. In Shape Casting: 5th International Symposium 2014 (pp. 51-57). Springer, Cham.

Egodawatta, A. K., Harrison, D. K., De Silva, A., & Haritos, G. (2004). Feasibility study on developing productivity and quality improved layered manufacturing method

for rapid prototyping/tooling/manufacture. Journal of materials processing technology, 149(1-3), 604-608.

Eiamsa-Ard, K., & Wannissorn, K. (2015). Conformal bubbler cooling for molds by metal deposition process. Computer-Aided Design, 69, 126-133.

Elkott, D. F., Elmaraghy, H. A., & Elmaraghy, W. H. (2002). Automatic sampling for CMM inspection planning of free-form surfaces. International Journal of Production Research, 40(11), 2653-2676.

Elliott, K. W., Curles, C. T., Hollingsworth, A., Zachary, D. P., Sisk, T. C., & Vaniman, M. D. (1997). U.S. Patent No. 5,694,742. Washington, DC: U.S. Patent and Trademark Office.

Elsoufi, L., Khalil, K., Charon, W., & Lachat, R. (2015). Influence of the Thermoplastic Type on the Thermal Evolution of a Piezoceramic Patch during the Manufacture of a Smart Thermoplastic Part by Injection Molding Process. Journal of Manufacturing Science and Engineering, 137(2), 021002.

Farotti, E., & Natalini, M. (2018). Injection molding. Influence of process parameters on mechanical properties of polypropylene polymer. A first study. Procedia Structural Integrity, 8, 256-264.

Fathi, S., & Dickens, P. (2012). Nozzle Wetting and Instabilities during Droplet Formation of Molten Nylon Materials in an Inkjet Printhead. Journal of Manufacturing Science and Engineering, 134(4), 041008.

Fei, N. C., Mehat, N. M., & Kamaruddin, S. (2013). Practical applications of Taguchi method for optimization of processing parameters for plastic injection moulding: a retrospective review. ISRN Industrial engineering, 2013.

Ferreira, J. C. (2004). Rapid tooling of die DMLS inserts for shoot-squeeze moulding (DISA) system. Journal of Materials Processing Technology, 155, 1111-1117.

Ferreira, J. C., Santos, E., Madureira, H., & Castro, J. (2006). Integration of VP/RP/RT/RE/RM for rapid product and process development. Rapid Prototyping Journal, 12(1), 18-25.

Folgar, C. E., Folgar, L. N., Cormier, D., & Hill, R. (2013). Multifunctional material direct printing for laser sintering systems. In Int. Solid Free. Fabr. Symp (pp. 282-296).

Frazier, W. E. (2014). Metal additive manufacturing: a review. Journal of Materials Engineering and Performance, 23(6), 1917-1928.

Fuller, S. B., Wilhelm, E. J., & Jacobson, J. M. (2002). Ink-jet printed nanoparticle microelectromechanical systems. Journal of Microelectromechanical systems, 11(1), 54-60.

Galantucci, L. M., & Spina, R. (2003). Evaluation of filling conditions of injection moulding by integrating numerical simulations and experimental tests. Journal of materials processing technology, 141(2), 266-275.

Galantucci, L. M., Lavecchia, F., & Percoco, G. (2009). Experimental study aiming to enhance the surface finish of fused deposition modeled parts. CIRP annals, 58(1), 189-192.

Galantucci, L. M., Percoco, G., & Spina, R. (2003). Evaluation of rapid prototypes obtained from reverse engineering. Proceedings of the Institution of Mechanical Engineers, Part B: Journal of Engineering Manufacture, 217(11), 1543-1552.

Galantucci, L. M., Percoco, G., & Spina, R. (2003). Telemanufacturing of reverse engineered parts: A case study. Proceedings of the Institution of Mechanical Engineers, Part B: Journal of Engineering Manufacture, 217(5), 727-731.

Gao, J., Chen, X., Zheng, D., Yilmaz, O., & Gindy, N. (2006). Adaptive restoration of complex geometry parts through reverse engineering application. Advances in Engineering Software, 37(9), 592-600.

Gao, J., Gindy, N., & Chen, X. (2006). An automated GD&T inspection system based on non-contact 3D digitization. International journal of production research, 44(1), 117-134.

Gao, W., Zhang, Y., Ramanujan, D., Ramani, K., Chen, Y., Williams, C. B.,& Zavattieri, P. D. (2015). The status, challenges, and future of additive manufacturing in engineering. Computer-Aided Design, 69, 65-89.

Garg, H. K., & Singh, R. (2013). Pattern development for manufacturing applications with fused deposition modelling-a case study. International Journal of Automotive and Mechanical Engineering, 7, 981.

Ghalme, S., Mankar, A., & Bhalerao, Y. J. (2016). Parameter optimization in milling of glass fiber reinforced plastic (GFRP) using DOE-Taguchi method. SpringerPlus, 5(1), 1376.

Ghazali, R., Sukri, A. E. E., Latif, A. R. A., Rasam, A. R. A., Latif, Z. A., & Samad, A. M. (2011, November). Evaluating the relationship between scanning resolution of laser scanner with the accuracy of the 3D model constructed. In Control System, Computing and Engineering (ICCSCE), 2011 IEEE International Conference on (pp. 590-595). IEEE.

Gibbons, G. J., Hansell, R. G., Norwood, A. J., & Dickens, P. M. (2003). Rapid laminated die-cast tooling. Assembly Automation, 23(4), 372-381.

Gibson, I., Rosen, D. W., & Stucker, B. (2010). Design for additive manufacturing. In Additive Manufacturing Technologies (pp. 299-332). Springer, Boston, MA.

Gibson, I., Rosen, D. W., & Stucker, B. (2010). The use of multiple materials in additive manufacturing. In Additive Manufacturing Technologies (pp. 436-449). Springer, Boston, MA.

Ginzburg, M., Galloro, J., Jäkle, F., Power-Billard, K. N., Yang, S., Sokolov, I., ... & Ozin, G. A. (2000). Layer-by-layer self-assembly of organic− organometallic polymer electrostatic superlattices using poly (ferrocenylsilanes). Langmuir, 16(24), 9609-9614.

Gojanović, D., & Nikolić, G. (2015). 3D printers-review of printing clothing, footwear and accessories. Tekstil: časopis za tekstilnu tehnologiju i konfekciju, 64(5-6), 190-199.

Gong, H., Rafi, K., Starr, T., & Stucker, B. (2012, August). Effect of defects on fatigue tests of as-built Ti-6Al-4V parts fabricated by selective laser melting. In Solid freeform fabrication symposium (pp. 499-506). University of Texas Austin, Texas.

González-Jorge, H., Riveiro, B., Armesto, J., & Arias, P. (2011). Standard artifact for the geometric verification of terrestrial laser scanning systems. Optics & Laser Technology, 43(7), 1249-1256.

Grijpma, D. W., Altpeter, H., Bevis, M. J., & Feijen, J. (2002). Improvement of the mechanical properties of poly (D, L-lactide) by orientation. Polymer international, 51(10), 845-851.

Guerrica-Echevarría, G., Eguiazabal, J. I., & Nazabal, J. (2001). Influence of the preparation method on the mechanical properties of a thermotropic liquid crystalline copolyester. Polymer testing, 20(4), 403-408.

Guo, Y., Sohel, F., Bennamoun, M., Wan, J., & Lu, M. (2015). A novel local surface feature for 3D object recognition under clutter and occlusion. Information Sciences, 293, 196-213.

Gupta, M., & Wang, K. K. (1993). Fiber orientation and mechanical properties of short-fiber-reinforced injection-molded composites: Simulated and experimental results. Polymer Composites, 14(5), 367-382.

Hakimian, E., & Sulong, A. B. (2012). Analysis of warpage and shrinkage properties of injection-molded micro gears polymer composites using numerical simulations assisted by the Taguchi method. Materials & Design, 42, 62-71.

Hall, M., & Krystofik, M. (2015). Conformal Cooling. Center of Excellence in Sustainable Manufacturing: Rochester Institute of Technology.

Hamdan, A., Sarhan, A. A., & Hamdi, M. (2012). An optimization method of the machining parameters in high-speed machining of stainless steel using coated carbide tool for best surface finish. The International Journal of Advanced Manufacturing Technology, 58(1-4), 81-91.

Hassan, H., Regnier, N., Pujos, C., Arquis, E., & Defaye, G. (2010). Modeling the effect of cooling system on the shrinkage and temperature of the polymer by injection molding. Applied Thermal Engineering, 30(13), 1547-1557.

Hay, R.R. and Spencer, P.R., HP Inc, 1986. Nozzle test apparatus and method for thermal ink jet systems. U.S. Patent 4,590,482.

Hayasi, M., & Asiabanpour, B. (2014). Close to CAD model curved-form adaptive slicing. Rapid Prototyping Journal, 20(2), 133-144.

He, Y., Wildman, R. D., Tuck, C. J., Christie, S. D., & Edmondson, S. (2016). An investigation of the behavior of solvent based polycaprolactone ink for material jetting. Scientific reports, 6, 20852.

Hearunyakij, M., Sontikaew, S., & Sriprapai, D. (2014). Improvement in the cooling performance of conformal mold cooling by using fin concept. Int J Min Metall Mech Eng, 2, 41-46.

Hilton, P. (2000). Rapid tooling: technologies and industrial applications. CRC press.

Himmer, T., Nakagawa, T., & Anzai, M. (1999). Lamination of metal sheets. Computers in Industry, 39(1), 27-33.

Himmer, T., Techel, A., Nowotny, S., & Beyer, E. (2003). Recent developments in metal laminated tooling by multiple laser processing. Rapid prototyping journal, 9(1), 24-29.

Ho, K., & Pehlke, R. D. (1985). Metal-mold interfacial heat transfer. Metallurgical Transactions B, 16(3), 585-594.

Hoekstra, N. (2000). Tool design and concurrent engineering using rapid tooling construction methods. age, 5, 1.

Hofmann, M. (2014). 3D printing gets a boost and opportunities with polymer materials.

Holder, g., villamizar, f. A. Y., martin, p. J., & salmoria, g. (2005), Investigation of the thermo-mechanical properties of rapid tooling materials for injection moulding.

Hopkinson, N., & Dickens, P. (1999). Study of ejection forces in the AIMTM process. Materials & design, 20(2-3), 99-105.

Hosaka, K., Tagami, J., Nishitani, Y., Yoshiyama, M., Carrilho, M., Tay, F. R., ... & Pashley, D. H. (2007). Effect of wet vs. dry testing on the mechanical properties of hydrophilic self-etching primer polymers. European journal of oral sciences, 115(3), 239-245.

http//www.steinbichler.com/products.

http://3dprintingindustry.com/2014 injection-molding-stratasys-worrell/ 3DP Injection Molding

http://www.stratasys.com/materials/polyjet/~/media/29592222B80C489BAC28803DB08C10E5.ashx

Huang, J., Lu, Y., Wang, Q., & Lin, F. (2013). Design and Fabrication of Conformal Cooling Channels with Vacuum Diffusion Bonding. Recent Patents on Chemical Engineering, 6(3), 176-183.

Huang, M. C., & Tai, C. C. (2001). The effective factors in the warpage problem of an injection-molded part with a thin shell feature. Journal of materials processing technology, 110(1), 1-9.

Ibrahim, M., Otsubo, T., Narahara, H., Koresawa, H., & Suzuki, H. (2006). Inkjet printing resolution study for multi-material rapid prototyping. JSME International Journal Series C Mechanical Systems, Machine Elements and Manufacturing, 49(2), 353-360.

Ilyas, I., Taylor, C., Dalgarno, K., & Gosden, J. (2010). Design and manufacture of injection mould tool inserts produced using indirect SLS and machining processes. Rapid Prototyping Journal, 16(6), 429-440.

Im, Y. T., & Walczyk, D. F. (2002). Development of a computer-aided manufacturing system for profiled edge lamination tooling. Journal of manufacturing science and engineering, 124(3), 754-761.

Ippolito, R., Iuliano, L., & Gatto, A. (1995). Benchmarking of rapid prototyping techniques in terms of dimensional accuracy and surface finish. CIRP Annals-Manufacturing Technology, 44(1), 157-160.

Isgro, G., Kleverlaan, C. J., Wang, H., & Feilzer, A. J. (2005). The influence of multiple firing on thermal contraction of ceramic materials used for the fabrication of layered all-ceramic dental restorations. Dental Materials, 21(6), 557-564.

Isgrò, G., Wang, H., Kleverlaan, C. J., & Feilzer, A. J. (2005). The effects of thermal mismatch and fabrication procedures on the deflection of layered all-ceramic discs. Dental Materials, 21(7), 649-655.

Jacobs, P. (1996). Stereolithography and other rapid prototyping and manufacturing technologies. SME., New York.

Jamal, A. M. M., Sarker, B. R., & Mondal, S. (2004). Optimal manufacturing batch size with rework process at a single-stage production system. Computers & Industrial Engineering, 47(1), 77-89.

Janaki Ram, G. D., Venugopal Reddy, A., Prasad Rao, K., & Madhusudhan Reddy, G. (2006). High temperature mechanical properties of Inconel 718 pulsed Nd–YAG laser welds. Materials at High Temperatures, 23(1), 29-37.

Jetley, S., & Low, D. K. (2006). A rapid tooling technique using a low melting point metal alloy for plastic injection molding. Journal of Industrial Technology, 22(3), 2-8.

Ji, C. H., Choi, M., Kim, S. C., Lee, S. H., Kim, S. H., Yee, Y., & Bu, J. U. (2006). An electrostatic scanning micromirror with diaphragm mirror plate and diamond-shaped reinforcement frame. Journal of Micromechanics and Microengineering, 16(5), 1033.

Juraeva, M., Ryu, K. J., & Song, D. J. (2013). Gate shape optimization using design of experiment to reduce the shear rate around the gate. International Journal of Automotive Technology, 14(4), 659-666.

Kaasalainen, S., Jaakkola, A., Kaasalainen, M., Krooks, A., & Kukko, A. (2011). Analysis of incidence angle and distance effects on terrestrial laser scanner intensity: Search for correction methods. Remote Sensing, 3(10), 2207-2221.

Kaasalainen, S., Niittymaki, H., Krooks, A., Koch, K., Kaartinen, H., Vain, A., & Hyyppa, H. (2010). Effect of target moisture on laser scanner intensity. IEEE Transactions on Geoscience and Remote Sensing, 48(4), 2128-2136.

Kakinuma, Y., Mori, M., Oda, Y., Mori, T., Kashihara, M., Hansel, A., & Fujishima, M. (2016). Influence of metal powder characteristics on product quality with directed energy deposition of Inconel 625. CIRP Annals, 65(1), 209-212.

Karunakaran, K. P., Bernard, A., Suryakumar, S., Dembinski, L., & Taillandier, G. (2012). Rapid manufacturing of metallic objects. Rapid Prototyping Journal, 18(4), 264-280.

Karunakaran, K. P., Sreenathbabu, A., & Pushpa, V. (2004). Hybrid layered manufacturing: direct rapid metal tool-making process. Proceedings of the Institution of Mechanical Engineers, Part B: Journal of Engineering Manufacture, 218(12), 1657-1665.

Karunakaran, K. P., Suryakumar, S., Chandrasekhar, U., & Bernard, A. (2010). Hybrid rapid manufacturing of metallic objects. International Journal of Rapid Manufacturing, 1(4), 433-455.

Kassim, N. (2012). New technique of producing removable complete denture using rapid tooling approach (Doctoral dissertation, Universiti Tun Hussein Onn Malaysia).

Kechagias, J., Stavropoulos, P., Koutsomichalis, A., Ntintakis, I., & Vaxevanidis, N. (2014, July). Dimensional Accuracy Optimization of Prototypes produced by PolyJet Direct 3D Printing Technology. In Proccedings of the 18th International Conference on Circuits, Systems, Communications and Computers.

Kenig, S., Ben-David, A., Omer, M., & Sadeh, A. (2001). Control of properties in injection molding by neural networks. Engineering Applications of Artificial Intelligence, 14(6), 819-823.

Khamis, S. Z., Othman, M. H., Hasan, S., & Ibrahim, M. H. I. (2017, August). Characterizetion of Flexural Strength, Warpage and Shrinkage of Polypropylene-Nanoclay-Nanocomposites Blend with Gigantochloa Scortechinii. In IOP Conference Series: Materials Science and Engineering (Vol. 226, No. 1, p. 012163). IOP Publishing.

Khan, M., Afaq, S. K., Khan, N. U., & Ahmad, S. (2014). Cycle time reduction in injection molding process by selection of robust cooling channel design. ISRN Mechanical Engineering, 2014.

Khondker, O. A., Yang, X., Usui, N., & Hamada, H. (2006). Mechanical properties of textile-inserted PP/PP knitted composites using injection–compression molding. Composites Part A: Applied Science and Manufacturing, 37(12), 2285-2299.

Kikuchi, H., & Koyama, K. (1996). Generalized warpage parameter. Polymer Engineering & Science, 36(10), 1309-1316.

Kikuchi, H., & Koyama, K. (1996). The relation between thickness and warpage in a disk injection molded from fiber reinforced PA66. Polymer Engineering & Science, 36(10), 1317-1325.

Kikuchi, H., & Koyama, K. (1996). Warpage, anisotropy, and part thickness. Polymer Engineering & Science, 36(10), 1326-1335.

Kim, M., Park, Y. B., Okoli, O. I., & Zhang, C. (2009). Processing, characterization, and modeling of carbon nanotube-reinforced multiscale composites. Composites Science and Technology, 69(3-4), 335-342.

Kim, Y. S., Park, Y. C., Ansari, S. G., Lee, B. S., & Shin, H. S. (2003). Effect of substrate temperature on the bonded states of indium tin oxide thin films deposited by plasma enhanced chemical vapor deposition. Thin Solid Films, 426(1-2), 124-131.

Kordás, K., Mustonen, T., Tóth, G., Jantunen, H., Lajunen, M., Soldano, C., ... & Ajayan, P. M. (2006). Inkjet printing of electrically conductive patterns of carbon nanotubes. Small, 2(8-9), 1021-1025.

Kovács, J. G., & Siklo, B. (2011). Test method development for deformation analysis of injection moulded plastic parts. Polymer Testing, 30(5), 543-547.

Kovács, J. G., & Sikló, B. Fiber reinforcement induced warpage on injection molded thermoplastics.

Kovács, J. G., Szabó, F., Kovács, N. K., Suplicz, A., Zink, B., Tábi, T., & Hargitai, H. (2015).Thermal simulations and measurements for rapid tool inserts in injection molding applications. Applied Thermal Engineering, 85, 44-51.

Kremer, D. M., Davis, R. W., Moore, E. F., Maslar, J. E., Burgess, D. R., & Ehrman, S. H. (2003). An investigation of particle dynamics in a rotating disk chemical vapor deposition reactor. Journal of the Electrochemical Society, 150(2), G127-G139.

Kruth, J. P. (1991). Material incress manufacturing by rapid prototyping techniques. CIRP Annals-Manufacturing Technology, 40(2), 603-614. Kruth, J. P., Wangutomatio

Kruth, J. P., Leu, M. C., & Nakagawa, T. (1998). Progress in additive manufacturing and rapid prototyping. Cirp Annals, 47(2), 525-540.

Kruth, J. P., Mercelis, P., Van Vaerenbergh, J., Froyen, L., & Rombouts, M. (2005). Binding mechanisms in selective laser sintering and selective laser melting. Rapid prototyping journal, 11(1), 26-36.

Kruth, J. P., Vandenbroucke, B., Van Vaerenbergh, J., & Mercelis, P. (2005). Benchmarking of different SLS/SLM processes as rapid manufacturing techniques. Laser, 1, 3D.

Kruth, J. P., Wang, X., Laoui, T., & Froyen, L. (2003). Lasers and materials in selective laser sintering. Assembly Automation, 23(4), 357-371.

Ku, T. W., Ha, B. K., Song, W. J., Kang, B. S., & Hwang, S. M. (2002). Finite element analysis of multi-stage deep drawing process for high-precision rectangular case with extreme aspect ratio. Journal of Materials Processing Technology, 130, 128-134.

Kumar, P., Singh, R., & Ahuja, I. P. S. (2015). Investigations on dimensional accuracy of the components prepared by hybrid investment casting. Journal of Manufacturing Processes, 20, 525-533.

Kumar, S., & Singh, A. K. (2018). Warpage and Shrinkage analysis and optimization of rapid tooling molded thin wall component using modified particle swarm algorithm. Journal of Advanced Manufacturing Systems.

Kumar, S., & Singh, A. K. (2018). FDM molded polymer tooling for plastic injection molding, International journal of advanced in materials science and engineering (IJAMSE) Vol. 7, No. 1, Jan 2018. DOI: 10.14810/ijamse.2018.7102

Kumar, S., & Singh, A. K., Pathak V.K (2019) Modelling and optimization of injection molding process for PBT/PET parts using modified particle swarm algorithm, International Journal of Engineering and Material Sciences, NISCAIR(IJEMS-9642)/18

Kuo, C. C., & Xu, W. C. (2018). Effects of different cooling channels on the cooling efficiency in the wax injection molding process. The International Journal of Advanced Manufacturing Technology, 1-9.

Kuram, E., Ozcelik, B., Yilmaz, F., Timur, G., & Sahin, Z. M. (2014). The effect of recycling number on the mechanical, chemical, thermal, and rheological properties of PBT/PC/ABS ternary blends: With and without glass-fiber. Polymer Composites, 35(10), 2074-2084.

Kurtaran, H., & Erzurumlu, T. (2006). Efficient warpage optimization of thin shell plastic parts using response surface methodology and genetic algorithm. The International Journal of Advanced Manufacturing Technology, 27(5-6), 468-472.

Kurtaran, H., Ozcelik, B., & Erzurumlu, T. (2005). Warpage optimization of a bus ceiling lamp base using neural network model and genetic algorithm. Journal of materials processing technology, 169(2), 314-319.

Kurtz, S. M., Pruitt, L., Jewett, C. W., Crawford, R. P., Crane, D. J., & Edidin, A. A. (1998). The yielding, plastic flow, and fracture behavior of ultra-high molecular weight polyethylene used in total joint replacements. Biomaterials, 19(21), 1989-2003.

Laeng, J., Stewart, J. G., & Liou, F. W. (2000). Laser metal forming processes for rapid prototyping-A review. International Journal of Production Research, 38(16), 3973-3996.

Lam, C. X. F., Mo, X. M., Teoh, S. H., & Hutmacher, D. W. (2002). Scaffold development using 3D printing with a starch-based polymer. Materials Science and Engineering: C, 20(1-2), 49-56.

Le Goff, R., Delaunay, D., Boyard, N., Jarny, Y., Jurkowski, T., & Deterre, R. (2009). On-line temperature measurements for polymer thermal conductivity estimation under injection molding conditions. International Journal of heat and mass transfer, 52(5-6), 1443-1450.

Lebrun, G., Gauvin, R., & Kendall, K. N. (1996). Experimental investigation of resin temperature and pressure during filling and curring in a flat steel RTM mould. Composites Part A: Applied Science and Manufacturing, 27(5), 347-356.

Lee, C. T., & Lee, C. C. (2014). On a hybrid particle swarm optimization method and its application in mechanism design. Proceedings of the Institution of Mechanical Engineers, Part C: Journal of Mechanical Engineering Science, 228(15), 2844-2857.

Lee, S. J., & Chang, D. Y. (2006). A laser sensor with multiple detectors for freeform surface digitization. The International Journal of Advanced Manufacturing Technology, 31(5-6), 474-482.

Lee, G. W., Park, M., Kim, J., Lee, J. I., & Yoon, H. G. (2006). Enhanced thermal conductivity of polymer composites filled with hybrid filler. Composites Part A: Applied science and manufacturing, 37(5), 727-734.

Lee, J. G., & Subramanian, K. N. (2007). Effects of TMF heating rates on damage accumulation and resultant mechanical behavior of Sn–Ag based solder joints. Microelectronics Reliability, 47(1), 118-131.

Lee, S. B., Lee, J. H., Chang, J. S., Moon, H. J., Kim, S. W., & An, K. (2002). Observation of scarred modes in asymmetrically deformed microcylinder lasers. Physical review letters, 88(3), 033903.

Lemeš, S., & Zaimović-Uzunović, N. (2009, October). Study of ambient light influence on laser 3D scanning. In Proceedings of the 7th International Conference on Industrial Tools and Material Processing Technologies (pp. 327-330).

Leo, V., & Cuvelliez, C. H. (1996). The effect of the packing parameters, gate geometry, and mold elasticity on the final dimensions of a molded part. Polymer Engineering & Science, 36(15), 1961-1971.

Levy, G. N., Schindel, R., & Kruth, J. P. (2003). Rapid manufacturing and rapid tooling with layer manufacturing (LM) technologies, state of the art and future perspectives. CIRP Annals-Manufacturing Technology,52(2), 589-609.

Li, C. G., & Li, C. L. (2008). Plastic injection mould cooling system design by the configuration space method. Computer-Aided Design, 40(3), 334-349.

Liang, Z., Lin, D., Zhao, J., Lu, Z., Liu, Y., Liu, C., ... & Cui, Y. (2016). Composite lithium metal anode by melt infusion of lithium into a 3D conducting scaffold with lithiophilic coating. Proceedings of the National Academy of Sciences, 113(11), 2862-2867.

Liao, S. J., Chang, D. Y., Chen, H. J., Tsou, L. S., Ho, J. R., Yau, H. T., ... & Su, Y. C. (2004). Optimal process conditions of shrinkage and warpage of thin-wall parts. Polymer Engineering & Science, 44(5), 917-928.

Liao, S. J., Hsieh, W. H., Wang, J. T., & Su, Y. C. (2004). Shrinkage and warpage prediction of injection-molded thin-wall parts using artificial neural networks. Polymer Engineering & Science, 44(11), 2029-2040.

Liao, W. C., & Hsu, S. L. C. (2004). High aspect ratio pattern transfer in imprint lithography using a hybrid mold. Journal of Vacuum Science & Technology B: Microelectronics and Nanometer Structures Processing, Measurement, and Phenomena, 22(6), 2764-2767.

Lin, J. C. (2002). Optimum cooling system design of a free-form injection mold using an abductive network. Journal of Materials Processing Technology, 120(1-3), 226-236.

Lin, Y., & Cunningham, G. A. (1995). A new approach to fuzzy-neural system modeling. IEEE Transactions on Fuzzy systems, 3(2), 190-198.

Liu, G. H., Wong, Y. S., Zhang, Y. F., & Loh, H. T. (2003). Error-based segmentation of cloud data for direct rapid prototyping. Computer-Aided Design, 35(7), 633-645.

Liu, H., Chen, Y., Tang, Y., Wei, S., & Niu, G. (2007). The microstructure, tensile properties, and creep behavior of as-cast Mg–(1–10)% Sn alloys. Journal of Alloys and Compounds, 440(1-2), 122-126.

Liu, J., & Shin, T. (2003). U.S. Patent Application No. 10/124,535.

Lours, P., Bui, H. V., Nafi, A., Mercier, O., & Bernhart, G. (2004). Rapid tooling for injection moulding process. In Materials Science Forum (Vol. 449, pp. 789-792). Trans Tech Publications.

Luecke, W. E., & Slotwinski, J. A. (2014). Mechanical properties of austenitic stainless steel made by additive manufacturing. Journal of research of the National Institute of Standards and Technology, 119, 398.

Manas, D., Manas, M., Stanek, M., & Danek, M. (2008). Improvement of plastic properties. Archives of Materials Science and Engineering, 32(2), 69-76.

Mansour, S., & Hague, R. (2003). Impact of rapid manufacturing on design for manufacture for injection moulding. Proceedings of the Institution of Mechanical Engineers, Part B: Journal of Engineering Manufacture, 217(4), 453-461.

Mansouri, A., Lathuiliere, A., Marzani, F. S., Voisin, Y., & Gouton, P. (2007). Toward a 3d multispectral scanner: an application to multimedia. IEEE multimedia, 14(1).

Mao, H. Q., Leong, K. W., Dang, W., Lo, H., Zhao, Z., Nowotnik, D. P., & English, J. P. (2003). U.S. Patent No. 6,600,010. Washington, DC: U.S. Patent and Trademark Office.

Martínez, S., Cuesta, E., Barreiro, J., & Alvarez, B. (2010). Methodology for comparison of laser digitizing versus contact systems in dimensional control. Optics and Lasers in Engineering, 48(12), 1238-1246.

Marques, S., Souza, A. F., Miranda, J. R., & Santos, R. F. F. (2014, October). Evaluating the conformal cooling system in moulds for plastic injection by CAE simulation. In 9th International Conference on Industrial Tools and Material Processing Technologies. Ljubljana, Eslovenia (pp. 9-11).

Martinez, A., Castany, J., & Aisa, J. (2011). Characterization of in-mold decoration process and influence of the fabric characteristics in this process. Materials and Manufacturing Processes, 26(9), 1164-1172

Martinez, A., Castany, J., & Mercado, D. (2011). Characterization of viscous response of a polymer during fabric IMD injection process by means a spiral mold. Measurement, 44(10), 1806-1818.

Martínez, S., Cuesta, E., Barreiro, J., & Álvarez, B. (2010). Analysis of laser scanning and strategies for dimensional and geometrical control. The International Journal of Advanced Manufacturing Technology, 46(5-8), 621-629.

Martínez-Mateo, I., Carrión-Vilches, F. J., Sanes, J., & Bermúdez, M. D. (2011). Surface damage of mold steel and its influence on surface roughness of injection molded plastic parts. Wear, 271(9-10), 2512-2516.

Mathivanan, D., & Parthasarathy, N. S. (2009). Prediction of sink depths using nonlinear modeling of injection molding variables. The International Journal of Advanced Manufacturing Technology, 43(7-8), 654-663.

Mathivanan, D., Nouby, M., & Vidhya, R. (2010). Minimization of sink mark defects in injection molding process–Taguchi approach. International Journal of Engineering, Science and Technology, 2(2), 13-22.

Mehat, N. M., & Kamaruddin, S. (2011). Investigating the effects of injection molding parameters on the mechanical properties of recycled plastic parts using the Taguchi method. Materials and Manufacturing Processes, 26(2), 202-209.

Mehat, N. M., & Kamaruddin, S. (2012). Quality control and design optimisation of plastic product using Taguchi method: a comprehensive review. International Journal of Plastics Technology, 16(2), 194-209.

Mehat, N. M., Zakarria, N. S., & Kamaruddin, S. (2014). Investigating the Effects of Blending Ratio and Injection Parameters on the Tensile Properties of Glass Fiber-Filled Nylon 66 Composite Gear. In Applied Mechanics and Materials (Vol. 548, pp. 43-47). Trans Tech Publications.

Melchels, F. P., Domingos, M. A., Klein, T. J., Malda, J., Bartolo, P. J., & Hutmacher, D. W. (2012). Additive manufacturing of tissues and organs. Progress in Polymer Science, 37(8), 1079-1104.

Mian, S. H., Mannan, M. A., & Al-Ahmari, A. (2015). Accuracy of a reverse-engineered mould using contact and non-contact measurement techniques. International Journal of Computer Integrated Manufacturing, 28(5), 419-436.

Michaels, S., Sachs, E. M., & Cima, M. J. (1992). Metal parts generation by three dimensional printing. In 1992 International Solid Freeform Fabrication Symposium.

Michii, T., Seto, M., Yamabe, M., Kubota, Y., Aoki, G., & Ohtsuka, H. (2008). Study on warpage behavior and filler orientation during injection molding. International Polymer Processing, 23(5), 419-429.

Mikołajewska, E., Macko, M., Ziarnecki, Ł., Stańczak, S., Kawalec, P., & Mikołajewski, D. (2014). 3D printing technologies in rehabilitation engineering

Minitab tutorial: http://www.minitab.com/, Minitab software

Moammer, A., & Dimitrov, D. (2010). Investigation of the impact of conformal cooling on the performance of injection moulds for the packaging industry.

Mohan, M., Ansari, M. N. M., & Shanks, R. A. (2017). Review on the effects of process parameters on strength, shrinkage, and warpage of injection molding plastic component. Polymer-Plastics Technology and Engineering, 56(1), 1-12.

Moore, J. P., & Williams, C. B. (2012, August). Fatigue characterization of 3D printed elastomer material. In International Solid Freeform Fabrication Symposium (pp. 641-655).

Morrow, W. R., Qi, H., Kim, I., Mazumder, J., & Skerlos, S. J. (2007). Environmental aspects of laser-based and conventional tool and die manufacturing. Journal of Cleaner Production, 15(10), 932-943.

Mott, M., & Evans, J. R. G. (1999). Zirconia/alumina functionally graded material made by ceramic ink jet printing. Materials Science and Engineering: A, 271(1-2), 344-352.

Mott, M., Song, J. H., & Evans, J. R. (1999). Microengineering of ceramics by direct ink-jet printing. Journal of the American Ceramic Society, 82(7), 1653-1658.

Mueller, B. (2012). Additive manufacturing technologies–Rapid prototyping to direct digital manufacturing. Assembly Automation, 32(2).

Mueller, B., & Kochan, D. (1999). Laminated object manufacturing for rapid tooling and patternmaking in foundry industry. Computers in Industry, 39(1), 47-53.

Muhammad Khan, S. Kamran Afaq, Nizar Ullah Khan and Saboor Ahmed, "Cycle Time Reduction in Injection Molding Procss by Selection of Robust Cooling Channel Design," Vol. 2014, Article ID 968484, ISRN Mechanical Engineering, Hindawi Publishing Corporation.

Murr, L. E., Gaytan, S. M., Martinez, E., Medina, F., & Wicker, R. B. (2012). Next generation orthopaedic implants by additive manufacturing using electron beam melting. International journal of biomaterials, 2012.

Murr, L. E., Gaytan, S. M., Ramirez, D. A., Martinez, E., Hernandez, J., Amato, K. N., ... & Wicker, R. B. (2012). Metal fabrication by additive manufacturing using laser and electron beam melting technologies. Journal of Materials Science & Technology, 28(1), 1-14.

Murr, L. E., Martinez, E., Amato, K. N., Gaytan, S. M., Hernandez, J., Ramirez, D. A., ... & Wicker, R. B. (2012). Fabrication of metal and alloy components by additive manufacturing: examples of 3D materials science. Journal of Materials Research and technology, 1(1), 42-54.

Muth, J. T., Vogt, D. M., Truby, R. L., Mengüç, Y., Kolesky, D. B., Wood, R. J., & Lewis, J. A. (2014). Embedded 3D printing of strain sensors within highly stretchable elastomers. Advanced Materials, 26(36), 6307-6312.

Myoung, J. M., Yoon, W. H., Lee, D. H., Yun, I., Bae, S. H., & Lee, S. Y. (2002). Effects of thickness variation on properties of ZnO thin films grown by pulsed laser deposition. Japanese Journal of Applied Physics, 41(1R), 28.

Nadkarni, A. V. (1993). Copper based alloys. Mechanical Properties of Metallic Composites, 293.

Nagahanumaiah, & Ravi, B. (2009). Effects of injection molding parameters on shrinkage and weight of plastic part produced by DMLS mold. Rapid Prototyping Journal, 15(3), 179-186.

Nagaoka, T., Ishiaku, U. S., Tomari, T., Hamada, H., & Takashima, S. (2005). Effect of molding parameters on the properties of PP/PP sandwich injection moldings. Polymer testing, 24(8), 1062-1070.

Naing, M. W., Chua, C. K., Leong, K. F., & Wang, Y. (2005). Fabrication of customised scaffolds using computer-aided design and rapid prototyping techniques. Rapid Prototyping Journal, 11(4), 249-259.

Nambiar, R. V., Lee, K. H., & Nagarajan, D. (2007). Stereolithography mold life extension using gas-assisted injection. Rapid Prototyping Journal, 13(2), 92-98.

Nasir, S. M., Ismail, K. A., & Shayfull, Z. (2016). Application of RSM to Optimize Moulding Conditions for Minimizing Shrinkage in Thermoplastic Processing. In Key Engineering Materials (Vol. 700, pp. 12-21). Trans Tech Publications.

Negi, S., Dhiman, S., & Kumar Sharma, R. (2014). Basics and applications of rapid prototyping neural network methods. Materials & Design, 31(1), 599-604.

Noble, J., Walczak, K., & Dornfeld, D. (2014). Rapid tooling injection molded prototypes: a case study in artificial photosynthesis technology. Procedia CIRP, 14, 251-256.

Nogueira, A. A., Pouzada, P. S., Martinho, P. G., & Pouzada, A. S. (2010). A new way to produce conformal cooling channels by RPT for moulding blocks of the hybrid moulds. In PMI 2010-Int. Conf. on Polymers & Moulds Innovations (pp. 2-6). Ghent University Association.

Noorani, R. (2006). Rapid prototyping: principles and applications.

Nylon Materials in an Inkjet Printhead. Journal of Manufacturing Science and Engineering, 134(4), 041008.

Oktem, H., Erzurumlu, T., & Uzman, I. (2007). Application of Taguchi optimization technique in determining plastic injection molding process parameters for a thin-shell part. Materials & design, 28(4), 1271-1278.

Ong, H. S., Chua, C. K., & Cheah, C. M. (2002). Rapid moulding using epoxy tooling resin. The International Journal of Advanced Manufacturing Technology, 20(5), 368-374.

Onuh, S. O., & Hon, K. K. B. (1998). Optimising build parameters for improved surface finish in stereolithography. International Journal of Machine Tools and Manufacture, 38(4), 329-342.

Onuh, S., Bennett, N., & Hughes, V. (2006). Reverse engineering and rapid tooling as enablers of agile manufacturing. International Journal of Agile Systems and Management, 1(1), 60-72.

Othman, M. H., Hasan, S., Ibrahim, M. H. I., & Khamis, S. Z. (2017). Optimum Injection Moulding Processing Condition to Reduce Shrinkage and Warpage for Polypropylene-Nanoclay-Bamboo Fibre with Compatibilizer. In Materials Science Forum (Vol. 889, pp. 51-55). Trans Tech Publications.

Othman, M. H., Hasan, S., Khamis, S. Z., Ibrahim, M. H. I., & Amin, S. Y. M. (2017). Optimisation of Injection Moulding Parameter towards Shrinkage and Warpage for Polypropylene-Nanoclay-Gigantochloa Scortechinii Nanocomposites. Procedia engineering, 184, 673-680.

Othman, M. H., Shamsudin, S., Hasan, S., & Rahman, M. N. A. (2012). The effects of injection moulding processing parameters and mould gate size towards weld line strength. In Advanced Materials Research (Vol. 488, pp. 801-805). Trans Tech Publications.

Othman, M. H., Yusof, M. A. M., Hasan, S., Ibrahim, M. H. I., Amin, S. Y. M., Marwah, O. M. F., ... & Shahbudin, S. N. A. (2017, August). Development of Mould of Rheology Test Sample via CadMould 3D-F Simulation. In IOP Conference Series: Materials Science and Engineering (Vol. 226, No. 1, p. 012159). IOP Publishing.

Ozcelik, B., & Erzurumlu, T. (2005). Determination of effecting dimensional parameters on warpage of thin shell plastic parts using integrated response surface method and genetic algorithm. International communications in heat and mass transfer, 32(8), 1085-1094.

Ozcelik, B., & Erzurumlu, T. (2006). Comparison of the warpage optimization in the plastic injection molding using ANOVA, neural network model and genetic algorithm. Journal of materials processing technology, 171(3), 437-445.

Ozcelik, B., & Sonat, I. (2009). Warpage and structural analysis of thin shell plastic in the plastic injection molding. Materials & Design, 30(2), 367-375.

Ozcelik, B., Ozbay, A., & Demirbas, E. (2010). Influence of injection parameters and mold materials on mechanical properties of ABS in plastic injection molding. International Communications in Heat and Mass Transfer, 37(9), 1359-1365.

P. Chavhan Injection Mold Development Using Unigraphics as CAD Software for Mass Scale Production of a Plastic Container

Palmer, A. E., & Colton, J. S. (2000). Failure mechanisms in stereolithography injection molding tooling. Polymer Engineering & Science, 40(6), 1395-1404.

Palmer, A. E., & Colton, J. S. (2000). The Effect of Feature Geometry on Stereolithography Tooling. Polymer Engineering and Science, 40(6), 1395-1404.

Panda, S., & Ray, M. C. (2006). Nonlinear analysis of smart functionally graded plates integrated with a layer of piezoelectric fiber reinforced composite. Smart materials and structures, 15(6), 1595.

Park, H. S., & Dang, X. P. (2010). Optimization of conformal cooling channels with array of baffles for plastic injection mold. International Journal of Precision Engineering and Manufacturing, 11(6), 879-890.

Park, H. S., & Dang, X. P. (2010). Structural optimization based on CAD–CAE integration and metamodeling techniques. Computer-Aided Design, 42(10), 889-902.

Park, H. S., & Dang, X. P. (2012). Design and simulation-based optimization of cooling channels for plastic injection mold. In New Technologies-Trends, Innovations and Research. InTech.

Park, K., & Ahn, J. H. (2004). Design of experiment considering two-way interactions and its application to injection molding processes with numerical analysis. Journal of Materials Processing Technology, 146(2), 221-227.

Park, Y. C., Tokiwa, H., Kakinuma, K., Watanabe, M., & Uchida, M. (2016). Effects of carbon supports on Pt distribution, ionomer coverage and cathode performance for polymer electrolyte fuel cells. Journal of Power Sources, 315, 179-191.

Pathak V.K, K. Sagar, Nayak C., Rao NRNS G. (2017) Evaluating Geometric Characteristics of Planar Surfaces using Improved Particle Swarm Optimization

Pathak, V. K., & Singh, A. K. (2017). Optimization of morphological process parameters in contactless laser scanning system using modified particle swarm algorithm. Measurement, 109, 27-35.

Pathak, V. K., Singh, A. K., Singh, R., & Chaudhary, H. (2017). A modified algorithm of Particle Swarm Optimization for form error evaluation. tm-Technisches Messen, 84(4), 272-292.

Pelham, R. J., & Wang, Y. L. (1999). High resolution detection of mechanical forces exerted by locomoting fibroblasts on the substrate. Molecular biology of the cell, 10(4), 935-945.

Perez, A. R. T., Roberson, D. A., & Wicker, R. B. (2014). Fracture surface analysis of 3D-printed tensile specimens of novel ABS-based materials. Journal of Failure Analysis and Prevention, 14(3), 343-353.

Pesci, A., & Teza, G. (2008). Effects of surface irregularities on intensity data from laser scanning: an experimental approach. Annals of Geophysics, 51(5-6), 839-848.

Pesci, A., & Teza, G. (2008). Terrestrial laser scanner and retro-reflective targets: an experiment for anomalous effects investigation. International journal of remote sensing, 29(19), 5749-5765.

Pesci, A., Teza, G., Bonali, E., Casula, G., & Boschi, E. (2013). A laser scanning-based method for fast estimation of seismic-induced building deformations. ISPRS journal of photogrammetry and remote sensing, 79, 185-198.

Pham, D. T., & Dimov, S. S. (2003). Rapid prototyping and rapid tooling—the key enablers for rapid manufacturing. Proceedings of the Institution of Mechanical Engineers, Part C: Journal of Mechanical Engineering Science, 217(1), 1-23.

Pham, D. T., & Gault, R. S. (1998). A comparison of rapid prototyping technologies. International Journal of machine tools and manufacture, 38(10-11), 1257-1287.

Pham, P. L., Kamen, A., & Durocher, Y. (2006). Large-scale transfection of mammalian cells for the fast production of recombinant protein. Molecular biotechnology, 34(2), 225-237.

Polosky, Q. (2004). U.S. Patent Application No. 10/739,721.

PolyJet Materials Data Sheet. (n.d.). Retrieved 7 8, 2013, from stratasys

Postawa, P., Kwiatkowski, D., & Bociaga, E. (2008). Influence of the method of heating/cooling moulds on the properties of injection moulding parts. Archives of Materials Science and Engineering, 31(2), 121-124.

Prashantha, K., Soulestin, J., Lacrampe, M. F., Lafranche, E., Krawczak, P., Dupin, G., & Claes, M. (2009). Taguchi analysis of shrinkage and warpage of injection-moulded polypropylene/multiwall carbon nanotubes nanocomposites. Express Polym Lett, 3(10), 630-638.

Prest, C.D., Poole, J.C., Stevick, J., Waniuk, T.A. and Pham, Q.T., Apple Inc and Crucible Intellectual Property LLC, 2013. Layer-by-layer construction with bulk metallic glasses. U.S. Patent Application 13/473,210.

Raffi, M., Rumaiz, A. K., Hasan, M. M., & Shah, S. I. (2007). Studies of the growth parameters for silver nanoparticle synthesis by inert gas condensation. Journal of Materials Research, 22(12), 3378-3384.

Rahim, S. Z. A., Sharif, S., Zain, A. M., Nasir, S. M., & Mohd Saad, R. (2016). Improving the quality and productivity of molded parts with a new design of conformal cooling channels for the injection molding process. Advances in Polymer Technology, 35(1).

Rahmati, S., & Dickens, P. (1997). Stereolithography for injection mould tooling. Rapid Prototyping Journal, 3(2), 53-60.

Rahmati, S., Rezaei, M. R., & Akbari, J. (2009). Design and manufacture of a wax injection tool for investment casting using rapid tooling. Tsinghua Science & Technology, 14, 108-115.

Ramakrishnan, R., & Mao, K. (2017). Minimization of Shrinkage in Injection Molding Process of Acetal Polymer Gear Using Taguchi DOE Optimization and ANOVA Method. International Journal of Mechanical and Industrial Technology, 4(2348-7593), 72-79.

Rambhau, I. A., Ashwinkumar, J. S., Rajendra, J. P., Narayan, K. N., & Patil, B. D. (2016). Design and Analysis of Cover Handle Bar Top (Injection moulding process).

Rayegani, F., & Onwubolu, G. C. (2014). Fused deposition modelling (FDM) process parameter prediction and optimization using group method for data handling

(GMDH) and differential evolution (DE). The International Journal of Advanced Manufacturing Technology, 73(1-4), 509-519.

Richard, B. M., McElfresh, P., & Williams, C. (2010). U.S. Patent No. 7,762,342. Washington, DC: U.S. Patent and Trademark Office.

Rivera, D. R., Brown, C. M., Ouzounov, D. G., Pavlova, I., Kobat, D., Webb, W. W., & Xu, C. (2011). Compact and flexible raster scanning multiphoton endoscope capable of imaging unstained tissue. Proceedings of the National Academy of Sciences, 108(43), 17598-17603.

Rodd, A. B., Cooper-White, J., Dunstan, D. E., & Boger, D. V. (2001). Gel point studies for chemically modified biopolymer networks using small amplitude oscillatory rheometry. Polymer, 42(1), 185-198.

Rodriguez, J. (2016, June). Use of additive manufacturing (AM) for mold inserts in injection molding. In 123rd ASEE Annual Conference and Exposition. American Society for Engineering Education.

Rosochowski, A., & Matuszak, A. (2000). Rapid tooling: the state of the art. Journal of materials processing technology, 106(1-3), 191-198.

Saboori, M., Bakhshi-Jooybari, M., Noorani-Azad, M., & Gorji, A. (2006). Experimental and numerical study of energy consumption in forward and backward rod extrusion. Journal of materials processing technology, 177(1-3), 612-616.

Sachs, E., Cima, M., Williams, P., Brancazio, D., & Cornie, J. (1992). Three dimensional printing: rapid tooling and prototypes directly from a CAD model. Journal of Engineering for Industry, 114(4), 481-488.

Sachs, E., Wylonis, E., Allen, S., Cima, M., & Guo, H. (2000). Production of injection molding tooling with conformal cooling channels using the three dimensional printing process. Polymer Engineering & Science, 40(5), 1232-1247.

SadAbadi, H., & Ghasemi, M. (2007). Effects of some injection molding process parameters on fiber orientation tensor of short glass fiber polystyrene composites (SGF/PS). Journal of Reinforced Plastics and Composites, 26(17), 1729-1741.

Sahebrao Ingole, D., Madhusudan Kuthe, A., Thakare, S. B., & Talankar, A. S. (2009). Rapid prototyping–a technology transfer approach for development of rapid tooling. Rapid Prototyping Journal, 15(4), 280-290.

Saifullah, A. B. M., & Masood, S. H. (2007). Finite element thermal analysis of conformal cooling channels in injection moulding. In 5th Australasian Congress on Applied Mechanics (ACAM 2007) (Vol. 1, pp. 337-341). Engineers Australia.

Saifullah, A. B. M., & Masood, S. H. (2007, December). Cycle time reduction in injection moulding with conformal cooling channels. In Proceedings of the International Conference on Mechanical Engineering (pp. 29-31).

Sanchis, P., Villalba, P., Cuesta, F., Håkansson, A., Griol, A., Galán, J. V., ... & Martí, J. (2009). Highly efficient crossing structure for silicon-on-insulator waveguides. Optics letters, 34(18), 2760-2762.

Sandström, T., & Lindau, S. (2013). U.S. Patent No. 8,442,302. Washington, DC: U.S. Patent and Trademark Office.

Sanghera, B., Naique, S., Papaharilaou, Y., & Amis, A. (2001). Preliminary study of rapid prototype medical models. Rapid Prototyping Journal, 7(5), 275-284.

Saunders, P., Orchard, N., Maropoulos, P. G., & Graves, A. P. (2010). Integrated design and dimensional measurement: A review of the state of the art. Proceedings of the 2010 ICMR, Durham, UK.

Schiele, N. R., Corr, D. T., Huang, Y., Raof, N. A., Xie, Y., & Chrisey, D. B. (2010). Laser-based direct-write techniques for cell printing. Biofabrication, 2(3), 032001.

Schwenke, H., Neuschaefer-Rube, U., Pfeifer, T., & Kunzmann, H. (2002). Optical methods for dimensional metrology in production engineering. CIRP Annals-Manufacturing Technology, 51(2), 685-699.

Shanmugam, S., Ramisetti, N. K., Misra, R. D. K., Mannering, T., Panda, D., & Jansto, S. (2007). Effect of cooling rate on the microstructure and mechanical properties of Nb-microalloyed steels. Materials Science and Engineering: A, 460, 335-343.

Shayfull, Z., Sharif, S., Zain, A. M., Ghazali, M. F., & Saad, R. M. (2014). Potential of conformal cooling channels in rapid heat cycle molding: a review. Advances in Polymer Technology, 33(1).

Shayfull, Z., Sharif, S., Zain, A. M., Saad, R. M., & Fairuz, M. A. (2013). Milled groove square shape conformal cooling channels in injection molding process. Materials and Manufacturing Processes, 28(8), 884-891.

Shen, Y. K., Liao, J. H., & Zhao, W. X. (2004). Study on warpage and shrinkage of flip chip encapsulation process. International communications in heat and mass transfer, 31(5), 693-702.

Sherwood, J. K., Riley, S. L., Palazzolo, R., Brown, S. C., Monkhouse, D. C., Coates, M., ... & Ratcliffe, A. (2002). A three-dimensional osteochondral composite scaffold for articular cartilage repair. Biomaterials, 23(24), 4739-4751.

Shi, Y., & Eberhart, R. C., (2000). Comparing inertia weights and constriction factors in particle swarm optimization. In Evolutionary Computation, 2000. Proceedings of the 2000 Congress on (Vol. 1, pp. 84-88). IEEE.

Shin, J. K., Kim, K. T., Jung, M. J., Yoon, S. S., Han, Y. S., & Lee, J. E. (2003). U.S. Patent No. 6,515,339. Washington, DC: U.S. Patent and Trademark Office.

Shinde, M. S., & Ashtankar, K. M. (2017). Additive manufacturing–assisted conformal cooling channels in mold manufacturing processes. Advances in Mechanical Engineering, 9(5), 1687814017699764.

Shinde, M. S., & Ashtankar, K. M. (2018). Effect of Different Shapes of Conformal Cooling Channel on the Parameters of Injection Molding. CMC-COMPUTERS MATERIALS & CONTINUA, 54(3), 287-306.

Shirazi, S. F. S., Gharehkhani, S., Mehrali, M., Yarmand, H., Metselaar, H. S. C., Kadri, N. A., & Osman, N. A. A. (2015). A review on powder-based additive manufacturing for tissue engineering: selective laser sintering and inkjet 3D printing. Science and Technology of Advanced Materials, 16(3), 033502.

Simchi, A., Petzoldt, F., & Pohl, H. (2003). On the development of direct metal laser sintering for rapid tooling. Journal of materials processing technology, 141(3), 319-328.

Singh, G., & Verma, A. (2017). A Brief Review on injection moulding manufacturing process. Materials Today: Proceedings, 4(2), 1423-1433.

Singh, R. (2014). Process capability analysis of fused deposition modelling for plastic components. Rapid Prototyping Journal, 20(1), 69-76.

Singraur, D. S., & Patil, B. (2016). Review on Performance Enhancement of Plastic Injection Molding using Conformal Cooling Channels. Internation Journal of Engineering Research and General Science, 4(4).

Siouris, S., Shepherd, T., Wilson, C., & Blakey, S. (2013). Development of an apparatus for the degradation of aviation gas turbine lubricants. Tribology Transactions, 56(2), 215-223.

Sirrine, J. M., Pekkanen, A. M., Nelson, A. M., Chartrain, N. A., Williams, C. B., & Long, T. E. (2015). 3D-printable biodegradable polyester tissue scaffolds for cell adhesion. Australian Journal of Chemistry, 68(9), 1409-1414.

Sivadasan M, N K Singh. N.K, Sood, A.K."Use of FDM in Investment Casting and risk of using SLS process" Intl.J.of Applied Research in Mechanical Engg (IJARME) ISSN No. 2231 –5950, Vol2 Issue-1(2012) pp 1-5.

Slizewski, A., Friess, M., & Semal, P. (2010). Surface scanning of anthropological specimens: nominal-actual comparison with low cost laser scanner and high end fringe light projection surface scanning systems. Quartär, 57, 179-187.

Snelling, D., Blount, H., Forman, C., Ramsburg, K., Wentzel, A., Williams, C., & Druschitz, A. (2013). The effects of 3D printed molds on metal castings. In International solid freeform fabrication symposium.

Snelling, D., Li, Q., Meisel, N., Williams, C. B., Batra, R. C., & Druschitz, A. P. (2015). Lightweight metal cellular structures fabricated via 3D printing of sand cast molds. Advanced Engineering Materials, 17(7), 923-932.

Snelling, D., Williams, C., & Druschitz, A. (2014). A comparison of binder burnout and mechanical characteristics of printed and chemically bonded sand molds. In SFF Symposium, Austin, TX.

Soar, R. C., & Dickens, P. M. (1997). Deflection and the Prevention ofIngress within Laminated Tooling for Pressure Die-Casting.

Soar, R. C., & Dickens, P. M. (1997, January). Design of laminated tooling for high-pressure die casting. In Rapid Product Development Technologies (Vol. 2910, pp. 198-210). International Society for Optics and Photonics.

Son, S., Park, H., & Lee, K. H. (2002). Automated laser scanning system for reverse engineering and inspection. International Journal of Machine Tools and Manufacture, 42(8), 889-897.

Sood, A. K., Ohdar, R. K., & Mahapatra, S. S. (2010). Parametric appraisal of mechanical property of fused deposition modelling processed parts. Materials & Design, 31(1), 287-295.

Sood, A. K., Ohdar, R. K., & Mahapatra, S. S. (2012). Experimental investigation and empirical modelling of FDM process for compressive strength improvement. Journal of Advanced Research, 3(1), 81-90.

Spina, R. (2006). Optimisation of injection moulded parts by using ANN-PSO approach. Journal of Achievements in Materials and Manufacturing Engineering, 15(1-2), 146-152.

Spina, R., Walach, P., Schild, J., & Hopmann, C. (2012). Analysis of lens manufacturing with injection molding. International Journal of Precision Engineering and Manufacturing, 13(11), 2087-2095.

Sreedharan, J., & Jeevanantham, A. K. (2018). Analysis of Shrinkages in ABS Injection Molding Parts for Automobile Applications. Materials Today: Proceedings, 5(5), 12744-12749.

Stevenson, W. H. (1993, May). Use of laser triangulation probes in coordinate measuring machines for part tolerance inspection and reverse engineering. In Industrial Applications of Optical Inspection, Metrology, and Sensing (Vol. 1821, pp. 406-415). International Society for Optics and Photonics.

Stucker, B. R. E. N. T. (2012, September). Additive manufacturing technologies: technology introduction and business implications. In Frontiers of Engineering: Reports on Leading-Edge Engineering from the 2011 Symposium, National Academies Press, Washington, DC, Sept (pp. 19-21).

Sukindar, N. A., Ariffin, M., & Anuar, M. K. (2016). An Analysis on Finding the Optimum Die Angle of Polylactic Acid in Fused Deposition Modelling. In Applied Mechanics and Materials (Vol. 835, pp. 254-259). Trans Tech Publications.

Swaelens, B., Pauwels, J. and Vancraen, W., Materialise NV, 1997. Method for supporting an object made by means of stereolithography or another rapid prototype production method. U.S. Patent 5,595,703.

Taghizadeh, S., Özdemir, A., & Uluer, O. (2013). Warpage prediction in plastic injection molded part using artificial neural network. Iranian Journal of Science and Technology. Transactions of Mechanical Engineering, 37(M2), 149.

Tai, S. H. E. N. (2001). Development of geomechanic model experiment techniques. Journal of Yangtze River Scientific Research Institute, 18(5), 32-36.

Tan, K. H., Chua, C. K., Leong, K. F., Naing, M. W., & Cheah, C. M. (2005). Fabrication and characterization of three-dimensional poly (ether-ether-ketone)/-hydroxyapatite biocomposite scaffolds using laser sintering. Proceedings of the Institution of Mechanical Engineers, Part H: Journal of Engineering in Medicine, 219(3), 183-194.

Tang, C. L., & Telle, J. M. (1976). U.S. Patent No. 3,983,507. Washington, DC: U.S. Patent and Trademark Office.

Tang, C., Shi, B., Gao, W., Chen, F., & Cai, Y. (2007). Strength and mechanical behavior of short polypropylene fiber reinforced and cement stabilized clayey soil. Geotextiles and Geomembranes, 25(3), 194-202.

Tang, S. H., Tan, Y. J., Sapuan, S. M., Sulaiman, S., Ismail, N., & Samin, R. (2007). The use of Taguchi method in the design of plastic injection mould for reducing warpage.Journal of Materials Processing Technology, 182(1-3), 418-426.

Tang, Y., Loh, H. T., Wong, Y. S., Fuh, J. Y. H., Lu, L., & Wang, X. (2003). Direct laser sintering of a copper-based alloy for creating three-dimensional metal parts. Journal of Materials Processing Technology, 140(1-3), 368-372.

Tavman, I. H. (1996). Thermal and mechanical properties of aluminum powder-filled high-density polyethylene composites. Journal of Applied Polymer Science, 62(12), 2161-2167.

Teza, G., Pesci, A., Genevois, R., & Galgaro, A. (2008). Characterization of landslide ground surface kinematics from terrestrial laser scanning and strain field computation. Geomorphology, 97(3-4), 424-437.

Thamizhmanii, S., Saparudin, S., & Hasan, S. (2007). Analyses of surface roughness by turning process using Taguchi method. Journal of Achievements in Materials and Manufacturing Engineering, 20(1-2), 503-506.

Thomas, S. W. (1992). Stereolithography simplifies tooling for reinforced rubber parts. Mechanical engineering, 114(7), 62.

Thorne, A., Kruth, A., Tunstall, D., Irvine, J. T., & Zhou, W. (2005). Formation, structure, and stability of titanate nanotubes and their proton conductivity. The Journal of Physical Chemistry B, 109(12), 5439-5444.

Tomori, T., Melkote, S., & Kotnis, M. (2004). Injection mold performance of machined ceramic filled epoxy tooling boards. Journal of materials processing technology, 145(1), 126-133.

Tong, Y., Shan, Y., & Feng, Z. (2010). Profile invalidation approaching rapid prototyping. Rapid Prototyping Journal, 16(2), 146-155.

Tornincasa, S., & Vezzetti, E. (2005). Feasibility study of a reverse engineering system benchmarking. Proceedings of ADM-Ingegraf.

Torres, R. A., Arellano-Ceja, J., Hernández-Hernández, M. E., & González-Núñez, R. (2007). Effects of the blending sequence and interfacial agent on the morphology and mechanical properties of injection molded PC/PP Blends. Polymer Bulletin, 59(2), 251-260.

Tóth, T., & Živčák, J. (2014). A Comparison of the Outputs of 3D Scanners. Procedia Engineering, 69, 393-401.

Trdnost, V. P. D. N. N., & Modelov, T. T. (2013). Influence of processing factors on the tensile strength of 3d-printed models. Materiali in tehnologije, 47(6), 781-788.

Tursi, D., & Bistany, S. P. (2000). Process and tooling factors affecting sink marks for amorphous and crystalline resins. Journal of Injection Molding Technology, 4(3), 114.

Vaezi, M., Safaeian, D., & Shakeri, M. (2011). Integration of reverse engineering and rapid technologies for rapid investment casting of gas turbine blades: A comparison between applicable rapid technologies for blade rapid investment casting was conducted and reported in this paper. Virtual and Physical Prototyping, 6(4), 225-239.

Vaezi, M., Seitz, H., & Yang, S. (2013). A review on 3D micro-additive manufacturing technologies. The International Journal of Advanced Manufacturing Technology, 67(5-8), 1721-1754.

Van Gestel, N., Cuypers, S., Bleys, P., & Kruth, J. P. (2009). A performance evaluation test for laser line scanners on CMMs. Optics and lasers in engineering, 47(3-4), 336-342.

Varady, T., Martin, R. R., & Cox, J. (1997). Reverse engineering of geometric models—an introduction. Computer-aided design, 29(4), 255-268.

Vezzetti, E., Nasi, A., Ramieri, G., Tornincasa, S., & Verze, L. (2005). Validation of a 3d laser scanner to acquire human face morphology.

Volpato, N., Solis, D. M., & Costa, C. A. (2016). An analysis of Digital ABS as a rapid tooling material for polymer injection moulding. International Journal of Materials and Product Technology, 52(1-2), 3-16.

Vukašinović, N., Korošec, M., & Duhovnik, J. E. (2010). The Influence of Surface Topology on the Accuracy of Laser Triangulation Scanning Results. Strojniski Vestnik/Journal of Mechanical Engineering, 56(1).

Walczyk, D. F., & Yoo, S. (2009). Design and fabrication of a laminated thermoforming tool with enhanced features. Journal of Manufacturing Processes, 11(1), 8-18.

Wang, J., & Shaw, L. L. (2006). Fabrication of functionally graded materials via inkjet color printing. Journal of the American Ceramic Society, 89(10), 3285-3289.

Wang, X., & Feng, C. X. (2002). Development of empirical models for surface roughness prediction in finish turning. The International Journal of Advanced Manufacturing Technology, 20(5), 348-356.

Wang, Y., Yu, K. M., Wang, C. C., & Zhang, Y. (2011). Automatic design of conformal cooling circuits for rapid tooling. Computer-Aided Design, 43(8), 1001-1010.

Wang, Y., Yu, K. M., & Wang, C. C. (2015). Spiral and conformal cooling in plastic injection molding. Computer-Aided Design, 63, 1-11.

Weng, F. T., & Her, M. G. (2002). Study of the batch production of micro parts using the EDM process. The international journal of advanced manufacturing technology, 19(4), 266-270.

Wilson, J. S., Virag, L., Di Achille, P., Karšaj, I., & Humphrey, J. D. (2013). Biochemomechanics of intraluminal thrombus in abdominal aortic aneurysms. Journal of biomechanical engineering, 135(2), 021011.

Wimpenny, D. I., Bryden, B., & Pashby, I. R. (2003). Rapid laminated tooling. Journal of materials processing technology, 138(1-3), 214-218.

Wohlers Report 2014 – 3D Printing and Additive Manufacturing State of the Industry, Annual 665 Worldwide Progress Report, Wohlers Associates, 2014.

Wohlers, T. (2011). Making products by using additive manufacturing. Manufacturing Engineering, 146(4).

Wong, H. S. P., Lee, H. Y., Yu, S., Chen, Y. S., Wu, Y., Chen, P. S., ... & Tsai, M. J. (2012). Metal–oxide RRAM. Proceedings of the IEEE, 100(6), 1951-1970.

Wu, T., & Tovar, A. Design for additive manufacturing of conformal cooling channels using thermal-fluid topology optimization and application in injection molds.

Wu, T., Upadhyaya, N., Acheson, D., & Tovar, a. Topology optimization of injection molds with lattice cooling.

X., Laoui, T., & Froyen, L. (2003). Lasers and materials in selective laser sintering. Assembly An, 23(4), 357-371.

Xi, F., & Shu, C. (1999). CAD-based path planning for 3-D line laser scanning. Computer-Aided Design, 31(7), 473-479.

Xie, D., Zhang, H., Shu, X., & Xiao, J. (2012). Fabrication of polymer micro-lens array with pneumatically diaphragm-driven drop-on-demand inkjet technology. Optics Express, 20(14), 15186-15195.

Xie, D., Zhang, H., Shu, X., Xiao, J., & Cao, S. (2010). Multi-materials drop-on-demand inkjet technology based on pneumatic diaphragm actuator. Science China Technological Sciences, 53(6), 1605-1611.

Xu, X., Sachs, E., & Allen, S. (2001). The design of conformal cooling channels in injection molding tooling. Polymer Engineering & Science, 41(7), 1265-1279.

Xu, Y., Zhang, Q., Zhang, W., & Zhang, P. (2015). Optimization of injection molding process parameters to improve the mechanical performance of polymer product against impact. The International Journal of Advanced Manufacturing Technology, 76(9-12), 2199-2208.

Yang, B. X., Shi, J. H., Pramoda, K. P., & Goh, S. H. (2008). Enhancement of the mechanical properties of polypropylene using polypropylene-grafted multiwalled carbon nanotubes. Composites Science and Technology, 68(12), 2490-2497.

Yang, H., Lim, J. C., Liu, Y., Qi, X., Yap, Y. L., Dikshit, V., ... & Wei, J. (2017). Performance evaluation of project multi-material jetting 3D printer. Virtual and Physical Prototyping, 12(1), 95-103.

Yang, J. G., Zhou, X. H., & Niu, Q. (2013). Model and simulation of water penetration in water-assisted injection molding. The International Journal of Advanced Manufacturing Technology, 67(1-4), 367-375.

Yang, Y. K. (2006). Optimization of injection-molding process for mechanical and tribological properties of short glass fiber and polytetrafluoroethylene reinforced polycarbonate composites with grey relational analysis: a case study. Polymer-Plastics Technology and Engineering, 45(7), 769-777.

Yang, Y., & Gao, F. (2006). Injection molding product weight: online prediction and control based on a nonlinear principal component regression model. Polymer Engineering & Science, 46(4), 540-548.

Yap, Y. L., & Yeong, W. Y. (2014). Additive manufacture of fashion and jewellery products: A mini review: This paper provides an insight into the future of 3D printing industries for fashion and jewellery products. Virtual and Physical Prototyping, 9(3), 195-201.

Yap, Y. L., & Yeong, W. Y. (2015). Shape recovery effect of 3D printed polymeric honeycomb: This paper studies the elastic behaviour of different honeycomb structures produced by polyjet technology. Virtual and Physical Prototyping, 10(2), 91-99.

Yau, H. T., Chen, C. Y., & Wilhelm, R. G. (2000). Registration and integration of multiple laser scanned data for reverse engineering of complex 3D models. International Journal of Production Research, 38(2), 269-285.

Yin, F., Mao, H., Hua, L., Guo, W., & Shu, M. (2011). Back propagation neural network modeling for warpage prediction and optimization of plastic products during injection molding. Materials & design, 32(4), 1844-1850.

Yin, S., Ren, Y., Guo, Y., Zhu, J., Yang, S., & Ye, S. (2014). Development and calibration of an integrated 3D scanning system for high-accuracy large-scale metrology. Measurement, 54, 65-76.

Yoo, J., Cima, M. J., Khanuja, S., & Sachs, E. M. (1993). Structural ceramic components by 3D printing. In Solid Freeform Fabrication Symposium (pp. 40-50).

Yoo, J., Cima, M., Sachs, E., & Suresh, S. (2008). Fabrication and microstructural control of advanced ceramic components by three dimensional printing. In Proceedings of the 19th Annual Conference on Composites, Advanced Ceramics, Materials, and Structures—B: Ceramic Engineering and Science Proceedings, John Wiley & Sons, Inc (pp. 755-762).

Zaimovic-Uzunovic, N., & Lemes, S. (2010). Influences of surface parameters on laser 3d scanning. In IMEKO Conference Proceedings: International Symposium on Measurement and Quality Control: Osaka, Japan (pp. D024-026).

Zeng, K., Pal, D., & Stucker, B. (2012, August). A review of thermal analysis methods in Laser Sintering and Selective Laser Melting. In Proceedings of Solid Freeform Fabrication Symposium Austin, TX (pp. 796-814).

Zhang, H., Xie, A., Shen, Y., Qiu, L., & Tian, X. (2012). Layer-by-layer inkjet printing of fabricating reduced graphene-polyoxometalate composite film for chemical sensors. Physical Chemistry Chemical Physics, 14(37), 12757-12763.

Zheng, Z. X., FU, K. X., & Chen, Z. Q. (2005). The application based on reverse engineering and rapid prototype technology in the product design [J]. Machinery Design & Manufacture, 1, 025.

Zheng, Z., Zhang, H. O., Wang, G. L., & Qian, Y. P. (2011). Finite element analysis on the injection molding and productivity of conformal cooling channel. Journal of Shanghai Jiaotong University (Science), 16(2), 231-235.

Zhil'tsova, T. V., Oliveira, M. S. A., & Ferreira, J. A. F. (2009). Relative influence of injection molding processing conditions on HDPE acetabular cups dimensional stability. Journal of materials processing technology, 209(8), 3894-3904.

Zwicke, F., Behr, M., & Elgeti, S. (2017, October). Predicting shrinkage and warpage in injection molding: Towards automatized mold design. In AIP Conference Proceedings (Vol. 1896, No. 1, p. 100001). AIP Publishing.

Publication/ Research Paper

Peer-reviewed Journal Publications

1. **Sagar Kumar** and Amit Kumar Singh. "Warpage and Shrinkage analysis and optimization of rapid tooling molded thin wall component using modified particle swarm algorithm" in Journal of Advanced Manufacturing Systems (JAMS) DOI/10.1142/S0219686719500045. (Scopus)
2. **Sagar Kumar,** Amit Kumar Singh, Vimal Kumar Pathak. "Modelling and optimization of injection molding process for PBT/PET parts using modified particle swarm algorithm" in Indian Journal of Engineering and Material Sciences (IJEMS), Ref: NISCAIR (IJEMS-9642)/18. (SCI)
3. **Sagar Kumar** and Amit Kumar Singh. "FDM modeled polymer tooling for Plastic Injection Molding" in International Journal of Advances in Materials Science and Engineering (IJAMSE) Vol.7, No.1, January 2018, DOI:10.14810/ijamse.2018.7102.
4. **Sagar Kumar** and Amit Kumar Singh. "Volumetric shrinkage estimation of benchmark parts developed from rapid tooling mold insert" Sadhana, submission id: SADH-D-18-00150 (Under review on 01-Feb-2018). (SCI)

International/ National Conferences

1. **Sagar Kumar** and Amit Kumar Singh. "Dimensional issues of polymer based rapid tooling mold inserts" *International Colloquium on Materials, Manufacturing and Metrology*. 2014, IIT Chennai, India.
2. **Sagar Kumar** and Amit Kumar Singh. "Dimensional Accuracy of RP pattern and RTV mold Using Taguchi technique" *International conference on AM, 3D printing and 3D scanning (ICAM-3D)*. Feb 2015, Chennai India.
3. **Sagar Kumar** and Amit Kumar Singh. "Integrated product design and development through rapid tooling for sustainable manufacturing" *National Conference on Sustainable manufacturing (NCSM-2015*) MNIT Jaipur, January 2015.

BRIEF BIO-DATA OF THE AUTHOR

Name: **Sagar Kumar**

Date of birth: February 20, 1988

Address for correspondence: Flat G1 Wing 03 Glory Apartment
Vinayak Enclaves, Near Gyan Vihar University
Ramnagariya, Jagatpura, Jaipur- 302025

Education:

Qualification	Discipline	University	Year of Passing	School/college
Ph.D.	Machine Design	Autonomous	2019	MNIT, Jaipur
M. Tech	CAD/CAM	Autonomous	2012	VNIT, Nagpur
B.E.	Mechanical	VTU, Belgaum	2010	Sir MVIT, Bangalore
Intermediate	Science	BIEC, Patna	2004	M.M. College, Patna
Matriculation	General	BSEB, Patna	2002	P.H.S, Patna

Teaching/Research Experience:

University/ Institute	Duration	Designation
ARMIET, Mumbai	Jun 2012- July 2013	Assistant Professor
MNIT, Jaipur, (Rajasthan)	Dec 2013- Feb 2019	Ph.D. Research Scholar